Transient Electromagnetic Waves in Nonlinear Media

Sjöberg, Daniel

2001

Transient Electromagnetic Waves in Nonlinear Media

Daniel Sjöberg

Doctoral Dissertation
Electromagnetic Theory

Lund 2001

Department of Electroscience
Lund Institute of Technology, Lund University
Box 118, S-221 00 Lund, Sweden

No. 23
ISSN 1402-8662
ISBN 91-7874-132-7

Printed in Sweden by KFS AB, Lund
March 2001

Abstract

This thesis is concerned with the propagation of transient electromagnetic waves in nonlinear media. It consists of a General Introduction and five scientific papers.

The General Introduction gives a broad overview of nonlinear electromagnetic phenomena. The emphasis is on the representation of the constitutive functional modeling the material's response to electromagnetic excitation, and the methods employed to analyze the combination of the constitutive functional and the Maxwell equations. Some applications of nonlinear electromagnetics are also discussed.

Paper I treats the inverse scattering problem for an isotropic, homogeneous, nonlinear slab, subjected to a normally incident field. It is shown that when both reflected and transmitted fields are measured, we can reconstruct both the nonlinear permittivity and permeability. When one of these functions is known, reflection data is sufficient to obtain the other.

Paper II gives a formulation of transient electromagnetic fields, that can be used to analyze wave propagation in homogeneous media. The source free Maxwell equations are treated as an eigenvalue problem, from which we deduce the propagating waves and their wave speeds. The analysis is applied to the case of obliquely incident waves on a semi-infinite, bianisotropic, nonlinear medium.

Paper III analyzes the propagation of electromagnetic waves in a waveguide filled with an isotropic, nonlinear material. The equations governing each waveguide mode are derived, and it is shown that the different modes couple to each other. This coupling is quantified, and a growth estimates is given for the induced modes.

Paper IV deals with discontinuous electromagnetic waves, shock waves. It is shown that in order for these waves to be stable, they must satisfy a number of conditions, similar to Lax's classical shock conditions. These conditions permit us to classify electromagnetic shock waves as slow, fast or intermediate shock waves.

Finally, Paper V investigates the uniqueness and continuous dependence on data for solutions of the quasi-linear Maxwell equations, when we also require them to satisfy an entropy condition. This condition is related to the second law of thermodynamics, that the energy that is not described by our model must be dissipated.

Sammanfattning (in Swedish)

Denna avhandling behandlar hur elektromagnetiska vågor utbreder sig i olika material. Vanligtvis antar man i elektromagnetiska problem att materialen är linjära, det vill säga om man vet att man får en viss utsignal från materialet vid en given insignal, så förväntar man sig att få två gånger så stor utsignal om man fördubblar insignalen. I avhandlingen försöker vi klara oss utan denna egenskap, och utvecklar metoder som inte behöver linjäritet för att behandla vågutbredning. Detta kan behövas för att beskriva fenomen där man använder mycket stora energier, och vi ger ett antal olika exempel på sådana situationer i den allmänna inledningen, som föregår de fem vetenskapliga artiklar som utgör huvuddelen av avhandlingen.

Olika problem som behandlas i detta verk är hur man kan tolka mätningar utförda på olinjära material, och hur vågutbredningen i materialen kan beskrivas. Vi undersöker dels material som har samma egenskaper i alla riktningar, så kallade isotropa material, som material som har särskilda egenskaper i någon riktning, så kallade anisotropa material. Det visar sig att man vanligtvis har två olika vågutbredningshastigheter i ett olinjärt material. Dessa hastigheter kallas karakteristiska hastigheter, som dessutom visar sig bero på hur starka vågor vi försöker skicka genom materialet.

Ett typiskt fenomen som inträffar med vågutbredning i olinjära material är så kallade chockvågor. Detta är vågor som kan börja som lugna och mjuka vågor, men efter en viss ändlig tids utbredning börjar de kantra och blir skarpare och skarpare. Ett typiskt exempel på detta är vattenvågor som kommer in mot en grund strand; då avståndet mellan vattenytan och botten minskar, kommer toppen av vågen att färdas snabbare än resten, varpå vågen till slut bryts och vi får de typiska bränningar som kan iakttas vid en strand. Det visar sig att det finns tre sorters elektromagnetiska chockvågor, som skiljer sig åt beroende på hur snabbt de utbreder sig i förhållande till de två karakteristiska hastigheterna som vi nämnde i förra stycket: de snabba, långsamma eller mellanliggande chockvågorna.

List of papers

This thesis consists of a General Introduction and the following scientific papers:

I. D. Sjöberg. Reconstruction of nonlinear material properties for homogeneous, isotropic slabs using electromagnetic waves. *Inverse Problems*, **15** (1999), 431–444.

II. D. Sjöberg. Simple wave solutions for the Maxwell equations in bianisotropic, nonlinear media, with application to oblique incidence. *Wave Motion*, **32** (2000), 217–232.

III. D. Sjöberg. Nonlinear waveguides. Technical Report LUTEDX/(TEAT-7088)/-1–26/(2000), Lund Institute of Technology.

IV. D. Sjöberg. Shock structure for electromagnetic waves in bianisotropic, nonlinear materials. Technical Report LUTEDX/(TEAT-7094)/(1–17/(2001), Lund Institute of Technology.

V. D. Sjöberg. On uniqueness and continuity for the quasi-linear, bianisotropic Maxwell equations, using an entropy condition. Technical Report LUTEDX/-(TEAT-7095)/(1–20/(2001), Lund Institute of Technology.

Acknowledgments

This thesis is not *the* result of my nearly five years of study as a postgraduate student. These past years have given me so much more than just a few scientific papers, and I would like to thank a few of the people who helped making it such a lovely time.

First of all is my supervisor, Prof. Gerhard Kristensson. Thank you for providing pleasant discussions and a wonderful introduction to the world of science. Your support, in science as well as in other matters, has been invaluable, and I will remember these years with joy.

I thank all present and former colleagues at the Department of Electroscience and the former Department of Electromagnetic Theory, for creating a stimulating atmosphere in which it has been a true delight to work. Special thanks go to Anders Karlsson, Elsbieta Szybicka and Mats Gustafsson, and my present and former fellow postgraduates Björn Widenberg, Igor Egorov, Ingegerd Åberg, Martin Åkerberg, Michael Andersson, Peter Waller, Sören Poulsen, and Thomas Craven-Bartle.

Towards the end of my fourth year, I received a travel grant from the Royal Physiographical Society in Lund (Kungliga fysiografiska sällskapet i Lund), which gave me the opportunity to visit the Department of Mathematics and Statistics at the University of Canterbury, Christchurch, New Zealand, and the Department of Mathematics and Computer Science at the University of Akron, Ohio, for a couple of months. This was a most rewarding trip, and I am truly grateful for the warm hospitality shown by these institutions. In particular, I thank Prof. David Wall of Christchurch and Prof. Kevin Kreider of Akron, for making these visits very memorable.

During the course of my studies, I have had the fortune of participating in several distracting activities: playing chess and working at rock festivals for my chess club Hultsfred, fighting for the rights of postgraduate students in Lund and Sweden through the Student Union at Lund Institute of Technology, playing floorball, badminton and squash, and, above all, laughing and having a wonderful time with friends and family. Thank you all for putting up with me through my ups and downs! And finally, a big hug to Tore, Siv, Magnus, Peter, Åsa, Alicia and Jesper!

Lund, March 2001 Daniel Sjöberg

Contents

General Introduction

Daniel Sjöberg

Linear Nonlinear

Figure 1: To the discussion on nonlinearity in the supermarket.

1 Introduction

How can we explain the term *nonlinear*? As the name suggests, it is a *non*-property, a nonlinear material is characterized by not having a property called "linear". This is a rather odd way of classifying things; instead of saying what they *are*, we try to say what they are *not*. However, the concept of linearity is deeply rooted in our everyday experiences. When we go to the supermarket and weigh the fruit we want to buy, we expect two oranges to weigh twice as much as one orange, and we also pay twice as much for two oranges as for one. This is the essence of linearity; when we get one output for a certain input, we expect to get twice as much when we double the input.

Strangely enough, the concept of linearity is upset in the same supermarket, when we come to the candy department. This is the residence of the signs saying "Buy three, pay for two!" Thus, we pay say 5 crowns for one chocolate bar, but when we buy three, we only pay 10 crowns, not 15! This is an example of *non*-linearity.

Another situation where we see that a linear model cannot apply, is the speed of cars on a highway. When there are few cars on the road, each driver is relatively free to choose his/her own speed. Though, when the number of cars increases, there is less space to maneuver in. This results in an overall reduction of speed, which ultimately may turn into a total standstill, as all commuters probably are aware of. This is an example of *saturation*, which is a typically nonlinear phenomenon.

The latter example of nonlinearity, *i.e.*, cars influencing each others speed on the highway, actually has many similarities with electromagnetic waves propagating in nonlinear materials. The nonlinearity of the cars is that the speed depends on how many cars there are. In the nonlinear materials we study in this thesis, the speed of the electromagnetic wave depends on the electromagnetic energy in the media, *i.e.*, the strengths of the electromagnetic fields. This causes waves with large amplitudes to travel slower than waves with small amplitudes, just as cars on an empty highway can travel much faster than the cars on a jammed one.

Mathematically, the statement that a function $f(x)$ is linear is equivalent to requiring the relation

$$f(\alpha x_1 + \beta x_2) = \alpha f(x_1) + \beta f(x_2) \tag{1.1}$$

to hold for all scalars α and β, and all x_1 and x_2. This property is very useful when analyzing a given problem. If we can write the input x as a sum of easily analyzed

Description	Symbol	SI unit
Electric field strength	$\boldsymbol{E}$	V/m
Magnetic field strength	$\boldsymbol{H}$	A/m
Electric flux density	$\boldsymbol{D}$	$\mathrm{As/m^2}$
Magnetic flux density	$\boldsymbol{B}$	$\mathrm{Vs/m^2}$
Electric current density	$\boldsymbol{J}$	$\mathrm{A/m^2}$
Polarization density	$\boldsymbol{P}$	$\mathrm{As/m^2}$
Magnetization density	$\boldsymbol{M}$	A/m
Poynting vector	$\boldsymbol{S}$	$\mathrm{W/m^2}$

Table 1: The electromagnetic fields and sources. The fields are related by the definitions $\boldsymbol{D} = \epsilon_0 \boldsymbol{E} + \boldsymbol{P}$, $\boldsymbol{B} = \mu_0(\boldsymbol{H} + \boldsymbol{M})$ and $\boldsymbol{S} = \boldsymbol{E} \times \boldsymbol{H}$. We could also include the scalar charge density ρ in this table, but it is not used in this thesis.

inputs x_1 and x_2, *i.e.*, $x = \alpha x_1 + \beta x_2$, we obtain the desired output $f(x)$ as the sum of the outputs for each of the easy signals, $\alpha f(x_1) + \beta f(x_2)$. Of course, this reasoning is effective only if it really is easy to solve the problem for the inputs x_1 and x_2. The theory for solving linear equations is extensively developed, and there often exist standard methods for solving the problem.

When the linearity property is no longer available, many of the methods used to solve linear problems break down. It often turns out that we have to take a few steps back, and refrain from using the most advanced algorithms that were successful in the linear case. This has the interesting consequence that we often have to return to the original, physical problem, and ask ourselves which aspects that we are *really* looking for. By taking a more abstract view on the problem, we also obtain a better understanding of the linear problem.

1.1 Notation

The notation used in this General Introduction is mostly standard. In the enclosed papers, we sometimes use a different notation, which is explained in each paper.

Vector quantities, such as the electric field strength $\boldsymbol{E}$, are written in bold italics, and its absolute value is $|\boldsymbol{E}| = \sqrt{E_1^2 + E_2^2 + E_3^2}$, where E_1, E_2 and E_3 are the cartesian components of the three-dimensional vector $\boldsymbol{E}$. We denote a point in space by $\boldsymbol{x} = (x_1, x_2, x_3)$, and the unit vector pointing in the direction of the coordinate x_i is denoted by $\hat{\boldsymbol{x}}_i$, where $i = 1, 2, 3$. The electromagnetic fields are given in Table 1, and some common constants are given in Table 2.

In this General Introduction, the emphasis is on the constitutive functional, *i.e.*, the relation between the field strengths $\boldsymbol{E}$ and $\boldsymbol{H}$, and the flux densities $\boldsymbol{D}$ and $\boldsymbol{B}$. This relation describes the material's response to electromagnetic excitation, and may depend on the history of the fields. We mostly study the relation between the polarization and the electric field strength, which we write $\boldsymbol{P} = \mathcal{P}\boldsymbol{E}$. The symbol $\mathcal{P}$ denotes an operator, which for every field $\boldsymbol{E}$ defined for all space and time, gives a polarization $\boldsymbol{P}$ for all space and time. Thus, when using this symbol, we implicitly

Description	Symbol	Value in SI units
Speed of light in vacuum	c_0	299 792 458 m/s
Permittivity of vacuum	ϵ_0	$8.854 \cdot 10^{-12}$ As/Vm
Permeability of vacuum	μ_0	$12.57 \cdot 10^{-7}$ Vs/Am
Wave impedance in vacuum	η_0	376.7 Ω

Table 2: The electromagnetic constants. The value for c_0 is exact, the exact value for μ_0 is $4\pi \cdot 10^{-7}$ Vs/Am, and ϵ_0 is derived from the exact relation $c_0^2 = 1/\epsilon_0\mu_0$. The wave impedance in vacuum is defined as $\eta_0 = \sqrt{\mu_0/\epsilon_0}$.

allow the polarization to depend on the electric field strength in a non-local way. In Section 3 we give some explicit examples of representations of this functional.

On occasions, we use the tensor notation $\chi_{ij}E_j$, where one or more indices are repeated, in this case j. It is then assumed that $\chi_{ij}E_j = \sum_{j=1}^{3} \chi_{ij}E_j$, *i.e.*, we sum over all repeated indices.

Differentiation with respect to a given variable, say t, is written ∂_t, indicating $\partial_t f(x,t) = \partial f(x,t)/\partial t = \lim_{h\to 0}(f(x,t+h) - f(x,t))/h$ when the limit is defined. The spatial derivatives are often denoted by the nabla operator, $\nabla = \sum_{i=1}^{3} \hat{\boldsymbol{x}}_i \partial_{x_i}$, which has the character of a vector.

We conclude this section by explicitly writing out the Maxwell equations,

$$\begin{cases} \nabla \times \boldsymbol{E} + \partial_t \boldsymbol{B} = \boldsymbol{0} \\ \nabla \times \boldsymbol{H} - \partial_t \boldsymbol{D} = \boldsymbol{J}, \end{cases} \tag{1.2}$$

which are the equations modeling the dynamics of the electromagnetic fields. Maxwell wrote his equations in a more complicated manner [47, 48], and the vector formulation above was introduced by Heaviside [27]. Extensive reference is made to this system of equations in the following.

2 Nonlinear materials and phenomena

Nonlinear materials and phenomena are present in many places in our everyday world. In this section we present three examples of a more technical nature, *i.e.*, ferromagnetic materials, electromechanical effects, and semiconducting materials.

2.1 Ferromagnetics

One of the first documented observations of a magnetic phenomenon is in Plato's dialogue *Ion*, where Socrates mentions Euripides' discovery of the magnet, a stone which attracts iron by an invisible force [52]. Today, we have learnt to classify magnetic materials as diamagnetic, paramagnetic, ferromagnetic, antiferromagnetic, or ferrimagnetic material [14, 39]. The most familiar among these are probably the ferromagnetic materials, which are named after their most known member; the latin word for iron is *ferrum*. Ferromagnetic effects are very strong, and a striking demonstration of this is that already the ancient greeks were able to observe them.

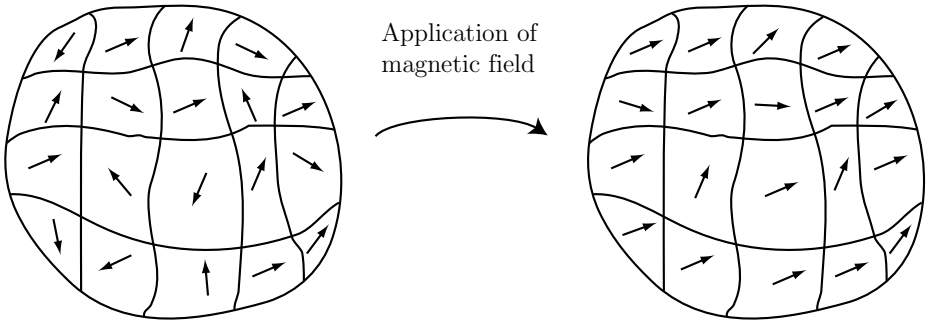

Figure 2: The alignment of domains when applying an external magnetic field. The configuration to the left shows the disordered domains in the absence of a magnetic field. When we apply an external magnetic field, the domains align themselves along the field (or rather: domains which are already aligned to the field grow on the expense of other domains). This alignment remains even after removing the external magnetic field.

Most people have had some experience with ferromagnets; since the materials can be permanently magnetized by placing them in a constant magnetic field and then removing the field, they are often used as permanent magnets, for instance in loudspeakers, motors and magnetic resonance imaging (MRI) [34]. That there is a remanent magnetization when the magnetic field is removed, is explained by the domain theory, proposed by Weiss in 1907 [68]. The idea is that there exist relatively large regions in the material, called domains, where the magnetic dipole moments of the individual atoms are aligned. This results in a strong local magnetic field, which maintains the alignment of the different domains even after the external magnetic field is removed, see Figure 2.

The remanent magnetization is an example of hysteresis, *i.e.*, that the magnetization depends on the history of the excitation of the material. The mathematical description of hysteresis is a complex matter. For a more detailed presentation of hysteresis we refer to the literature [9, 31, 34, 64, 67].

2.2 Electromechanical effects

Electromagnetic fields are defined through observations on how charged particles interact with other particles, and this interaction is represented by various kinds of forces. There are many other forces than electromagnetic ones, which sometimes must be taken into account in order to present an accurate model. In this section, we present two effects that can be modeled by the combination of electromagnetic theory and continuum mechanics: magnetohydrodynamics and piezoelectricity. A thorough review of the equations obtained when combining the Maxwell equations with the equations of continuum mechanics is found in [15, 16], and [45] also has related material.

Magnetohydrodynamics is the study of a conductive fluid in a magnetic field. Since the charged particles in the fluid experience a force from the magnetic field, this often drastically influences the behavior of the fluid. In order to describe this

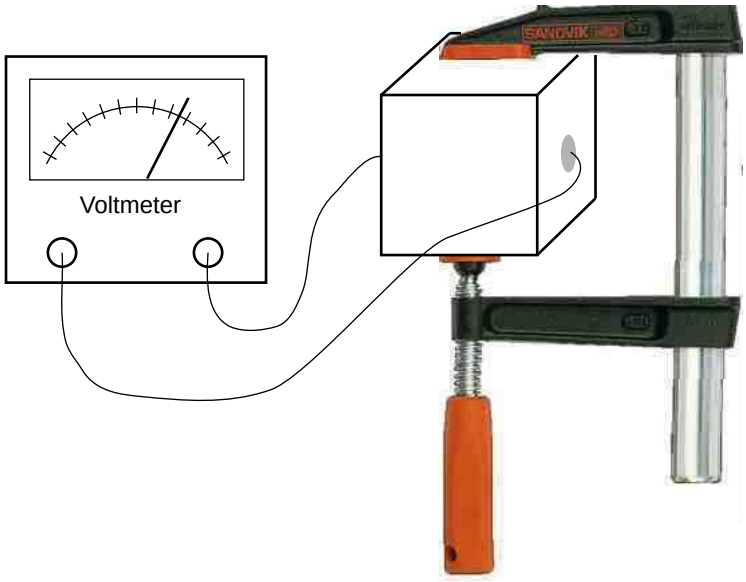

Figure 3: A piezoelectric crystal. When the crystal is compressed, a voltage is induced. The converse is also true: when applying a voltage to the crystal, a deformation is induced.

behavior, we have to combine the Maxwell equations describing the magnetic field with the Navier-Stokes equations describing the fluid movement. This leads to a complicated nonlinear system of equations, with applications ranging from entrapment of very hot plasmas in fusion experiments, over the pumping of liquid metals, to the dynamics of galaxies. We refer the interested reader to the review articles [3, 22] and references therein, and some textbooks treating magnetohydrodynamics are [2, 16, 33, 45].

Piezoelectricity, from the greek word *piezein* for press, is the effect where a mechanical pressure on a crystal induces a voltage across the crystal. The effect is reciprocal in the sense that we can also induce mechanical stresses and strains in the crystal by applying a voltage to it, see Figure 3. Thus, a piezoelectric crystal can be used to convert electric to mechanic energy, and vice versa. Piezoelectricity is usually treated with linear theories, but for large strains and voltages, nonlinear corrections are necessary. Among the applications of piezoelectric materials we mention transducers (generators of ultrasonic vibrations) and the crystal pickup in a phonograph. Textbook treatments of piezoelectricity are found in [14, 15, 45].

2.3 Semiconductors

One of the major reasons for the explosive progress in electronics is the understanding of semiconducting materials that has evolved over the last century. A characteristic property of a semiconducting material is that its intrinsic, relatively poor conductivity, can be dramatically changed by introducing impurities in the material, a process known as doping [39, p. 206]. By combining semiconducting crystals with different kinds of doping, we can build important circuit elements such

as the diode and the transistor. A characteristic property of these elements is that their behavior is altered by a bias. For instance, the diode usually lets through current of a given sign, say positive, but blocks negative currents. This means that by adding a large bias current I to a small signal current $i < |I|$ through the diode, the diode only lets the signal through if $I > 0$, since $I + i < 0$ if $I < 0$. This is obviously not a linear behavior.

3 Mathematical models of nonlinear materials

The reaction of materials when subjected to electromagnetic excitation can be modeled by a constitutive functional. The reaction is described by the polarization $\boldsymbol{P}$ and the magnetization $\boldsymbol{M}$, and the constitutive functional is the mapping from the excitation to these fields. There is some freedom of choice as to which combination of electric and magnetic fields should be considered as excitation. It is generally agreed that the electric field strength $\boldsymbol{E}$ is the primary electric field instead of $\boldsymbol{D}$, but in the literature both $\boldsymbol{B}$ and $\boldsymbol{H}$ are used as the primary magnetic field. The former is preferable when dealing with relativistic applications [32, 40], whereas the latter admits a formalism more suited for the computational aspects we are treating in this thesis. Thus, we choose to study the mapping

$$(\boldsymbol{E}, \boldsymbol{H}) \to (\boldsymbol{P}, \boldsymbol{M}), \tag{3.1}$$

and treat the magnetic field strength $\boldsymbol{H}$ as the primary magnetic field. The fields $\boldsymbol{D}$ and $\boldsymbol{B}$ are then found from the definitions $\boldsymbol{D} = \epsilon_0 \boldsymbol{E} + \boldsymbol{P}$ and $\boldsymbol{B} = \mu_0(\boldsymbol{H} + \boldsymbol{M})$.

The constitutive functional can be represented in a number of ways. One common approach is to find a large class of functionals, which can be used to represent almost anything, and then impose a number of axioms concerning the model behavior. These axioms are often based on phenomenological observations of physical phenomena, and lead to restrictions on the parameters defining the mathematical model. Some of the most common are

Causality: The material should not generate a response until it is excited.

Continuity: A small change in the excitation should only result in a small change in the response.

Time invariance: There is no origin of time. The material does not age, and experiments are repeatable.

Locality: The response does not depend appreciably on excitation that is distant in space and/or time.

Passivity: The material may only dissipate electromagnetic energy, not generate it, *i.e.*, the second law of thermodynamics must be satisfied.

Several other axioms are often used, see for instance [15, 24, 37]. Among these we mention pointwise spatial dependence, linearity and objectivity.

In practice, other requirements also come into play. If we are aiming at using the constitutive functional to make a simulation, we must be able to calculate it efficiently, and if we want to solve an inverse problem, we need a model with as few parameters as possible. A model with few parameters is also helpful to obtain a physical intuition for the problem.

For the models presented in the following subsections, most of the above properties are obvious. However, the passivity requires a somewhat deeper analysis, a brief outline of which is presented here. We must consider the full dynamics of the problem, *i.e.*, the constitutive relation in conjunction with the Maxwell equations. From the Maxwell equations we obtain the Poynting theorem, see for instance [32, p. 259], [40, p. 13] or [58, p. 132],

$$\nabla \cdot (\boldsymbol{E} \times \boldsymbol{H}) + \boldsymbol{E} \cdot \partial_t \boldsymbol{D} + \boldsymbol{H} \cdot \partial_t \boldsymbol{B} + \boldsymbol{E} \cdot \boldsymbol{J} = 0. \tag{3.2}$$

This equation is the balance law for electromagnetic energy. The requirement that a constitutive model is (pointwise) passive, is satisfied if the relation

$$\int_{-\infty}^{t} (\boldsymbol{E} \cdot \partial_{t'} \boldsymbol{D} + \boldsymbol{H} \cdot \partial_{t'} \boldsymbol{B}) \, \mathrm{d}t' \geq 0, \tag{3.3}$$

holds for every t and every point in space [20, 24, 37]. This relation is difficult to analyze for a general representation of the constitutive relation, and we refer to [42] for a discussion of passivity in nonlinear media.

When discussing the various representations of the constitutive functional below, we usually consider the mapping of the electric field strength $\boldsymbol{E}$ to the electric polarization density $\boldsymbol{P}$, *i.e.*, $\boldsymbol{P} = \mathcal{P}\boldsymbol{E}$, where $\mathcal{P}$ denotes the constitutive functional. The representations are easily adapted to other, more complicated, situations.

3.1 General representation of a linear functional

From the Schwartz kernel theorem [29, p. 128], we know that a general, linear, continuous operator $\mathcal{P}$ has the representation

$$[\mathcal{P}\boldsymbol{E}]_i(\boldsymbol{x}, t) = \iint \chi_{ij}(\boldsymbol{x}, t; \boldsymbol{x}', t') E_j(\boldsymbol{x}', t') \, \mathrm{d}^3\boldsymbol{x}' \, \mathrm{d}t', \tag{3.4}$$

where the integration is performed over $\mathbb{R}^3 \times \mathbb{R}$, and summation over j is assumed. It is common to deal only with causal relations, invariant under translations in time and pointwise defined. Under these assumptions, the general constitutive relation above reduces to a convolution in time,

$$[\mathcal{P}\boldsymbol{E}]_i(\boldsymbol{x}, t) = \int_{-\infty}^{t} \chi_{ij}(\boldsymbol{x}, t - t') E_j(\boldsymbol{x}, t') \, \mathrm{d}t'. \tag{3.5}$$

The advantage with this representation is that it is general, *i.e.*, it can represent any linear, time-invariant constitutive functional $\mathcal{P}$. The disadvantage is that it is often numerically inefficient: in order to calculate the response at a given point

in time and space, we need to compute an integral over all preceding times. It is also difficult to give an exact criterion on χ_{ij} that guarantees passivity, unless we transform the problem to the frequency domain [24, 41].

Of course, the nonlinear constitutive relations in the following subsections can also be applied to linear materials, which demonstrates that there are alternatives to the convolution representation of the functional.

3.2 General representation of a weakly nonlinear functional

When a functional is weakly nonlinear, it may be expanded in a Volterra series, which is a generalization of the usual series expansion applied to functions [66]. It is written

$$\mathcal{P}\boldsymbol{E} = \boldsymbol{P}^{(1)} + \boldsymbol{P}^{(2)} + \boldsymbol{P}^{(3)} + \cdots, \tag{3.6}$$

where the explicit representation of the i:th component of the n:th term in this series in a homogeneous material is

$$P_i^{(n)}(\boldsymbol{x}, t) = \int \cdots \int \chi^{(n)}_{i,p_1\ldots p_n}(t - t_1, \ldots, t - t_n) E_{p_1}(\boldsymbol{x}, t_1) \cdots E_{p_n}(\boldsymbol{x}, t_n)\, \mathrm{d}t_1 \cdots \mathrm{d}t_n, \tag{3.7}$$

and summation over the indices $p_1, \ldots, p_n$ is assumed. This is a reasonable representation of a weakly nonlinear constitutive functional, and is for example used in the analysis of nonlinear microwave circuits [46], and nonlinear optics [16, p. 631]. See also the discussion on the nonlinear transfer functional in Section 4.5.

It is interesting to study the frequency domain representation of the Volterra series, and to this end we introduce the four-dimensional Fourier transform $\mathcal{F}_4$ of a scalar function f as

$$\begin{cases} \hat{f}(\boldsymbol{k}, \omega) = [\mathcal{F}_4 f](\boldsymbol{k}, \omega) = \iint f(\boldsymbol{x}, t) \mathrm{e}^{-\mathrm{i}(\boldsymbol{k}\cdot\boldsymbol{x} - \omega t)}\, \mathrm{d}^3\boldsymbol{x}\, \mathrm{d}t \\ f(\boldsymbol{x}, t) = [\mathcal{F}_4^{-1} \hat{f}](\boldsymbol{x}, t) = \dfrac{1}{(2\pi)^4} \iint \hat{f}(\boldsymbol{k}, \omega) \mathrm{e}^{\mathrm{i}(\boldsymbol{k}\cdot\boldsymbol{x} - \omega t)}\, \mathrm{d}^3\boldsymbol{k}\, \mathrm{d}\omega \end{cases} \tag{3.8}$$

where the transformed function is indicated by a hat. Applying this transform to the n:th order term above, we obtain (after some calculations as in [57])

$$\begin{aligned} P_i^{(n)}(\boldsymbol{k}, \omega) = \frac{1}{(2\pi)^{4n-4}} \int \cdots \int \int \cdots \int \\ \hat{\chi}^{(n)}_{i,p_1\ldots p_n}(\omega_1, \ldots, \omega_n) \hat{E}_{p_1}(\boldsymbol{k}_1, \omega_1) \cdots \hat{E}_{p_n}(\boldsymbol{k}_n, \omega_n) \delta(\boldsymbol{k} - \sum_{i=1}^{n} \boldsymbol{k}_i) \delta(\omega - \sum_{i=1}^{n} \omega_i) \\ \mathrm{d}^3\boldsymbol{k}_1 \cdots \mathrm{d}^3\boldsymbol{k}_n\, \mathrm{d}\omega_1 \cdots \mathrm{d}\omega_n, \end{aligned} \tag{3.9}$$

where δ denotes the Dirac distribution. From this relation, we identify the important phase matching criterion in the generation of harmonics, *i.e.*, in order to generate a field with frequency ω and wave vector $\boldsymbol{k}$ from n fields with frequencies ω_i and wave

vectors $\boldsymbol{k}_i$, where $i = 1, \ldots, n$, we must require

$$\omega = \sum_{i=1}^{n} \omega_i, \quad \text{and} \quad \boldsymbol{k} = \sum_{i=1}^{n} \boldsymbol{k}_i. \tag{3.10}$$

From (3.9) it is seen that there is generally little to gain by Fourier transforming the equations, as we can for linear equations. The Fourier transform of the convolutions reduces to a product only for the linear term, *i.e.*, $[\mathcal{F}_4 \boldsymbol{P}^{(1)}](\boldsymbol{k}, \omega) = \hat{\chi}^{(1)}(\omega)\hat{\boldsymbol{E}}(\boldsymbol{k}, \omega)$, whereas the higher order terms remain rather complicated after transformation. A further complication is that if each pair of frequency and wave vector should be associated to a propagating wave, they must satisfy the dispersion relation relevant for the linearized medium, *i.e.*, frequency is a function of wave vector (or vice versa), $\omega_i = \Omega(\boldsymbol{k}_i)$. However, when dealing with a fixed frequency it is still useful to do the analysis in the frequency domain, especially if the generation of harmonics is limited. This is the common approach in nonlinear optics [5, 7, 55], where the frequency is fixed by the frequency of a strong laser beam and its harmonics, and the wave vectors are given by the directions of the beams.

Since the n:th order susceptibility $\chi^{(n)}(t_1, \ldots, t_n)$ has n continuous arguments, the Volterra series representation requires huge amounts of data. Sometimes this can be reduced by expressing the functions $\chi^{(i)}$, $i \geq 2$, in the function $\chi^{(1)}$ associated with the linear response. For weak nonlinearities, it is often found that $\chi^{(2)}$ is proportional to the cube of $\chi^{(1)}$, written as

$$\chi^{(2)}(t_1, t_2) = a \int \chi^{(1)}(t')\chi^{(1)}(t_1 - t')\chi^{(1)}(t_2 - t')\,\mathrm{d}t', \tag{3.11}$$

where a is a proportionality constant. This is called Miller's rule, and is usually stated in the frequency domain as

$$\hat{\chi}^{(2)}(\omega_1, \omega_2) = a\hat{\chi}^{(1)}(\omega_1 + \omega_2)\hat{\chi}^{(1)}(\omega_1)\hat{\chi}^{(1)}(\omega_2), \tag{3.12}$$

see for instance [7, p. 27], [16, p. 655] and [53, p. 786]. It was discovered empirically by observing that the quotient between the above quantities is almost constant for materials not having a microscopic center of symmetry [49]. This relation may be of interest when solving an inverse scattering problem, where it would be practically impossible to resolve all of $\chi^{(n)}$ since it depends on n continuous variables. Using Miller's rule, an inverse scattering algorithm as in [51] can be designed to search for the region where $a \neq 0$, *i.e.*, the region of a scatterer where the nonlinear interaction takes place.

3.3 Variables of state

A less memory-intense representation of the constitutive functional than the Volterra series in the previous subsection can be achieved by introducing variables of state, which in their turn are given by a functional operating on the excitation. One common model is the Lorentz model, where $\mathcal{P}\boldsymbol{E} = \boldsymbol{P}$ and $\boldsymbol{P}$ satisfies the ordinary differential equation

$$\partial_t^2 \boldsymbol{P} + \nu \partial_t \boldsymbol{P} + \omega_0^2(\boldsymbol{P} - \beta|\boldsymbol{P}|^2\boldsymbol{P}) = \omega_\mathrm{p}^2 \epsilon_0 \boldsymbol{E}, \tag{3.13}$$

where ν is the collision frequency, ω_0 is the resonance frequency and ω_p is the plasma frequency of the material. This model is used as a simple model for the displacement of the electron cloud surrounding the atom, when subjected to an external electric field $\boldsymbol{E}$, see [7, p. 29] and [16, p. 652]. The term multiplied by ω_0^2 is proportional to the restoring force acting on the electron, and the cubic term represents a nonlinear correction to this restoring force for large displacements (large $\boldsymbol{P}$). The parameter β is related to a typical polarization at which the nonlinear effects become noticeable.

Another common model is the Debye model, which describes how molecules with permanent dipole moments align themselves to an external electric field on an average. It is written

$$\partial_t \boldsymbol{P} + \frac{1}{\tau}\boldsymbol{P} = \boldsymbol{F}(\boldsymbol{E}, \boldsymbol{P}), \tag{3.14}$$

where the parameter τ is the relaxation time, and $\boldsymbol{F}$ is a function of $\boldsymbol{E}$ and $\boldsymbol{P}$, representing the aligning force. For small $|\boldsymbol{P}|$, this function is proportional to $\boldsymbol{E}$.

A third important example is the Landau-Lifshitz model for the magnetization in ferromagnetic material, see [44, pp. 284–313], [43] and [16, p. 465], where the constitutive functional giving the magnetization is $\mathcal{M}\boldsymbol{H} = \boldsymbol{M}$, and $\boldsymbol{M}$ satisfies the differential equation

$$\partial_t \boldsymbol{M} = \gamma\mu_0 \boldsymbol{M} \times \boldsymbol{H}_\mathrm{eff} - \frac{\lambda}{M^2}\boldsymbol{M} \times (\boldsymbol{M} \times \boldsymbol{H}_\mathrm{eff}), \tag{3.15}$$

which describes the conservation of angular momentum. The parameter γ is the gyromagnetic ratio, which is negative, and λ is a small parameter introducing a phenomenological damping. The effective magnetic field strength $\boldsymbol{H}_\mathrm{eff}$ is given by the gradient of the Landau-Lifshitz free energy with respect to $\boldsymbol{M}$, and we refer to [44, pp. 284–313] and [16, p. 465] for further details. The field $\boldsymbol{H}_\mathrm{eff}$ can often be considered as equal to the external field strength $\boldsymbol{H}$, but when considering anisotropy, domain walls and other ferromagnetic phenomena, additional terms must be included. A recent review of problems and possibilities for this and related models is given in [67].

The advantage of using a variables of state representation of nonlinear, dispersive constitutive functionals, is that we often obtain a direct coupling to the physical phenomena we are modeling. This representation is also numerically efficient for transient wave propagation, when combined with a finite difference algorithm for the Maxwell equations.

3.4 Instantaneous response

In the representations presented above, we have taken memory effects into account, *i.e.*, the polarization depends on earlier time values of the electric field. When we neglect all memory effects, the constitutive functional reduces to a function [15, p. 631],

$$[\mathcal{P}\boldsymbol{E}](\boldsymbol{x}, t) = \boldsymbol{P}(\boldsymbol{E}(\boldsymbol{x}, t)), \tag{3.16}$$

which expresses that the polarization at a given point in time and space depends only on the electric field at the same point in space and time. An explicit example

is the classical Kerr model [53, p. 751],

$$\boldsymbol{P}(\boldsymbol{E}) = \chi_1 \boldsymbol{E} + \chi_3 |\boldsymbol{E}|^2 \boldsymbol{E}, \tag{3.17}$$

and the saturated Kerr model [42, 63]

$$\boldsymbol{P}(\boldsymbol{E}) = \chi_1 \boldsymbol{E} + (\chi_\mathrm{S} - \chi_1) \frac{|\boldsymbol{E}|^2}{E_\mathrm{S}^2 + |\boldsymbol{E}|^2} \boldsymbol{E}. \tag{3.18}$$

The parameter E_S is a typical field strength at which the material response begins to saturate, *i.e.*, for $|\boldsymbol{E}| \ll E_\mathrm{S}$ we have $\boldsymbol{P} \approx \chi_1 \boldsymbol{E} + \chi_3 |\boldsymbol{E}|^2 \boldsymbol{E}$, where $\chi_3 = (\chi_\mathrm{S} - \chi_1) E_\mathrm{S}^{-2}$, but for $|\boldsymbol{E}| \gg E_\mathrm{S}$ we have $\boldsymbol{P} \approx \chi_\mathrm{S} \boldsymbol{E}$. This shows that this model is linear for large field strengths.

The instantaneous response is a reasonable model when the variation of the applied field strength $\boldsymbol{E}$ is much slower than the materials resonance frequencies. Throughout the papers in this thesis, we use a model with a nonlinear, instantaneous response.

4 Analysis methods

So far, we have only given representations of the constitutive functional, without considering its combination with the equations governing the dynamics of the electromagnetic fields, the Maxwell equations. In this section we present some methods used in studying transient nonlinear electromagnetics, preferably wave propagation.

4.1 Linearization

Since there exist powerful methods of analysis for linear problems, it is desirable to use them whenever possible. This is indeed possible even when studying nonlinear models, for instance in a classical small signal analysis, where the nonlinearity manifests in the establishment of an operating point, which is only slightly perturbed by the signal. Probably the most familiar example is in circuit theory, treating amplifiers built on transistors and other nonlinear elements. For the transistor, we may assume a relatively large bias current, which sets the operating mode of the transistor. We then add a small signal current, which can be treated with linear methods since its amplitude is not large enough to disturb the operating point, see Figure 4.

The linearization approach is feasible if we can divide the excitation in two parts, where the dominating one can be treated in some known manner (for instance when it is static). It is then possible to create a linear model for the small signal, where the parameters depend on the dominating excitation.

4.2 Numerical methods

Even if an analytical solution may be desirable in order to obtain physical intuition regarding a given problem, it is necessary to use some sort of numerical method to

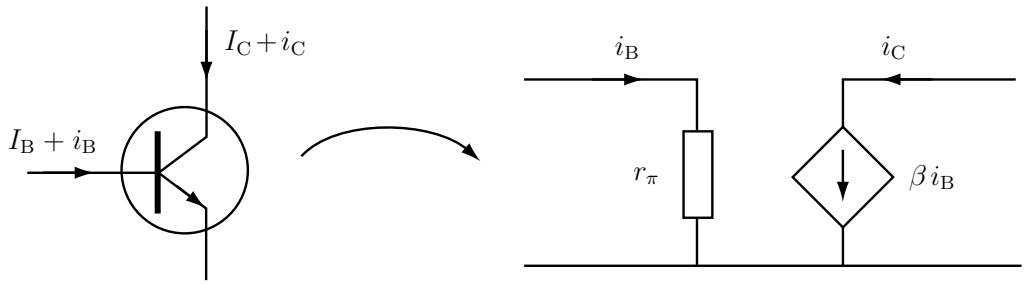

Figure 4: A small signal scheme modeling a transistor. The total base current is $I_B + i_B$, where the bias current I_B is much larger than the signal current i_B. The total collector current $I_C + i_C$ is similarly decomposed. The amplification factor β and the resistance r_π in the scheme for the signal currents i_B and i_C depend on I_B.

calculate the solution. In this section, we briefly describe two important techniques, the finite difference method, and the finite element method. The key word here is "finite", which reflects the fact that it is often easier to use a local description of the phenomena, consistent with our wish that the constitutive relation should only depend on its neighborhood.

The numerical methods described here are essentially linear, and the nonlinearity can be handled by linearizing the equations locally, although we give no details of this.

4.2.1 Finite differences

The finite difference methods is based upon the idea of approximating the derivatives in a given differential equation by finite differences, *i.e.*, $\partial_t \boldsymbol{E} \approx (\boldsymbol{E}(t + \Delta t) - \boldsymbol{E}(t))/\Delta t$, with Δt small and fixed. This is a natural and successful approach, and is one of the dominating numerical methods for calculating transient fields. In computational electromagnetics, it is known as the FDTD method, where FDTD spells out as Finite Differences in the Time Domain. For constitutive relations with no couplings between electric and magnetic fields, the Yee staggered grid algorithm, first presented in [70], is the dominant one, due to its slightly lower memory demand than standard discretizations and the relatively easy implementation of boundary conditions.

The finite difference method often uses an equidistant grid, which permits easy implementation of the code. However, sometimes it is desirable to use an automatic mesh generator, that can adapt the grid to a complicated geometry. Whether defined on an equidistant or an irregular grid, it is often the termination of the grid that is the most problematic one, since we cannot define all spatial derivatives on the boundary. Therefore, the dominating part of the actual code in a finite difference algorithm is often concerned with how to terminate the grid in order not to generate any nonphysical solutions. Some general references on finite difference methods are [21, 23, 59, 61].

4.2.2 Finite elements

The method of finite elements is originally based on a variational approach to the problem, *i.e.*, it is based on minimizing a given functional [12]. One means of formulating the method is by projection: the sought function is expanded in a set of basis functions, and the equations which it satisfies are then projected on a set of test functions. This results in a system of algebraic equations, which can be solved for the coefficients of the basis functions, *i.e.*, the function itself. When using basis and test functions with compact support, we obtain the finite element method. There are several books treating the finite element method in electromagnetics [35, 56, 65].

4.3 Asymptotic methods

Sometimes we are only interested in the dominating contribution to a given problem. If we can identify very small and/or very large parameters, it is often possible to do an asymptotic analysis, where we essentially make a power series expansion in the large/small parameters. Denoting the small parameter by δ, this means we are looking for a solution of the form $\boldsymbol{E} = \boldsymbol{E}_0 + \delta\boldsymbol{E}_1 + \delta^2\boldsymbol{E}_2 + \cdots$. Sometimes it is easy to find the first few terms in this series, which then should approximate the solution well if δ is small.

4.3.1 Born approximation for weak nonlinearities

The Born approximation is a general method to treat problems with small perturbations. The idea is to treat the perturbations as sources to the unperturbed problem, which in the nonlinear case is a kind of linearization. The method is best understood by an example. The propagation of electromagnetic waves in a non-magnetic material, where $\boldsymbol{B} = \mu_0\boldsymbol{H}$, is modeled by the equation

$$\nabla^2\boldsymbol{E} - c_0^{-2}\partial_t^2\boldsymbol{E} = \mu_0\partial_t^2\mathcal{P}\boldsymbol{E}, \tag{4.1}$$

where ∇^2 denotes the Laplace operator $\sum_{i=1}^{3}\partial_{x_i}^2$. If we separate the functional $\mathcal{P}$ in a linear and a nonlinear part, *i.e.*, $\mathcal{P} = \mathcal{P}_{\mathrm{L}} + \mathcal{P}_{\mathrm{NL}}$, this can be written

$$\nabla^2\boldsymbol{E} - c_0^{-2}\partial_t^2\left(1 + \epsilon_0^{-1}\mathcal{P}_{\mathrm{L}}\right)\boldsymbol{E} = \mu_0\partial_t^2\mathcal{P}_{\mathrm{NL}}\boldsymbol{E}. \tag{4.2}$$

We denote the left hand side with $\mathcal{L}\boldsymbol{E}$ and the right hand side with $\mathcal{S}\boldsymbol{E}$, where $\mathcal{L}$ is a linear differential operator. Assume there exist suitable methods to solve the equation $\mathcal{L}\boldsymbol{E} = \boldsymbol{F}$, where $\boldsymbol{F}$ is a given function of space and time, and that the nonlinear operator $\mathcal{S} = \mu_0\partial_t^2\mathcal{P}_{\mathrm{NL}}$ can be considered small. It is then reasonable to consider the sequence $\{\boldsymbol{E}_n\}_{n=0}^{\infty}$, where $\boldsymbol{E}_0$ solves the equation $\mathcal{L}\boldsymbol{E}_0 = \boldsymbol{0}$ with the relevant initial/boundary values corresponding to the excitation (incident field), and the remaining elements in the sequence are found from the iterative scheme

$$\mathcal{L}\boldsymbol{E}_n = \mathcal{S}\boldsymbol{E}_{n-1}, \quad n \geq 1, \tag{4.3}$$

where zero initial/boundary values are assumed, see Figure 5. This is the Born iterative procedure [53, p. 742], which is likely to give a good approximation for

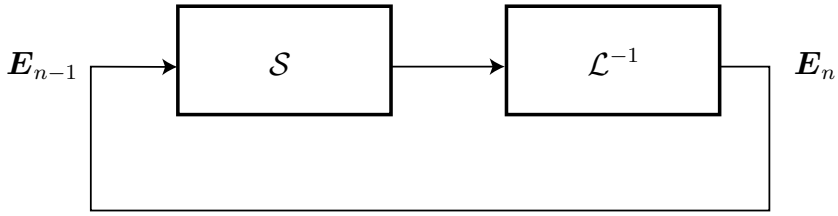

Figure 5: The Born iteration. The starting solution $\boldsymbol{E}_0$ is found from solving the linear equation $\mathcal{L}\boldsymbol{E}_0 = \boldsymbol{0}$ with the relevant initial/boundary values.

small nonlinearities or, equivalently, small field strengths. The convergence of this procedure is not treated in this thesis. Its usefulness depends very much on the algorithm used to solve the linear equation $\mathcal{L}\boldsymbol{E}_n = \mathcal{S}\boldsymbol{E}_{n-1}$, and in practice the iteration stops after one or two iterations.

4.3.2 Multiple scale analysis

A prominent feature of nonlinear differential equations is that there often occur interesting phenomena at different scales. Small nonlinear effects may be neglected at small propagation lengths or simulation times, but when we try to propagate a wave a long distance, the nonlinear effects accumulate and ultimately affects the appearence of the wave. A means of analyzing this difference is the method of multiple scales [4, 38]. In this method, we introduce an explicit microscopic scale and an explicit macroscopic scale, and consider the fields to depend separately on these variables. It is customary to identify a small parameter, which is the quotient between the microscopic scale and the macroscopic scale, and make a series expansion of the fields in this parameter. An example of a situation where a multiple scale analysis gives good results is found in Figure 6; the wavelength of the signal represents the microscopic scale, and the slowly increasing phase shift represents the macroscopic scale.

4.3.3 Vanishing viscosity regularization

Some nonlinear equations allow discontinuous solutions, which is problematic in numerical implementations. One way to deal with this problem, is the vanishing viscosity regularization. Ever since the exact solution of the viscous Burger's equation was discovered independently by Hopf [28] and Cole [11], this has been used as a means of obtaining microscopically smooth solutions, which appears as discontinuous solutions on a macroscopic scale. It is a singular perturbation technique, which basically consists in adding a small multiple of a derivative of higher order than the equation considered [38]. We typically write

$$\begin{cases} \nabla \times \boldsymbol{E} + \partial_t \boldsymbol{B} = \eta_0 \delta \nabla^2 \boldsymbol{H} \\ -\nabla \times \boldsymbol{H} + \partial_t \boldsymbol{D} + \boldsymbol{J} = \eta_0^{-1} \delta \nabla^2 \boldsymbol{E} \end{cases} \tag{4.4}$$

where the scalar parameter δ is small, has units of length and represents the microscopic scale. The idea is that the right hand side comes into play only when there

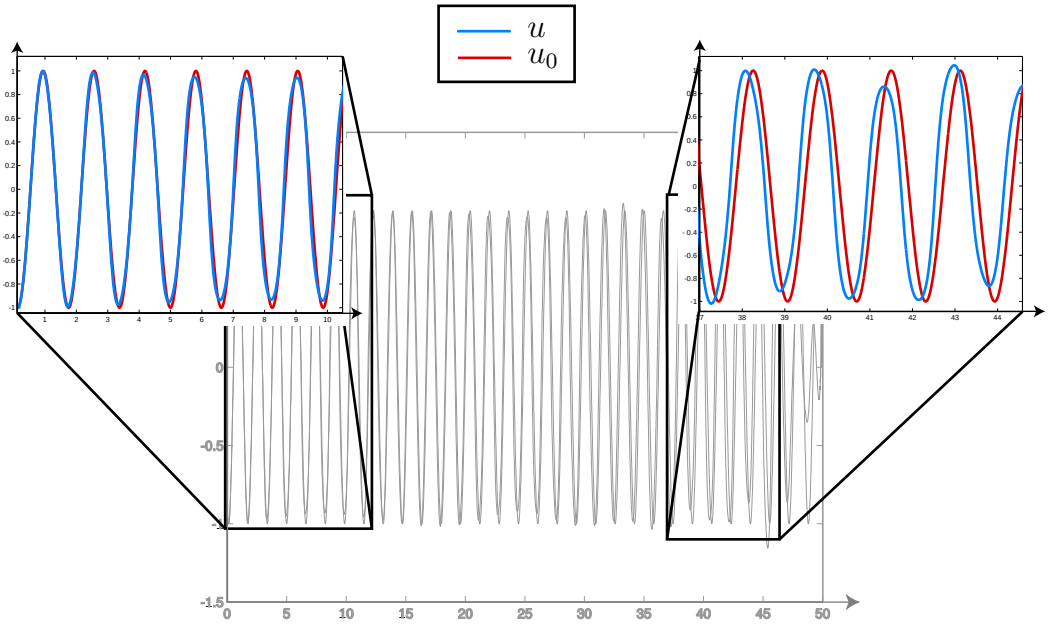

Figure 6: An example of cumulative effects of small nonlinearities. A sinusoidal signal is propagated through a waveguide filled with a weakly nonlinear material, see Figure 7 for the geometry of the problem. The plots show the nonlinear solution u and the linearized solution u_0 as functions of x, which is the coordinate along the waveguide. For small x the solutions correspond well, but for large x they differ by a phase shift. The dominant effect of the small nonlinearity in this case is a small phase shift, which becomes important after long propagation lengths. It can be shown that the phase shift grows approximately linearly with x.

are large spatial gradients of the fields, and when this happens, we should have a parabolic equation (such as the heat equation, $u_t = u_{xx}$), which in the nonlinear case almost always has smooth solutions [62, pp. 327–332]. Thus, it seems likely that the vanishing viscosity helps smoothing out shocks, which is also the case in practice. It is very difficult to verify the method mathematically for systems of equations, but there is strong empirical evidence for its validity since it is the basis of some successful finite difference schemes, such as the Lax-Friedrichs scheme in one spatial dimension [21, p. 181].

4.4 Canonical problems

Much experience and physical intuition is obtained by simple examples. If we want to study the effects of nonlinearities, it is often advantageous to study homogeneous materials, and isolate the contributions which originate directly from the nonlinearity. In this subsection, we present three canonical equations, which have proved to give valuable insights to the wave propagation. The equations should be supplemented with initial/boundary values to make sense, but they are left out for simplicity in this presentation. In this subsection, we have adopted a notation which assumes that all variables are dimensionless, in order to make the mathemat-

ical structure clear. Whitham's book [69] is a wonderful source for further studies of similar examples.

4.4.1 Quasi-linear conservation laws

Equations describing physical phenomena are often in the form of conservation or balance laws. A typical conservation law is the balance of momentum, where the time derivative of the momentum is balanced by the divergence of the stress tensor. The mathematical construction relevant to this kind of models is a quasi-linear system of balance laws in n spatial variables, which we write

$$\partial_t \boldsymbol{u} + \sum_{i=1}^{n} \partial_{x_i} \boldsymbol{f}_i(\boldsymbol{x}, t, \boldsymbol{u}) = \boldsymbol{g}(\boldsymbol{x}, t, \boldsymbol{u}). \tag{4.5}$$

When $\boldsymbol{g} = \boldsymbol{0}$ it is customary to use the term conservation law instead of balance law. Quasi-linear means that the equation is linear in its highest order derivatives; in this case, we deal only with first-order derivatives, which means the functions $\boldsymbol{f}$ and $\boldsymbol{g}$ may only depend on $\boldsymbol{u}$, not the derivatives of $\boldsymbol{u}$. Note that the Maxwell equations can be put in this form,

$$\partial_t \begin{pmatrix} \boldsymbol{D} \\ \boldsymbol{B} \end{pmatrix} + \sum_{i=1}^{3} \partial_{x_i} \begin{pmatrix} -\hat{\boldsymbol{x}}_i \times \boldsymbol{H} \\ \hat{\boldsymbol{x}}_i \times \boldsymbol{E} \end{pmatrix} = \begin{pmatrix} -\boldsymbol{J} \\ \boldsymbol{0} \end{pmatrix}, \tag{4.6}$$

although the situation is complicated by the form of the constitutive relations. One interesting point on quasi-linear conservation laws is that they exhibit shock solutions, which is further explored in papers IV and V of this thesis. A review of the present mathematical understanding of systems of conservation laws is given in [54].

4.4.2 Nonlinear Klein-Gordon equation

When the wave propagation is confined geometrically to a cylindrical structure such as in a waveguide, the typical equation governing the propagation is the Klein-Gordon equation. The geometry is shown in Figure 7, and the wave propagation through the waveguide is described by the scalar equation

$$-\partial_x^2 u + \partial_t^2 u + u + u^3 = 0. \tag{4.7}$$

This is one of the simplest wave equations which exhibits both nonlinearity and dispersion. A discussion of the classical mathematical questions of existence and uniqueness is given in [30, pp. 145–185], and a multiple scale analysis is performed in [38, pp. 522–531]. See also Figure 6 for a numerical demonstration of the nonlinearity in this equation for small u.

The propagation of electromagnetic waves in a waveguide is treated in Paper III, where a slightly different version of the nonlinear Klein-Gordon equation is derived.

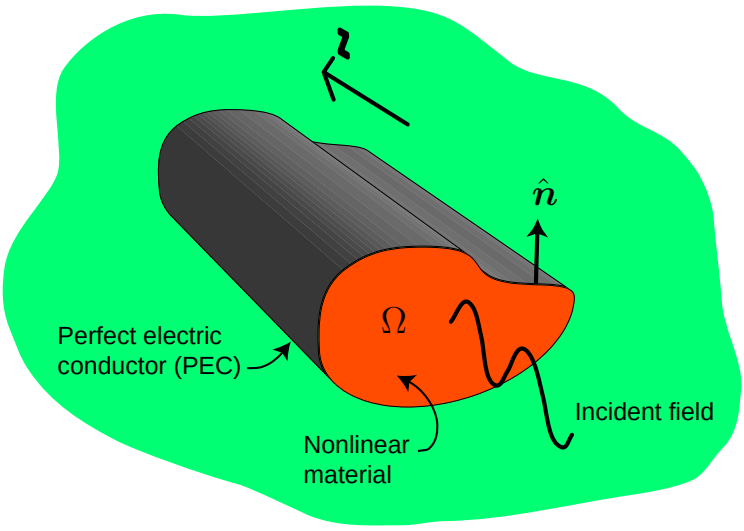

Figure 7: The geometry of a waveguide. The idea is to confine the propagation of electromagnetic waves to the inside of a tube with metallic walls.

4.4.3 Nonlinear Schrödinger equation

The nonlinear Schrödinger equation is the archetype model for nonlinear waves with a carrier frequency, and is typically used to describe the propagation of solitons. It arises in a number of physical situations, and is typically written [60]

$$\mathrm{i}\partial_\tau \psi + \nabla^2 \psi + g|\psi|^2\psi = 0, \tag{4.8}$$

where ψ is the slowly varying envelope, and τ is the time relative to the wave front. The parameter g may be positive or negative, corresponding to an attracting or a repulsive nonlinearity, respectively. The nonlinear Schrödinger equation can be viewed as a dispersion relation, which must be satisfied in order to prevent the solutions on the carrier frequency from blowing up. It is suitable for materials with weak nonlinearities, and nonresonant carrier frequencies. A recent review of the nonlinear Schrödinger equation is given in [60], and the first experimental evidence of solitons was given in [50].

4.5 The nonlinear transfer functional

We define the transfer functional $\mathcal{H}$ as the operator which gives the output signal $\boldsymbol{E}_{\text{out}}$ when operating on the input signal $\boldsymbol{E}_{\text{in}}$, *i.e.*, $\boldsymbol{E}_{\text{out}} = \mathcal{H}\boldsymbol{E}_{\text{in}}$. In this section we assume the fields $\boldsymbol{E}_{\text{in}}$ and $\boldsymbol{E}_{\text{out}}$ depend only on time, *i.e.*, we have fixed the measurement locations. If the nonlinearity is weak, this functional can be expanded in a Volterra series as in Section 3.2, which makes it possible to generalize the concept of a transfer function from the linear analysis [46]. However, it is necessary to define a separate transfer function for each order of interaction, such that we can expand the output signal as $\boldsymbol{E}_{\text{out}} = \boldsymbol{E}^{(1)}_{\text{out}} + \boldsymbol{E}^{(2)}_{\text{out}} + \boldsymbol{E}^{(3)}_{\text{out}} + \cdots$, where the i:th

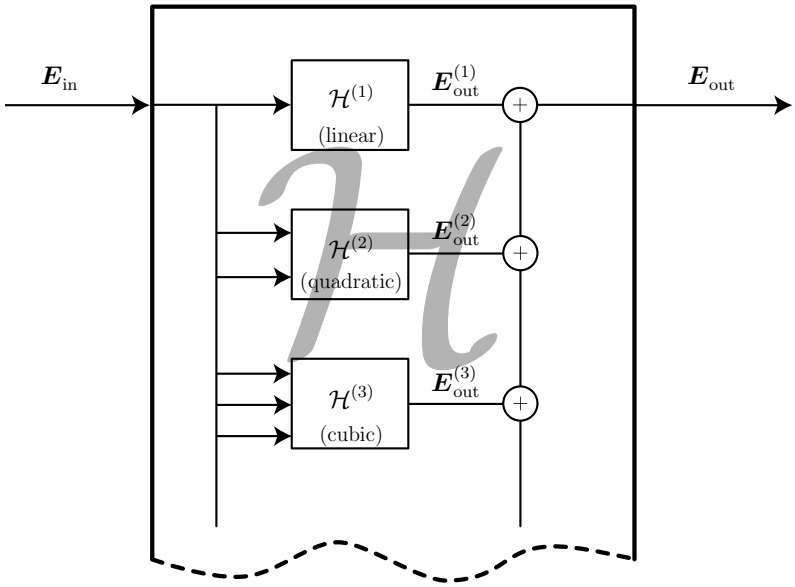

Figure 8: The Volterra series expansion of the nonlinear transfer functional as a "black box". The output signal $\boldsymbol{E}_{\text{out}}$ is related to the input signal $\boldsymbol{E}_{\text{in}}$ through the nonlinear transfer functional $\mathcal{H}$ as $\boldsymbol{E}_{\text{out}} = \mathcal{H}\boldsymbol{E}_{\text{in}} = \boldsymbol{E}^{(1)}_{\text{out}} + \boldsymbol{E}^{(2)}_{\text{out}} + \cdots$. The transfer functional may for instance represent the propagation of a wave through a medium or the reflection operator from a scattering experiment.

component of the n:th term is

$$E^{(n)}_{\text{out},i}(t) = \int \cdots \int H^{(n)}_{i,p_1\ldots p_n}(t-t_1,\ldots,t-t_n) E_{\text{in},p_1}(t_1)\cdots E_{\text{in},p_n}(t_n)\,\mathrm{d}t_1\cdots\mathrm{d}t_n, \quad (4.9)$$

and summation is assumed over the indices $p_1,\ldots,p_n$. This can be seen as a decomposition of the transfer functional $\mathcal{H}$, see Figure 8. The functions $H^{(n)}$ contain information of the experiment we are conducting, and may typically be used to obtain material parameters. Since the relation between $\boldsymbol{E}_{\text{out}}$ and $\boldsymbol{E}_{\text{in}}$ is linear in the functions $H^{(n)}$, the determination of these functions from knowledge of $\boldsymbol{E}_{\text{in}}$ and $\boldsymbol{E}_{\text{out}}$ is a linear deconvolution problem. It is possible to identify the Fourier transformed functions $\hat{H}^{(n)}(\omega_1,\cdots,\omega_n)$ from harmonic inputs $\boldsymbol{E}_{\text{in}}$ [46], and it turns out that usually all higher order functions can be expressed in the linear function $\hat{H}^{(1)}$, consistent with Miller's rule presented in Section 3.2. The deconvolution is usually very computationally intensive.

5 Applications

There are many applications in which nonlinear electromagnetic effects are important. Among these we mention basic semiconductor devices such as diodes and transistors [46], magnetic recording, the Kerr and Pockels cells used in nonlinear

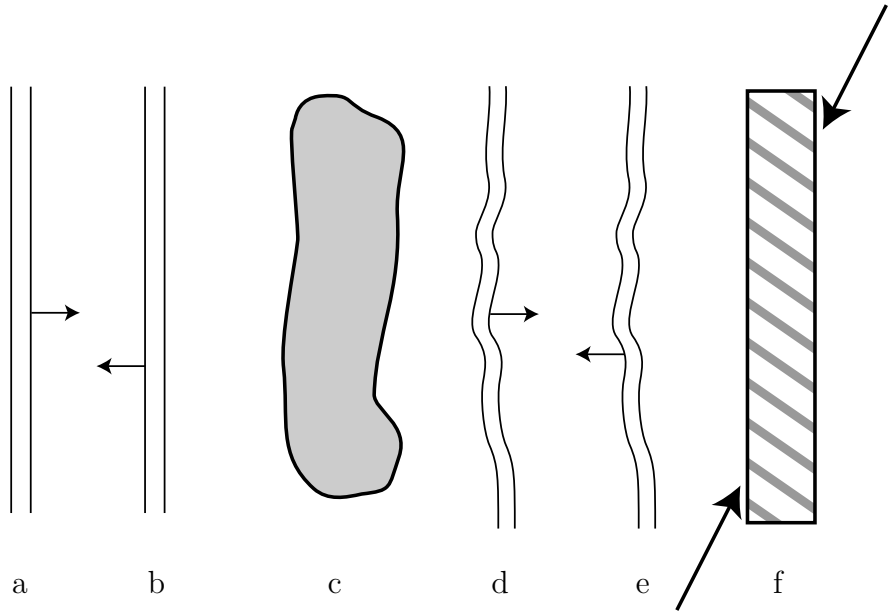

Figure 9: The phase conjugate mirror. An incident wave (a) encounters an obstacle (c), whereupon the wavefront is distorted (d). Two strong, counterpropagating beams, create a standing wave pattern in the nonlinear material (f), which is experienced as a grating by the incident weak beam. The resulting reflected wave (e) has exactly the same wave front as the incident wave, but is propagating in the oppposite direction. After passing through the distorting medium, the wave front is restored.

optics [7, 53], and electromechanical devices such as transducers and piezoelectric crystals. Another interesting application is a system for tracking down skiers buried in avalanches; by using a passive nonlinear reflector fastened on the skier, the frequency of a scanning signal is doubled, which allows for easy detection of the skier (if the rescue crew is quick, the skier may even be alive!). In this section, we give a brief presentation of three other applications: the phase conjugate mirror, shock generation, and solitons.

5.1 Phase conjugate mirror

An area of recent interest in acoustics is time-reversal mirrors, see [17–19] and [36, pp. 133–171]. In nonlinear optics, the corresponding effect is known as phase conjugate mirrors. The effect was first achieved experimentally in 1977 [6], and is treated in most textbooks on nonlinear optics, see for instance [7, pp. 241–257] and [53, pp. 758–761]. The idea is to use two strong, counterpropagating laser beams, which create a standing wave pattern. In a nonlinear material, where the refractive index depends on the electric field intensity, this induces a grating with a period of roughly half a wavelength. This grating causes an incident, weak beam to be reflected as usual, only that it is traveling "backwards in time", see Figure 9.

This effect can be used to cancel dispersion effects in optical fibers, by introducing

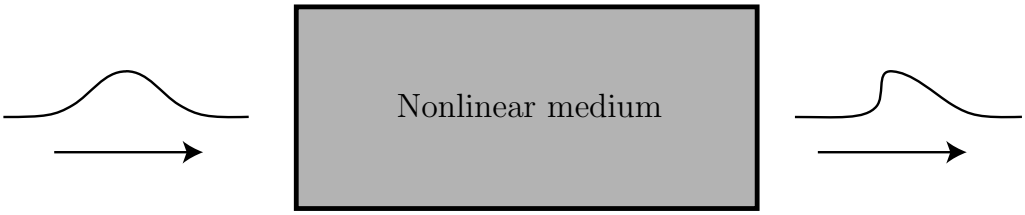

Figure 10: The profile of a pulse changes as it propagates through a nonlinear medium. This can be used to create strong pulses with short rise-time.

a phase conjugator half-way in the fiber; the phase conjugated (or equivalently: the time reversed) wave will then be perfectly restored at the other end if the optical fiber has the same properties on both sides of the conjugator. However, the situation is complicated by losses in the fiber, which often makes it more important to regenerate the signal altogether at given points along the fiber.

5.2 Pulse sharpening and shock generation

It is difficult to generate fast rise-time pulses with high voltage. For instance, it is possible to use spark gaps to generate strong pulses with fast rise-time, but the repetition rate is often relatively limited and the electrodes tend to erode quickly [8]. One way around this problem, is to use a pulse with a relatively slow rise-time, and send it through a nonlinear medium. Since different amplitudes travel with different speeds, the pulse steepens as it propagates through the medium, until it reaches a rise-time roughly given by the lowest resonance frequency of the material, see Figure 10.

The steepening of a pulse as it propagates through a nonlinear medium is mathematically described as the formation of a shock wave, *i.e.*, a discontinuous wave. Recently, a few papers on experiments concerning electromagnetic shock waves have been published [8, 10, 13], and in Paper IV we discuss the nature of an electromagnetic shock wave in detail.

5.3 Solitons

The electromagnetic shock, an application of which was described in the previous subsection, is a manifestation of the steepening effect of a nonlinear medium. Another effect which is important for the propagation of electromagnetic waves is dispersion, *i.e.*, the property that different frequencies travel with different speeds. This often results in a broadening of the pulse, and it is clear that there must exist an interesting interplay between the nonlinear steepening effects and the dispersive broadening. For instance, when the two effects exactly balance each other, the shape of the pulse should be unchanged as it propagates. When this occurs, the pulse is called a soliton.

The fact that solitons travel without changing their shape, makes them attractive to use in communications. Indeed, much of the research on solitons is focused on the possibilities of using them in communications with optical fibers [1, 25, 26, 50].

References

[1] G. P. Agrawal. *Nonlinear fiber optics*. Academic Press, San Diego, 1995.

[2] H. Alfvén and C.-G. Fälthammar. *Cosmical Electrodynamics*. Oxford University Press, New York, second edition, 1963.

[3] G. Bekefi and S. C. Brown. Plasma physics: Waves and radiation processes in plasma. *Am. J. Phys*, **34**, 1001, 1966.

[4] C. M. Bender and S. A. Orszag. *Advanced Mathematical Methods for Scientists and Engineers*. McGraw-Hill, New York, 1978.

[5] N. Bloembergen. *Nonlinear Optics*. W. A. Benjamin, Inc., Reading, Massachusetts, 1977.

[6] D. M. Bloom and G. C. Bjorklund. Conjugate wave-front generation and image reconstruction by four-wave mixing. *Appl. Phys. Lett.*, **31**(9), 592–594, November 1977.

[7] R. W. Boyd. *Nonlinear Optics*. Academic Press, San Diego, 1992.

[8] G. Branch and P. W. Smith. Fast-rise-time electromagnetic shock waves in nonlinear, ceramic dielectrics. *J. Phys. D: Applied Phys.*, **29**(8), 2170–2178, August 1996.

[9] M. Brokate and J. Sprekels. *Hysteresis and Phase Transitions*. Springer-Verlag, Berlin, 1996.

[10] C. Brooker, N. Altieri, G. Eastwood, R. Hoad, and J. E. Dolan. 90kV 1800A 85ps rise time electromagnetic shock line for UWB applications. *Electronics Letters*, **35**(25), 2210–2212, December 1999.

[11] J. D. Cole. On a quasilinear parabolic equation occurring in aerodynamics. *Quart. Appl. Math.*, **9**, 225–236, 1951.

[12] R. L. Courant. Variational methods for the solution of problems of equilibrium and vibration. *Bulletin of the American Mathematical Society*, **49**, 1–23, 1943.

[13] J. E. Dolan. Simulation of shock waves in ferrite-loaded coaxial transmission lines with axial bias. *J. Phys. D: Applied Phys.*, **32**(15), 1826–1831, August 1999.

[14] R. S. Elliott. *Electromagnetics: History, Theory, and Applications*. IEEE Press, New York, 1993.

[15] A. C. Eringen and G. A. Maugin. *Electrodynamics of Continua I*. Springer-Verlag, New York, 1990.

[16] A. C. Eringen and G. A. Maugin. *Electrodynamics of Continua II*. Springer-Verlag, New York, 1990.

[17] M. Fink. Time-reversed acoustics. *Scientific American*, **281**(5), 91–97, November 1999.

[18] M. Fink. Time-reversal mirrors. *J. Phys. D: Applied Phys.*, **26**, 1333–1350, 1993.

[19] M. Fink and C. Prada. Acoustic time-reversal mirrors. *Inverse Problems*, **17**(1), R1–R38, February 2001.

[20] J. Fridén, G. Kristensson, and A. Sihvola. Effect of dissipation on the constitutive relations of bi-anisotropic media–the optical response. *Electromagnetics*, **17**(3), 251–267, 1997.

[21] E. Godlewski and P.-A. Raviart. *Numerical Approximation of Hyperbolic Systems of Conservation Laws*. Springer-Verlag, Berlin, 1996.

[22] C. L. Grabbe. Plasma waves and instabilities. *Am. J. Phys*, **52**, 970, 1984.

[23] B. Gustafsson, H.-O. Kreiss, and J. Oliger. *Time Dependent Problems and Difference Methods*. John Wiley & Sons, New York, 1995.

[24] M. Gustafsson. *Wave Splitting in Direct and Inverse Scattering Problems*. PhD thesis, Lund Institute of Technology, Department of Electromagnetic Theory, P.O. Box 118, S-211 00 Lund, Sweden, 2000. `http://www.es.lth.se/home/mats`.

[25] A. Hasegawa. *Optical Solitons in Fibers*. Springer-Verlag, Berlin Heidelberg, 1990.

[26] A. Hasegawa and Y. Kodama. *Solitons in Optical Communications*. Clarendon Press, Oxford, 1995.

[27] O. Heaviside. Electromagnetic induction and its propagation, part 1. *Electrician*, pages 178–180, January 1885.

[28] E. Hopf. The partial differential equation $u_t + uu_x = \mu u_{xx}$. *Comm. Pure Appl. Math.*, **3**, 201–230, 1950.

[29] L. Hörmander. *The Analysis of Linear Partial Differential Operators I*. Grundlehren der mathematischen Wissenschaften 256. Springer-Verlag, Berlin Heidelberg, 1983.

[30] L. Hörmander. *Lectures on Nonlinear Hyperbolic Differential Equations*. Number 26 in Mathémathiques & Applications. Springer-Verlag, Berlin, 1997.

[31] K. Huang. *Statistical Mechanics*. John Wiley & Sons, New York, second edition, 1987.

[32] J. D. Jackson. *Classical Electrodynamics*. John Wiley & Sons, New York, third edition, 1999.

[33] A. Jeffrey. *Magnetohydrodynamics*. Oliver and Boyd, Ediburgh, 1966.

[34] D. Jiles. *Introduction to Magnetism and Magnetic Materials*. Chapman & Hall, New York, 1998.

[35] J. Jin. *The Finite Element Method in Electromagnetics*. John Wiley & Sons, New York, 1993.

[36] B. L. G. Jonsson. *Directional Decomposition in Anisotropic Heterogeneous Media for Acoustic and Electromagnetic Fields*. PhD thesis, Royal Institute of Technology, Stockholm, Sweden, 2001.

[37] A. Karlsson and G. Kristensson. Constitutive relations, dissipation and reciprocity for the Maxwell equations in the time domain. *J. Electro. Waves Applic.*, **6**(5/6), 537–551, 1992.

[38] J. Kevorkian and J. D. Cole. *Multiple Scale and Singular Perturbation Methods*. Springer-Verlag, Berlin, 1996.

[39] C. Kittel. *Introduction to Solid State Physics*. John Wiley & Sons, New York, 6 edition, 1986.

[40] J. A. Kong. *Electromagnetic Wave Theory*. John Wiley & Sons, New York, 1986.

[41] H.-O. Kreiss and J. Lorenz. *Initial-Boundary Value Problems and the Navier-Stokes Equations*. Academic Press, San Diego, 1989.

[42] G. Kristensson and D. J. N. Wall. Direct and inverse scattering for transient electromagnetic waves in nonlinear media. *Inverse Problems*, **14**, 113–137, 1998.

[43] L. D. Landau and E. M. Lifshitz. On the theory of the dispersion of magnetic permeability in ferromagnetic bodies. *Physik. Z. Sowjetunion*, **8**, 153–169, 1935. Reprinted by Gordon and Breach, Science Publishers, "Collected Papers of L. D. Landau", D. Ter Haar, editor, 1965, pp. 101–114.

[44] L. D. Landau and E. M. Lifshitz. *Statistical Physics, Part 2*. Butterworth-Heinemann, Linacre House, Jordan Hill, Oxford, 1980.

[45] L. D. Landau, E. M. Lifshitz, and L. P. Pitaevskiĭ. *Electrodynamics of Continuous Media*. Pergamon, Oxford, second edition, 1984.

[46] S. A. Maas. *Nonlinear Microwave Circuits*. IEEE Press, New York, 1988.

[47] J. C. Maxwell. *A Treatise on Electricity and Magnetism*, volume 1. Dover Publications, New York, 1954.

[48] J. C. Maxwell. *A Treatise on Electricity and Magnetism*, volume 2. Dover Publications, New York, 1954.

[49] R. C. Miller. *Appl. Phys. Lett.*, **5**, 17, 1964.

[50] L. F. Mollenauer, R. H. Stolen, and J. P. Gordon. Experimental observation of picosecond pulse narrowing and solitons in optical fibers. *Phys. Rev. Lett.*, **45**(13), 1095–1098, September 1980.

[51] M. Norgren. Optimization approaches to frequency-domain inverse problems for Kerr-like and non-Kerr-like nonlinear media. *Mathematics and Computers in Simulation*, **50**(5–6), 533–575, December 1998.

[52] Plato. *Ion*. 380 B.C.

[53] B. E. A. Saleh and M. C. Teich. *Fundamentals of Photonics*. John Wiley & Sons, New York, 1991.

[54] D. Serre. Systems of conservation laws: A challenge for the XXIst century. In B. Engquist and W. Schmid, editors, *Mathematics Unlimited — 2001 and Beyond*, pages 1061–1080. Springer-Verlag, Berlin, 2001.

[55] Y. R. Shen. *Principles of Nonlinear Optics*. John Wiley & Sons, New York, 1984.

[56] P. P. Silvester and G. Pelosi. *Finite Elements for Wave Electromagnetics: Methods and Techniques*. IEEE Press, New York, 1994.

[57] D. Sjöberg. *Direct and Inverse Scattering of Electromagnetic Waves in Nonlinear Media*. Licentiate thesis, Lund Institute of Technoloy, Department of Electromagnetic Theory, Lund University, P.O. Box 118, S-221 00 Lund, Sweden, 1999. LUTEDX/(TEAT-1012)/1–25/(1999).

[58] J. A. Stratton. *Electromagnetic Theory*. McGraw-Hill, New York, 1941.

[59] J. C. Strikwerda. *Finite Difference Schemes and Partial Differential Equations*. Chapman & Hall, New York, 1989.

[60] C. Sulem and P.-L. Sulem. *The Nonlinear Schrödinger Equation: Self-Focusing and Wave Collapse*. Springer-Verlag, Berlin, 1999.

[61] A. Taflove. *Computational electrodynamics: The Finite-Difference Time-Domain Method*. Artech House, Boston, London, 1995.

[62] M. Taylor. *Partial Differential Equations III: Nonlinear Equations*. Springer-Verlag, New York, 1996.

[63] V. Tikhonenko, J. Christou, and B. Luther-Davies. Three-dimensional bright spatial soliton collision and fusion in a saturable nonlinear medium. *Phys. Rev. Lett.*, **76**, 2698–2701, 1996.

[64] A. Visintin. *Differential Models of Hysteresis*. Springer-Verlag, Berlin, 1994.

[65] J. L. Volakis, A. Chatterjee, and L. C. Kempel. *Finite Element Method for Electromagnetics*. IEEE Press, New York, 1998.

[66] V. Volterra. *Theory of functional and of integral and integro-differential equations*. Dover Publications, New York, 1959.

[67] E. Weinan. Selected problems in materials science. In B. Engquist and W. Schmid, editors, *Mathematics Unlimited — 2001 and Beyond*, pages 407–432. Springer-Verlag, Berlin, 2001.

[68] P. Weiss. L'hypothèse du champ moléculaire et la propriété ferromagnétique. *J. Physique*, **6**, 661–690, 1907.

[69] G. B. Whitham. *Linear and nonlinear waves*. John Wiley & Sons, New York, 1974.

[70] K. S. Yee. Numerical solution of initial boundary value problems involving Maxwell's equations in isotropic media. *IEEE Trans. Antennas Propagat.*, **14**, 302–307, March 1966.

Reconstruction of nonlinear material properties for homogeneous, isotropic slabs using electromagnetic waves

Paper I

Daniel Sjöberg

Based on: D. Sjöberg. Reconstruction of nonlinear material properties for homogeneous, isotropic slabs using electromagnetic waves. *Inverse Problems*, **15** (1999), 431–444.

Abstract

This paper addresses the inverse problem of reconstructing a medium's instantaneous, nonlinear response to electromagnetic excitation. Using reflection and transmission data for an almost arbitrary incident field on a homogeneous slab, we are able to obtain the nonlinear constitutive relations for both electric and magnetic fields, with virtually no assumptions made on the specific form of the relations. It is shown that for a nonmagnetic material, reflection data suffices to obtain the electrical nonlinear response. We also show that the algorithms are well posed. Numerical examples illustrate the analysis presented in this paper.

1 Introduction

There has been an increased interest in nonlinear electromagnetic materials recently, much due to the progresses in nonlinear optics. This is especially so for the nonlinear effects in optical fibers, *i.e.*, the experimental verification of soliton solutions [13, 14, 21], and the use of different field-dependent scattering mechanisms for amplification of a propagating signal [1]. Some chaotic effects have also been studied [10].

The research in this field is largely conducted in the frequency domain, where the nonlinearities manifest in the generation of multiple frequencies. In this paper, we study nonlinear effects in the time domain, where the nonlinearities rather cause the steepening of a propagating pulse. This steepening may ultimately turn into a shock solution, where the pulse becomes discontinuous after a finite propagation time, although we will endeavour to avoid shock solutions in this paper.

We study a material which has an instantaneous, nonlinear response, *i.e.*, we do not consider memory effects of any kind. We further assume the material to be passive, isotropic and homogeneous, and solve the problem of reconstructing the constitutive relations. Then we are able to reconstruct the nonlinear relation between $\boldsymbol{E}$ and $\boldsymbol{D}$ as well as between $\boldsymbol{H}$ and $\boldsymbol{B}$ with reflection and transmission data from a finite slab for an (almost) arbitrary input signal. Since no further assumptions have to be made regarding the specific form of the constitutive relations, the reconstruction is model independent.

Previous work in the field include the propagation of pulses in nonlinear slabs, where the paper by Kazakia and Venkataraman deserves special attention [18]. They have obtained an analytical solution for the propagation of a step function through a slab with some special constitutive functions. Reference [24] presents a method to solve the reflection and refraction problem at oblique incidence on a nonlinear half space. The wave propagation in more complicated nonlinear materials has appeared, *i.e.*, mixed nonlinearities [19], bi-anisotropic and bi-isotropic media [5], and nonlinearities in chiral media [2, 23].

Though much work has been done on the direct problem of wave propagation in nonlinear media, our solution of the inverse problem of reconstructing the material seems to be novel. It extends and improves the results in [20], where the inverse problem is solved for a nonmagnetic material, based on measurements inside the material.

In Section 2 we formulate the stratified Maxwell equations, introduce the constitutive relations for the studied materials and try to interprete the dynamics in terms known from the linear case. The main theory is contained in Section 3, where we formulate the necessary boundary conditions and state the solution to our inverse problems. Some numerical results are contained in Section 4.

2 Prerequisites

2.1 The Maxwell equations in one spatial dimension

In a source-free environment the Maxwell equations are

$$\begin{aligned} \nabla \times \boldsymbol{E}(\boldsymbol{r},t) + \partial_t \boldsymbol{B}(\boldsymbol{r},t) &= 0 \\ \nabla \times \boldsymbol{H}(\boldsymbol{r},t) - \partial_t \boldsymbol{D}(\boldsymbol{r},t) &= 0. \end{aligned}$$

Since we wish to study a homogeneous medium, it is sufficient to observe variations for only one direction. We thus assume that the fields depend on only one spatial variable, say z, in a Cartesian coordinate system (x, y, z). Then the curl operator can be written $\nabla \times = \hat{z} \times \mathbf{I}\partial_z = \mathbf{J}\partial_z$, where $\mathbf{J}$ denotes a rotation $\pi/2$ around the z-axis, and the Maxwell equations become

$$\begin{aligned} \mathbf{J} \cdot \partial_z \boldsymbol{E}(z,t) + \partial_t \boldsymbol{B}(z,t) &= 0 \\ \mathbf{J} \cdot \partial_z \boldsymbol{H}(z,t) - \partial_t \boldsymbol{D}(z,t) &= 0. \end{aligned}$$

We now assume the fields to be linearly polarized and the material to be isotropic, *i.e.*, the $\boldsymbol{D}$ and $\boldsymbol{B}$ fields are parallel to the $\boldsymbol{E}$ and $\boldsymbol{H}$ fields, respectively, which vary only in amplitude. This means we can write the Maxwell equations in a scalar form,

$$\begin{aligned} \partial_z E(z,t) + \partial_t B(z,t) &= 0 \\ \partial_z H(z,t) + \partial_t D(z,t) &= 0, \end{aligned}$$

where E and D denote an arbitrary transversal component, say x, of $\mathbf{J} \cdot \boldsymbol{E}$ and $\mathbf{J} \cdot \boldsymbol{D}$, respectively. H and B denote the corresponding component of $\boldsymbol{H}$ and $\boldsymbol{B}$, respectively. The geometry of the scattering situation studied in this paper is depicted in Figure 1.

2.2 Constitutive relations, passive materials

We consider the field strengths E and H to be the primary fields, and the flux densities D and B as effects of these. If we assume that the material responds instantaneous to excitation, we are studying the following situation:

$$\begin{aligned} D(z,t) &= \varepsilon_0 F_{\mathrm{e}}(E(z,t)) \\ B(z,t) &= \frac{1}{c_0} F_{\mathrm{m}}(\eta_0 H(z,t)), \end{aligned}$$

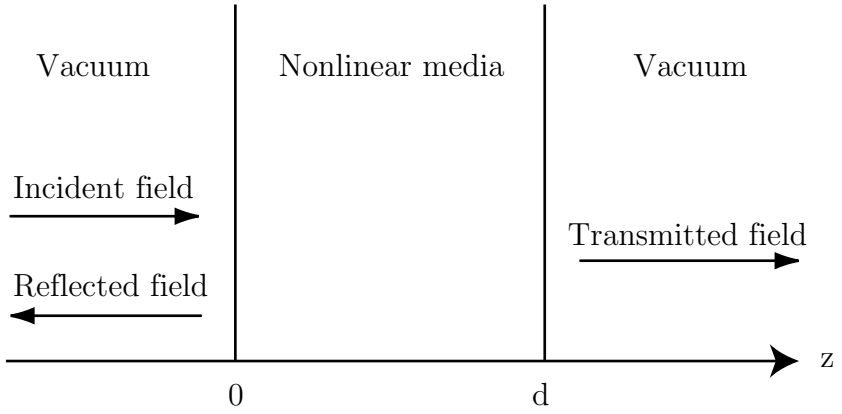

Figure 1: The scattering geometry studied in this paper.

where the constants $c_0 = 1/\sqrt{\varepsilon_0\mu_0}$ (speed of light in vacuum), ε_0 (permittivity of vacuum), and $\eta_0 = \sqrt{\mu_0/\varepsilon_0}$ (wave impedance of vacuum) are explicit for convenience. As usual, μ_0 denotes the permeability of vacuum. The functions $F_{\mathrm{e}}(E)$ and $F_{\mathrm{m}}(\eta_0 H)$ are continuously differentiable scalar functions of one variable, and generalize the linear optical responses, $F_{\mathrm{e}}^{\mathrm{lin}}(E) = \varepsilon_r E$ and $F_{\mathrm{m}}^{\mathrm{lin}}(\eta_0 H) = \mu_r \eta_0 H$. This kind of nonlinear constitutive response with similar dynamics is investigated in [20], [3, Chap. 2], and [11, Chap. 6]. In nonlinear optics similar relations are often used, although frequently in the context of the frequency domain [1, 4].

Some thermodynamic restrictions can be put on the constitutive relations [6], but these deal mainly with the symmetry of cross terms, *i.e.*, $\frac{\partial D}{\partial H}$ and $\frac{\partial B}{\partial E}$, which we do not take into account here. Reference [20] discusses the restrictions on the functions F_{e} and F_{m} in order to model passive media; though they call it dissipative.[1] The result is that for a passive, nonmagnetic material, $F_{\mathrm{e}}'(x) \geq a > 0$ is a *sufficient* condition. In this paper we generalize this to materials which also have $F_{\mathrm{m}}'(x) \geq b > 0$, and call these *positive passive*.

When demanding isotropy, we have the implication that a change of sign in the electric and magnetic fields leads to a change of sign in the electric and magnetic fluxes, *i.e.*, $(E, H) \to (-E, -H) \Rightarrow (D, B) \to (-D, -B)$. This is also true for crystals with an *inversion symmetry*, see [4, Chap. 1] for further discussions of material properties. This property implies that the constitutive functions should be odd functions of their argument, which will be important in the following.

Eliminating the D and B fields using the constitutive relations, the scalar Maxwell equations become

$$\begin{aligned} \partial_z E + \frac{1}{c_0} F_{\mathrm{m}}' \partial_t \eta_0 H &= 0 \\ \partial_z \eta_0 H + \frac{1}{c_0} F_{\mathrm{e}}' \partial_t E &= 0, \end{aligned} \tag{2.1}$$

where we have dropped the arguments of the functions F_{m}', F_{e}' for simplicity.

[1] With a passive material we mean that the electromagnetic energy produced in a region is nonpositive for all times, *i.e.*, the material is not active.

2.3 The dynamics as a symmetric system, physical interpretation

Though it is possible to directly introduce the well known Riemann invariants $\frac{1}{2}(\int_0^E \sqrt{F_{\mathrm{e}}'(x)}\,dx \pm \int_0^{\eta_0 H} \sqrt{F_{\mathrm{m}}'(x)}\,dx)$ as in [3, Sec. 2.4] or [11, Sec. 6.13], we wish to follow a different approach, where we try to interprete our variables and make comparisons to the linear case. We start by formulating the dynamics as

$$\begin{pmatrix} F_{\mathrm{e}}'\partial_t E \\ F_{\mathrm{m}}'\partial_t \eta_0 H \end{pmatrix} + c_0 \begin{pmatrix} 0 & 1 \\ 1 & 0 \end{pmatrix} \partial_z \begin{pmatrix} E \\ \eta_0 H \end{pmatrix} = 0,$$

which after division by the square root of the derivative of F_{e} and F_{m} leads to

$$\begin{pmatrix} \sqrt{F_{\mathrm{e}}'}\partial_t E \\ \sqrt{F_{\mathrm{m}}'}\partial_t \eta_0 H \end{pmatrix} + c_0 \begin{pmatrix} 0 & \frac{1}{\sqrt{F_{\mathrm{e}}'F_{\mathrm{m}}'}} \\ \frac{1}{\sqrt{F_{\mathrm{e}}'F_{\mathrm{m}}'}} & 0 \end{pmatrix} \begin{pmatrix} \sqrt{F_{\mathrm{e}}'}\partial_z E \\ \sqrt{F_{\mathrm{m}}'}\partial_z \eta_0 H \end{pmatrix} = 0.$$

We now introduce the functions,

$$g_{\mathrm{e}}(E) = \int_0^E \sqrt{F_{\mathrm{e}}'(x)}\,dx$$
$$g_{\mathrm{m}}(\eta_0 H) = \int_0^{\eta_0 H} \sqrt{F_{\mathrm{m}}'(x)}\,dx.$$

These functions can be thought of as the generalizations of the linear expressions $\sqrt{\varepsilon_r}E$ and $\sqrt{\mu_r}\eta_0 H$. The product of the derivative of the functions, $g_{\mathrm{e}}'g_{\mathrm{m}}'$, which appears in the wave speed below, can be viewed as the generalization of $\sqrt{\varepsilon_r\mu_r}$, the relative refractive index. Furthermore, for an isotropic, positive passive material, the g-functions are odd and monotone, since the integrands are always even and positive. With these new functions we can write the dynamics as

$$\partial_t \begin{pmatrix} g_{\mathrm{e}}(E) \\ g_{\mathrm{m}}(\eta_0 H) \end{pmatrix} + \frac{c_0}{g_{\mathrm{e}}'(E)g_{\mathrm{m}}'(\eta_0 H)} \begin{pmatrix} 0 & 1 \\ 1 & 0 \end{pmatrix} \partial_z \begin{pmatrix} g_{\mathrm{e}}(E) \\ g_{\mathrm{m}}(\eta_0 H) \end{pmatrix} = 0,$$

which in the new variables $u_1 = g_{\mathrm{e}}(E)$ and $u_2 = g_{\mathrm{m}}(\eta_0 H)$ is the symmetric system

$$\partial_t \begin{pmatrix} u_1 \\ u_2 \end{pmatrix} + c(u_1, u_2) \begin{pmatrix} 0 & 1 \\ 1 & 0 \end{pmatrix} \partial_z \begin{pmatrix} u_1 \\ u_2 \end{pmatrix} = 0, \tag{2.2}$$

where the wave speed c is

$$c(u_1, u_2) = \frac{c_0}{g_{\mathrm{e}}'(g_{\mathrm{e}}^{-1}(u_1))g_{\mathrm{m}}'(g_{\mathrm{m}}^{-1}(u_2))} = c_0 \left(\frac{d}{du_1} g_{\mathrm{e}}^{-1}(u_1)\right)\left(\frac{d}{du_2} g_{\mathrm{m}}^{-1}(u_2)\right). \tag{2.3}$$

This result generalizes the nonmagnetic case given in [20].

3 Methods to solve the inverse problem

In this section we demonstrate the methods used to solve the propagation problem and to resolve the boundary conditions. We also state our inverse problems of reconstructing the materials constitutive relations.

3.1 Wave splitting

The symmetric system (2.2) can be written as a system of one-dimensional wave equations with the wave splitting [8, 9, 20],

$$\begin{pmatrix} u_1 \\ u_2 \end{pmatrix} = \begin{pmatrix} 1 & 1 \\ 1 & -1 \end{pmatrix} \begin{pmatrix} u^+ \\ u^- \end{pmatrix} \quad \Leftrightarrow \quad \begin{pmatrix} u^+ \\ u^- \end{pmatrix} = \frac{1}{2} \begin{pmatrix} 1 & 1 \\ 1 & -1 \end{pmatrix} \begin{pmatrix} u_1 \\ u_2 \end{pmatrix}.$$

This change of variables is exactly the introduction of the Riemann invariants of the one-dimensional Maxwell equations, which was mentioned in Section 2.3. The dynamics (2.2) now becomes

$$\partial_t \begin{pmatrix} u^+ \\ u^- \end{pmatrix} + c(u^+ + u^-, u^+ - u^-) \begin{pmatrix} 1 & 0 \\ 0 & -1 \end{pmatrix} \partial_z \begin{pmatrix} u^+ \\ u^- \end{pmatrix} = 0, \tag{3.1}$$

with c defined by (2.3). This is a system of one-dimensional wave equations, which couple only through the wave speed c.

Analytical solutions for the wave propagation have been found in [18, 22] for some special constitutive relations. These solutions could be used to benchmark an algorithm for the wave propagation, though this is not performed in this work.

3.2 Propagation along characteristics

We can solve the propagation problem of the system (3.1) via the method of characteristics. A characteristic curve for this kind of differential equation is one on which the dependent variables are constant. We study the development of the variables $u^\pm(z,t)$ on the paths $(z,t) = (\zeta^\pm(\tau), \tau)$, where $\zeta^\pm(\tau) = \zeta_0 \pm \int_0^\tau c(\boldsymbol{u}')\, d\tau'$. The notation $c(\boldsymbol{u}')$ is short hand for $c(\boldsymbol{u}(\zeta^\pm(\tau'), \tau'))$, and $\boldsymbol{u} = (u^+, u^-)$. The variation of $u^\pm(z,t)$ along these curves are

$$\frac{d}{d\tau} u^\pm(\zeta^\pm(\tau), \tau) = \frac{\partial u^\pm}{\partial t} + \frac{d\zeta^\pm(\tau)}{d\tau} \frac{\partial u^\pm}{\partial z} = \frac{\partial u^\pm}{\partial t} \pm c(\boldsymbol{u}) \frac{\partial u^\pm}{\partial z} = 0,$$

since $u^\pm$ satisfy the differential equations $u_t \pm c u_z = 0$. Thus, we conclude that u^+ is constant along the characteristic path $\zeta(\tau) = \zeta_0 + \int_0^\tau c(\boldsymbol{u}')\, d\tau'$, and u^- is constant along the characteristic path $\zeta(\tau) = \zeta_0 - \int_0^\tau c(\boldsymbol{u}')\, d\tau'$.

This means we can find the values of the fields at a point (z,t) if we can trace the characteristics to some boundary where they are known. If only one of the waves is present, it is particularly simple; then the characteristics are straight lines, with a slope given by the boundary values [20].

We see that since the slope of the characteristics is governed by the boundary values, they may cross each other if we do not choose these boundary values carefully. When two characteristics cross each other, we have two possible solutions to the wave equation, and a *shock* occurs.

Theorem 3.1 in [20] concerns the extent of the shock-free region for one-way wave propagation in a semi-infinite media with given boundary conditions. This can be used to estimate how fast the incident field may vary in order not to create

a shock in the slab. The suitable boundary conditions are $u^+(z,0) = u^-(z,0) = 0$, $u^+(0,t) = h(t)$ and $u^-(0,t) = 0$, for which the theorem states that there can be no shock in the region $0 \leq z \leq d$ if $\sup\left\{-\frac{d}{dt}\frac{1}{c(u^+(0,t),u^-(0,t))}\right\} = \sup\left\{-\frac{d}{dt}\frac{1}{c(h(t),0)}\right\} \leq \frac{1}{d}$. Since $\frac{c_0}{c(u^+,0)} = g_{\rm e}'(g_{\rm e}^{-1}(u^+))g_{\rm m}'(g_{\rm m}^{-1}(u^+))$, the condition will be

$$\sup_t\left\{-(\frac{g_{\rm e}''}{g_{\rm e}'}g_{\rm m}' + g_{\rm e}'\frac{g_{\rm m}''}{g_{\rm m}'})h'\right\} \leq \frac{c_0}{d}. \tag{3.2}$$

We see, that we can always avoid shocks by using a signal with sufficiently small variation, *i.e.*, the derivative of $h(t)$ should be small compared to $1/(\frac{g_{\rm e}''}{g_{\rm e}'}g_{\rm m}' + g_{\rm e}'\frac{g_{\rm m}''}{g_{\rm m}'})$. Also, if this quantity and h' have the same sign, there is no risk of a shock. With positive second derivatives of $g_{\rm e,m}$, this means that shocks can only occur when $h' < 0$, *i.e.*, on the decreasing part of a signal.

3.3 Boundary conditions

Since we want to study propagation in a nonlinear slab, we must solve the problem of satisfying the boundary conditions. In this paper, we are studying a slab imbedded in vacuum. The generalization to more general linear materials follows from the method used.

The solution is based on the wave splitting, which allows us to determine in which direction the energy of the fields are travelling. In the surrounding vacuum, the splitting corresponds to the appropriate identification of incident, reflected and transmitted field. The boundary conditions we have to satisfy are the usual, *i.e.*, continuity of the tangential electric and magnetic field strengths. Since we are assuming normal incidence, this means continuity of the total fields E and H. Inside the slab, the electric and magnetic fields can be expressed as

$$E_{\rm slab} = g_{\rm e}^{-1}(u^+ + u^-)$$
$$\eta_0 H_{\rm slab} = g_{\rm m}^{-1}(u^+ - u^-).$$

In vacuum, the magnetic field strength is related to the electric field strength via $\eta_0 H^\pm = \pm E^\pm$, where the $\pm$ indicate right(left) propagating fields, *i.e.*, waves travelling towards higher(lower) z-values.

It is possible to define differential reflection and transmission coefficients relating infinitesimal changes in the incident field to infinitesimal changes in the reflected and transmitted field, respectively, *i.e.*, $dE^r = r\cdot dE^i$ and $dE^t = t\cdot dE^i$. These differential coefficients look exactly like the linear expressions, where the square roots of the permittivity and permeability $\sqrt{\varepsilon}$ and $\sqrt{\mu}$ are replaced by $\sqrt{F_{\rm e}'(E)}$ and $\sqrt{F_{\rm m}'(\eta_0 H)}$, respectively. This method is used in [18] to solve the boundary problem, but in this paper we will prefer to simply state the boundary conditions in explicit form and solve these numerically for the desired fields when implementing the forward problem.

3.3.1 The left boundary

In vacuum, $z < 0$, we have an incident field from the left E^i, and a reflected field into vacuum, E^r. In the slab two fields are present: a right propagating field u^+, and a left propagating field u^-. The continuity of electric and magnetic fields implies that

$$\begin{cases} E^i + E^r = g_{\mathrm{e}}^{-1}(u^+ + u^-) \\ E^i - E^r = g_{\mathrm{m}}^{-1}(u^+ - u^-) \end{cases} \quad \Leftrightarrow \quad \begin{cases} g_{\mathrm{e}}(E^i + E^r) = u^+ + u^- \\ g_{\mathrm{m}}(E^i - E^r) = u^+ - u^-. \end{cases} \tag{3.3}$$

This gives two, generally nonlinear, equations from which the desired fields u^+ and E^r can be determined:

$$\begin{cases} 2E^i = g_{\mathrm{e}}^{-1}(u^+ + u^-) + g_{\mathrm{m}}^{-1}(u^+ - u^-) \\ 2u^- = g_{\mathrm{e}}(E^i + E^r) - g_{\mathrm{m}}(E^i - E^r). \end{cases}$$

The incident field is given, but also the left propagating field u^- can be thought of as known. This is because this field can be traced back in time via a characteristic curve into the slab, and is therefore, from a computational point of view, known. Since the g-functions are monotone for a positive passive material, their inverses are too. This means that the right hand sides of the equations above, treated as functions of u^+ and E^r, are invertible, and we can find all desired fields numerically.

3.3.2 The right boundary

At the right boundary, $z = d$, we have just a transmitted field in the vacuum, but we still have both right and left propagating fields in the slab. Continuity of the fields now gives

$$\begin{cases} E^t = g_{\mathrm{e}}^{-1}(u^+ + u^-) \\ E^t = g_{\mathrm{m}}^{-1}(u^+ - u^-) \end{cases} \quad \Leftrightarrow \quad \begin{cases} g_{\mathrm{e}}(E^t) = u^+ + u^- \\ g_{\mathrm{m}}(E^t) = u^+ - u^-. \end{cases} \tag{3.4}$$

From this we get the following equations to determine u^- and E^t:

$$\begin{cases} 2u^+ = g_{\mathrm{e}}(E^t) + g_{\mathrm{m}}(E^t) \\ 2u^- = g_{\mathrm{e}}(E^t) - g_{\mathrm{m}}(E^t). \end{cases}$$

We can consider the field u^+ as known, since it can be traced back in time into the slab. The same conclusions as above about the solvability of these equations apply here.

3.4 Inverse problems

The objective of this paper is to find methods from which the material properties can be obtained from measurements outside the slab, *i.e.*, the incident, reflected, and transmitted fields.

3.4.1 Reflection

If we can ignore the left-propagating field at the left boundary, *i.e.*, $u^- = 0$, the boundary conditions (3.3) become

$$E^i + E^r = g_{\mathrm{e}}^{-1}(u^+)$$
$$E^i - E^r = g_{\mathrm{m}}^{-1}(u^+).$$

A situation where this approximation applies is a half space (see [20]) or a sufficiently thick slab, where the reflection from the right boundary, $z = d$, does not appear until after some time. This delay is at least one completed roundtrip for a wave propagating with maximal speed, $2d/(\sup_{\boldsymbol{u}} c(\boldsymbol{u}))$. For the models considered in this paper, the speed is maximal for infinitesimally small fields, *i.e.*, when the right propagating field at the left boundary, $u^+(0,t)$, is equal to zero until $t = 0$, there will be no left propagating field at the left boundary, $u^-(0,t)$, separated from zero until $t > 2d/c(0)$.

In the case of the approximation $u^- = 0$, the relation between the measurable quantities $E^i + E^r$ and $E^i - E^r$ becomes

$$g_{\mathrm{e}}(E^i + E^r) = g_{\mathrm{m}}(E^i - E^r),$$

and the composite function $g_{\mathrm{e}}^{-1}(g_{\mathrm{m}}(\cdot))$ (or its inverse $g_{\mathrm{m}}^{-1}(g_{\mathrm{e}}(\cdot))$) can be determined. The fields $E = \pm g_{\mathrm{e}}^{-1}(g_{\mathrm{m}}(\eta_0 H))$ are the electric fields which combined with $\eta_0 H$ gives a right(left) propagating wave in the slab. Differentiating this relation, we get $dE = \pm \frac{g'_{\mathrm{m}}(\eta_0 H)}{g'_{\mathrm{e}}(E)} \eta_0 dH$, which lets us define a differential wave impedance relative to vacuum as $\frac{g'_{\mathrm{m}}(\eta_0 H)}{g'_{\mathrm{e}}(E)}$.

In nonlinear optics, the materials can often be considered as nonmagnetic. This implies $g_{\mathrm{m}}(x) = x$, and we can easily determine the electric response function g_{e}, from which we get F_{e} or the wave speed c. We see that the range of the input signal E^i puts bounds on the domain of the reconstructed function g_{e}. Thus, we can not gain information on how the material responds to fields greater than those we probe with, unless we extrapolate our results.

3.4.2 Transmission

If we neglect the fields that are reflected at the right boundary, $z = d$, we are considering a problem where the wave speed depends on only one variable, and the u^+-fields propagate independently of the u^--fields. This means that the characteristic curves for the right-going fields are straight lines, which can be used to our advantage. Since the left propagating wave induced by an internal reflection is in general rather small compared with the direct wave, this is an acceptable approximation.

We assume that for $z = 0+$, the right propagating field $u^+(0,t)$ considered as a function of time has a pulse shape, *i.e.*, it is continuous with finite support, and has only one extremum, *e.g.*, a maximum. This implies that there are two times for which u^+ assumes the same value, *i.e.*, $u^+(0,t_1) = u^+(0,t_1+\tau)$ for some time separation τ. Since the wave speed depends only on u^+ when we neglect the left

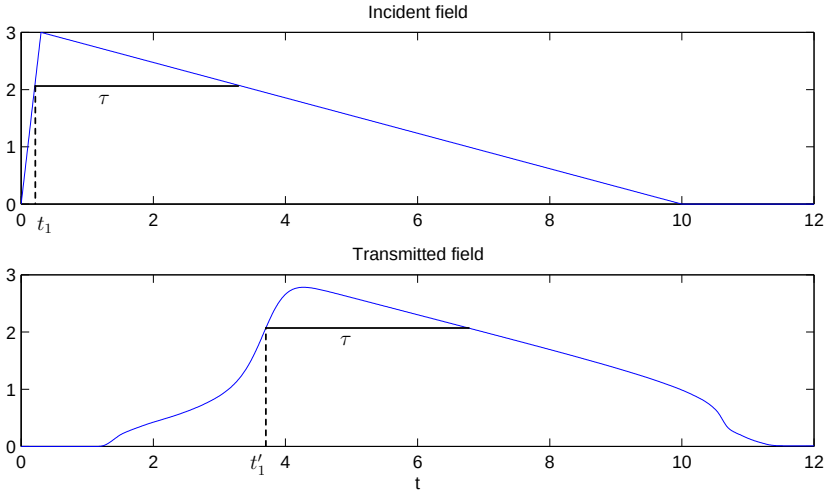

Figure 2: Method for extracting the travel time for different field amplitudes. Since equal amplitudes travel with equal speed, they arrive with the same time separation and the travel time is $t_1' - t_1$.

propagating field u^-, these two points of equal amplitude will travel with the same speed, and thus appear with the same time separation on the right side of the slab, *i.e.*, $u^+(d, t_1') = u^+(d, t_1' + \tau)$ for some time t_1'. This can be used to find the propagation time corresponding to the amplitude in question, $t_1' - t_1$, and thereby the wave speed $c(u^+) = d/(t_1' - t_1)$.

One complication is that we can only measure the fields outside the slab, but using the boundary conditions (3.3) and (3.4),

$$\begin{cases} 2u^+ = g_{\mathrm{e}}(E^i + E^r) + g_{\mathrm{m}}(E^i - E^r) \\ 2u^+ = g_{\mathrm{e}}(E^t) + g_{\mathrm{m}}(E^t), \end{cases}$$

we find that there is a one-to-one correspondence between the incident field strength and the u^+-level, and between the transmitted field strength and the u^+-level. This means that if $E^i(t_1) = E^i(t_1+\tau)$, then there is a time t_1' for which $E^t(t_1') = E^t(t_1'+\tau)$, and we can find our transmission time $t_1' - t_1$.

In other words, we take a segment of a certain length τ of the time axis, and fit this into the curves $E^i(t)$ and $E^t(t)$. The time difference between the fits is the travel time for this particular amplitude, see Figure 2. This does not work with shock solutions, but the only consequence is that we cannot get any information on the travel time for the amplitudes over which the shock occurs.

We have the following relationships determined by reflection data and transmission time:

$$E^i + E^r = g_{\mathrm{e}}^{-1}(g_{\mathrm{m}}(E^i - E^r))$$
$$c(E^i + E^r, E^i - E^r) = \frac{c_0}{g_{\mathrm{e}}'(E^i + E^r) g_{\mathrm{m}}'(E^i - E^r)}.$$

If we denote the measurable quantities $E^i + E^r$ and $E^i - E^r$ by e and h, we have

the experimentally determined functions

$$\begin{aligned} e(h) &= g_{\mathrm{e}}^{-1}(g_{\mathrm{m}}(h)) \\ c(e,h) &= \frac{c_0}{g_{\mathrm{e}}'(e)g_{\mathrm{m}}'(h)}. \end{aligned} \tag{3.5}$$

The derivative of e with respect to h is $\frac{de}{dh} = \frac{g_{\mathrm{m}}'(h)}{g_{\mathrm{e}}'(e)}$, corresponding to the differential wave impedance. We can thus find $g_{\mathrm{e}}'(e)^2 = F_{\mathrm{e}}'(e)$ and $g_{\mathrm{m}}'(h)^2 = F_{\mathrm{m}}'(h)$ by combining these relations:

$$\begin{aligned} F_{\mathrm{e}}'(e) = \frac{c_0\frac{dh}{de}}{c(e,h(e))} \quad &\Rightarrow \quad F_{\mathrm{e}}(e) = \int_0^{h(e)} \frac{c_0 dh'}{c(e(h'),h')} \\ F_{\mathrm{m}}'(h) = \frac{c_0\frac{de}{dh}}{c(e(h),h)} \quad &\Rightarrow \quad F_{\mathrm{m}}(h) = \int_0^{e(h)} \frac{c_0 de'}{c(e',h(e'))}. \end{aligned} \tag{3.6}$$

From these expressions we conclude that there is a one-to-one correspondence between $F_{\mathrm{e,m}}$ and $c(e,h)$ once the relation between e and h is given. Since this is given by $g_{\mathrm{e}}(e) - g_{\mathrm{m}}(h) = 0$, and $g_{\mathrm{e,m}}$ are monotone functions, this is a one-to-one relation. With shockfree propagation of a pulseshaped signal, the transmitted signal should also be pulseshaped, see *e.g.*, the example in Figure 2. Then the wavespeed $c(e,h(e)) = c(e(h),h)$ must be unique, and we conclude that the reconstructed functions are unique, always exist, and depend continuously on the data. Thus the algorithm is well posed.

3.5 Implementation of the forward problem

In order to obtain the reflected and transmitted fields from the slab, an algorithm using finite differences has been implemented in MATLAB. The algorithm is based on interpolating the wave speed and fields between two neighboring points in the grid with a linear function, and tracing the characteristics back one time step. The tracing is made by searching for the point in the grid for which the interpolated wave speed points to the new grid point. The method is described in [12, Chap. 8].

This method does not handle discontinuous solutions very well, but rather smears the discontinuity over 10-20 grid points. Since we never use shock solutions in our reconstruction algorithm, this is not a problem. When tested, the travel time for shocks seems to be correct, though.

For numerical reasons, it is advantageous to scale the problem. We have access to two different scalings; one scales the spacetime and one scales the fields. The scaling is most obvious when looking at the original Maxwell equations,

$$\partial_z \begin{pmatrix} E \\ \eta_0 H \end{pmatrix} + \frac{1}{c_0} \begin{pmatrix} 0 & F_{\mathrm{m}}'(\eta_0 H) \\ F_{\mathrm{e}}'(E) & 0 \end{pmatrix} \partial_t \begin{pmatrix} E \\ \eta_0 H \end{pmatrix} = 0.$$

When multiplying this equation by a factor a, and introducing the new fields $\tilde{E} = aE$ and $\tilde{H} = a\eta_0 H$, we get

$$\partial_z \begin{pmatrix} \tilde{E} \\ \tilde{H} \end{pmatrix} + \frac{1}{c_0} \begin{pmatrix} 0 & F_{\mathrm{m}}'(\tilde{H}/a) \\ F_{\mathrm{e}}'(\tilde{E}/a) & 0 \end{pmatrix} \partial_t \begin{pmatrix} \tilde{E} \\ \tilde{H} \end{pmatrix} = 0.$$

There is no problem incorporating the factor $\frac{1}{a}$ in the constitutive relations, *e.g.*, when $F_{\mathrm{e}}'(E) = \varepsilon_1 + \varepsilon_3 E^2$, we have $F_{\mathrm{e}}'(\tilde{E}/a) = \varepsilon_1 + \frac{\varepsilon_3}{a^2}\tilde{E}^2 = \varepsilon_1 + \tilde{\varepsilon}_3\tilde{E}^2 = \tilde{F}_{\mathrm{e}}{}'(\tilde{E})$. We see that the fields can be quite arbitrarily scaled, as long as we scale the constitutive relations as well. In our simulations, we have chosen to use a factor a such that the nonlinear terms in the constitutive relations are of the same order as the linear ones, when using a numerical field strength of a few units.

We also see that we still have the possibility to scale the spacetime, since this only effects the differential operators. Note that this is true only for homogeneous media; for inhomogenous media we would have to scale the constitutive relations once again. In our simulations, we have chosen to scale the spacetime so that the vacuum wave speed c_0 is 1, and the slab has width 1. The slab is discretized with 100 grid points in space, and the step size in time is chosen the same as that in space. This guarantees that when tracing the characteristics back in time, we stay within the nearest grid points in space.

Since we can scale the field strength and spacetime individually, and must avoid shock solutions but still have substantial nonlinear effects, our results will apply to situations with either strong fields and short propagation distances, or weak fields and long propagation distances. Of course, the concepts strong–weak and short–long, must be related to the exact physical media being modeled.

4 Numerical results

4.1 Reflection

When implementing this reconstruction, it is difficult not committing the inverse crime, *i.e.*, using the same algorithm for both simulating data and reconstructing the constitutive functions, leading to a perfect match [7, p. 121].

It is therefore meaningless to present *any* results for reconstruction with pure reflection data, unless some measured data is available, which is not the case at the present time. The reconstruction is anyway used in the transmission reconstruction, where we get good results.

4.2 Transmission

Simulations have been run, giving reflection and transmission data for a given input signal and the constitutive relations

$$F_{\mathrm{e}}(E) = 1.5E + 2\frac{E^3}{1+E^2}$$
$$F_{\mathrm{m}}(H) = H + 2\frac{H^3}{1+H^2},$$

where we have used the scaling in Section 3.5 to define dimensionless variables and functions. These constitutive relations describe a Kerr material with saturation, *i.e.*, it behaves as a material with a nonlinear behavior for weak fields, and as a linear material for strong fields.

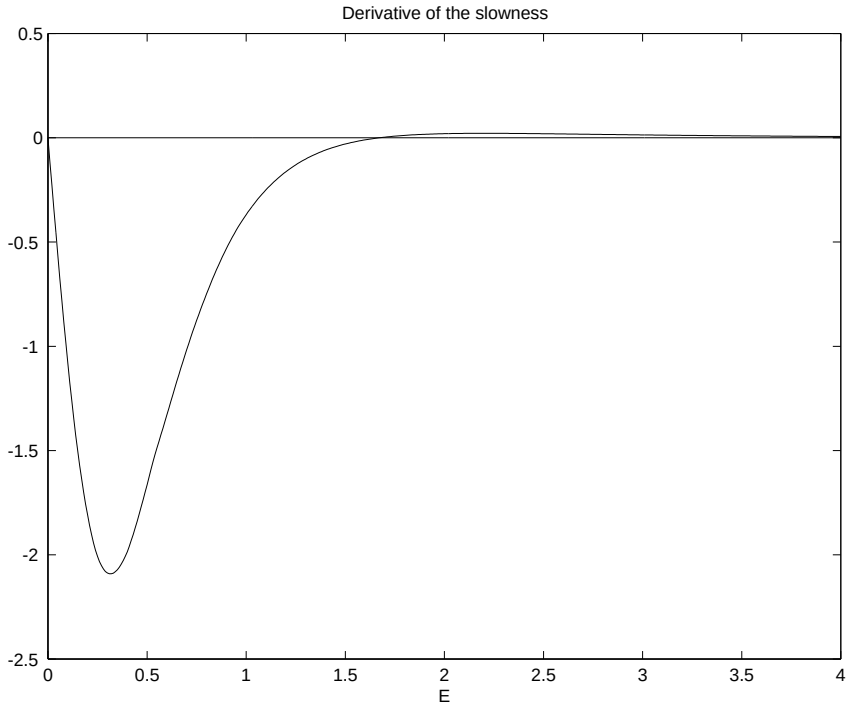

Figure 3: Graph of $-\frac{\partial}{\partial E}\frac{c_0}{c(E,H(E))}$. Observe that it is slightly positive for large field strengths, about 0.022.

We have previously stated that the condition (3.2) must be satisfied to avoid shock solutions. Figure 3 depicts the function which, when multiplied with $\frac{\partial E^i}{\partial t}$, should be less than $c_0/d = 1$. Since the function is mostly negative, we see that the greatest danger is when $\frac{\partial E^i}{\partial t} < 0$, *i.e.*, on the trailing edge of the pulse. This can be avoided by using an incident field wich decays sufficiently slow. When the derivative is positive, there is an upper limit on $\frac{\partial E^i}{\partial t}$ set by the reciprocal of the greatest positive value of the function in Figure 3, *i.e.*, $1/0.022 = 46$. Thus, we can use an incident field which rises very rapidly, but not instantly. We want it to rise fast enough so that its peak value is obtained before the reflected field at the back has returned; this gives us an exact map of the relation $g_{\mathrm{e}}(E) = g_{\mathrm{m}}(H)$, since then $g_{\mathrm{e}}(E) - g_{\mathrm{m}}(H) = 2u^- = 0$. The incident field used is depicted in Figure 4.

It should be stressed that it is not necessary to make the measurement of reflected and transmitted fields simultaneously. This is because the reflected field is only used to establish the relation between the electric and the magnetic fields necessary to create only a forward propagating field u^+, *i.e.*, $E = g_{\mathrm{e}}^{-1}(g_{\mathrm{m}}(H))$.

Figures 4 and 5 show the calculated fields and the reconstructed constitutive functions. The fields are calculated using the full forward problem, *i.e.*, the left propagating field u^- in the slab is present. The mean relative error in the reconstruction was 2.3% for F_{e} and 2.5% for F_{m}.

The algorithm is based on neglecting the field reflected from the back edge. To investigate the validity of this approximation the following test has been made. The left propagating field was neglected in the solution of the forward problem,

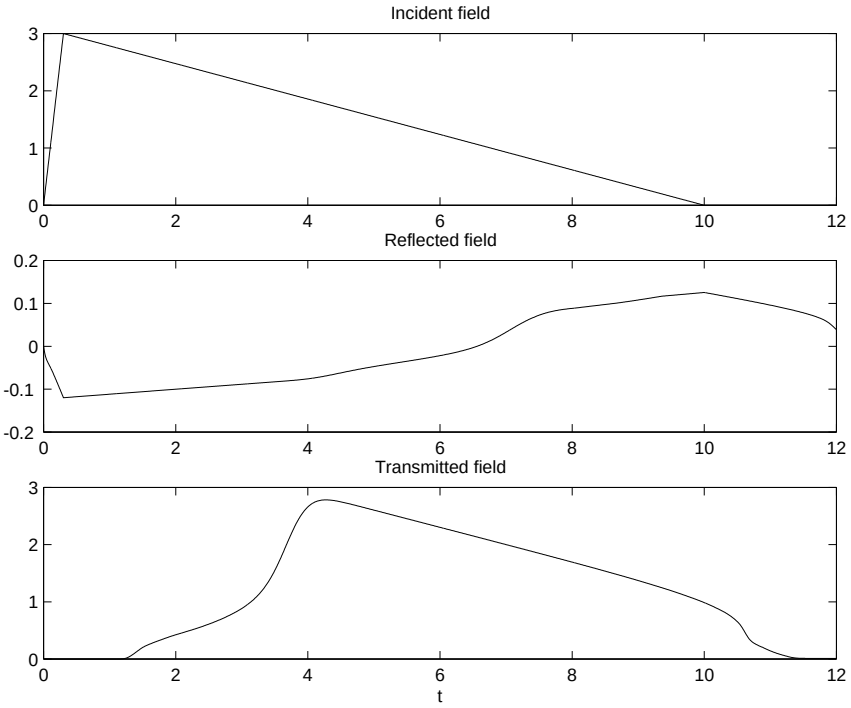

Figure 4: Incident, reflected and transmitted fields.

i.e., we used straight characteristics. Then we used the full forward problem, and compared the travel times obtained in the two cases. The mean relative difference between them was 0.19%, which shows that the approximation is good, at least for the materials studied in this paper.

In Figure 6 we have depicted the travel time as a function of the incident field strength for the two methods, as well as the difference between them. It is clearly seen that the greatest difference in travel time is for small field strengths. Remember that the expression for the slowness is $\frac{c_0}{c(u^+,u^-)} = g'_{\rm e}(u^+ + u^-)g'_{\rm m}(u^+ - u^-)$, which means that the error in travel time when neglecting u^- should be small when u^+ is relatively large.

5 Discussion and conclusions

It has been shown that it is possible to reconstruct the constitutive functions of a nonlinear slab, with the help of reflection and transmission data, not necessarily measured simultaneously. The algorithm is based on the fact that equal amplitudes travel with almost equal and constant speeds. When one of the constitutive functions is known, for instance for a nonmagnetic material, the other function is obtained with reflection data only. The algorithm seems to be robust and simple, and may be useful for measuring instantaneous nonlinear effects, with virtually no assumptions made on the specific form of the constitutive function, *i.e.*, the inverse algorithm is model independent.

Since the algorithm is based on shock free propagation, it is necessary to con-

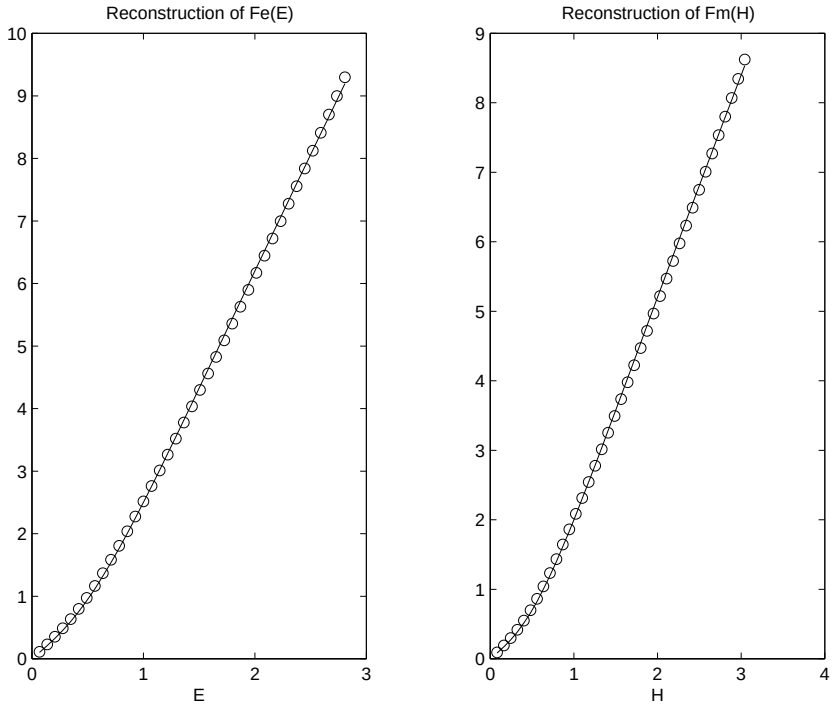

Figure 5: Reconstructed functions, from the fields in Figure 4. The circles are the reconstructed values, and the solid lines are the true functions.

struct a suitable input signal. When measuring reflected and transmitted field simultaneously, the input signal should rise fast enough so that its maximum is reached before the first reflection from the back boundary turns up, and then decrease slow enough not to create a shock in the transmitted field. This may be a difficult field to create.

The neglection of u^- in the propagation corresponds to the first term in a series expansion of the slowness at $u^- = 0$, *i.e.*, $\frac{c_0}{c(u^+,u^-)} = \frac{c_0}{c(u^+,0)} + O(u^-)$. The term $O(u^-)$ is proportional not only to u^- but also to the derivative of the slowness, which is proportional to the second derivative of the constitutive relations. A material is defined as weakly nonlinear if this second derivative is small compared to the reciprocal of the field strength. We then expect our method to work well for such materials, since the neglected term is a product of two small quantities. The series approach can in principle be used to establish a definite bound on the error in travel time, deduced directly from the constitutive relations. Though, this is a formidable problem, which is under current research. A rigorous analysis of such an expansion of the slowness may also be used to further develop the reconstruction algorithm presented in this paper, and will probably clarify which properties of the constitutive relations are important for the wave propagation.

An interesting fact is that it is conceivable to have a material with nonlinear behavior in both electric and magnetic fields. If the media changes from being dominantly electric to being dominantly magnetic, or vice versa, we may get a very small reflection for a very strong incident wave. This might have some implications on the theory of nonreflecting materials, or provide a new kind of electric shutter.

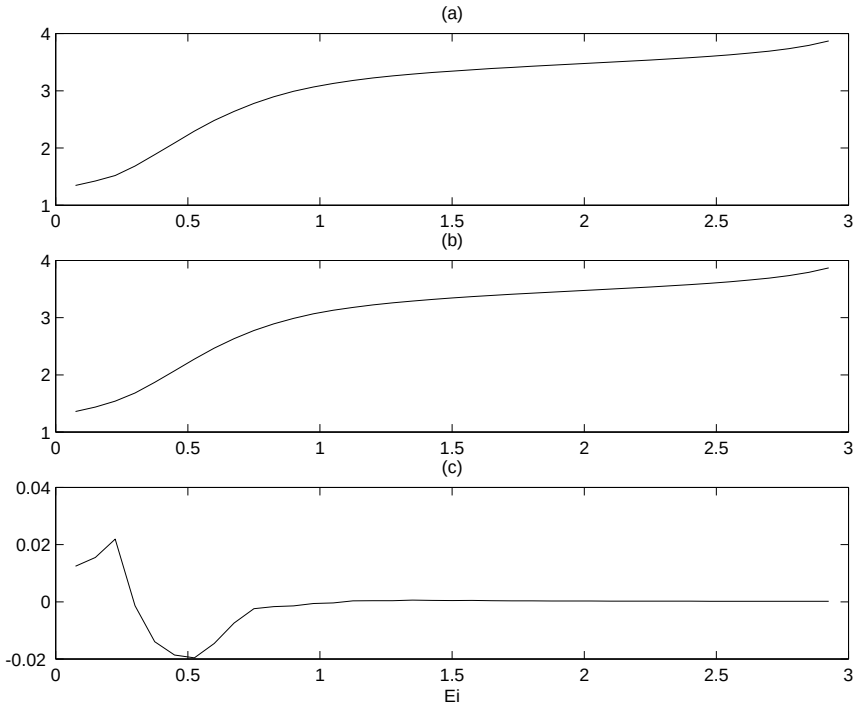

Figure 6: Amplitude-dependent travel time as a function of the incident field strength. (a) Travel time when using straight characteristics, *i.e.*, neglecting the left propagating field u^-. (b) Travel time when using the full forward problem. (c) The difference in travel time for the two methods.

6 Acknowledgment

The author wishes to express his sincere gratitude to Prof. G. Kristensson for valuable discussions and suggestions during this project.

The work reported in this paper is partially supported by a grant from the Swedish Research Council for Engineering Sciences, and its support is gratefully acknowledged.

References

[1] G. P. Agrawal. *Nonlinear fiber optics*. Academic Press, San Diego, 1995.

[2] F. G. Bass, G. Y. Slepyan, S. A. Maksimenko, and A. Lakhtakia. Time-domain Beltrami-Maxwell solitons in certain nonlinear chiral media. *Microwave Opt. Techn. Lett.*, **9**(4), 218–221, July 1995.

[3] F. Bloom. *Mathematical problems of classical nonlinear electromagnetic theory*. Longman Scientific & Technical, Burnt Mill, Harlow, England, 1993.

[4] R. W. Boyd. *Nonlinear Optics*. Academic Press, San Diego, 1992.

[5] D. Censor and Y. Ben-Shimol. Wave propagation in weakly nonlinear bi-anisotropic and bi-isotropic media. *J. Electro. Waves Applic.*, **11**, 1763–1779, 1997.

[6] B. D. Coleman and E. H. Dill. Thermodynamic restrictions on the constitutive equations of electromagnetic theory. *Z. angew. Math. Phys.*, **22**, 691–702, 1971.

[7] D. Colton and R. Kress. *Inverse Acoustic and Electromagnetic Scattering Theory*. Springer-Verlag, Berlin, 1992.

[8] J. P. Corones, M. E. Davison, and R. J. Krueger. The effects of dissipation in one-dimensional inverse problems. In A. J. Devaney, editor, *Inverse Optics, Proceedings of the SPIE*, pages 107–114, Bellingham, WA, 1983. Proc. SPIE 413, SPIE.

[9] M. E. Davison and R. C. Winther. A general approach to splitting and invariant imbedding for linear wave equations. *J. Math. Anal. Appl.*, **188**(1), 158–181, 1994.

[10] M. de Magistris, G. Miano, L. Verolino, C. Visone, and E. Zamparelli. A numerical analysis of the behaviour of the Galerkin equations relevant to electromagnetic wave propagation in nonlinear media. *IEEE Trans. Magnetics*, **30**, 3196–3199, 1994.

[11] A. C. Eringen and G. A. Maugin. *Electrodynamics of Continua I.* Springer-Verlag, New York, 1990.

[12] B. Gustafsson, H.-O. Kreiss, and J. Oliger. *Time Dependent Problems and Difference Methods*. John Wiley & Sons, New York, 1995.

[13] A. Hasegawa. *Optical Solitons in Fibers*. Springer-Verlag, Berlin Heidelberg, 1990.

[14] A. Hasegawa and Y. Kodama. *Solitons in Optical Communications*. Clarendon Press, Oxford, 1995.

[15] L. Hörmander. *Lectures on Nonlinear Hyperbolic Differential Equations*. Number 26 in Mathémathiques & Applications. Springer-Verlag, Berlin, 1997.

[16] F. John. *Partial Differential Equations*. Springer-Verlag, New York, fourth edition, 1982.

[17] R. M. Joseph and A. Taflove. FDTD Maxwell's equations models for nonlinear electrodynamics and optics. *IEEE Trans. Antennas Propagat.*, **45**, 364–374, 1997.

[18] J. Y. Kazakia and R. Venkataraman. Propagation of electromagnetic waves in a nonlinear dielectric slab. *Z. angew. Math. Phys.*, **26**, 61–76, 1975.

[19] A. Kluwick and E. A. Cox. Nonlinear waves in materials with mixed nonlinearity. *Wave Motion*, **27**, 23–41, 1998.

[20] G. Kristensson and D. J. N. Wall. Direct and inverse scattering for transient electromagnetic waves in nonlinear media. *Inverse Problems*, **14**, 113–137, 1998.

[21] L. F. Mollenauer, R. H. Stolen, and J. P. Gordon. Experimental observation of picosecond pulse narrowing and solitons in optical fibers. *Phys. Rev. Lett.*, **45**(13), 1095–1098, September 1980.

[22] C. Rogers, H. M. Cekirge, and A. Askar. Electromagnetic wave propagation in non-linear dielectric media. *Acta Mech.*, **26**, 59–73, 1977.

[23] G. Y. Slepyan, S. A. Maksimenko, F. G. Bass, and A. Lakhtakia. Nonlinear electromagnetics in chiral media: Self-action of waves. *Phys. Rev. E*, **52**(1), 1049–1058, July 1995.

[24] J. Veldhuis and H. Blok. Reflection and refraction of electromagnetic waves by the plane boundary of a non-linear medium: application of the simple wave theory. *J. Phys. A: Math. Gen.*, **11**(8), 1663–1680, 1978.

Simple wave solutions for the Maxwell equations in bianisotropic, nonlinear media, with application to oblique incidence

Paper II

Daniel Sjöberg

Based on: D. Sjöberg. Simple wave solutions for the Maxwell equations in bianisotropic, nonlinear media, with application to oblique incidence. *Wave Motion*, **32** (2000), 217–232.

Abstract

We analyze the propagation of electromagnetic waves in nonlinear, bianisotropic, nondispersive, homogeneous media using simple waves and six-vector formalism. The Maxwell equations are formulated as an eigenvalue problem, whose solutions are equivalent to the characteristic propagation directions. We solve the oblique incidence of plane waves in vacuum on a half space of nonlinear material, and present a method to calculate the reflected and transmitted fields for all angles of incidence and all polarizations of the incident field. Numerical examples for reflection and transmission illustrate the field dependence of the Brewster angle, and the birefringence of an anisotropic material.

1 Introduction

Wave propagation in nonlinear media is a wide and quickly expanding area. In particular, the nonlinear optics field has been very prosperous [1, 3]. One of the most exciting areas is that of solitons, *i.e.*, pulses which have a very specific shape, in which the nonlinear steepening effects are precisely balanced by the dispersive broadening, thereby producing a pulse that is temporally and spatially unchanged during propagation. This delicate balance can only be understood by studying both contributing effects. In this paper, we are devoted to the nonlinear effects which occur in materials with no memory, *i.e.*, no dispersion.

Whereas the linear dispersion has been thoroughly investigated, *e.g.*, [4, 14, 20], the nonlinear properties may not have received enough attention. Some early works are summarized in [2], and especially the papers on wave propagation in nonlinear dielectrics [5, 6, 17, 21, 32] are relevant. A prominent feature of nonlinear wave propagation, where the nonlinearity acts as an amplitude-dependent wave speed, is the formation of shock waves. These are discontinuous waves, which must be interpreted in a generalized way as weak solutions, see *e.g.*, [31, pp. 369–373], and the theory of these has been thoroughly studied [15, 18, 28, 37]. It is often argued that the shock waves are eliminated by the linear dispersion, see *e.g.*, [1, pp. 117–120], but since we are ignoring dispersion in this study, we expect our model to be accurate only when we are not in the vicinity of any shock formations.

An often encountered problem when studying nonlinear materials is that of finding suitable constitutive relations. In the treatise of Eringen and Maugin [9, 10], the constitutive relations for virtually every reasonable situation are presented. Some important thermodynamic restrictions are presented in [8]. The derivation of constitutive relations from a quantum mechanical point of view is presented in [3], and some theory about nonlinear dielectrics is found in [7].

This paper aims to improve the understanding of a nonlinear optical response, *i.e.*, an instantaneous nonlinear response. Earlier works, as reported above, have often made some important restrictions, such as assuming the material to be isotropic or uniaxial. Here we present a theory describing wave propagation in bianisotropic materials. We show that a generalized form of plane waves, called simple waves, can

be used to analyze the wave propagation, and we reformulate the Maxwell equations as an eigenvalue problems. A brief presentation on simple waves in partial differential equations is given in [19, p. 52], and a more extensive treatment is given in [16, Chap. 3]. There are also some related results in [13, p. 47].

The paper is organized as follows: in Sections 2 and 3 we present the simple wave Ansatz and the six-vector formalism, which are the basic tools used in this paper. This is applied to the Maxwell equations in Section 4, which transforms the dynamics into an eigenvalue problem. Special notice is taken to isotropic media. In Section 5 we introduce the theory on how to classify materials. We then apply our formalism in Section 6 to the problem of a plane wave obliquely impinging on a nonlinear half space and solve the problem of finding the reflected and transmitted fields. Some results on suitable conditions on the Brewster angles are also presented, as well as numerical results for reflection and transmission.

2 Simple wave Ansatz

Plane waves constitute a powerful tool in the analysis of wave phenomena in linear materials. The concept of plane waves transforms the problem of three spatial dimensions into a problem along the propagation direction. Simple waves are the generalization of this concept. They have previously been used in the description of nonlinear electromagnetic waves [5, 6], and are explained in basic books on partial differential equations [19, p. 52]. They also determine the characteristics of the wave equation.

The simple wave Ansatz is suitable for materials which respond instantaneously to excitation, and states that the fields depend only upon a scalar parameter, which we denote ϕ. This parameter is a function of space and time. For an isotropic, linear media the simple wave Ansatz reduces to the usual phase function, $\phi(\boldsymbol{r}, t) = \boldsymbol{k}\cdot\boldsymbol{r} - \omega t$.

It is obvious that if a quantity u depends on space and time as $u(\boldsymbol{r}, t) = u(\phi(\boldsymbol{r}, t))$, the spatial gradient $\nabla\phi$ represents a propagation direction. We identify the quantity $-\frac{\nabla\phi/\phi_t}{|\nabla\phi/\phi_t|}$ as the propagation direction and $|\phi_t|/|\nabla\phi|$ as the propagation speed, where ϕ_t denotes the time derivative of ϕ. The minus sign comes from implicit differentiation of the equation $\phi(\boldsymbol{r}, t) = \text{constant}$, which is the equation of the wave front.

3 Six-vector formalism

When describing bianisotropic phenomena, it is often advantageous to use the six-vector formalism, see *e.g.*, [25]. In this approach, no real distinction between the electric and magnetic fields is made, but they are treated as components of a single

field. We define our fields as

$$\begin{cases} \mathsf{e} = \begin{pmatrix} \sqrt{\epsilon_0}\boldsymbol{E} \\ \sqrt{\mu_0}\boldsymbol{H} \end{pmatrix} \\ \mathsf{d} = \begin{pmatrix} \frac{1}{\sqrt{\epsilon_0}}\boldsymbol{D} \\ \frac{1}{\sqrt{\mu_0}}\boldsymbol{B} \end{pmatrix} \end{cases} \tag{3.1}$$

where ϵ_0 and μ_0 denote the permittivity and permeability of vacuum, respectively. The components of the six-vector fields now all have the same dimension, *i.e.*, $\sqrt{\text{energy/volume}}$.

To distinguish between three-vectors and six-vectors, we denote the former by bold-faced italic letters, and the latter by sans-serif letters, *i.e.*, the notation in [25]. Three-dimensional dyadics are denoted by uppercase bold-faced roman letters, and six-dimensional dyadics by uppercase sans-serif letters. The exception is the material six-dyadic, which is denoted by $\boldsymbol{\varepsilon}$. The unit three vector is denoted by a hat, *e.g.*, the unit three vector in the z direction is denoted $\hat{\boldsymbol{z}}$.

The scalar product between two six-vectors a and b is defined as $\mathsf{a}\cdot\mathsf{b} = \sum_{i=1}^{6} a_i b_i$. Operations with three-vectors on six-vectors are understood in the obvious manner, *i.e.*, the scalar and cross products are

$$\boldsymbol{v}\cdot\mathsf{e} = \begin{pmatrix} \boldsymbol{v}\cdot\sqrt{\epsilon_0}\boldsymbol{E} \\ \boldsymbol{v}\cdot\sqrt{\mu_0}\boldsymbol{H} \end{pmatrix}, \quad \text{and} \quad \boldsymbol{v}\times\mathsf{e} = \begin{pmatrix} \boldsymbol{v}\times\sqrt{\epsilon_0}\boldsymbol{E} \\ \boldsymbol{v}\times\sqrt{\mu_0}\boldsymbol{H} \end{pmatrix}. \tag{3.2}$$

We often use the three-dimensional dyadic $[\mathbf{I} - \hat{\boldsymbol{z}}\hat{\boldsymbol{z}}]$, which projects out the x and y components, on six-dimensional dyadics. This is defined as

$$[\mathbf{I} - \hat{\boldsymbol{z}}\hat{\boldsymbol{z}}]\cdot\begin{pmatrix} \mathbf{A}_{11} & \mathbf{A}_{12} \\ \mathbf{A}_{21} & \mathbf{A}_{22} \end{pmatrix} = \begin{pmatrix} [\mathbf{I} - \hat{\boldsymbol{z}}\hat{\boldsymbol{z}}]\cdot\mathbf{A}_{11} & [\mathbf{I} - \hat{\boldsymbol{z}}\hat{\boldsymbol{z}}]\cdot\mathbf{A}_{12} \\ [\mathbf{I} - \hat{\boldsymbol{z}}\hat{\boldsymbol{z}}]\cdot\mathbf{A}_{21} & [\mathbf{I} - \hat{\boldsymbol{z}}\hat{\boldsymbol{z}}]\cdot\mathbf{A}_{22} \end{pmatrix}. \tag{3.3}$$

Using the six-dyadic $\mathsf{J} = \begin{pmatrix} \mathbf{0} & -\mathbf{I} \\ \mathbf{I} & \mathbf{0} \end{pmatrix}$, which is formed from the three-dimensional identity dyadic $\mathbf{I}$, we write the source free Maxwell equations as

$$[\nabla\times\mathsf{J}]\cdot\mathsf{e} + \frac{1}{c_0}\partial_t\mathsf{d} = 0, \tag{3.4}$$

where c_0 denotes the wave speed in vacuum, $1/\sqrt{\epsilon_0\mu_0}$. The spatial differential operator ∇ is treated as a three-vector, and is merged with the six-dyadic J to form the operator

$$\nabla\times\mathsf{J} = \begin{pmatrix} \mathbf{0} & -\nabla\times\mathbf{I} \\ \nabla\times\mathbf{I} & \mathbf{0} \end{pmatrix} = \begin{pmatrix} 0 & 0 & 0 & 0 & \partial_z & -\partial_y \\ 0 & 0 & 0 & -\partial_z & 0 & \partial_x \\ 0 & 0 & 0 & \partial_y & -\partial_x & 0 \\ 0 & -\partial_z & \partial_y & 0 & 0 & 0 \\ \partial_z & 0 & -\partial_x & 0 & 0 & 0 \\ -\partial_y & \partial_x & 0 & 0 & 0 & 0 \end{pmatrix}, \tag{3.5}$$

as in [12]. The explicit matrix representation in cartesian coordinates is seen to be symmetric.

4 The Maxwell equations as an eigenvalue problem

The constitutive relation for a material with no memory, *i.e.*, where the fluxes d depend only upon the present values of the field strengths e, can be written

$$\mathsf{d}(\boldsymbol{r},t) = \mathsf{d}(\mathsf{e}(\boldsymbol{r},t)). \tag{4.1}$$

We now apply the simple wave Ansatz together with the constitutive relation,

$$\begin{cases} \mathsf{e}(\boldsymbol{r},t) = \mathsf{e}(\phi(\boldsymbol{r},t)) \\ \mathsf{d}(\boldsymbol{r},t) = \mathsf{d}(\mathsf{e}(\phi(\boldsymbol{r},t))). \end{cases} \tag{4.2}$$

This means that the curl operator turns into a cross product, $\nabla \times \mathsf{e} = \nabla\phi \times \mathsf{e}'$, and the time derivative becomes $\partial_t \mathsf{d} = [\nabla_e \mathsf{d}] \cdot \mathsf{e}' \partial_t \phi$, where the prime denotes differentiation with respect to ϕ. The operator ∇_e denotes the field gradient operator, *i.e.*, $[\nabla_e \mathsf{d}]_{nm} = \frac{\partial}{\partial e_m} d_n(\mathsf{e})$. Since we write the linear constitutive relations as $\mathsf{d} = \boldsymbol{\varepsilon} \cdot \mathsf{e}$, where $\boldsymbol{\varepsilon}$ is a six-dyadic, we denote $[\nabla_e \mathsf{d}]$ by $\boldsymbol{\varepsilon}(\mathsf{e})$, and often suppress the argument to obtain a less cumbersome notation.

The dyadic $\boldsymbol{\varepsilon}$ is postulated to be positive definite and symmetric, and is thus invertible. In the linear case, it is possible to show that $\boldsymbol{\varepsilon}$ has to be a symmetric, positive definite dyadic in order to model passive media [12]. The assumptions made on the dyadic $\boldsymbol{\varepsilon}$ is a natural generalization of the result in the linear case.

With the simple wave Ansatz, the Maxwell equations contain the generic field $\mathsf{e}' = \frac{\mathrm{d}}{\mathrm{d}\phi}\mathsf{e}$. However, for reasons that become more obvious below we prefer to use the time derivative, $\dot{\mathsf{e}} = \partial_t \mathsf{e} = \mathsf{e}' \partial_t \phi$. This choice also becomes advantageous when implementing the equations later on. Since $\phi(\boldsymbol{r},t) =$ constant is the equation for the wave front, we identify the wave slowness $1/c$ and the propagation direction $\hat{\boldsymbol{k}}$ of the simple wave by the following expressions,

$$\begin{cases} \dfrac{1}{c} = \dfrac{|\nabla\phi|}{|\partial_t\phi|} \\ \hat{\boldsymbol{k}} = -\dfrac{\nabla\phi/\partial_t\phi}{|\nabla\phi/\partial_t\phi|} = -\dfrac{\nabla\phi}{\partial_t\phi} c. \end{cases} \tag{4.3}$$

Using these expressions, we write the Maxwell equations as

$$-\frac{1}{c}[\hat{\boldsymbol{k}} \times \mathsf{J}] \cdot \dot{\mathsf{e}} + \frac{1}{c_0}\boldsymbol{\varepsilon} \cdot \dot{\mathsf{e}} = 0. \tag{4.4}$$

This is an eigenvalue problem, which becomes more obvious in the form

$$\frac{c}{c_0}\dot{\mathsf{e}} = \boldsymbol{\varepsilon}^{-1} \cdot [\hat{\boldsymbol{k}} \times \mathsf{J}] \cdot \dot{\mathsf{e}}. \tag{4.5}$$

Comparison with the matrix representation of $\nabla \times \mathsf{J}$ in (3.5) shows that $[\hat{\boldsymbol{k}} \times \mathsf{J}]$ is a symmetric dyadic.[1]

[1] A dyadic $\mathbf{A}$ is symmetric if it is equal to its transpose $\mathbf{A}^{\mathrm{T}}$ defined by $\mathbf{A}^{\mathrm{T}} \cdot \boldsymbol{v} = \boldsymbol{v} \cdot \mathbf{A}$, *i.e.*, $\mathbf{A}$ is symmetric if $\mathbf{A} \cdot \boldsymbol{v} = \boldsymbol{v} \cdot \mathbf{A}$. This is identical to the demand that its matrix representation is symmetric.

The solution to (4.5) gives conditions on the wave speed and propagation direction in terms of the fields. In the linear case, only the directions of the field will be important, but for nonlinear materials there is also a dependence on the amplitude. For an isotropic material, where

$$\boldsymbol{\varepsilon}(\mathsf{e}) = \begin{pmatrix} \epsilon(E)\mathbf{I} & \mathbf{0} \\ \mathbf{0} & \mu(H)\mathbf{I} \end{pmatrix}, \tag{4.6}$$

the conditions derived from (4.5) are

$$c = \frac{c_0}{\sqrt{\epsilon(E)\mu(H)}} \quad \text{and} \quad \begin{cases} \hat{\boldsymbol{k}} \cdot \dot{\mathsf{e}} = 0 \\ \dot{\boldsymbol{E}} \cdot \dot{\boldsymbol{H}} = 0 \end{cases} \quad \Rightarrow \quad \dot{\mathsf{e}} = \begin{pmatrix} \frac{1}{\sqrt{\epsilon}}\boldsymbol{v} \\ \frac{1}{\sqrt{\mu}}\hat{\boldsymbol{k}} \times \boldsymbol{v} \end{pmatrix}, \tag{4.7}$$

where the three-vector $\boldsymbol{v}$ is orthogonal to $\hat{\boldsymbol{k}}$. Observe that it is the direction of the *derivatives* of the fields that are important, not the fields themselves.

For a given propagation direction $\hat{\boldsymbol{k}}$ the dyadic $\boldsymbol{\varepsilon}^{-1} \cdot [\hat{\boldsymbol{k}} \times \mathsf{J}]$ has six eigenvectors $\dot{\mathsf{e}}_j$, $j = 1, \ldots, 6$. Since the dyadic is not symmetric, these solutions are not guaranteed to be mutually orthogonal. We symmetrize the dyadic by

$$\frac{c}{c_0}(\sqrt{\boldsymbol{\varepsilon}} \cdot \dot{\mathsf{e}}_j) = \left[\sqrt{\boldsymbol{\varepsilon}}^{-1} \cdot [\hat{\boldsymbol{k}} \times \mathsf{J}] \cdot \sqrt{\boldsymbol{\varepsilon}}^{-1}\right] \cdot (\sqrt{\boldsymbol{\varepsilon}} \cdot \dot{\mathsf{e}}_j), \tag{4.8}$$

where we have used the square root of the positive definite and symmetric dyadic $\boldsymbol{\varepsilon}$, which is also positive definite and symmetric. It is concluded that the eigenvectors $\sqrt{\boldsymbol{\varepsilon}} \cdot \dot{\mathsf{e}}_j$ are real and orthogonal, which implies that the eigenvectors $\dot{\mathsf{e}}_j$ are real and linearly independent. The dyadic $\sqrt{\boldsymbol{\varepsilon}}^{-1} \cdot [\hat{\boldsymbol{k}} \times \mathsf{J}] \cdot \sqrt{\boldsymbol{\varepsilon}}^{-1}$ is a congruence transformation (see *e.g.*, [11, p. 251]) of $[\hat{\boldsymbol{k}} \times \mathsf{J}]$, which has the (double) eigenvalues -1, 0 and 1. Since the signs of the eigenvalues are preserved under congruence transforms, we conclude that for a given propagation direction $\hat{\boldsymbol{k}}$ there are two modes propagating in the $+\hat{\boldsymbol{k}}$-direction (positive eigenvalues) and two modes propagating in the $-\hat{\boldsymbol{k}}$-direction (negative eigenvalues), while two modes do not propagate with respect to $\hat{\boldsymbol{k}}$ at all (zero eigenvalue). The last two can be written explicitly as $\dot{\mathsf{e}}_{5,6} = \binom{\pm\hat{\boldsymbol{k}}}{\hat{\boldsymbol{k}}}$.

5 Classification of materials

Materials are often classified as, *e.g.*, isotropic, bi-isotropic or uniaxial depending on the invariance under symmetry transformations. In our formulation, the natural way to classify the materials is by the corresponding invariance of the dyadic $\boldsymbol{\varepsilon}(\mathsf{e})$. This is motivated by the following way of writing the constitutive relations (4.1):

$$\mathsf{d}(\mathsf{e}) = \int_0^{\mathsf{e}} \boldsymbol{\varepsilon}(\mathsf{e}') \cdot \mathrm{d}\mathsf{e}', \tag{5.1}$$

where the integral should be understood in terms of integration along a parameterized curve in $\mathbb{R}^6$. The prime is not to be confused with time differentiation, it is

only denoting the integration variable. When applying a rotation of coordinates $\mathbf{S}$ on the field strength e, we get

$$\mathsf{d}(\mathbf{S}\cdot\mathsf{e}) = \int_0^{\mathbf{S}\cdot\mathsf{e}} \boldsymbol{\varepsilon}(\mathsf{e}')\cdot \mathrm{d}\mathsf{e}' = \int_0^{\mathsf{e}} \boldsymbol{\varepsilon}(\mathbf{S}\cdot\mathsf{e}'')\cdot\mathbf{S}\cdot\mathrm{d}\mathsf{e}'', \tag{5.2}$$

where we have made the change of variables $\mathsf{e}' = \mathbf{S}\cdot\mathsf{e}''$. Materials are classified depending on which group of transformations $\mathbf{S}$ that satisfies $\mathsf{d}(\mathbf{S}\cdot\mathsf{e}) = \mathbf{S}\cdot\mathsf{d}(\mathsf{e})$, *i.e.*, which group of transformations that satisfies $\mathbf{S}^{-1}\cdot\boldsymbol{\varepsilon}(\mathbf{S}\cdot\mathsf{e}'')\cdot\mathbf{S} = \boldsymbol{\varepsilon}(\mathsf{e}'')$.

Materials that satisfy this relation for all rotations $\mathbf{S}$ are called bi-isotropic. This implies that

$$\boldsymbol{\varepsilon}(\mathsf{e}) = \begin{pmatrix} \epsilon(E,H)\mathbf{I} & \xi(E,H)\mathbf{I} \\ \zeta(E,H)\mathbf{I} & \mu(E,H)\mathbf{I} \end{pmatrix}, \tag{5.3}$$

describes a bi-isotropic material, where ϵ, ξ, ζ and μ are scalar functions of the field strengths. Common restrictions on constitutive relations, [8, 12], state that $\xi = \zeta$, and if they are equal to zero, the material is said to be isotropic. When $\xi = \zeta$ is non-zero, we have a nonreciprocal material, see, *e.g.*, [22, p. 403], [20] and [29, Chap. 8]. The possible existence of linear, nonreciprocal, bi-isotropic materials has been thoroughly questioned and debated [24, 30, 33, 35], but since they do not cause any problem in our formalism, we choose not to exclude them from the analysis. The argument for existence of nonlinear, nonreciprocal, bi-isotropic materials has to be reexamined.

6 Oblique incidence

To demonstrate the possible application of the simple wave approach, we analyze the problem of a plane electromagnetic wave obliquely impinging from vacuum on a nonlinear half space. The problem has been studied to some extent by Broer and Sarluy in [5, 6], though they specialize their treatment to a uniaxial material with nonlinearity in electric field only, where the optical axis is in a special direction. An approach similar to ours has been undertaken by Veldhuis and Blok in [36], where they study the oblique incidence of plane waves on an isotropic, nonlinear material. Here, we solve the problem with arbitrary nonlinearities in both electric and magnetic field, as well as arbitrary bianisotropy.

6.1 Geometry and boundary conditions

The geometry of the problem is depicted in Figure 1. The incident field, $\mathsf{e}^{\mathrm{i}}(\boldsymbol{r},t)$, is a plane wave, and we make the Ansatz

$$\begin{cases} \mathsf{e}^{\mathrm{i}}(\boldsymbol{r},t) = \mathsf{e}(\hat{\boldsymbol{k}}^{\mathrm{i}}\cdot\boldsymbol{r} - c_0 t) \\ \mathsf{e}^{\mathrm{r}}(\boldsymbol{r},t) = \mathsf{e}(\hat{\boldsymbol{k}}^{\mathrm{r}}\cdot\boldsymbol{r} - c_0 t) \\ \mathsf{e}^{\mathrm{t}}(\boldsymbol{r},t) = \sum \mathsf{e}^{\mathrm{t}}_j(\phi_j(\boldsymbol{r},t)), \end{cases} \tag{6.1}$$

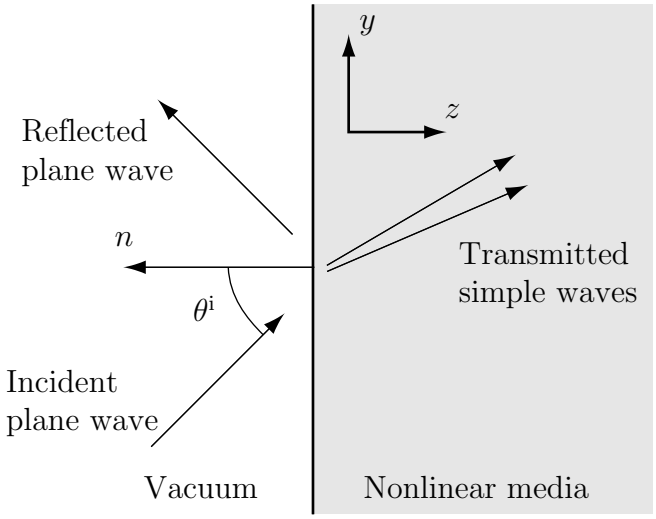

Figure 1: The geometry of the problem of oblique incidence.

where c_0 denotes the wave speed in vacuum. We thus assume that the transmitted field, $\mathsf{e}^{\mathrm{t}}(\boldsymbol{r}, t)$, may consist of several simple waves, as we can expect from the linear, anisotropic case. The number of those is restricted to two in Section 6.5. The usual boundary conditions apply, *i.e.*, the tangential components of the field strengths should be continuous and the normal component of the fluxes should be continuous (no sources at the interface). We write this as

$$\begin{cases} \mathsf{e}^{\mathrm{i}}_{\parallel} + \mathsf{e}^{\mathrm{r}}_{\parallel} = \mathsf{e}^{\mathrm{t}}_{\parallel} \\ \hat{\boldsymbol{z}} \cdot (\mathsf{d}^{\mathrm{i}} + \mathsf{d}^{\mathrm{r}}) = \hat{\boldsymbol{z}} \cdot \mathsf{d}^{\mathrm{t}}. \end{cases} \tag{6.2}$$

The latter condition is not used in the present analysis.

6.2 Reflection law and Snell's law

Since the boundary conditions (6.2) must hold for all times on the surface $z = 0$, we can differentiate them with respect to both time and y. The simple wave Ansatz and (4.3) implies that $\partial_y \phi = -\frac{1}{c} k_y \partial_t \phi$, where $k_y = \hat{\boldsymbol{y}} \cdot \hat{\boldsymbol{k}}$. Using this result and $\mathsf{e}^{\mathrm{t}}(\boldsymbol{r}, t) = \sum \mathsf{e}^{\mathrm{t}}_j(\phi_j(\boldsymbol{r}, t))$ we write the time and y derivative of the tangential fields as

$$\begin{cases} \dot{\mathsf{e}}^{\mathrm{i}}_{\parallel} + \dot{\mathsf{e}}^{\mathrm{r}}_{\parallel} = \sum (\dot{\mathsf{e}}^{\mathrm{t}}_j)_{\parallel} \\ \dfrac{1}{c_0} k^{\mathrm{i}}_y \dot{\mathsf{e}}^{\mathrm{i}}_{\parallel} + \dfrac{1}{c_0} k^{\mathrm{r}}_y \dot{\mathsf{e}}^{\mathrm{r}}_{\parallel} = \sum \dfrac{1}{c_j(\mathsf{e}^{\mathrm{t}})} k^{\mathrm{t}}_{yj} (\dot{\mathsf{e}}^{\mathrm{t}}_j)_{\parallel}. \end{cases} \tag{6.3}$$

These conditions are satisfied if the following holds:

$$k^{\mathrm{i}}_y = k^{\mathrm{r}}_y = \frac{c_0}{c_j(\mathsf{e}^{\mathrm{t}})} k^{\mathrm{t}}_{yj}, \tag{6.4}$$

for all values of j, which is also known as phase-matching [22, p. 104]. It is conjectured that this is the only solution to (6.3).[2]

The quotient between the wave speeds corresponds to the refractive index, and since k_y^{i} and k_{yj}^{t} are the sines of the angles of incidence and transmission, respectively, (6.4) is the well-known Snell's law. This is a purely kinematic law, so it is not surprising that it is valid also in the nonlinear case. Note that since there are several possible values for the wave speed c_j, there are several possible angles of transmission.

Since the propagation directions are normalized and there is no propagation in the x-direction, we now also have the usual reflection law for the reflected field, *i.e.*,

$$\hat{\boldsymbol{k}}^{\mathrm{r}} = k_y^{\mathrm{i}}\hat{\boldsymbol{y}} - k_z^{\mathrm{i}}\hat{\boldsymbol{z}}. \tag{6.5}$$

The transmitted field is more complicated, since it involves the wave speed, which may depend on the field strength.

6.3 Decomposition of the propagation direction

It seems natural to consider a decomposition of the propagation direction $\hat{\boldsymbol{k}}$ in (4.5) in a y and a z part. Using Snell's law and $|\hat{\boldsymbol{k}}_j^{\mathrm{t}}| = 1$, we find

$$\frac{c_0}{c_j}\hat{\boldsymbol{k}}_j^{\mathrm{t}} = \frac{c_0}{c_j}k_{yj}^{\mathrm{t}}\hat{\boldsymbol{y}} + \frac{c_0}{c_j}k_{zj}^{\mathrm{t}}\hat{\boldsymbol{z}} = k_y^{\mathrm{i}}\hat{\boldsymbol{y}} + \frac{c_0}{c_j}\sqrt{1-(\frac{c_j}{c_0}k_y^{\mathrm{i}})^2}\,\hat{\boldsymbol{z}}. \tag{6.6}$$

Using the eigenvalue problem (4.5) for each simple wave in the nonlinear material, we get

$$\begin{aligned}
\boldsymbol{\varepsilon}\cdot\dot{\mathsf{e}}_j^{\mathrm{t}} &= \frac{c_0}{c_j}[\hat{\boldsymbol{k}}_j^{\mathrm{t}}\times\mathsf{J}]\cdot\dot{\mathsf{e}}_j^{\mathrm{t}}\\
[\boldsymbol{\varepsilon} - k_y^{\mathrm{i}}\hat{\boldsymbol{y}}\times\mathsf{J}]\cdot\dot{\mathsf{e}}_j^{\mathrm{t}} &= \frac{c_0}{c_j}k_{zj}^{\mathrm{t}}[\hat{\boldsymbol{z}}\times\mathsf{J}]\cdot\dot{\mathsf{e}}_j^{\mathrm{t}}\\
\frac{c_j}{c_0}\frac{1}{k_{zj}^{\mathrm{t}}}\dot{\mathsf{e}}_j^{\mathrm{t}} &= [\boldsymbol{\varepsilon} - k_y^{\mathrm{i}}\hat{\boldsymbol{y}}\times\mathsf{J}]^{-1}\cdot[\hat{\boldsymbol{z}}\times\mathsf{J}]\cdot\dot{\mathsf{e}}_j^{\mathrm{t}}.
\end{aligned} \tag{6.7}$$

Since the dyadic $[\boldsymbol{\varepsilon} - k_y^{\mathrm{i}}\hat{\boldsymbol{y}}\times\mathsf{J}]^{-1}\cdot[\hat{\boldsymbol{z}}\times\mathsf{J}]$ is independent of j, all simple waves in the nonlinear material are found from the same eigenvalue problem,

$$\lambda_j\mathsf{a}_j = [\boldsymbol{\varepsilon} - k_y^{\mathrm{i}}\hat{\boldsymbol{y}}\times\mathsf{J}]^{-1}\cdot[\hat{\boldsymbol{z}}\times\mathsf{J}]\cdot\mathsf{a}_j, \tag{6.8}$$

where λ_j denotes the number $c_j/(c_0k_{zj}^{\mathrm{t}})$ and a_j is shorthand for $\dot{\mathsf{e}}_j^{\mathrm{t}}$. The corresponding problem for the vacuum fields is easily found,

$$\pm\frac{1}{k_z^{\mathrm{i}}}\dot{\mathsf{e}}^{\mathrm{i,r}} = [\mathsf{I} - k_y^{\mathrm{i}}\hat{\boldsymbol{y}}\times\mathsf{J}]^{-1}\cdot[\hat{\boldsymbol{z}}\times\mathsf{J}]\cdot\dot{\mathsf{e}}^{\mathrm{i,r}}, \tag{6.9}$$

where the $\pm$ comes from $k_z^{\mathrm{r}} = -k_z^{\mathrm{i}}$. The dyadic $[\mathsf{I} - k_y^{\mathrm{i}}\hat{\boldsymbol{y}}\times\mathsf{J}]^{-1}$ is positive definite, since $|k_y^{\mathrm{i}}| < 1$. If all eigenvalues to $\boldsymbol{\varepsilon}$ are greater than one, *i.e.*, the material is denser than vacuum, the dyadic $[\boldsymbol{\varepsilon} - k_y^{\mathrm{i}}\hat{\boldsymbol{y}}\times\mathsf{J}]^{-1}$ is also positive definite.

[2] It is shown later in the text that the vectors $(\dot{\mathsf{e}}_j^{\mathrm{t}})_{\parallel}$ are linearly independent, which supports this conjecture.

6.4 Properties of the eigenvectors

The eigenvalue problem (6.8) is put in a symmetric form in the same manner as in Section 4. We observe that $[\boldsymbol{\varepsilon} - k_y^{\mathrm{i}}\hat{\boldsymbol{y}} \times \mathsf{J}]$ is positive definite and symmetric. In this section we temporarily denote this dyadic C. By multiplying (6.8) with $\sqrt{\mathsf{C}}$, which is also positive definite and symmetric, we obtain

$$\begin{aligned} \lambda_j \sqrt{\mathsf{C}} \cdot \mathsf{a}_j &= \sqrt{\mathsf{C}}^{-1} \cdot [\hat{\boldsymbol{z}} \times \mathsf{J}] \cdot \sqrt{\mathsf{C}}^{-1} \cdot \sqrt{\mathsf{C}} \cdot \mathsf{a}_j \\ \lambda_j \mathsf{u}_j &= \left[\sqrt{\mathsf{C}}^{-1} \cdot [\hat{\boldsymbol{z}} \times \mathsf{J}] \cdot \sqrt{\mathsf{C}}^{-1}\right] \cdot \mathsf{u}_j. \end{aligned} \tag{6.10}$$

The λ_j:s are now eigenvalues to a symmetric dyadic, which implies that they are real. The symmetric dyadic $\sqrt{\mathsf{C}}^{-1} \cdot [\hat{\boldsymbol{z}} \times \mathsf{J}] \cdot \sqrt{\mathsf{C}}^{-1}$ is a congruence transformation of $[\hat{\boldsymbol{z}} \times \mathsf{J}]$, which has the (double) eigenvalues -1, 0 and 1. Since the signs are preserved under congruence transformations, the eigenvalues can be characterized by

$$\begin{cases} \lambda_{1,2} > 0 \\ \lambda_{3,4} < 0 \\ \lambda_{5,6} = 0. \end{cases} \tag{6.11}$$

Since the u_j:s are eigenvectors to a symmetric dyadic, they are real and mutually orthogonal. This implies that $\mathsf{a}_j = \sqrt{\mathsf{C}}^{-1} \cdot \mathsf{u}_j$ are linearly independent vectors. The eigenvectors corresponding to $\lambda_{5,6}$ can be constructed from $\mathsf{a}_{5,6} = \binom{\pm\hat{\boldsymbol{z}}}{\hat{\boldsymbol{z}}}$, which implies that $\mathsf{a}_{1,2,3,4}$ are the only eigenvectors needed to form the tangential fields.

The sign of the eigenvalue indicates in which direction each mode represented by an eigenvector is propagating, *i.e.*, $\mathsf{a}_{1,2}$ represent waves propagating in the $+z$-direction and $\mathsf{a}_{3,4}$ represent waves propagating in the $-z$-direction, while $\mathsf{a}_{5,6}$ represent waves which do not propagate with respect to z at all.

6.5 Transmission

Temporarily introduce the dyadic

$$\mathsf{A} = k_z^{\mathrm{i}}[\mathbf{I} - \hat{\boldsymbol{z}}\hat{\boldsymbol{z}}] \cdot [\mathsf{I} - k_y^{\mathrm{i}}\hat{\boldsymbol{y}} \times \mathsf{J}]^{-1} \cdot [\hat{\boldsymbol{z}} \times \mathsf{J}]. \tag{6.12}$$

From (6.9) we see that $\dot{\mathsf{e}}_{\parallel}^{\mathrm{i,r}} = \pm\mathsf{A} \cdot \dot{\mathsf{e}}_{\parallel}^{\mathrm{i,r}}$. By multiplying the boundary condition $\dot{\mathsf{e}}_{\parallel}^{\mathrm{i}} + \dot{\mathsf{e}}_{\parallel}^{\mathrm{r}} = \dot{\mathsf{e}}_{\parallel}^{\mathrm{t}}$ with A we now have

$$\dot{\mathsf{e}}_{\parallel}^{\mathrm{i}} - \dot{\mathsf{e}}_{\parallel}^{\mathrm{r}} = \mathsf{A} \cdot \dot{\mathsf{e}}_{\parallel}^{\mathrm{t}}. \tag{6.13}$$

In the previous section, we found that only the eigenvectors $\mathsf{a}_{1,2,3,4}$ involve the tangential fields. Specifically, $\mathsf{a}_{1,2}$ correspond to waves travelling in the $+z$-direction. To this end, the transmitted tangential field is expanded as

$$\dot{\mathsf{e}}_{\parallel}^{\mathrm{t}} = \sum_{j=1}^{2} \alpha_j [\mathbf{I} - \hat{\boldsymbol{z}}\hat{\boldsymbol{z}}] \cdot \mathsf{a}_j, \tag{6.14}$$

provided there are no sources in the region $z > 0$, *i.e.*, no waves travelling in the $-z$-direction. We have now restricted the number of simple waves in the nonlinear material to two. From (6.8) follows

$$\begin{aligned}\mathsf{A}\cdot[\mathbf{I}-\hat{\boldsymbol{z}}\hat{\boldsymbol{z}}]\cdot\mathsf{a}_j &= k_z^{\mathrm{i}}[\mathbf{I}-\hat{\boldsymbol{z}}\hat{\boldsymbol{z}}]\cdot[\mathsf{I}-k_y^{\mathrm{i}}\hat{\boldsymbol{y}}\times\mathsf{J}]^{-1}\cdot[\hat{\boldsymbol{z}}\times\mathsf{J}]\cdot[\mathbf{I}-\hat{\boldsymbol{z}}\hat{\boldsymbol{z}}]\cdot\mathsf{a}_j\\ &= \lambda_j k_z^{\mathrm{i}}[\mathbf{I}-\hat{\boldsymbol{z}}\hat{\boldsymbol{z}}]\cdot[\mathsf{I}-k_y^{\mathrm{i}}\hat{\boldsymbol{y}}\times\mathsf{J}]^{-1}\cdot[\boldsymbol{\varepsilon}-k_y^{\mathrm{i}}\hat{\boldsymbol{y}}\times\mathsf{J}]\cdot\mathsf{a}_j,\end{aligned} \tag{6.15}$$

where we have used $[\hat{\boldsymbol{z}}\times\mathsf{J}]\cdot[\mathbf{I}-\hat{\boldsymbol{z}}\hat{\boldsymbol{z}}]=[\hat{\boldsymbol{z}}\times\mathsf{J}]$. The dyadic

$$\begin{aligned}\mathsf{B} &= [\mathsf{I}-k_y^{\mathrm{i}}\hat{\boldsymbol{y}}\times\mathsf{J}]^{-1}\cdot[\boldsymbol{\varepsilon}-k_y^{\mathrm{i}}\hat{\boldsymbol{y}}\times\mathsf{J}]\\ &= \mathsf{I}+[\mathsf{I}-k_y^{\mathrm{i}}\hat{\boldsymbol{y}}\times\mathsf{J}]^{-1}\cdot[\boldsymbol{\varepsilon}-\mathsf{I}]\end{aligned} \tag{6.16}$$

is positive definite with eigenvalues greater than one. The boundary conditions are

$$\begin{cases}\dot{\mathsf{e}}_{\parallel}^{\mathrm{i}}+\dot{\mathsf{e}}_{\parallel}^{\mathrm{r}}=\displaystyle\sum_{j=1}^{2}\alpha_j[\mathbf{I}-\hat{\boldsymbol{z}}\hat{\boldsymbol{z}}]\cdot\mathsf{a}_j\\ \dot{\mathsf{e}}_{\parallel}^{\mathrm{i}}-\dot{\mathsf{e}}_{\parallel}^{\mathrm{r}}=\displaystyle\sum_{j=1}^{2}\alpha_j\lambda_j k_z^{\mathrm{i}}[\mathbf{I}-\hat{\boldsymbol{z}}\hat{\boldsymbol{z}}]\cdot\mathsf{B}\cdot\mathsf{a}_j.\end{cases} \tag{6.17}$$

By adding these equations, we eliminate the reflected field, and obtain

$$2\dot{\mathsf{e}}_{\parallel}^{\mathrm{i}}=\sum_{j=1}^{2}\alpha_j[\mathbf{I}-\hat{\boldsymbol{z}}\hat{\boldsymbol{z}}]\cdot[\mathsf{I}+\lambda_j k_z^{\mathrm{i}}\mathsf{B}]\cdot\mathsf{a}_j. \tag{6.18}$$

The only unknown quantities in this equation are the coefficients α_j. If we multiply the equation by $\mathsf{a}_{1,2}$ from the left, we obtain a 2×2 system, which is used to extract the coefficients $\alpha_{1,2}$:

$$\begin{cases}2\mathsf{a}_1\cdot\dot{\mathsf{e}}_{\parallel}^{\mathrm{i}}=\alpha_1\mathsf{a}_1\cdot[\mathbf{I}-\hat{\boldsymbol{z}}\hat{\boldsymbol{z}}]\cdot[\mathsf{I}+\lambda_1 k_z^{\mathrm{i}}\mathsf{B}]\cdot\mathsf{a}_1+\alpha_2\mathsf{a}_1\cdot[\mathbf{I}-\hat{\boldsymbol{z}}\hat{\boldsymbol{z}}]\cdot[\mathsf{I}+\lambda_2 k_z^{\mathrm{i}}\mathsf{B}]\cdot\mathsf{a}_2\\ 2\mathsf{a}_2\cdot\dot{\mathsf{e}}_{\parallel}^{\mathrm{i}}=\alpha_1\mathsf{a}_2\cdot[\mathbf{I}-\hat{\boldsymbol{z}}\hat{\boldsymbol{z}}]\cdot[\mathsf{I}+\lambda_1 k_z^{\mathrm{i}}\mathsf{B}]\cdot\mathsf{a}_1+\alpha_2\mathsf{a}_2\cdot[\mathbf{I}-\hat{\boldsymbol{z}}\hat{\boldsymbol{z}}]\cdot[\mathsf{I}+\lambda_2 k_z^{\mathrm{i}}\mathsf{B}]\cdot\mathsf{a}_2.\end{cases} \tag{6.19}$$

This system is always solvable provided the following determinant is non-zero:

$$\begin{aligned}\Delta =&(\mathsf{a}_1\cdot[\mathbf{I}-\hat{\boldsymbol{z}}\hat{\boldsymbol{z}}]\cdot[\mathsf{I}+\lambda_1 k_z^{\mathrm{i}}\mathsf{B}]\cdot\mathsf{a}_1)(\mathsf{a}_2\cdot[\mathbf{I}-\hat{\boldsymbol{z}}\hat{\boldsymbol{z}}]\cdot[\mathsf{I}+\lambda_2 k_z^{\mathrm{i}}\mathsf{B}]\cdot\mathsf{a}_2)\\ &-(\mathsf{a}_2\cdot[\mathbf{I}-\hat{\boldsymbol{z}}\hat{\boldsymbol{z}}]\cdot[\mathsf{I}+\lambda_1 k_z^{\mathrm{i}}\mathsf{B}]\cdot\mathsf{a}_1)(\mathsf{a}_1\cdot[\mathbf{I}-\hat{\boldsymbol{z}}\hat{\boldsymbol{z}}]\cdot[\mathsf{I}+\lambda_2 k_z^{\mathrm{i}}\mathsf{B}]\cdot\mathsf{a}_2)\\ =&(\mathsf{a}_1\cdot\mathsf{v}_1)(\mathsf{a}_2\cdot\mathsf{v}_2)-(\mathsf{a}_2\cdot\mathsf{v}_1)(\mathsf{a}_1\cdot\mathsf{v}_2)\\ =&\mathsf{a}_1\cdot(\mathsf{v}_1\mathsf{v}_2-\mathsf{v}_2\mathsf{v}_1)\cdot\mathsf{a}_2,\end{aligned} \tag{6.20}$$

where we have introduced the vectors $\mathsf{v}_{1,2}=[\mathbf{I}-\hat{\boldsymbol{z}}\hat{\boldsymbol{z}}]\cdot[\mathsf{I}+\lambda_{1,2}k_z^{\mathrm{i}}\mathsf{B}]\cdot\mathsf{a}_{1,2}=\mathsf{R}_{1,2}\cdot\mathsf{a}_{1,2}$. The dyadics $\mathsf{R}_{1,2}$ are positive semi-definite, where the semi-definiteness comes from the projection $[\mathbf{I}-\hat{\boldsymbol{z}}\hat{\boldsymbol{z}}]$. It is conjectured that these properties imply $\Delta>0$.

Using the explicit inverse of a 2×2-matrix, we can write the solution to (6.19) as

$$\begin{cases} \alpha_1 = \dfrac{2}{\Delta}\Big\{(\mathsf{a}_2 \cdot [\mathbf{I} - \hat{\boldsymbol{z}}\hat{\boldsymbol{z}}] \cdot [\mathsf{I} + \lambda_2 k_z^{\mathrm{i}} \mathsf{B}] \cdot \mathsf{a}_2)(\mathsf{a}_1 \cdot \dot{\mathsf{e}}_{\parallel}^{\mathrm{i}}) \\ \qquad\qquad -(\mathsf{a}_1 \cdot [\mathbf{I} - \hat{\boldsymbol{z}}\hat{\boldsymbol{z}}] \cdot [\mathsf{I} + \lambda_2 k_z^{\mathrm{i}} \mathsf{B}] \cdot \mathsf{a}_2)(\mathsf{a}_2 \cdot \dot{\mathsf{e}}_{\parallel}^{\mathrm{i}})\Big\} \\ \alpha_2 = \dfrac{2}{\Delta}\Big\{(\mathsf{a}_1 \cdot [\mathbf{I} - \hat{\boldsymbol{z}}\hat{\boldsymbol{z}}] \cdot [\mathsf{I} + \lambda_1 k_z^{\mathrm{i}} \mathsf{B}] \cdot \mathsf{a}_1)(\mathsf{a}_2 \cdot \dot{\mathsf{e}}_{\parallel}^{\mathrm{i}}) \\ \qquad\qquad -(\mathsf{a}_2 \cdot [\mathbf{I} - \hat{\boldsymbol{z}}\hat{\boldsymbol{z}}] \cdot [\mathsf{I} + \lambda_1 k_z^{\mathrm{i}} \mathsf{B}] \cdot \mathsf{a}_1)(\mathsf{a}_1 \cdot \dot{\mathsf{e}}_{\parallel}^{\mathrm{i}})\Big\}. \end{cases} \tag{6.21}$$

This can be written as $\alpha_{1,2} = \frac{2}{\Delta}\mathsf{b}_{1,2} \cdot \dot{\mathsf{e}}_{\parallel}^{\mathrm{i}}$ by introducing the vectors

$$\begin{cases} \mathsf{b}_1 = (\mathsf{a}_2 \cdot [\mathbf{I} - \hat{\boldsymbol{z}}\hat{\boldsymbol{z}}] \cdot [\mathsf{I} + \lambda_2 k_z^{\mathrm{i}} \mathsf{B}] \cdot \mathsf{a}_2)\mathsf{a}_1 - (\mathsf{a}_1 \cdot [\mathbf{I} - \hat{\boldsymbol{z}}\hat{\boldsymbol{z}}] \cdot [\mathsf{I} + \lambda_2 k_z^{\mathrm{i}} \mathsf{B}] \cdot \mathsf{a}_2)\mathsf{a}_2 \\ \mathsf{b}_2 = (\mathsf{a}_1 \cdot [\mathbf{I} - \hat{\boldsymbol{z}}\hat{\boldsymbol{z}}] \cdot [\mathsf{I} + \lambda_1 k_z^{\mathrm{i}} \mathsf{B}] \cdot \mathsf{a}_1)\mathsf{a}_2 - (\mathsf{a}_2 \cdot [\mathbf{I} - \hat{\boldsymbol{z}}\hat{\boldsymbol{z}}] \cdot [\mathsf{I} + \lambda_1 k_z^{\mathrm{i}} \mathsf{B}] \cdot \mathsf{a}_1)\mathsf{a}_1. \end{cases} \tag{6.22}$$

The map between $\mathsf{a}_{1,2}$ and $\mathsf{b}_{1,2}$ has the same determinant as the map between the coefficients $\alpha_{1,2}$ and the incident field, *i.e.*, Δ, which was assumed greater than zero above. This implies that the vectors $\mathsf{b}_{1,2}$ are linearly independent.

We now formulate the relation $\dot{\mathsf{e}}_{\parallel}^{\mathrm{t}} = \sum_{j=1}^{2} \alpha_j [\mathbf{I} - \hat{\boldsymbol{z}}\hat{\boldsymbol{z}}] \cdot \mathsf{a}_j$ as a dyadic relation between incident and transmitted fields,

$$\begin{aligned} \dot{\mathsf{e}}_{\parallel}^{\mathrm{t}} =& \frac{2}{\Delta}[\mathbf{I} - \hat{\boldsymbol{z}}\hat{\boldsymbol{z}}] \cdot [\mathsf{a}_1\mathsf{b}_1 + \mathsf{a}_2\mathsf{b}_2] \cdot \dot{\mathsf{e}}_{\parallel}^{\mathrm{i}} \\ =& \mathsf{T}_{\parallel} \cdot \dot{\mathsf{e}}_{\parallel}^{\mathrm{i}}, \end{aligned} \tag{6.23}$$

where we have introduced the notation $\mathsf{T}_{\parallel}$ for the transmission dyadic acting on the tangential fields. Since the transmitted field consists of only the modes $\mathsf{a}_{1,2}$, the transmission dyadic extends to the total transmitted field:

$$\dot{\mathsf{e}}^{\mathrm{t}} = \frac{2}{\Delta}[\mathsf{a}_1\mathsf{b}_1 + \mathsf{a}_2\mathsf{b}_2] \cdot \dot{\mathsf{e}}_{\parallel}^{\mathrm{i}} = \mathsf{T} \cdot \dot{\mathsf{e}}_{\parallel}^{\mathrm{i}}. \tag{6.24}$$

Since the vectors $\mathsf{b}_{1,2}$ are linearly independent, they represent the two different polarizations of the incident field which generate the two possible modes $\mathsf{a}_{1,2}$ in the nonlinear material.

6.6 Reflection and Brewster angles

It is well known that at certain angles and polarizations of the incident field there is no reflected field at all — the Brewster angles [22, 26, 27]. From (6.17) we see that the reflected field can be written

$$2\dot{\mathsf{e}}_{\parallel}^{\mathrm{r}} = \sum_{j=1}^{2} \alpha_j [\mathbf{I} - \hat{\boldsymbol{z}}\hat{\boldsymbol{z}}] \cdot [\mathsf{I} - \lambda_j k_z^{\mathrm{i}} \mathsf{B}] \cdot \mathsf{a}_j. \tag{6.25}$$

Using $\alpha_{1,2} = \frac{2}{\Delta}\mathsf{b}_{1,2} \cdot \dot{\mathsf{e}}^{\mathrm{i}}_{\parallel}$ we find the following relationship between the reflected and incident field:

$$\begin{aligned} 2\dot{\mathsf{e}}^{\mathrm{r}}_{\parallel} =& \frac{2}{\Delta}\Big[\left\{[\mathbf{I} - \hat{\boldsymbol{z}}\hat{\boldsymbol{z}}] \cdot [\mathsf{I} - \lambda_1 k^{\mathrm{i}}_z \mathsf{B}] \cdot \mathsf{a}_1\right\} \mathsf{b}_1 \\ &+ \left\{[\mathbf{I} - \hat{\boldsymbol{z}}\hat{\boldsymbol{z}}] \cdot [\mathsf{I} - \lambda_2 k^{\mathrm{i}}_z \mathsf{B}] \cdot \mathsf{a}_2\right\} \mathsf{b}_2\Big] \cdot \dot{\mathsf{e}}^{\mathrm{i}}_{\parallel} \\ =& \frac{2}{\Delta}[\mathbf{I} - \hat{\boldsymbol{z}}\hat{\boldsymbol{z}}] \cdot [\mathsf{b}'_1\mathsf{b}_1 + \mathsf{b}'_2\mathsf{b}_2] \cdot \dot{\mathsf{e}}^{\mathrm{i}}_{\parallel} \\ =& 2\mathsf{R}_{\parallel} \cdot \dot{\mathsf{e}}^{\mathrm{i}}_{\parallel}. \end{aligned} \tag{6.26}$$

This is the reflection dyadic $\mathsf{R}_{\parallel}$ for the tangential fields, which is represented as a factorization in the simple dyads $\mathsf{b}'_1\mathsf{b}_1$ and $\mathsf{b}'_2\mathsf{b}_2$, where $\mathsf{b}'_{1,2} = [\mathsf{I} - \lambda_{1,2} k^{\mathrm{i}}_z \mathsf{B}] \cdot \mathsf{a}_{1,2}$.

Since the vectors $\mathsf{b}_{1,2}$ are linearly independent, we see that the Brewster angles are characterized by

$$\begin{cases} \dot{\mathsf{e}}^{\mathrm{i}}_{\parallel} = \beta[\mathbf{I} - \hat{\boldsymbol{z}}\hat{\boldsymbol{z}}] \cdot \mathsf{b}_j \\ 0 = [\mathbf{I} - \hat{\boldsymbol{z}}\hat{\boldsymbol{z}}] \cdot [\mathsf{I} - \lambda_j k^{\mathrm{i}}_z \mathsf{B}] \cdot \mathsf{a}_j \end{cases} \quad j = 1, 2, \tag{6.27}$$

where β is a scalar. This means that if the incident field is polarized along b_j and a_j is in the null space of $[\mathbf{I} - \hat{\boldsymbol{z}}\hat{\boldsymbol{z}}] \cdot [\mathsf{I} - \lambda_j k^{\mathrm{i}}_z \mathsf{B}]$, there is no reflected field. These conditions determine the possible Brewster angles. We have

$$\begin{aligned} 0 &= [\mathbf{I} - \hat{\boldsymbol{z}}\hat{\boldsymbol{z}}] \cdot [\mathsf{I} - \lambda_j k^{\mathrm{i}}_z \mathsf{B}] \cdot \mathsf{a}_j \\ &= [\mathbf{I} - \hat{\boldsymbol{z}}\hat{\boldsymbol{z}}] \cdot [\mathsf{I} - \frac{c_j}{c_0}\frac{k^{\mathrm{i}}_z}{k^{\mathrm{t}}_{zj}}(\mathsf{I} + [\mathsf{I} - k^{\mathrm{i}}_y \hat{\boldsymbol{y}} \times \mathsf{J}]^{-1} \cdot [\boldsymbol{\varepsilon} - \mathsf{I}])] \cdot \mathsf{a}_j \\ &= [\mathbf{I} - \hat{\boldsymbol{z}}\hat{\boldsymbol{z}}] \cdot [\mathsf{I} - \frac{c_j}{c_0}\frac{k^{\mathrm{i}}_z}{k^{\mathrm{t}}_{zj}}(\mathsf{I} + \frac{1}{(k^{\mathrm{i}}_z)^2}[\mathsf{I} + k^{\mathrm{i}}_y \hat{\boldsymbol{y}} \times \mathsf{J} - (k^{\mathrm{i}}_y)^2 \hat{\boldsymbol{y}}\hat{\boldsymbol{y}}] \cdot [\boldsymbol{\varepsilon} - \mathsf{I}])] \cdot \mathsf{a}_j, \end{aligned} \tag{6.28}$$

where we have introduced the explicit inverse $[\mathsf{I} - k^{\mathrm{i}}_y \hat{\boldsymbol{y}} \times \mathsf{J}]^{-1} = \frac{1}{(k^{\mathrm{i}}_z)^2}[\mathsf{I} + k^{\mathrm{i}}_y \hat{\boldsymbol{y}} \times \mathsf{J} - (k^{\mathrm{i}}_y)^2 \hat{\boldsymbol{y}}\hat{\boldsymbol{y}}]$, which can be verified by straightforward calculations. The y-component of this equation is

$$\begin{aligned} 0 &= \hat{\boldsymbol{y}} \cdot \mathsf{a}_j - \frac{c_j}{c_0}\frac{k^{\mathrm{i}}_z}{k^{\mathrm{t}}_{zj}}(\hat{\boldsymbol{y}} + \frac{1}{(k^{\mathrm{i}}_z)^2}[\hat{\boldsymbol{y}} - (k^{\mathrm{i}}_y)^2 \hat{\boldsymbol{y}}] \cdot [\boldsymbol{\varepsilon} - \mathsf{I}]) \cdot \mathsf{a}_j \\ &= \hat{\boldsymbol{y}} \cdot \mathsf{a}_j - \frac{c_j}{c_0}\frac{k^{\mathrm{i}}_z}{k^{\mathrm{t}}_{zj}}(\hat{\boldsymbol{y}} + \hat{\boldsymbol{y}} \cdot [\boldsymbol{\varepsilon} - \mathsf{I}]) \cdot \mathsf{a}_j \\ &= \hat{\boldsymbol{y}} \cdot \mathsf{a}_j - \frac{c_j}{c_0}\frac{k^{\mathrm{i}}_z}{k^{\mathrm{t}}_{zj}}\hat{\boldsymbol{y}} \cdot \boldsymbol{\varepsilon} \cdot \mathsf{a}_j. \end{aligned} \tag{6.29}$$

6.6.1 Isotropic materials

In Section 4 it was shown that a propagating field in an isotropic material is described by $\mathsf{a}_j = \begin{pmatrix} \boldsymbol{v}_j/\sqrt{\epsilon} \\ \hat{\boldsymbol{k}} \times \boldsymbol{v}_j/\sqrt{\mu} \end{pmatrix}$, where the three-vector $\boldsymbol{v}_j$ is orthogonal to $\hat{\boldsymbol{k}}$, and the only possible wave speed is $\frac{c_j}{c_0} = \frac{1}{\sqrt{\epsilon\mu}}$. In the remainder of this section, we suppress the index j,

and separate the two modes in the end. The Brewster angles can now be found from the y-component defined above. By explicitly considering both electric and magnetic fields we have

$$\begin{aligned}\hat{\boldsymbol{y}}\cdot\begin{pmatrix}\frac{1}{\sqrt{\epsilon}}\boldsymbol{v}\\ \frac{1}{\sqrt{\mu}}\hat{\boldsymbol{k}}^{\mathrm{t}}\times\boldsymbol{v}\end{pmatrix}&=\frac{1}{\sqrt{\epsilon\mu}}\frac{k_z^{\mathrm{i}}}{k_z^{\mathrm{t}}}\hat{\boldsymbol{y}}\cdot\begin{pmatrix}\sqrt{\epsilon}\boldsymbol{v}\\ \sqrt{\mu}\hat{\boldsymbol{k}}^{\mathrm{t}}\times\boldsymbol{v}\end{pmatrix}\\ \begin{pmatrix}\frac{1}{\sqrt{\epsilon}}\hat{\boldsymbol{y}}\cdot\boldsymbol{v}\\ \frac{1}{\sqrt{\mu}}k_z^{\mathrm{t}}\hat{\boldsymbol{z}}\cdot(\boldsymbol{v}\times\hat{\boldsymbol{y}})\end{pmatrix}&=\frac{k_z^{\mathrm{i}}}{k_z^{\mathrm{t}}}\begin{pmatrix}\frac{1}{\sqrt{\mu}}\hat{\boldsymbol{y}}\cdot\boldsymbol{v}\\ \frac{1}{\sqrt{\epsilon}}k_z^{\mathrm{t}}\hat{\boldsymbol{z}}\cdot(\boldsymbol{v}\times\hat{\boldsymbol{y}})\end{pmatrix}.\end{aligned}\tag{6.30}$$

It is now concluded that one of the following sets of conditions have to be satisfied in order to satisfy the Brewster angle criterion.

$$\begin{cases}\hat{\boldsymbol{y}}\cdot\boldsymbol{v}=0\\ \sqrt{\epsilon}k_z^{\mathrm{t}}=\sqrt{\mu}k_z^{\mathrm{i}}\end{cases}\quad\text{or}\quad\begin{cases}\hat{\boldsymbol{z}}\cdot(\boldsymbol{v}\times\hat{\boldsymbol{y}})=0\\ \sqrt{\mu}k_z^{\mathrm{t}}=\sqrt{\epsilon}k_z^{\mathrm{i}}.\end{cases}\tag{6.31}$$

Observe that $\hat{\boldsymbol{z}}\cdot(\boldsymbol{v}\times\hat{\boldsymbol{y}})=0$ is equivalent to $\hat{\boldsymbol{x}}\cdot\boldsymbol{v}=0$, *i.e.*, the first set of conditions corresponds to TE-polarization and the second to TM-polarization. Remember that $k_z^{\mathrm{i}}=\cos\theta^{\mathrm{i}}$ and $k_z^{\mathrm{t}}=\cos\theta^{\mathrm{t}}$, where $\theta^{\mathrm{i,t}}$ denote the angles of incidence and transmission, respectively, and we have recovered the well known results for linear isotropic materials. Since we in general have $\theta^{\mathrm{t}}<\theta^{\mathrm{i}}$, only one of the above possible Brewster angles is feasible.

An interesting question is whether it always suffices to study the y-component of our original Brewster-angle-condition in (6.27). This is a problem that goes beyond the scope of this paper.

6.7 Algorithm for the direct problem

In this section we summarize the algorithm for solving the direct problem of propagating the incident field through a boundary between vacuum and a nonlinear, nondispersive, homogeneous, bianisotropic halfspace.

We have to calculate the eigenvectors $\mathsf{a}_{1,2}$, the eigenvalues $\lambda_{1,2}$ and the dyadic B to obtain the reflection and transmission dyadics. These quantities are determined from the relations

$$\begin{cases}\lambda_j\mathsf{a}_j=[\boldsymbol{\varepsilon}-k_y^{\mathrm{i}}\hat{\boldsymbol{y}}\times\mathsf{J}]^{-1}\cdot[\hat{\boldsymbol{z}}\times\mathsf{J}]\cdot\mathsf{a}_j\\ \mathsf{B}=[\mathsf{I}-k_y^{\mathrm{i}}\hat{\boldsymbol{y}}\times\mathsf{J}]^{-1}\cdot[\boldsymbol{\varepsilon}-k_y^{\mathrm{i}}\hat{\boldsymbol{y}}\times\mathsf{J}],\end{cases}\tag{6.32}$$

i.e., we have to solve an eigenvalue problem (first row), extract the eigenvectors corresponding to positive eigenvalues, and calculate the dyadic B. These calculations are evaluated at the transmitted field values at a specific time. The dyadics are supposed to act on time derivatives of the fields. We discretize the problem with central differences in time, and use the previously calculated values for the transmitted fields in the solution of the eigenvalue problem.

Once we have calculated the tangential fields, it is an easy task to obtain the normal components of the fields. For the transmitted fields these are already given

by the transmission dyadic, see (6.24), and for the reflected field they are given by the relation $\hat{\boldsymbol{k}}^{\mathrm{r}} \cdot \dot{\mathsf{e}}^{\mathrm{r}} = 0$, which implies $\dot{\mathsf{e}}^{\mathrm{r}}_z = -\frac{k^{\mathrm{r}}_y}{k^{\mathrm{r}}_z}\dot{\mathsf{e}}^{\mathrm{r}}_y$.

The algorithm can be summarized as follows, where the indices denote at which time level the different quantities are to be evaluated.

$$\begin{aligned}
(\text{eigenvalue problem})_j &\Rightarrow (\lambda_{1,2})_j, (\mathsf{a}_{1,2})_j \\
(\mathsf{B})_j &= \mathsf{B}((\mathsf{e}^{\mathrm{t}})_j) \\
(\mathsf{T})_j &= \mathsf{T}((\lambda_{1,2})_j, (\mathsf{a}_{1,2})_j, (\mathsf{B})_j) \\
(\mathsf{R}_{\parallel})_j &= \mathsf{R}_{\parallel}((\lambda_{1,2})_j, (\mathsf{a}_{1,2})_j, (\mathsf{B})_j) \\
(\dot{\mathsf{e}}^{\mathrm{i}}_{\parallel})_j &= \frac{(\mathsf{e}^{\mathrm{i}}_{\parallel})_{j+1} - (\mathsf{e}^{\mathrm{i}}_{\parallel})_{j-1}}{2\Delta t} \\
(\mathsf{e}^{\mathrm{t}})_{j+1} &= (\mathsf{e}^{\mathrm{t}})_{j-1} + 2\Delta t(\mathsf{T})_j \cdot (\dot{\mathsf{e}}^{\mathrm{i}}_{\parallel})_j \\
(\mathsf{e}^{\mathrm{r}}_{\parallel})_{j+1} &= (\mathsf{e}^{\mathrm{r}}_{\parallel})_{j-1} + 2\Delta t(\mathsf{R}_{\parallel})_j \cdot (\dot{\mathsf{e}}^{\mathrm{i}}_{\parallel})_j \\
(\mathsf{e}^{\mathrm{r}}_z)_{j+1} &= -\frac{k^{\mathrm{r}}_y}{k^{\mathrm{r}}_z}(\mathsf{e}^{\mathrm{r}}_y)_{j+1}
\end{aligned} \tag{6.33}$$

6.8 Numerical examples

When implementing the equations in a computer program, it is advantageous to scale the problem. The Maxwell equations are

$$[\nabla \times \mathsf{J}] \cdot \mathsf{e} + \frac{1}{c_0}\boldsymbol{\varepsilon}(\mathsf{e}) \cdot \partial_t \mathsf{e} = 0, \tag{6.34}$$

and we introduce the dimensionless variables

$$\begin{cases}
\tilde{t} = t/t_0 \\
\tilde{\boldsymbol{r}} = \boldsymbol{r}/(c_0 t_0) \\
\tilde{\mathsf{e}} = \mathsf{e}/e_0 \\
\tilde{\boldsymbol{\varepsilon}}(\tilde{\mathsf{e}}) = \boldsymbol{\varepsilon}(e_0\tilde{\mathsf{e}})
\end{cases} \tag{6.35}$$

where t_0 and e_0 are scalar constants, corresponding to a characteristic time and energy density, respectively. Using these variables, the Maxwell equations turn into

$$[\tilde{\nabla} \times \mathsf{J}] \cdot \tilde{\mathsf{e}} + \tilde{\boldsymbol{\varepsilon}} \cdot \partial_{\tilde{t}}\tilde{\mathsf{e}} = 0, \tag{6.36}$$

where the scaling constants t_0 and e_0 enable us to use dimensionless space-time and field strengths of reasonable numerical sizes. This scaling is also presented in [23, 34].

6.8.1 Reflection

The algorithm in Section 6.7 has been implemented for a nonlinear, anisotropic material, and the result is depicted in Figure 2. The constitutive relation is characterized by the six-dyadic $\boldsymbol{\varepsilon}$, which is represented in the xyz-coordinate system as

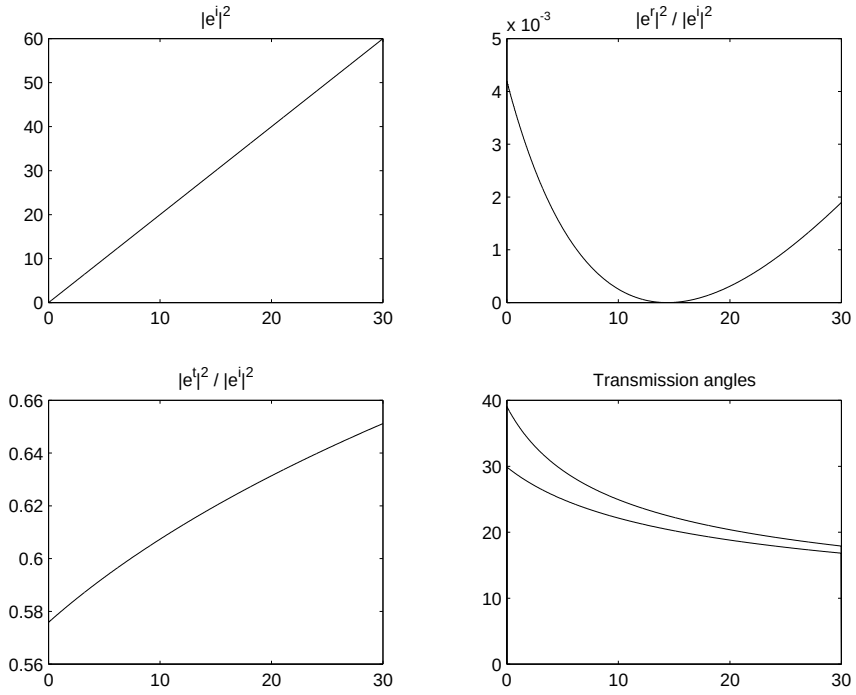

Figure 2: Oblique incidence on an anisotropic Kerr material, described by (6.37). The diagrams show the square of the incident field versus time, $|\tilde{\mathsf{e}}^{\mathrm{r}}|^2/|\tilde{\mathsf{e}}^{\mathrm{i}}|^2$ and $|\tilde{\mathsf{e}}^{\mathrm{t}}|^2/|\tilde{\mathsf{e}}^{\mathrm{i}}|^2$ versus time, respectively, and the two possible transmission angles versus time. Observe that since the square of the incident field is proportional to time, the horizontal scales can be used both as time and energy density of the incident field.

$$\tilde{\boldsymbol{\varepsilon}}(\tilde{\mathsf{e}}) = \begin{bmatrix} 2+\tilde{E}^2 & 0 & 0 & 0 & 0 & 0 \\ 0 & 3+\tilde{E}^2 & 0 & 0 & 0 & 0 \\ 0 & 0 & 4+\tilde{E}^2 & 0 & 0 & 0 \\ 0 & 0 & 0 & 1 & 0 & 0 \\ 0 & 0 & 0 & 0 & 1 & 0 \\ 0 & 0 & 0 & 0 & 0 & 1 \end{bmatrix}, \tag{6.37}$$

where we have decomposed the six-vector according to $\tilde{\mathsf{e}} = \binom{\tilde{\boldsymbol{E}}}{\tilde{\boldsymbol{H}}}$, and used the notation $|\tilde{\boldsymbol{E}}| = \tilde{E}$ for the absolute value of the three-vector $\tilde{\boldsymbol{E}}$. Thus, the material is non-magnetic, anisotropic with principal axes in the xyz-directions, and has a nonlinear permittivity depending on the square of the electric field strength. The angle of incidence, 63°, is chosen so that the Brewster angle is apparent. The incident field has the magnetic field perpendicular to the plane of incidence, *i.e.*, in the x-direction,

$$\tilde{\mathsf{e}}^{\mathrm{i}}(\tilde{\boldsymbol{r}},\tilde{t}) = f(\tilde{t}-\hat{\boldsymbol{k}}^{\mathrm{i}}\cdot\tilde{\boldsymbol{r}})\begin{pmatrix} -\hat{\boldsymbol{k}}^{\mathrm{i}}\times\hat{\boldsymbol{x}} \\ \hat{\boldsymbol{x}} \end{pmatrix}, \quad f(\tilde{t}) = \begin{cases} \sqrt{\tilde{t}} & \tilde{t}\geq 0 \\ 0 & \tilde{t}<0. \end{cases} \tag{6.38}$$

The time dependence of the amplitude of the incident field has been chosen so that its square, which in vacuum is the field energy density, depends linearly on time. This implies that the horizontal scales in Figure 2 can be used both as time and energy density. We see that the energy reflection coefficient $|\tilde{\mathsf{e}}^{\mathrm{r}}|^2/|\tilde{\mathsf{e}}^{\mathrm{i}}|^2$ and $|\tilde{\mathsf{e}}^{\mathrm{t}}|^2/|\tilde{\mathsf{e}}^{\mathrm{i}}|^2$ (which is *not* the energy transmission coefficient) depends strongly on the incident energy.

It is clearly seen that the Brewster angle occurs when the incident energy is approximately 15. Had the principle axis of the material not been in the xyz-directions, we would have needed another polarization of the incident field to obtain a reflected field that is zero.

The possible transmission angles start off as clearly separated, as can be expected for an anisotropic material, but become more and more equal as the incident energy increases. This can be interpreted from the material dyadic (6.37): when the electric field strength grows, the diagonal elements become essentially $\tilde{E}^2$. Thus the material becomes more and more isotropic, *i.e.*, it has only one possible angle of transmission. Observe that due to our choice of polarization of the incident field, only one of the modes is excited in this example.

6.8.2 Transmission

Up til now we have only dealt with the reflected field in vacuum and the transmitted field just inside the nonlinear material. We now wish to propagate this field some distance into the nonlinear material, and briefly return to the physical variables for clarity. We observe that the transmitted field satisfies a translational invariance in t and y,

$$\mathsf{e}^{\mathrm{t}}(\boldsymbol{r},t) = \mathsf{e}^{\mathrm{t}}(z, t - \frac{y\sin\theta^{\mathrm{i}}}{c_0}), \tag{6.39}$$

which implies that the derivatives in t and y are proportional,

$$\partial_y = -\frac{\sin\theta^{\mathrm{i}}}{c_0}\partial_t, \tag{6.40}$$

consistent with the simple wave approach. Assuming no propagation in the x-direction, the Maxwell equations

$$[\hat{\boldsymbol{y}} \times \mathsf{J}] \cdot \partial_y \mathsf{e}^{\mathrm{t}} + [\hat{\boldsymbol{z}} \times \mathsf{J}] \cdot \partial_z \mathsf{e}^{\mathrm{t}} + \frac{1}{c_0}\boldsymbol{\varepsilon} \cdot \partial_t \mathsf{e}^{\mathrm{t}} = 0 \tag{6.41}$$

are now turned into a system of one-dimensional equations,

$$\frac{1}{c_0}\partial_t \mathsf{e}^{\mathrm{t}} = -[\boldsymbol{\varepsilon}(\mathsf{e}^{\mathrm{t}}) - \sin\theta^{\mathrm{i}}\hat{\boldsymbol{y}} \times \mathsf{J}]^{-1} \cdot [\hat{\boldsymbol{z}} \times \mathsf{J}] \cdot \partial_z \mathsf{e}^{\mathrm{t}}. \tag{6.42}$$

This is used to propagate the transmitted field by a finite difference algorithm. We use a leap-frog scheme, approximating the derivatives with central differences. In our scaled variables this gives the following scheme, where $(\tilde{\mathsf{e}}^{\mathrm{t}})_n^m = \tilde{\mathsf{e}}^{\mathrm{t}}(\tilde{y}=0, n\Delta\tilde{z}, m\Delta\tilde{t})$,

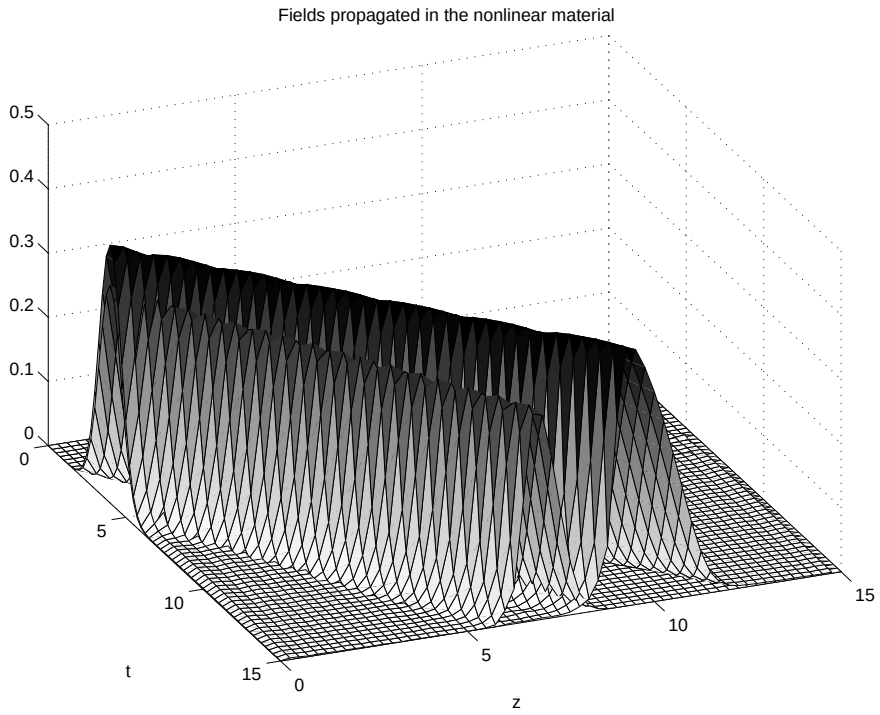

Figure 3: The x and y components of the transmitted electric field, each corresponding to exactly one of the two propagating modes. Due to the anisotropy, the modes have different polarization and propagation direction.

$$\frac{(\tilde{\mathsf{e}}^{\mathrm{t}})_n^{m+1} - (\tilde{\mathsf{e}}^{\mathrm{t}})_n^{m-1}}{2\Delta\tilde{t}} = -[\tilde{\boldsymbol{\varepsilon}}((\tilde{\mathsf{e}}^{\mathrm{t}})_n^m) - \sin\theta^{\mathrm{i}}\hat{\boldsymbol{y}} \times \mathsf{J}]^{-1} \cdot [\hat{\boldsymbol{z}} \times \mathsf{J}] \cdot \frac{(\tilde{\mathsf{e}}^{\mathrm{t}})_{n+1}^m - (\tilde{\mathsf{e}}^{\mathrm{t}})_{n-1}^m}{2\Delta\tilde{z}} \quad (6.43)$$

We use this algorithm for the same material as in Section 6.8.1, but with a Gaussian shaped incident field,

$$\tilde{\mathsf{e}}^{\mathrm{i}}(\tilde{\boldsymbol{r}}, \tilde{t}) = f(\tilde{t} - \hat{\boldsymbol{k}}^{\mathrm{i}} \cdot \tilde{\boldsymbol{r}}) \begin{pmatrix} \hat{\boldsymbol{v}} \\ \hat{\boldsymbol{k}}^{\mathrm{i}} \times \hat{\boldsymbol{v}} \end{pmatrix}, \quad f(\tilde{t}) = \exp(-(\tilde{t} - 4)^2). \quad (6.44)$$

The electric field is polarized in the direction $\hat{\boldsymbol{v}} = (\hat{\boldsymbol{x}} + \hat{\boldsymbol{k}}^{\mathrm{i}} \times \hat{\boldsymbol{x}})/\sqrt{2}$, to ensure that both modes are excited in the anisotropic material. From Figure 3 we see that the anisotropy of the material causes the two modes to travel in different directions, and the nonlinearity causes a change of shape in each of the modes. The latter implies that the region of existence of the simple waves is in general bounded, since the waves ultimately turn into shocks. This is also stated in [36].

7 Conclusions

In this paper, we have introduced the concept of simple waves, as a means to analyze wave propagation problems in nonlinear materials with instantaneous response. We have applied the method to the problem of oblique incidence of a plane electromagnetic wave on a nonlinear material, and found that the direct problem can be solved for all materials and all possible polarizations of the incident wave.

The drawback of the simple wave solutions, is that they do not apply to materials with dispersion, *i.e.*, materials with memory. Our mathematical model with instantaneous nonlinearity, predicts that *all* reasonable waves eventually turn into shocks. It is often argued that the presence of linear dispersion eliminates these shocks, see *e.g.*, [1, pp. 117–120]. Therefore, we can expect our model to be accurate only when there is no shock-like behavior and the dispersion effects are small, *i.e.*, for sufficiently smooth and slowly varying pulses. It is possible to calculate what propagation distances are necessary for the shock to develop, which means we can estimate the region of validity for our model.

8 Acknowledgments

The author wishes to express his sincere gratitude to Professor Gerhard Kristensson for invaluable support and encouragement during the work presented in this paper. The author's colleagues at the Department of Electromagnetic Theory are also acknowledged for valuable discussions and suggestions.

The work reported in this paper is partially supported by a grant from the Swedish Research Council for Engineering Sciences, and its support is gratefully acknowledged.

References

[1] G. P. Agrawal. *Nonlinear fiber optics.* Academic Press, San Diego, 1995.

[2] F. Bloom. *Mathematical problems of classical nonlinear electromagnetic theory.* Longman Scientific & Technical, Burnt Mill, Harlow, England, 1993.

[3] R. W. Boyd. *Nonlinear Optics.* Academic Press, San Diego, 1992.

[4] L. Brillouin. *Wave propagation and group velocity.* Academic Press, New York, 1960.

[5] L. J. F. Broer. Wave propagation in non-linear media. *Z. angew. Math. Phys.*, **16**, 18–26, 1965.

[6] L. J. F. Broer and P. H. A. Sarluy. On simple waves in non-linear dielectric media. *Physica*, **30**, 1421–1432, 1964.

[7] A. Chelkowski. *Dielectric Physics.* Elsevier Science Publishers, Amsterdam, 1980.

[8] B. D. Coleman and E. H. Dill. Thermodynamic restrictions on the constitutive equations of electromagnetic theory. *Z. angew. Math. Phys.*, **22**, 691–702, 1971.

[9] A. C. Eringen and G. A. Maugin. *Electrodynamics of Continua I.* Springer-Verlag, New York, 1990.

[10] A. C. Eringen and G. A. Maugin. *Electrodynamics of Continua II*. Springer-Verlag, New York, 1990.

[11] H. Goldstein. *Classical Mechanics*. Addison-Wesley, Reading, MA, USA, second edition, 1980.

[12] M. Gustafsson. Time domain theory of the macroscopic Maxwell equations. Technical Report LUTEDX/(TEAT-7062)/1–24/(1997), Lund Institute of Technology, Department of Electromagnetic Theory, P.O. Box 118, S-211 00 Lund, Sweden, 1997.

[13] L. Hörmander. *Lectures on Nonlinear Hyperbolic Differential Equations*. Number 26 in Mathémathiques & Applications. Springer-Verlag, Berlin, 1997.

[14] J. D. Jackson. *Classical Electrodynamics*. John Wiley & Sons, New York, third edition, 1999.

[15] A. Jeffrey. Wave propagation and electromagnetic shock wave formation in transmission lines. *J. Math. and Mech.*, **15**(1), 1–13, 1966.

[16] A. Jeffrey. *Quasilinear hyperbolic systems and waves*. Research Notes in Mathematics. Pitman, London, 1976.

[17] A. Jeffrey. Non-dispersive wave propagation in nonlinear dielectrics. *Z. angew. Math. Phys.*, **19**, 741–745, 1968.

[18] A. Jeffrey and V. P. Korobeinikov. Formation and decay of electromagnetic shock waves. *Z. angew. Math. Phys.*, **20**, 440–447, 1969.

[19] F. John. *Partial Differential Equations*. Springer-Verlag, New York, fourth edition, 1982.

[20] A. Karlsson and G. Kristensson. Constitutive relations, dissipation and reciprocity for the Maxwell equations in the time domain. *J. Electro. Waves Applic.*, **6**(5/6), 537–551, 1992.

[21] J. Y. Kazakia and R. Venkataraman. Propagation of electromagnetic waves in a nonlinear dielectric slab. *Z. angew. Math. Phys.*, **26**, 61–76, 1975.

[22] J. A. Kong. *Electromagnetic Wave Theory*. John Wiley & Sons, New York, 1986.

[23] G. Kristensson and D. J. N. Wall. Direct and inverse scattering for transient electromagnetic waves in nonlinear media. *Inverse Problems*, **14**, 113–137, 1998.

[24] A. Lakhtakia and W. S. Weiglhofer. Are linear, nonreciprocal, bi-isotropic media forbidden? *IEEE Trans. Microwave Theory Tech.*, **42**(9), 1715–1716, 1994.

[25] I. V. Lindell, A. H. Sihvola, and K. Suchy. Six-vector formalism in electromagnetics of bi-anisotropic media. *J. Electro. Waves Applic.*, **9**(7/8), 887–903, 1995.

[26] I. V. Lindell, A. H. Sihvola, S. A. Tretyakov, and A. J. Viitanen. *Electromagnetic Waves in Chiral and Bi-isotropic Media*. Artech House, Boston, London, 1994.

[27] I. V. Lindell, A. H. Sihvola, and A. J. Viitanen. Plane-wave reflection from a bi-isotropic (nonreciprocal chiral) interface. *Microwave Opt. Techn. Lett.*, **5**(2), 79–81, 1992.

[28] J. D. Logan. *An Introduction to Nonlinear Partial Differential Equations*. John Wiley & Sons, New York, 1994.

[29] E. J. Post. *Formal Structure of Electromagnetics*. North-Holland, Amsterdam, 1962.

[30] R. E. Raab and A. H. Sihvola. On the existence of linear non-reciprocal bi-isotropic (NRBI) media. *J. Phys. A: Math. Gen.*, **30**, 1335–1344, 1997.

[31] R. D. Richtmyer. *Principles of Advanced Mathematical Physics*, volume 1. Springer-Verlag, New York, 1978.

[32] C. Rogers, H. M. Cekirge, and A. Askar. Electromagnetic wave propagation in non-linear dielectric media. *Acta Mech.*, **26**, 59–73, 1977.

[33] A. Sihvola. Are nonreciprocal, bi-isotropic materials forbidden indeed? *IEEE Trans. Microwave Theory Tech.*, **43**(9), 2160–2162, 1995.

[34] D. Sjöberg. Reconstruction of nonlinear material properties for homogeneous, isotropic slabs using electromagnetic waves. *Inverse Problems*, **15**(2), 431–444, April 1999.

[35] B. D. H. Tellegen. The gyrator, a new electric network element. *Philips Res. Rep.*, **3**, 81–101, 1948.

[36] J. Veldhuis and H. Blok. Reflection and refraction of electromagnetic waves by the plane boundary of a non-linear medium: application of the simple wave theory. *J. Phys. A: Math. Gen.*, **11**(8), 1663–1680, 1978.

[37] G. B. Whitham. *Linear and nonlinear waves*. John Wiley & Sons, New York, 1974.

Nonlinear waveguides

Daniel Sjöberg

Paper III

Based on: D. Sjöberg. Nonlinear waveguides. Technical Report LUTEDX/(TEAT-7088)/1–26/(2000), Lund Institute of Technology.

Abstract

We investigate the propagation of electromagnetic waves in a waveguide filled with a nonlinear material. The electromagnetic field is expanded in the usual eigenmodes of the waveguide, and the coupling between the modes is quantified. We derive the wave equations governing each mode, with special emphasis on the situation with a dominant TE-mode. The result is a strictly hyperbolic system of nonlinear partial differential equations for the dominating mode, whereas the minor modes satisfy hyperbolic systems of linear, nonstationary, partial differential equations. A growth estimate is given for the minor modes.

1 Introduction

Electromagnetic waves can be guided in space by a hollow waveguide, where the walls are perfect electric conductors. This can be used to guide waves traveling from one point to another, and provide a controlled environment in which measurements can be made. In order to be able to interpret these measurements, we need to investigate what influence the waveguide structure and material or filling have on the wave propagation.

The waves can be decomposed in modes, which can be defined as the eigenfunctions of a transversal differential operator. These modes are orthogonal, and the wave equation for each mode decouples completely from the other modes for a linear, homogeneous filling. When the waveguide is filled with a nonlinear material, the equations no longer decouple, but it is still motivated to use the standard waveguide modes due to the possibility of using the resulting equations with a mode-matching algorithm in direct and inverse scattering problems [3, 16, 18].

In this paper we study the propagation of transient waves in nonlinear waveguides, *i.e.*, waves generated by an arbitrary signal. The theory of linear waveguides is well established since the major efforts during the second world war. The analysis is often made in the frequency domain, but since the nonlinear filling not only couples the modes but also induces a coupling between the different frequency components, we choose to treat the problem entirely in the time domain. The propagation of transient waves has been treated for linear materials in *e.g.*, [2, 6, 12], and some general references are [5, 15] and [10, Ch. 8].

There has been a number of papers on nonlinear waveguides. Some recent contributions consider the problem of self focusing, where the field energy inside the waveguide moves closer to the center as the wave propagates. A few early studies are found in [4, 11] and a more recent is [17]. The paper [19] discusses a problem similar to ours, where a modal expansion of the fields is attempted in a dielectric slab waveguide for a fixed frequency. The resulting equations are mainly used to determine where the energy will be localized.

This paper is organized as follows. In Section 2 we introduce the Maxwell equations and the instantaneous constitutive relations. The waveguide geometry is presented in Section 3, and the relevant expansion functions are derived. This is mostly established theory, but presented in a slightly different manner. Specifically,

the starting point is not the Helmholtz' equation, but a system of vector-valued equations. The eigenvalue zero now plays a different rôle. We use the expansion functions to obtain wave equations for each mode in Section 4, and the explicit results for a parallel plate waveguide are calculated in Section 5. Since even this simple example proves very challenging, we make the reasonable assumption that almost all the energy is contained in one mode in Section 6, which enables us to derive a system of quasilinear, homogeneous, hyperbolic differential equations for the dominant mode, and a system of inhomogeneous hyperbolic equations with source terms for the minor modes. Some energy relations are derived for both the dominant and the minor modes, allowing an estimate of the growth of the minor modes. The final conclusions and discussions are given in Section 7.

2 Preliminaries

In this paper we use a slight modification of the Heaviside-Lorentz units [10, p. 781], where the electromagnetic fields are scaled so that they all have the physical dimension $\sqrt{\text{energy/volume}}$,

$$\begin{cases} \boldsymbol{E} = \sqrt{\epsilon_0}\,\boldsymbol{E}_{\text{SI}} \\ \boldsymbol{H} = \sqrt{\mu_0}\,\boldsymbol{H}_{\text{SI}}, \end{cases} \qquad \begin{cases} \boldsymbol{D} = 1/\sqrt{\epsilon_0}\,\boldsymbol{D}_{\text{SI}} \\ \boldsymbol{B} = 1/\sqrt{\mu_0}\,\boldsymbol{B}_{\text{SI}}, \end{cases} \tag{2.1}$$

where $\boldsymbol{E}$ and $\boldsymbol{H}$ are the electric and magnetic field strength, respectively, and $\boldsymbol{D}$ and $\boldsymbol{B}$ are the electric and magnetic flux density, respectively. ϵ_0 is the permittivity of vacuum, and μ_0 is the permeability of vacuum. The speed of light in vacuum is $1/\sqrt{\epsilon_0\mu_0} = c_0$. We use instantaneous, isotropic constitutive relations, see [8, p. 231] and [20],

$$\begin{cases} \boldsymbol{D}(\boldsymbol{r},t) = F_{\text{e}}(E(\boldsymbol{r},t)^2)\boldsymbol{E}(\boldsymbol{r},t) \\ \boldsymbol{B}(\boldsymbol{r},t) = F_{\text{m}}(H(\boldsymbol{r},t)^2)\boldsymbol{H}(\boldsymbol{r},t), \end{cases} \tag{2.2}$$

where F_{e} and F_{m} are dimensionless functions of $E(\boldsymbol{r},t)^2 = |\boldsymbol{E}(\boldsymbol{r},t)|^2$ and $H(\boldsymbol{r},t)^2 = |\boldsymbol{H}(\boldsymbol{r},t)|^2$, respectively. We use the squared absolute values as arguments instead of the absolute values themselves, since this is beneficial in the final equations. The above constitutive relations imply that the time derivative of the fluxes can be written

$$\begin{cases} \partial_t \boldsymbol{D} = [F_{\text{e}}(E^2)\mathbf{I} + 2F'_{\text{e}}(E^2)\boldsymbol{E}\boldsymbol{E}] \cdot \partial_t \boldsymbol{E} = \boldsymbol{\epsilon}(\boldsymbol{E}) \cdot \partial_t \boldsymbol{E} \\ \partial_t \boldsymbol{B} = [F_{\text{m}}(H^2)\mathbf{I} + 2F'_{\text{m}}(H^2)\boldsymbol{H}\boldsymbol{H}] \cdot \partial_t \boldsymbol{H} = \boldsymbol{\mu}(\boldsymbol{H}) \cdot \partial_t \boldsymbol{H}. \end{cases} \tag{2.3}$$

We see that nonlinear, isotropic materials are described by non-diagonal dyadics $\boldsymbol{\epsilon}$ and $\boldsymbol{\mu}$. However, we refrain from this formulation of the time derivative in this paper. We now write the source free Maxwell equations as

$$\begin{cases} -\nabla \times \boldsymbol{H} + \dfrac{1}{c_0}\partial_t \boldsymbol{D} = \mathbf{0} \\ \nabla \times \boldsymbol{E} + \dfrac{1}{c_0}\partial_t \boldsymbol{B} = \mathbf{0} \end{cases} \implies \begin{cases} -\nabla \times \boldsymbol{H} + \dfrac{1}{c_0}\partial_t \left(F_{\text{e}}(E^2)\boldsymbol{E}\right) = \mathbf{0} \\ \nabla \times \boldsymbol{E} + \dfrac{1}{c_0}\partial_t \left(F_{\text{m}}(H^2)\boldsymbol{H}\right) = \mathbf{0}. \end{cases} \tag{2.4}$$

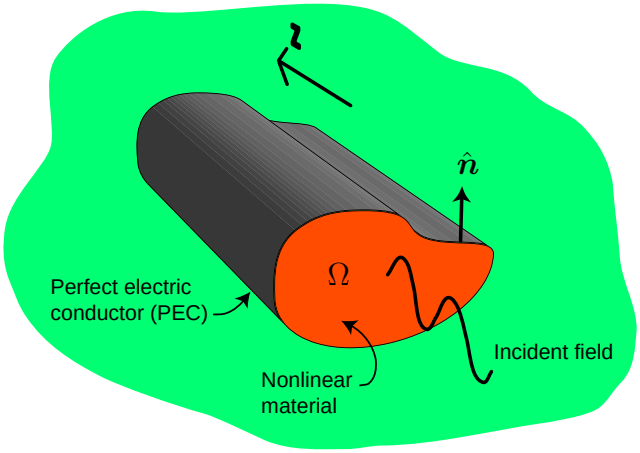

Figure 1: The geometry of a waveguide. The cross section of the cylinder is denoted by Ω, and the outward unit normal at the surface is denoted by $\hat{\boldsymbol{n}}$.

The purpose of the following section is to find suitable expansion functions for the fields $\boldsymbol{E}$ and $\boldsymbol{H}$, which simplifies the analysis of these equations.

3 Derivation of the expansion functions

The geometry of the waveguide is depicted in Figure 1. We wish to use the Maxwell equations to study propagation along the waveguide, *i.e.*, in the z-direction. To this end, we decompose the spatial differential operators and write the Maxwell equations as

$$\begin{cases} -\hat{\boldsymbol{z}} \times \partial_z \boldsymbol{H} + \dfrac{1}{c_0} \partial_t \left(F_{\mathrm{e}}(E^2) \boldsymbol{E} \right) = \nabla_{\mathrm{T}} \times \boldsymbol{H} \\ \hat{\boldsymbol{z}} \times \partial_z \boldsymbol{E} + \dfrac{1}{c_0} \partial_t \left(F_{\mathrm{m}}(H^2) \boldsymbol{H} \right) = -\nabla_{\mathrm{T}} \times \boldsymbol{E} \end{cases} \tag{3.1}$$

where $\nabla_{\mathrm{T}} = \hat{\boldsymbol{x}}\partial_x + \hat{\boldsymbol{y}}\partial_y$ and $\hat{\boldsymbol{x}}$, $\hat{\boldsymbol{y}}$, and $\hat{\boldsymbol{z}}$ denote the unit vector in the x, y, and z direction, respectively. The goal is now to get rid of the transversal dependence of the fields, and we start by simplifying the right hand side of this system of equations. We do this by searching for eigenfunctions of the transverse curl operators, which is a diagonalization of the transverse differential operator.

3.1 Eigenfunctions of the transverse curl operators

We see that the right hand side of (3.1) can be formulated as a differential operator applied to the pair of fields $\boldsymbol{E}$ and $\boldsymbol{H}$. It is natural to look for eigenfunctions to this operator, and we formulate the eigenproblem

$$\begin{pmatrix} \mathbf{0} & -\mathrm{i}\nabla_{\mathrm{T}} \times \mathbf{I} \\ \mathrm{i}\nabla_{\mathrm{T}} \times \mathbf{I} & \mathbf{0} \end{pmatrix} \begin{pmatrix} \boldsymbol{E}_n \\ \boldsymbol{H}_n \end{pmatrix} = \lambda_n \begin{pmatrix} \boldsymbol{E}_n \\ \boldsymbol{H}_n \end{pmatrix}, \tag{3.2}$$

where we have included the imaginary unit i so that the operator is self-adjoint in the scalar product

$$\left(\begin{pmatrix}\boldsymbol{E}_m\\ \boldsymbol{H}_m\end{pmatrix},\begin{pmatrix}\boldsymbol{E}_n\\ \boldsymbol{H}_n\end{pmatrix}\right)=\iint_\Omega(\boldsymbol{E}_m\cdot\boldsymbol{E}_n^*+\boldsymbol{H}_m\cdot\boldsymbol{H}_n^*)\,\mathrm{d}x\,\mathrm{d}y. \tag{3.3}$$

The self-adjointness can be shown by straight-forward calculations using integration by parts and the boundary condition $\hat{\boldsymbol{n}}\times\boldsymbol{E}=\boldsymbol{0}$, which is the usual boundary condition for a perfect electric conductor. Once we have established that the transverse curl operator in (3.2) is self-adjoint, we also know that all eigenvalues λ_n are real.

3.1.1 Boundary conditions

The boundary condition $\hat{\boldsymbol{n}}\times\boldsymbol{E}=\boldsymbol{0}$ is the only one needed for the analysis of the three-dimensional Maxwell equations, but we must check that our eigenproblem (3.2) does not imply inconsistent boundary conditions for the magnetic field strength. In this section we investigate which boundary conditions are imposed by the Maxwell equations, and compare them with those imposed by the eigenproblem.

We first note that since we have $\nabla\cdot\boldsymbol{B}=0$, we also have $\hat{\boldsymbol{n}}\cdot\boldsymbol{B}=0$ at the boundary. With $\boldsymbol{B}=F_{\mathrm{m}}(H^2)\boldsymbol{H}$, this implies $\hat{\boldsymbol{n}}\cdot\boldsymbol{H}=0$ at the boundary. Ampère's law $\nabla\times\boldsymbol{H}-\partial_t\boldsymbol{D}=\boldsymbol{0}$ must be satisfied on the boundary of the waveguide, which implies

$$\hat{\boldsymbol{n}}\times(\nabla\times\boldsymbol{H})-\hat{\boldsymbol{n}}\times\partial_t\boldsymbol{D}=\hat{\boldsymbol{n}}\times(\nabla\times\boldsymbol{H})=\boldsymbol{0} \tag{3.4}$$

on the boundary, since $\hat{\boldsymbol{n}}\times\boldsymbol{D}=\hat{\boldsymbol{n}}\times F_{\mathrm{e}}(E^2)\boldsymbol{E}=\boldsymbol{0}$. A closer look at this equation reveals that the z component of $\hat{\boldsymbol{n}}\times(\nabla\times\boldsymbol{H})=\boldsymbol{0}$ is

$$\hat{\boldsymbol{n}}\cdot\partial_z\boldsymbol{H}-(\hat{\boldsymbol{n}}\cdot\nabla_{\mathrm{T}})H_z=0\quad\Rightarrow\quad(\hat{\boldsymbol{n}}\cdot\nabla_{\mathrm{T}})H_z=0, \tag{3.5}$$

where the implication follows from the fact that $\hat{\boldsymbol{n}}$ is independent of z and therefore $\hat{\boldsymbol{n}}\cdot\partial_z\boldsymbol{H}=0$. The two conditions $\hat{\boldsymbol{n}}\cdot\boldsymbol{H}=0$ and $(\hat{\boldsymbol{n}}\cdot\nabla_{\mathrm{T}})H_z=0$ are precisely the boundary conditions implied by our eigenvalue problem.

Note carefully that we still have no conditions on $\hat{\boldsymbol{n}}\cdot\boldsymbol{E}$ and $(\hat{\boldsymbol{z}}\times\hat{\boldsymbol{n}})\cdot\boldsymbol{H}$. These components relate to the charge and current density on the walls of the waveguide, and can be used to study waveguides with a finite conductivity as in many textbooks, *e.g.*, [10, p. 366], [14, p. 317] and [5, p. 340]. This is not a problem we deal with in this paper.

3.1.2 Canonical problems

We show that the eigenproblem (3.2) implies the two-dimensional Helmholtz equation when $\lambda_n\neq0$ and all necessary derivatives exist. By applying the operator three

times, we have

$$\begin{aligned}
\lambda_n^3 \begin{pmatrix} \boldsymbol{E}_n \\ \boldsymbol{H}_n \end{pmatrix} &= \begin{pmatrix} \mathbf{0} & -\mathrm{i}\nabla_\mathrm{T} \times \mathbf{I} \\ \mathrm{i}\nabla_\mathrm{T} \times \mathbf{I} & \mathbf{0} \end{pmatrix}^3 \begin{pmatrix} \boldsymbol{E}_n \\ \boldsymbol{H}_n \end{pmatrix} \\
&= \begin{pmatrix} \mathbf{0} & -\mathrm{i}\nabla_\mathrm{T} \times \mathbf{I} \\ \mathrm{i}\nabla_\mathrm{T} \times \mathbf{I} & \mathbf{0} \end{pmatrix} \begin{pmatrix} \nabla_\mathrm{T} \times \nabla_\mathrm{T} \times \mathbf{I} & \mathbf{0} \\ \mathbf{0} & \nabla_\mathrm{T} \times \nabla_\mathrm{T} \times \mathbf{I} \end{pmatrix} \begin{pmatrix} \boldsymbol{E}_n \\ \boldsymbol{H}_n \end{pmatrix} \\
&= \begin{pmatrix} \mathbf{0} & -\mathrm{i}\nabla_\mathrm{T} \times \mathbf{I} \\ \mathrm{i}\nabla_\mathrm{T} \times \mathbf{I} & \mathbf{0} \end{pmatrix} \begin{pmatrix} \nabla_\mathrm{T}\nabla_\mathrm{T} - \nabla_\mathrm{T}^2 \mathbf{I} & \mathbf{0} \\ \mathbf{0} & \nabla_\mathrm{T}\nabla_\mathrm{T} - \nabla_\mathrm{T}^2 \mathbf{I} \end{pmatrix} \begin{pmatrix} \boldsymbol{E}_n \\ \boldsymbol{H}_n \end{pmatrix} \\
&= -\nabla_\mathrm{T}^2 \begin{pmatrix} \mathbf{0} & -\mathrm{i}\nabla_\mathrm{T} \times \mathbf{I} \\ \mathrm{i}\nabla_\mathrm{T} \times \mathbf{I} & \mathbf{0} \end{pmatrix} \begin{pmatrix} \boldsymbol{E}_n \\ \boldsymbol{H}_n \end{pmatrix} \\
&= -\nabla_\mathrm{T}^2 \lambda_n \begin{pmatrix} \boldsymbol{E}_n \\ \boldsymbol{H}_n \end{pmatrix},
\end{aligned} \tag{3.6}$$

where we have used that the curl of any gradient is zero and that the Laplace operator ∇_T^2 commutes with the curl operator. Thus, when $\lambda_n \neq 0$ the eigenproblem (3.2) implies the usual Helmholtz equation for the cross section,

$$\begin{cases}
\nabla_\mathrm{T}^2 \begin{pmatrix} \boldsymbol{E}_n \\ \boldsymbol{H}_n \end{pmatrix} + \lambda_n^2 \begin{pmatrix} \boldsymbol{E}_n \\ \boldsymbol{H}_n \end{pmatrix} = 0 & \text{in } \Omega \\
\hat{\boldsymbol{n}} \times \boldsymbol{E} = \mathbf{0} & \text{on } \partial\Omega \\
\hat{\boldsymbol{n}} \cdot \boldsymbol{H} = 0 & \text{on } \partial\Omega \\
(\hat{\boldsymbol{n}} \cdot \nabla_\mathrm{T}) H_z = 0 & \text{on } \partial\Omega.
\end{cases} \tag{3.7}$$

Since all components can be found from the z-components using the original eigenproblem (3.2), we now formulate the scalar canonical problems

$$\begin{aligned}
\text{TE} \quad &\begin{cases} \nabla_\mathrm{T}^2 \phi_n^\mathrm{TE} + (\lambda_n^\mathrm{TE})^2 \phi_n^\mathrm{TE} = 0 & \text{in } \Omega \\ \dfrac{\partial \phi_n^\mathrm{TE}}{\partial n} = 0 & \text{on } \partial\Omega \end{cases} \\
\text{TM} \quad &\begin{cases} \nabla_\mathrm{T}^2 \phi_n^\mathrm{TM} + (\lambda_n^\mathrm{TM})^2 \phi_n^\mathrm{TM} = 0 & \text{in } \Omega \\ \phi_n^\mathrm{TM} = 0 & \text{on } \partial\Omega, \end{cases}
\end{aligned} \tag{3.8}$$

where the acronyms TE and TM stand for a solution with Transverse Electric field or Transverse Magnetic field, respectively. That is, ϕ_n^TE is associated with the z-component of the magnetic field strength $\boldsymbol{H}_n$, and ϕ_n^TM is associated with the z-component of the electric field strength $\boldsymbol{E}_n$.

What about the eigenfunctions when $\lambda_n = 0$? Since they satisfy $\nabla_\mathrm{T} \times \boldsymbol{E}_n = \nabla_\mathrm{T} \times \boldsymbol{H}_n = \mathbf{0}$, they can be written as gradients of a scalar function [1, p. 66]. But the canonical problems above supply us with a complete set of scalar functions on Ω, and after considering the appropriate boundary conditions we deduce $\boldsymbol{E}_n = \nabla_\mathrm{T} \phi_n^\mathrm{TM}$ and $\boldsymbol{H}_n = \nabla_\mathrm{T} \phi_n^\mathrm{TE}$ for these eigenfunctions.[1]

[1] The case $\lambda = 0$ is also associated with the TEM modes, but for a simply connected geometry as the hollow waveguide, these do not appear. The TEM modes are also gradients of a scalar function ϕ, but for these modes this function satisfies $\nabla_\mathrm{T}^2 \phi = 0$ in Ω, which only has constant solutions in a simply connected geometry with homogeneous boundary conditions.

We normalize the canonical solutions ϕ_n^{TE} and ϕ_n^{TM} by requiring

$$\begin{cases} \iint_\Omega (\lambda_n^{\mathrm{TE}}\phi_n^{\mathrm{TE}})^2 \,\mathrm{d}x\,\mathrm{d}y = 1 \\ \iint_\Omega (\lambda_n^{\mathrm{TM}}\phi_n^{\mathrm{TM}})^2 \,\mathrm{d}x\,\mathrm{d}y = 1 \end{cases} \Leftrightarrow \quad \begin{cases} \iint_\Omega |\nabla_{\mathrm{T}}\phi_n^{\mathrm{TE}}|^2 \,\mathrm{d}x\,\mathrm{d}y = 1 \\ \iint_\Omega |\nabla_{\mathrm{T}}\phi_n^{\mathrm{TM}}|^2 \,\mathrm{d}x\,\mathrm{d}y = 1. \end{cases} \tag{3.9}$$

This implies that the scalar eigenfunctions are dimensionless. We summarize our results by expressing the vector eigenfunctions of the original transverse curl operator in the canonical, scalar functions ϕ_n^{TE} and ϕ_n^{TM},

$$\begin{pmatrix} \boldsymbol{E}_n \\ \boldsymbol{H}_n \end{pmatrix} = \begin{cases} \begin{pmatrix} -\hat{\boldsymbol{z}} \times \nabla_{\mathrm{T}}\phi_n^{\mathrm{TE}} \\ \mathrm{i}\lambda_n^{\mathrm{TE}}\phi_n^{\mathrm{TE}}\hat{\boldsymbol{z}} \end{pmatrix}, & \begin{pmatrix} \boldsymbol{0} \\ \nabla_{\mathrm{T}}\phi_n^{\mathrm{TE}} \end{pmatrix}, \\ \begin{pmatrix} \mathrm{i}\lambda_n^{\mathrm{TM}}\phi_n^{\mathrm{TM}}\hat{\boldsymbol{z}} \\ \hat{\boldsymbol{z}} \times \nabla_{\mathrm{T}}\phi_n^{\mathrm{TM}} \end{pmatrix}, & \begin{pmatrix} \nabla_{\mathrm{T}}\phi_n^{\mathrm{TM}} \\ \boldsymbol{0} \end{pmatrix}, \end{cases} \tag{3.10}$$

where the rightmost eigenfunctions correspond to the solutions with $\lambda = 0$. We see that the complex conjugate of the above eigenfunctions are also eigenfunctions, corresponding to the change $\lambda \to -\lambda$. When we use the letter λ in the remainder of this paper, we mean $\lambda > 0$.

3.2 Real-valued expansion functions

The vector eigenfunctions in (3.10) constitute a complete system for expansion of electromagnetic fields in a waveguide [5, p. 329]. Though, since they are complex vectors, we need to use complex expansion coefficients in order to get real-valued fields. By explicitly writing out the real and imaginary values of the scalar expansion coefficients, we have the expansion

$$\begin{aligned} \begin{pmatrix} \boldsymbol{E} \\ \boldsymbol{H} \end{pmatrix} = \sum_n & \frac{1}{2}(u_n^{\mathrm{TE}} - \mathrm{i}w_n^{\mathrm{TE}}) \begin{pmatrix} -\hat{\boldsymbol{z}} \times \nabla_{\mathrm{T}}\phi_n^{\mathrm{TE}} \\ \mathrm{i}\lambda_n^{\mathrm{TE}}\phi_n^{\mathrm{TE}}\hat{\boldsymbol{z}} \end{pmatrix} + \frac{1}{2}v_n^{\mathrm{TE}} \begin{pmatrix} \boldsymbol{0} \\ \nabla_{\mathrm{T}}\phi_n^{\mathrm{TE}} \end{pmatrix} \\ & + \frac{1}{2}(u_n^{\mathrm{TM}} - \mathrm{i}w_n^{\mathrm{TM}}) \begin{pmatrix} \mathrm{i}\lambda_n^{\mathrm{TM}}\phi_n^{\mathrm{TM}}\hat{\boldsymbol{z}} \\ \hat{\boldsymbol{z}} \times \nabla_{\mathrm{T}}\phi_n^{\mathrm{TM}} \end{pmatrix} + \frac{1}{2}v_n^{\mathrm{TM}} \begin{pmatrix} \nabla_{\mathrm{T}}\phi_n^{\mathrm{TM}} \\ \boldsymbol{0} \end{pmatrix} \\ & + \text{complex conjugate terms}, \end{aligned} \tag{3.11}$$

where the expansion coefficients u_n^{TE}, w_n^{TE}, v_n^{TE}, u_n^{TM}, w_n^{TM} and v_n^{TM} are real-valued scalar functions of z and t. Note carefully that the functions $\nabla_{\mathrm{T}}\phi_n^{\mathrm{TE}}$ and $\nabla_{\mathrm{T}}\phi_n^{\mathrm{TM}}$ are real-valued, and are therefore multiplied with real-valued expansion coefficients w_n^{TE} and w_n^{TM}. The summation is taken over $n = 1, 2, \ldots$, with the eigenvalues arranged in ascending order, $0 < \lambda_1 \leq \lambda_2 \leq \cdots$. After adding the complex conjugate terms

this is

$$\begin{aligned}\begin{pmatrix}\boldsymbol{E}\\ \boldsymbol{H}\end{pmatrix} &= \sum_n u_n^{\mathrm{TE}}\begin{pmatrix}-\hat{\boldsymbol{z}}\times\nabla_{\mathrm{T}}\phi_n^{\mathrm{TE}}\\ \mathbf{0}\end{pmatrix} + v_n^{\mathrm{TE}}\begin{pmatrix}\mathbf{0}\\ \nabla_{\mathrm{T}}\phi_n^{\mathrm{TE}}\end{pmatrix} + w_n^{\mathrm{TE}}\begin{pmatrix}\mathbf{0}\\ \lambda_n^{\mathrm{TE}}\phi_n^{\mathrm{TE}}\hat{\boldsymbol{z}}\end{pmatrix}\\ &\quad + u_n^{\mathrm{TM}}\begin{pmatrix}\mathbf{0}\\ \hat{\boldsymbol{z}}\times\nabla_{\mathrm{T}}\phi_n^{\mathrm{TM}}\end{pmatrix} + v_n^{\mathrm{TM}}\begin{pmatrix}\nabla_{\mathrm{T}}\phi_n^{\mathrm{TM}}\\ \mathbf{0}\end{pmatrix} + w_n^{\mathrm{TM}}\begin{pmatrix}\lambda_n^{\mathrm{TM}}\phi_n^{\mathrm{TM}}\hat{\boldsymbol{z}}\\ \mathbf{0}\end{pmatrix}\\ &= \sum_n u_n^{\mathrm{TE}}\boldsymbol{U}_n^{\mathrm{TE}} + v_n^{\mathrm{TE}}\boldsymbol{V}_n^{\mathrm{TE}} + w_n^{\mathrm{TE}}\boldsymbol{W}_n^{\mathrm{TE}}\\ &\quad + u_n^{\mathrm{TM}}\boldsymbol{U}_n^{\mathrm{TM}} + v_n^{\mathrm{TM}}\boldsymbol{V}_n^{\mathrm{TM}} + w_n^{\mathrm{TM}}\boldsymbol{W}_n^{\mathrm{TM}},\end{aligned} \tag{3.12}$$

where we have introduced the real-valued six-vector expansion functions $\boldsymbol{U}_n^{\mathrm{TE}}(x,y)$, $\boldsymbol{V}_n^{\mathrm{TE}}(x,y)$ etc. The fact that these expansion functions are derived from an eigenvalue problem, gives us strong orthogonality results, *i.e.*,

$$\begin{cases}(\boldsymbol{U}_m^{\mathrm{TE}},\boldsymbol{U}_n^{\mathrm{TE}}) = (\boldsymbol{V}_m^{\mathrm{TE}},\boldsymbol{V}_n^{\mathrm{TE}}) = (\boldsymbol{W}_m^{\mathrm{TE}},\boldsymbol{W}_n^{\mathrm{TE}}) = \delta_{m,n}\\ (\boldsymbol{U}_m^{\mathrm{TM}},\boldsymbol{U}_n^{\mathrm{TM}}) = (\boldsymbol{V}_m^{\mathrm{TM}},\boldsymbol{V}_n^{\mathrm{TM}}) = (\boldsymbol{W}_m^{\mathrm{TM}},\boldsymbol{W}_n^{\mathrm{TM}}) = \delta_{m,n}\\ \text{all other combinations} = 0,\end{cases} \tag{3.13}$$

where $\delta_{m,n}$ denotes the Kronecker delta, $\delta_{m,m} = 1$, $\delta_{m,n} = 0$ for $m \neq n$. We also see that our expansion functions $\boldsymbol{U}_n^{\mathrm{TE}}(x,y)$ etc have the physical dimension $(\text{length})^{-1}$, and thus the expansion coefficients $u_n^{\mathrm{TE}}(z,t)$ etc have the physical dimension $\sqrt{\text{energy/length}}$.

4 Decomposition in modes

We continue the analysis by taking the scalar product of the expansion functions with the Maxwell equations (3.1), in order to remove the transverse dependence. If we denote an arbitrary expansion function by $\boldsymbol{\Psi}_m$, this means we wish to study the equation

$$\begin{aligned}\iint_\Omega \boldsymbol{\Psi}_m \cdot \Bigg[&\begin{pmatrix}\mathbf{0} & -\hat{\boldsymbol{z}}\times\mathbf{I}\\ \hat{\boldsymbol{z}}\times\mathbf{I} & \mathbf{0}\end{pmatrix}\partial_z\begin{pmatrix}\boldsymbol{E}\\ \boldsymbol{H}\end{pmatrix} + \frac{1}{c_0}\partial_t\begin{pmatrix}F_{\mathrm{e}}(E^2)\boldsymbol{E}\\ F_{\mathrm{m}}(H^2)\boldsymbol{H}\end{pmatrix}\\ &+ \begin{pmatrix}\mathbf{0} & -\nabla_{\mathrm{T}}\times\mathbf{I}\\ \nabla_{\mathrm{T}}\times\mathbf{I} & \mathbf{0}\end{pmatrix}\begin{pmatrix}\boldsymbol{E}\\ \boldsymbol{H}\end{pmatrix}\Bigg]\,\mathrm{d}x\,\mathrm{d}y = 0.\end{aligned} \tag{4.1}$$

for each possible $\boldsymbol{\Psi}_m$.

4.1 Linear terms

We examine the expansion of the various terms in the Maxwell equations, starting with the z part of the curl operator,

$$\begin{aligned}\begin{pmatrix}\mathbf{0} & -\hat{\boldsymbol{z}}\times\mathbf{I}\\ \hat{\boldsymbol{z}}\times\mathbf{I} & \mathbf{0}\end{pmatrix}\partial_z\begin{pmatrix}\boldsymbol{E}\\ \boldsymbol{H}\end{pmatrix} &= \sum_n \partial_z u_n^{\mathrm{TE}}\boldsymbol{V}_n^{\mathrm{TE}} + \partial_z v_n^{\mathrm{TE}}\boldsymbol{U}_n^{\mathrm{TE}}\\ &\quad + \partial_z u_n^{\mathrm{TM}}\boldsymbol{V}_n^{\mathrm{TM}} + \partial_z v_n^{\mathrm{TM}}\boldsymbol{U}_n^{\mathrm{TM}},\end{aligned} \tag{4.2}$$

which is proved by straight-forward calculations from the expansion (3.12). The last term is the transverse part of the curl operator, which is

$$\begin{pmatrix} \mathbf{0} & -\nabla_{\mathrm{T}} \times \mathbf{I} \\ \nabla_{\mathrm{T}} \times \mathbf{I} & \mathbf{0} \end{pmatrix} \begin{pmatrix} \boldsymbol{E} \\ \boldsymbol{H} \end{pmatrix} = \sum_n \lambda_n^{\mathrm{TE}} u_n^{\mathrm{TE}} \boldsymbol{W}_n^{\mathrm{TE}} - \lambda_n^{\mathrm{TE}} w_n^{\mathrm{TE}} \boldsymbol{U}_n^{\mathrm{TE}} + \lambda_n^{\mathrm{TM}} u_n^{\mathrm{TM}} \boldsymbol{W}_n^{\mathrm{TM}} - \lambda_n^{\mathrm{TM}} w_n^{\mathrm{TM}} \boldsymbol{U}_n^{\mathrm{TM}}. \tag{4.3}$$

So far, all our work is well known from the corresponding linear analysis, and the orthogonality relations (3.13) makes it easy to evaluate the linear terms in integral (4.1). We now turn our attention to the nonlinear term.

4.2 Nonlinear term

The only term left is the middle term in (4.1), which contains the nonlinear contribution. We remind that the integral to be evaluated is

$$\partial_t \iint_\Omega \boldsymbol{\Psi}_m \cdot \begin{pmatrix} F_{\mathrm{e}}(E^2)\boldsymbol{E} \\ F_{\mathrm{m}}(H^2)\boldsymbol{H} \end{pmatrix} \mathrm{d}x\, \mathrm{d}y. \tag{4.4}$$

For the time being, we ignore the time derivative and consider the exact form of this integral for each possible expansion function $\boldsymbol{\Psi}_m$, since many cross terms drop out immediately. For the TE modes this means

$$\begin{cases} \boldsymbol{U}_m^{\mathrm{TE}}: & \sum_n u_n^{\mathrm{TE}}(\boldsymbol{U}_m^{\mathrm{TE}}, F_{\mathrm{e}}(E^2)\boldsymbol{U}_n^{\mathrm{TE}}) + v_n^{\mathrm{TM}}(\boldsymbol{U}_m^{\mathrm{TE}}, F_{\mathrm{e}}(E^2)\boldsymbol{V}_n^{\mathrm{TM}}) \\ \boldsymbol{V}_m^{\mathrm{TE}}: & \sum_n u_n^{\mathrm{TM}}(\boldsymbol{V}_m^{\mathrm{TE}}, F_{\mathrm{m}}(H^2)\boldsymbol{U}_n^{\mathrm{TM}}) + v_n^{\mathrm{TE}}(\boldsymbol{V}_m^{\mathrm{TE}}, F_{\mathrm{m}}(H^2)\boldsymbol{V}_n^{\mathrm{TE}}) \\ \boldsymbol{W}_m^{\mathrm{TE}}: & \sum_n w_n^{\mathrm{TE}}(\boldsymbol{W}_m^{\mathrm{TE}}, F_{\mathrm{m}}(H^2)\boldsymbol{W}_n^{\mathrm{TE}}), \end{cases} \tag{4.5}$$

and for the TM modes

$$\begin{cases} \boldsymbol{U}_m^{\mathrm{TM}}: & \sum_n u_n^{\mathrm{TM}}(\boldsymbol{U}_m^{\mathrm{TM}}, F_{\mathrm{m}}(H^2)\boldsymbol{U}_n^{\mathrm{TM}}) + v_n^{\mathrm{TE}}(\boldsymbol{U}_m^{\mathrm{TM}}, F_{\mathrm{m}}(H^2)\boldsymbol{V}_n^{\mathrm{TE}}) \\ \boldsymbol{V}_m^{\mathrm{TM}}: & \sum_n u_n^{\mathrm{TE}}(\boldsymbol{V}_m^{\mathrm{TM}}, F_{\mathrm{e}}(E^2)\boldsymbol{U}_n^{\mathrm{TE}}) + v_n^{\mathrm{TM}}(\boldsymbol{V}_m^{\mathrm{TM}}, F_{\mathrm{e}}(E^2)\boldsymbol{V}_n^{\mathrm{TM}}) \\ \boldsymbol{W}_m^{\mathrm{TM}}: & \sum_n w_n^{\mathrm{TM}}(\boldsymbol{W}_m^{\mathrm{TM}}, F_{\mathrm{e}}(E^2)\boldsymbol{W}_n^{\mathrm{TM}}). \end{cases} \tag{4.6}$$

Since the scalar products contain the functions $F_{\mathrm{e}}(E^2)$ and $F_{\mathrm{m}}(H^2)$, the remaining terms do not simplify, and the different modes couple to each other. It seems as if our modal analysis breaks down, and of course it does if we want an exact result. Though, we argue that the nonlinearity has its strongest effects in the wave propagation, *i.e.*, it might be permissible to ignore the nonlinear effect over the cross section to some extent. We are able to do this in a manner that preserves some of the coupling between the modes.

An obvious approach is to expand $F_\mathrm{e}(E^2)$ and $F_\mathrm{m}(H^2)$ in a Taylor series and explicitly calculate the corresponding integrals. Since the expressions for $E^2(x,y,z,t)$ and $H^2(x,y,z,t)$ are rather complex, we wish to delay this approach for a while. For a hint of the expressions involved we refer to Appendix A. Instead we suggest to substitute $E^2(x,y,z,t)$ and $H^2(x,y,z,t)$ with some suitable functions independent of the transverse variables x and y, *i.e.*, $\tilde{E}^2(z,t)$ and $\tilde{H}^2(z,t)$,

$$\begin{cases} F_\mathrm{e}(E^2) = F_\mathrm{e}(\tilde{E}^2) + [F_\mathrm{e}(E^2) - F_\mathrm{e}(\tilde{E}^2)] \\ F_\mathrm{m}(H^2) = F_\mathrm{m}(\tilde{H}^2) + [F_\mathrm{m}(H^2) - F_\mathrm{m}(\tilde{H}^2)], \end{cases} \tag{4.7}$$

and treat the terms in square brackets as perturbations which are ignored. Since the factors $F_\mathrm{e}(\tilde{E}^2)$ and $F_\mathrm{m}(\tilde{H}^2)$ are independent of x and y, they can be pulled out of the scalar products in (4.5) and (4.6), and we can then use orthogonality. Though, as we show in Section 4.3, we must generally choose a different $\tilde{E}^2$ and $\tilde{H}^2$ for each expansion function $\boldsymbol{\Psi}_m$, which we denote by an index m, $\tilde{E}^2_m$ and $\tilde{H}^2_m$. The resulting equations are deduced from (4.2), (4.3), (4.5) and (4.6) as

$$\begin{cases} \boldsymbol{U}^\mathrm{TE}_m: & \partial_z v^\mathrm{TE}_m + \dfrac{1}{c_0}\partial_t\left(F_\mathrm{e}(\tilde{E}^2_m)u^\mathrm{TE}_m\right) - \lambda^\mathrm{TE}_m w^\mathrm{TE}_m = 0 \\ \boldsymbol{V}^\mathrm{TE}_m: & \partial_z u^\mathrm{TE}_m + \dfrac{1}{c_0}\partial_t\left(F_\mathrm{m}(\tilde{H}^2_m)v^\mathrm{TE}_m\right) = 0 \\ \boldsymbol{W}^\mathrm{TE}_m: & \dfrac{1}{c_0}\partial_t\left(F_\mathrm{m}(\tilde{H}^2_m)w^\mathrm{TE}_m\right) + \lambda^\mathrm{TE}_m u^\mathrm{TE}_m = 0 \end{cases} \tag{4.8}$$

for the TE-modes, and

$$\begin{cases} \boldsymbol{U}^\mathrm{TM}_m: & \partial_z v^\mathrm{TM}_m + \dfrac{1}{c_0}\partial_t\left(F_\mathrm{m}(\tilde{H}^2_m)u^\mathrm{TM}_m\right) - \lambda^\mathrm{TM}_m w^\mathrm{TM}_m = 0 \\ \boldsymbol{V}^\mathrm{TM}_m: & \partial_z u^\mathrm{TM}_m + \dfrac{1}{c_0}\partial_t\left(F_\mathrm{e}(\tilde{E}^2_m)v^\mathrm{TM}_m\right) = 0 \\ \boldsymbol{W}^\mathrm{TM}_m: & \dfrac{1}{c_0}\partial_t\left(F_\mathrm{e}(\tilde{E}^2_m)w^\mathrm{TM}_m\right) + \lambda^\mathrm{TM}_m u^\mathrm{TM}_m = 0 \end{cases} \tag{4.9}$$

for the TM-modes. We see that the equations are strictly hyperbolic[2], and the equation structure is exactly the same for both TE- and TM-modes, only the functions F_e and F_m must be interchanged.

In the next section we discuss the approximation leading to this result, but we must first consider an important detail. Each of the systems (4.8) and (4.9) must be supplemented by three initial conditions (three dependent variables, three equations, three conditions), but only two initial conditions can be chosen independent of each other. Since we know that $\nabla \cdot \boldsymbol{B} = \nabla \cdot \boldsymbol{D} = 0$ inside the waveguide, we must introduce the additional constraints

$$-\lambda^\mathrm{TE}_m F_\mathrm{m}(\tilde{H}^2_m)v^\mathrm{TE}_m(z,0) + \partial_z\left(F_\mathrm{m}(\tilde{H}^2_m)w^\mathrm{TE}_m(z,0)\right) = 0 \tag{4.10}$$

[2] A system of partial differential equations $\partial_t \boldsymbol{u} + \mathbf{A}(\boldsymbol{u})\partial_z \boldsymbol{u} = \mathbf{0}$ is strictly hyperbolic if all eigenvalues of the matrix $\mathbf{A}(\boldsymbol{u})$ are real and distinct [9, p. 573]. In our case, it can be shown that there is one positive eigenvalue, one negative eigenvalue and one zero eigenvalue.

and

$$-\lambda_m^{\mathrm{TM}} F_{\mathrm{e}}(\tilde{E}_m^2) v_m^{\mathrm{TM}}(z,0) + \partial_z \left(F_{\mathrm{e}}(\tilde{E}_m^2) w_m^{\mathrm{TM}}(z,0) \right) = 0 \tag{4.11}$$

to maintain compatibility with the original equations. Note that λ_m^{TE} and λ_m^{TM} correspond to the x and y derivatives. The above constraints can be reformulated as

$$\lambda_m^{\mathrm{TE}} v_m^{\mathrm{TE}}(z,0) = \partial_z w_m^{\mathrm{TE}}(z,0) + \partial_z \ln F_{\mathrm{m}}(\tilde{H}_m^2(z,0)) \tag{4.12}$$

and

$$\lambda_m^{\mathrm{TM}} v_m^{\mathrm{TM}}(z,0) = \partial_z w_m^{\mathrm{TM}}(z,0) + \partial_z \ln F_{\mathrm{e}}(\tilde{E}_m^2(z,0)), \tag{4.13}$$

which may be nontrivial to satisfy. These constraints can also be derived from the last two lines in (4.8) and (4.9), respectively.

4.3 Estimate of the approximation

To estimate the approximation we made in the previous section, we look at the electric field only. We use a Taylor expansion of the function $F_{\mathrm{e}}(\tilde{E}_m^2)$ in the vicinity of the (so far) unknown argument $\tilde{E}_m^2$. Since the explicit representation of $E^2 = \boldsymbol{E}\cdot\boldsymbol{E}$ is rather complicated if we use the expansion functions $\boldsymbol{U}_n^{\mathrm{TE}}$, $\boldsymbol{V}_n^{\mathrm{TM}}$ and $\boldsymbol{W}_n^{\mathrm{TM}}$ (see Appendix A), we formulate the expansion of the electric field in a somewhat more abstract, but compact, manner,

$$\boldsymbol{E} = \sum_n f_n(z,t)\boldsymbol{E}_n(x,y) \quad \Rightarrow \quad E^2 = \boldsymbol{E}\cdot\boldsymbol{E} = \sum_{kl} f_k f_l \boldsymbol{E}_k \cdot \boldsymbol{E}_l, \tag{4.14}$$

where $(\boldsymbol{E}_m, \boldsymbol{E}_n) = \delta_{mn}$, *i.e.*, we drop the distinction between functions having or not having a z-component. This means the index n also includes variations of TE- and TM-modes etc. The error we wish to estimate is formulated as the scalar product

$$(\boldsymbol{E}_m, [F_{\mathrm{e}}(E^2) - F_{\mathrm{e}}(\tilde{E}_m^2)]\boldsymbol{E}), \tag{4.15}$$

and upon expanding $F_{\mathrm{e}}(E^2)$ in a Taylor series we see that this term is at most $\mathcal{O}(F_{\mathrm{e}}''(\tilde{E}^2)\iint_\Omega (E^2-\tilde{E}^2)^2 E\,\mathrm{d}x\,\mathrm{d}y)$ if

$$F_{\mathrm{e}}'(\tilde{E}^2)(\boldsymbol{E}_m, [E^2 - \tilde{E}_m^2]\boldsymbol{E}) = 0. \tag{4.16}$$

This can be accomplished by choosing

$$\tilde{E}_m^2 = \frac{1}{f_m}(\boldsymbol{E}_m, E^2\boldsymbol{E}) = \sum_{nkl} \frac{f_k f_l f_n}{f_m}(\boldsymbol{E}_m, \boldsymbol{E}_k \cdot \boldsymbol{E}_l \boldsymbol{E}_n), \tag{4.17}$$

which of course is the *exact* result for a Kerr material, *i.e.*, $F_{\mathrm{e}}(E^2) = 1 + E^2$. For other materials this represents an approximation to the first order in a Taylor series expansion of the constitutive function $F_{\mathrm{e}}(E^2)$, and we see that this choice of $\tilde{E}_m^2$ is equivalent to the Taylor expansion suggested on page 81. However, by delaying the introduction of the Taylor expansion until this stage, we have gained an opportunity to make other choices of $\tilde{E}_m^2$, depending on the situation at hand.

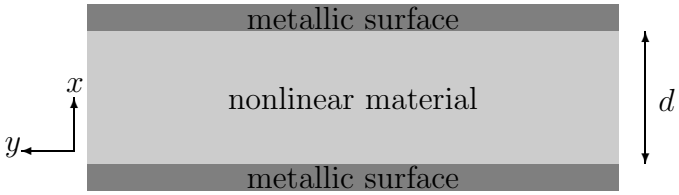

Figure 2: The parallel plate waveguide.

It is clear that we in general must choose a different $\tilde{E}_m^2$ for different $\boldsymbol{E}_m$. We can calculate the scalar products $(\boldsymbol{E}_m, \boldsymbol{E}_k \cdot \boldsymbol{E}_l \boldsymbol{E}_n)$ analytically for a few geometries, especially the rectangular and the parallel plate waveguide. For general geometries, we must resort to numerical calculations of the scalar products. In the following section, we show that even when we can calculate everything analytically, the problem is still quite a challenge.

5 Parallel plate waveguide with non-magnetic material

We analyze one of the simplest possible waveguides, *i.e.*, the parallel plate waveguide filled with a non-magnetic material. The geometry is depicted in Figure 2, and the expansion functions are

$$\begin{cases} \boldsymbol{U}_n^{\mathrm{TE}} = \begin{pmatrix} -\sqrt{\frac{2}{d}}\sin(\frac{n\pi x}{d})\hat{\boldsymbol{y}} \\ \boldsymbol{0} \end{pmatrix}, & \boldsymbol{U}_n^{\mathrm{TM}} = \begin{pmatrix} \boldsymbol{0} \\ \sqrt{\frac{2}{d}}\cos(\frac{n\pi x}{d})\hat{\boldsymbol{y}} \end{pmatrix}, \\ \boldsymbol{V}_n^{\mathrm{TE}} = \begin{pmatrix} \boldsymbol{0} \\ \sqrt{\frac{2}{d}}\sin(\frac{n\pi x}{d})\hat{\boldsymbol{x}} \end{pmatrix}, & \boldsymbol{V}_n^{\mathrm{TM}} = \begin{pmatrix} \sqrt{\frac{2}{d}}\cos(\frac{n\pi x}{d})\hat{\boldsymbol{x}} \\ \boldsymbol{0} \end{pmatrix}, \\ \boldsymbol{W}_n^{\mathrm{TE}} = \begin{pmatrix} \boldsymbol{0} \\ \sqrt{\frac{2}{d}}\cos(\frac{n\pi x}{d})\hat{\boldsymbol{z}} \end{pmatrix}, & \boldsymbol{W}_n^{\mathrm{TM}} = \begin{pmatrix} \sqrt{\frac{2}{d}}\sin(\frac{n\pi x}{d})\hat{\boldsymbol{z}} \\ \boldsymbol{0} \end{pmatrix}. \end{cases} \tag{5.1}$$

If the two plates are held at different potentials, we also have the TEM-mode,

$$\boldsymbol{U}^{\mathrm{TEM}} = \begin{pmatrix} \sqrt{\frac{1}{d}}\hat{\boldsymbol{x}} \\ \boldsymbol{0} \end{pmatrix}, \quad \boldsymbol{V}^{\mathrm{TEM}} = \begin{pmatrix} \boldsymbol{0} \\ \sqrt{\frac{1}{d}}\hat{\boldsymbol{y}} \end{pmatrix}, \quad \boldsymbol{W}^{\mathrm{TEM}} = \begin{pmatrix} \boldsymbol{0} \\ \boldsymbol{0} \end{pmatrix}, \tag{5.2}$$

but we assume the TEM-mode to be absent in this section. The full expansion of the scalar products $(\boldsymbol{E}_m, \boldsymbol{E}_k \cdot \boldsymbol{E}_l \boldsymbol{E}_n)$ with arbitrary expansion functions is given in

appendix A. The only non-zero scalar products we need to compute are

$$\begin{aligned}(\boldsymbol{U}_m^{\mathrm{TE}}, \boldsymbol{U}_k^{\mathrm{TE}} \cdot \boldsymbol{U}_l^{\mathrm{TE}} \boldsymbol{U}_n^{\mathrm{TE}}) &= (\boldsymbol{U}_m^{\mathrm{TE}}, \boldsymbol{W}_k^{\mathrm{TM}} \cdot \boldsymbol{W}_l^{\mathrm{TM}} \boldsymbol{U}_n^{\mathrm{TE}}) \\ &= (\boldsymbol{W}_m^{\mathrm{TM}}, \boldsymbol{U}_k^{\mathrm{TE}} \cdot \boldsymbol{U}_l^{\mathrm{TE}} \boldsymbol{W}_n^{\mathrm{TM}}) = (\boldsymbol{W}_m^{\mathrm{TM}}, \boldsymbol{W}_k^{\mathrm{TM}} \cdot \boldsymbol{W}_l^{\mathrm{TM}} \boldsymbol{W}_n^{\mathrm{TM}}) \\ &= \frac{4}{d^2} \int_{x=0}^{d} \sin \frac{m\pi x}{d} \sin \frac{k\pi x}{d} \sin \frac{l\pi x}{d} \sin \frac{n\pi x}{d} \, \mathrm{d}x \\ &= \frac{1}{2d} [-\delta_{m,k+l+n} + \delta_{m,-k+l+n} + \delta_{m,k-l+n} - \delta_{m,-k-l+n} \\ &\quad + \delta_{m,k+l-n} - \delta_{m,-k+l-n} - \delta_{m,k-l-n} + \delta_{m,-k-l-n}],\end{aligned} \tag{5.3}$$

and

$$\begin{aligned}(\boldsymbol{U}_m^{\mathrm{TE}}, \boldsymbol{V}_k^{\mathrm{TM}} \cdot \boldsymbol{V}_l^{\mathrm{TM}} \boldsymbol{U}_n^{\mathrm{TE}}) &= (\boldsymbol{W}_m^{\mathrm{TM}}, \boldsymbol{V}_k^{\mathrm{TM}} \cdot \boldsymbol{V}_l^{\mathrm{TM}} \boldsymbol{W}_n^{\mathrm{TM}}) \\ &= \frac{4}{d^2} \int_{x=0}^{d} \sin \frac{m\pi x}{d} \cos \frac{k\pi x}{d} \cos \frac{l\pi x}{d} \sin \frac{n\pi x}{d} \, \mathrm{d}x \\ &= \frac{1}{2d} [\delta_{m,k+l+n} + \delta_{m,-k+l+n} + \delta_{m,k-l+n} + \delta_{m,-k-l+n} \\ &\quad - \delta_{m,k+l-n} - \delta_{m,-k+l-n} - \delta_{m,k-l-n} - \delta_{m,-k-l-n}],\end{aligned} \tag{5.4}$$

and

$$\begin{aligned}(\boldsymbol{V}_m^{\mathrm{TM}}, \boldsymbol{U}_k^{\mathrm{TE}} \cdot \boldsymbol{U}_l^{\mathrm{TE}} \boldsymbol{V}_n^{\mathrm{TM}}) &= (\boldsymbol{V}_m^{\mathrm{TM}}, \boldsymbol{W}_k^{\mathrm{TM}} \cdot \boldsymbol{W}_l^{\mathrm{TM}} \boldsymbol{V}_n^{\mathrm{TM}}) \\ &= \frac{4}{d^2} \int_{x=0}^{d} \cos \frac{m\pi x}{d} \sin \frac{k\pi x}{d} \sin \frac{l\pi x}{d} \cos \frac{n\pi x}{d} \, \mathrm{d}x \\ &= \frac{1}{2d} [-\delta_{m,k+l+n} + \delta_{m,-k+l+n} + \delta_{m,k-l+n} - \delta_{m,-k-l+n} \\ &\quad - \delta_{m,k+l-n} + \delta_{m,-k+l-n} + \delta_{m,k-l-n} - \delta_{m,-k-l-n}].\end{aligned} \tag{5.5}$$

It is now clear that, even for the simplest cases, we have a formidable problem. For instance, we see that each mode generally couple to infinitely many others, sometimes with a nondecreasing coupling factor. This means that in order to proceed, we should impose some more restrictions on the problem.

6 Dominant TE mode in a non-magnetic material

In the previous section it is shown that (4.17) is quite complicated to handle explicitly. In this section, we look at a simplified case for a nonmagnetic material ($F_{\mathrm{m}}(H^2) = 1$), where almost all the energy is contained in the first TE-mode, which we denote TE_1. This mode is chosen since it generally corresponds to the lowest eigenvalue λ_1 [7, p. 410], and should be the easiest to generate. The assumption of a dominant TE_1 mode implies

$$|u_1^{\mathrm{TE}}|, |v_1^{\mathrm{TE}}|, |w_1^{\mathrm{TE}}| \gg \text{all other expansion coefficients.} \tag{6.1}$$

The expansion coefficients v_1^{TE} and w_1^{TE} are associated with the magnetic field, and do not enter our calculations below. Therefore we study only the case $|u_1^{\mathrm{TE}}| \to \infty$.

6.1 Leading terms for $\boldsymbol{U}_m^{\mathrm{TE}}$

With the above assumption on the relative sizes of the expansion coefficients, we deduce in Appendix A.3 that the leading term for the dominant mode $\boldsymbol{U}_1^{\mathrm{TE}}$ is

$$\tilde{E}_{\mathrm{u1}}^2 = (u_1^{\mathrm{TE}})^2 \alpha_{\mathrm{u1}}, \tag{6.2}$$

where the index "u1" is used to indicate the relation to the expansion function $\boldsymbol{U}_1^{\mathrm{TE}}$. For the other TE-modes, we have

$$\tilde{E}_{\mathrm{u}m}^2 = (u_1^{\mathrm{TE}})^2 \alpha_{\mathrm{u}m} + \frac{(u_1^{\mathrm{TE}})^3}{u_m^{\mathrm{TE}}} \beta_{\mathrm{u}m} + \mathcal{O}(u_1^{\mathrm{TE}} u_m^{\mathrm{TE}}), \tag{6.3}$$

and the constants α_{u1}, $\alpha_{\mathrm{u}m}$ and $\beta_{\mathrm{u}m}$ are defined in Appendix A.3 as

$$\begin{cases} \alpha_{\mathrm{u1}} = \iint_\Omega |\nabla_{\mathrm{T}} \phi_1^{\mathrm{TE}}|^4 \,\mathrm{d}x\,\mathrm{d}y \\ \alpha_{\mathrm{u}m} = \iint_\Omega |\nabla_{\mathrm{T}} \phi_m^{\mathrm{TE}}|^2 |\nabla_{\mathrm{T}} \phi_1^{\mathrm{TE}}|^2 \,\mathrm{d}x\,\mathrm{d}y + 2 \iint_\Omega |\nabla_{\mathrm{T}} \phi_m^{\mathrm{TE}} \cdot \nabla_{\mathrm{T}} \phi_1^{\mathrm{TE}}|^2 \,\mathrm{d}x\,\mathrm{d}y \\ \beta_{\mathrm{u}m} = \iint_\Omega \nabla_{\mathrm{T}} \phi_m^{\mathrm{TE}} \cdot \nabla_{\mathrm{T}} \phi_1^{\mathrm{TE}} |\nabla_{\mathrm{T}} \phi_1^{\mathrm{TE}}|^2 \,\mathrm{d}x\,\mathrm{d}y \end{cases} \tag{6.4}$$

Notice that the first term in $\tilde{E}_{\mathrm{u}m}^2$ is one order less in u_1^{TE} than the second. This term is needed since the second will cancel in the wavespeed factor. As soon as $\beta_{\mathrm{u}m} \neq 0$, the second term can be very large for infinitesimal u_m^{TE}. This is the origin of the mode coupling, and causes the excitation of new modes which were not present in the beginning. This is made more clear in the sections to follow. Figure 3 shows the distribution of this factor for the rectangular and circular waveguides.

In Section 4.2 we ignored the time derivative in order to calculate a scalar product. It is now time to bring that operator back to life, and calculate the time derivative $\partial_t \left(F_{\mathrm{e}}(\tilde{E}_{\mathrm{u}m}^2) u_m^{\mathrm{TE}} \right)$. For the dominant mode this is

$$\begin{aligned} \partial_t \left(F_{\mathrm{e}}(\tilde{E}_{\mathrm{u1}}^2) u_1^{\mathrm{TE}} \right) &= \partial_t \left(F_{\mathrm{e}}((u_1^{\mathrm{TE}})^2 \alpha_{\mathrm{u1}}) u_1^{\mathrm{TE}} \right) \\ &= [F_{\mathrm{e}}(\tilde{E}_{\mathrm{u1}}^2) + 2F_{\mathrm{e}}'(\tilde{E}_{\mathrm{u1}}^2)(u_1^{\mathrm{TE}})^2 \alpha_{\mathrm{u1}}] \partial_t u_1^{\mathrm{TE}} \end{aligned} \tag{6.5}$$

and for the other TE-modes it is

$$\begin{aligned} \partial_t \left(F_{\mathrm{e}}(\tilde{E}_{\mathrm{u}m}^2) u_m^{\mathrm{TE}} \right) &= \partial_t \left(F_{\mathrm{e}} \left(\frac{(u_1^{\mathrm{TE}})^3}{u_m^{\mathrm{TE}}} \beta_{\mathrm{u}m} + (u_1^{\mathrm{TE}})^2 \alpha_{\mathrm{u}m} \right) u_m^{\mathrm{TE}} \right) \\ &= [F_{\mathrm{e}}(\tilde{E}_{\mathrm{u}m}^2) - F_{\mathrm{e}}'(\tilde{E}_{\mathrm{u}m}^2) \frac{(u_1^{\mathrm{TE}})^3}{u_m^{\mathrm{TE}}} \beta_{\mathrm{u}m}] \partial_t u_m^{\mathrm{TE}} \\ &\quad + F_{\mathrm{e}}'(\tilde{E}_{\mathrm{u}m}^2)[3(u_1^{\mathrm{TE}})^2 \beta_{\mathrm{u}m} + 2u_1^{\mathrm{TE}} u_m^{\mathrm{TE}} \alpha_{\mathrm{u}m}] \partial_t u_1^{\mathrm{TE}}. \end{aligned} \tag{6.6}$$

Expanding $F_{\mathrm{e}}(\tilde{E}_{\mathrm{u}m}^2)$ in a Taylor series suggests that $F_{\mathrm{e}}(\tilde{E}_{\mathrm{u}m}^2) - F_{\mathrm{e}}'(\tilde{E}_{\mathrm{u}m}^2) \frac{(u_1^{\mathrm{TE}})^3}{u_m^{\mathrm{TE}}} \beta_{\mathrm{u}m} \approx F_{\mathrm{e}}((u_1^{\mathrm{TE}})^2 \alpha_{\mathrm{u}m})$, *i.e.*, the factor multiplying $\partial_t u_m^{\mathrm{TE}}$ should be approximated without

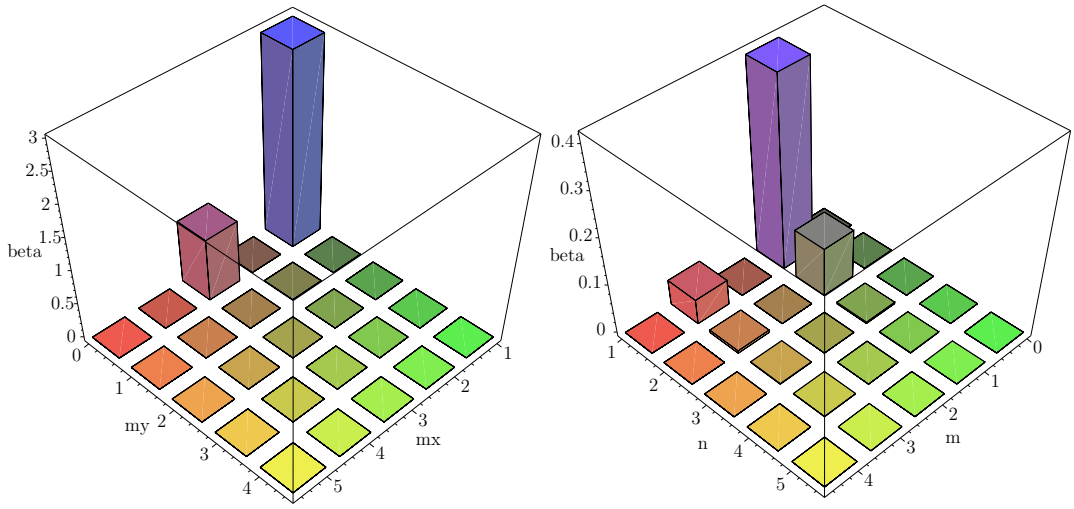

Figure 3: The distribution of the amplitude of the coupling factor $|\beta_{\mathrm{um}}|$ for a waveguide with rectangular (left) and circular (right) cross section. The index m is in both cases composed of two indices (m_x and m_y for the rectangular waveguide, and m and n for the circular). The tall bars correspond to α_{u1}.

any dependence on u_m^{TE}. This implies

$$\partial_t \left(F_{\mathrm{e}}(\tilde{E}^2_{\mathrm{um}}) u_m^{\mathrm{TE}} \right) = F_{\mathrm{e}}((u_1^{\mathrm{TE}})^2 \alpha_{\mathrm{um}}) \partial_t u_m^{\mathrm{TE}} + F'_{\mathrm{e}}(\tilde{E}^2_{\mathrm{um}})[3(u_1^{\mathrm{TE}})^2 \beta_{\mathrm{um}} + 2u_1^{\mathrm{TE}} u_m^{\mathrm{TE}} \alpha_{\mathrm{um}}] \partial_t u_1^{\mathrm{TE}}, \quad (6.7)$$

i.e., the wave speed for TE-mode m depends only on the dominant mode. As is shown in the next section, this is valid for the TM-modes as well.

6.2 Leading terms for $\boldsymbol{V}_m^{\mathrm{TM}}$ and $\boldsymbol{W}_m^{\mathrm{TM}}$

In Appendix A.3 it is shown that the leading term for $\boldsymbol{V}_m^{\mathrm{TM}}$ has the exact same structure as for $\tilde{E}^2_{\mathrm{vm}}$,

$$\tilde{E}^2_{\mathrm{vm}} = (u_1^{\mathrm{TE}})^2 \alpha_{\mathrm{vm}} + \frac{(u_1^{\mathrm{TE}})^3}{v_m^{\mathrm{TM}}} \beta_{\mathrm{vm}}, \quad (6.8)$$

where the constants α_{vm} and β_{vm} are integrals similar to α_{um} and β_{um}. Calculations analogous to the previous subsection give

$$\partial_t \left(F_{\mathrm{e}}(\tilde{E}^2_{\mathrm{vm}}) v_m^{\mathrm{TM}} \right) = F_{\mathrm{e}}((u_1^{\mathrm{TE}})^2 \alpha_{\mathrm{vm}}) \partial_t v_m^{\mathrm{TM}} + F'_{\mathrm{e}}(\tilde{E}^2_{\mathrm{vm}})[3(u_1^{\mathrm{TE}})^2 \beta_{\mathrm{vm}} + 2u_1^{\mathrm{TE}} v_m^{\mathrm{TM}} \alpha_{\mathrm{vm}}] \partial_t u_1^{\mathrm{TE}}. \quad (6.9)$$

Appendix A.3 also shows that the leading term for $\boldsymbol{W}_m^{\mathrm{TM}}$ is

$$\tilde{E}^2_{\mathrm{wm}} = (u_1^{\mathrm{TE}})^2 \alpha_{\mathrm{wm}}, \quad (6.10)$$

where the constants $\alpha_{\mathrm{w}m}$ are integrals similar to $\alpha_{\mathrm{u}m}$. Finally, we have the time derivative

$$\partial_t \left(F_{\mathrm{e}}(\tilde{E}^2_{\mathrm{w}m}) w_m^{\mathrm{TM}} \right) = F_{\mathrm{e}}(\tilde{E}^2_{\mathrm{w}m}) \partial_t v_m^{\mathrm{TM}} + 2F'_{\mathrm{e}}(\tilde{E}^2_{\mathrm{w}m}) u_1^{\mathrm{TE}} w_m^{\mathrm{TM}} \alpha_{\mathrm{w}m} \partial_t u_1^{\mathrm{TE}}. \tag{6.11}$$

Here, the factor multiplying $\partial_t w_m^{\mathrm{TM}}$ is explicitly independent of w_m^{TM}.

6.3 Resulting equations for a dominant TE mode

The equations for the dominant mode is

$$\begin{cases} \partial_z v_1^{\mathrm{TE}} + \dfrac{1}{c_0} \partial_t \left(F_{\mathrm{e}}((u_1^{\mathrm{TE}})^2 \alpha_{\mathrm{u}1}) u_1^{\mathrm{TE}} \right) - \lambda_1^{\mathrm{TE}} w_1^{\mathrm{TE}} = 0 \\ \partial_z u_1^{\mathrm{TE}} + \dfrac{1}{c_0} \partial_t v_1^{\mathrm{TE}} = 0 \\ \dfrac{1}{c_0} \partial_t w_1^{\mathrm{TE}} + \lambda_1^{\mathrm{TE}} u_1^{\mathrm{TE}} = 0 \end{cases} \tag{6.12}$$

and

$$\begin{cases} \partial_z v_m^{\mathrm{TE}} + F_{\mathrm{e}}((u_1^{\mathrm{TE}})^2 \alpha_{\mathrm{u}m}) \dfrac{1}{c_0} \partial_t u_m^{\mathrm{TE}} - \lambda_m^{\mathrm{TE}} w_m^{\mathrm{TE}} \\ \qquad = -F'_{\mathrm{e}}(\tilde{E}^2_{\mathrm{u}m}) [3(u_1^{\mathrm{TE}})^2 \beta_{\mathrm{u}m} + 2u_1^{\mathrm{TE}} u_m^{\mathrm{TE}} \alpha_{\mathrm{u}m}] \dfrac{1}{c_0} \partial_t u_1^{\mathrm{TE}} \\ \partial_z u_m^{\mathrm{TE}} + \dfrac{1}{c_0} \partial_t v_m^{\mathrm{TE}} = 0 \\ \dfrac{1}{c_0} \partial_t w_m^{\mathrm{TE}} + \lambda_m^{\mathrm{TE}} u_m^{\mathrm{TE}} = 0 \end{cases} \tag{6.13}$$

for the rest of the TE-modes. For the TM-modes, we have

$$\begin{cases} \partial_z v_m^{\mathrm{TM}} + \dfrac{1}{c_0} \partial_t u_m^{\mathrm{TM}} - \lambda_m^{\mathrm{TM}} w_m^{\mathrm{TM}} = 0 \\ \partial_z u_m^{\mathrm{TM}} + F_{\mathrm{e}}((u_1^{\mathrm{TE}})^2 \alpha_{\mathrm{v}m}) \dfrac{1}{c_0} \partial_t v_m^{\mathrm{TM}} \\ \qquad = -F'_{\mathrm{e}}(\tilde{E}^2_{\mathrm{v}m}) [3(u_1^{\mathrm{TE}})^2 \beta_{\mathrm{v}m} + 2u_1^{\mathrm{TE}} v_m^{\mathrm{TM}} \alpha_{\mathrm{v}m}] \dfrac{1}{c_0} \partial_t u_1^{\mathrm{TE}} \\ F_{\mathrm{e}}((u_1^{\mathrm{TE}})^2 \alpha_{\mathrm{w}m}) \dfrac{1}{c_0} \partial_t w_m^{\mathrm{TM}} + \lambda_m^{\mathrm{TM}} u_m^{\mathrm{TM}} = -2F'_{\mathrm{e}}(\tilde{E}^2_{\mathrm{w}m}) u_1^{\mathrm{TE}} w_m^{\mathrm{TM}} \alpha_{\mathrm{w}m} \dfrac{1}{c_0} \partial_t u_1^{\mathrm{TE}} \end{cases} \tag{6.14}$$

Some conclusions from these equations are

- The model is suitable when the dominant mode is not affected by the minor modes. It is modeled by a system of quasi-linear partial differential equations without source terms, which can be reduced to the scalar problem $-\partial_z^2 u + \partial_t^2 \left(F(u^2) u \right) + \lambda^2 u = 0$.
- The minor modes travel through an inhomogeneous medium with source terms. Both the inhomogeneity and the source terms are induced by the dominant mode.

6.4 Energy for the dominant mode

By multiplying the first, second and third equation in (6.12) by u_1^{TE}, v_1^{TE} and w_1^{TE}, respectively, and adding the equations, we obtain

$$\partial_z(u_1^{\mathrm{TE}}v_1^{\mathrm{TE}}) + u_1^{\mathrm{TE}}\frac{1}{c_0}\partial_t\left(F_{\mathrm{e}}((u_1^{\mathrm{TE}})^2\alpha_{\mathrm{u1}})u_1^{\mathrm{TE}}\right) + \frac{1}{c_0}\partial_t\left(\frac{(v_1^{\mathrm{TE}})^2}{2} + \frac{(w_1^{\mathrm{TE}})^2}{2}\right) = 0. \quad (6.15)$$

After some algebra, we find that this can be written as

$$\partial_z(u_1^{\mathrm{TE}}v_1^{\mathrm{TE}}) + \frac{1}{c_0}\partial_t\left(\frac{G((u_1^{\mathrm{TE}})^2\alpha_{\mathrm{u1}})}{\alpha_{\mathrm{u1}}} + \frac{(v_1^{\mathrm{TE}})^2}{2} + \frac{(w_1^{\mathrm{TE}})^2}{2}\right) = 0, \quad (6.16)$$

if we introduce the energy density function

$$\begin{aligned} G((u_1^{\mathrm{TE}})^2\alpha_{\mathrm{u1}}) &= \alpha_{\mathrm{u1}}\int_0^{u_1^{\mathrm{TE}}} [F_{\mathrm{e}}(u^2\alpha_{\mathrm{u1}}) + 2F_{\mathrm{e}}'(u^2\alpha_{\mathrm{u1}})u^2\alpha_{\mathrm{u1}}]u\,\mathrm{d}u \\ &= \frac{1}{2}\int_0^{(u_1^{\mathrm{TE}})^2\alpha_{\mathrm{u1}}} [F_{\mathrm{e}}(x) + 2F_{\mathrm{e}}'(x)x]\,\mathrm{d}x. \end{aligned} \quad (6.17)$$

This is exactly the energy density for propagation in an unbounded medium; the influence of the waveguide is reduced to a scaling constant α_{u1}. The energy density function can be calculated explicitly for some common cases. For the Kerr medium, where $F_{\mathrm{e}}(E^2) = 1 + E^2$, we have

$$G(u^2) = \frac{1}{2}u^2 + \frac{3}{4}u^4. \quad (6.18)$$

It is easy to show that for a medium where F_{e} can be expanded in a polynomial series, the energy density can be expressed in a related series. Another medium which has been used is the saturated Kerr medium [13, 21, 22], where $F_{\mathrm{e}}(E^2) = 1+E^2/(1+E^2)$. The energy density for this medium is

$$G(u^2) = \frac{1}{2}\left(\frac{2u^4}{1+u^2} + \ln(1+u^2)\right). \quad (6.19)$$

Integrating (6.16) over z and $0 \le t \le T$, we have

$$\begin{aligned} &\int\left(\frac{G((u_1^{\mathrm{TE}})^2\alpha_{\mathrm{u1}})}{\alpha_{\mathrm{u1}}} + \frac{(v_1^{\mathrm{TE}})^2}{2} + \frac{(w_1^{\mathrm{TE}})^2}{2}\right)\mathrm{d}z\Big|_{t=T} \\ &\quad = \int\left(\frac{G((u_1^{\mathrm{TE}})^2\alpha_{\mathrm{u1}})}{\alpha_{\mathrm{u1}}} + \frac{(v_1^{\mathrm{TE}})^2}{2} + \frac{(w_1^{\mathrm{TE}})^2}{2}\right)\mathrm{d}z\Big|_{t=0} \end{aligned} \quad (6.20)$$

since the parts associated with the z derivative correspond to the field values at infinity, and can be assumed to disappear for finite times T. This means that the energy of the dominant mode is conserved in this approximation.

6.5 Estimate of the mode-spreading

We have shown that one of the most distinct features of nonlinearity in propagation of guided waves is that the modes are no longer independent, but rather couple in an intricate manner. In the case of a dominant mode, this coupling appears as creating inhomogeneities and source terms for the minor modes. In this section we estimate how fast these minor modes grow when the dominant mode is known.

We refrain from using the explicit representation of the source terms in equations (6.12), (6.13) and (6.14), and return to the generic case

$$\begin{cases} \partial_z v_m^{\mathrm{TE}} + \dfrac{1}{c_0}\partial_t \left(F_{\mathrm{e}}(\tilde{E}_{\mathrm{um}}^2) u_m^{\mathrm{TE}} \right) - \lambda_m^{\mathrm{TE}} w_m^{\mathrm{TE}} = 0 \\ \partial_z u_m^{\mathrm{TE}} + \dfrac{1}{c_0}\partial_t v_m^{\mathrm{TE}} = 0 \\ \dfrac{1}{c_0}\partial_t w_m^{\mathrm{TE}} + \lambda_m^{\mathrm{TE}} u_m^{\mathrm{TE}} = 0 \end{cases} \tag{6.21}$$

where $\tilde{E}_{\mathrm{um}}^2 = \alpha_{\mathrm{um}} (u_1^{\mathrm{TE}})^2 + \beta_{\mathrm{um}} \frac{(u_1^{\mathrm{TE}})^3}{u_m^{\mathrm{TE}}}$. The differential energy equation is now

$$\partial_z (u_m^{\mathrm{TE}} v_m^{\mathrm{TE}}) + u_m^{\mathrm{TE}} \frac{1}{c_0}\partial_t \left(F_{\mathrm{e}}(\tilde{E}_{\mathrm{um}}^2) u_m^{\mathrm{TE}} \right) + \frac{1}{c_0}\partial_t \left(\frac{(v_m^{\mathrm{TE}})^2}{2} + \frac{(w_m^{\mathrm{TE}})^2}{2} \right) = 0. \tag{6.22}$$

For the dominant mode, we found a total energy, *i.e.*, a total time derivative. This is no longer possible, but a step in the desired direction is

$$\begin{aligned} \partial_z \left(u_m^{\mathrm{TE}} v_m^{\mathrm{TE}} \right) + \frac{1}{c_0}\partial_t \left(F_{\mathrm{e}}(\tilde{E}_{\mathrm{um}}^2) \frac{(u_m^{\mathrm{TE}})^2}{2} + \frac{(v_m^{\mathrm{TE}})^2}{2} + \frac{(w_m^{\mathrm{TE}})^2}{2} \right) \\ = \frac{(u_m^{\mathrm{TE}})^2}{2} \frac{1}{c_0}\partial_t F_{\mathrm{e}}(\tilde{E}_{\mathrm{um}}^2). \end{aligned} \tag{6.23}$$

Integrating this equation over z, implies

$$\begin{aligned} &\partial_t \int \left(F_{\mathrm{e}}(\tilde{E}_{\mathrm{um}}^2) \frac{(u_m^{\mathrm{TE}})^2}{2} + \frac{(v_m^{\mathrm{TE}})^2}{2} + \frac{(w_m^{\mathrm{TE}})^2}{2} \right) \mathrm{d}z \\ &\quad = \int \frac{(u_m^{\mathrm{TE}})^2}{2} \partial_t F_{\mathrm{e}}(\tilde{E}_{\mathrm{um}}^2) \, \mathrm{d}z \\ &\quad = \int F_{\mathrm{e}}(\tilde{E}_{\mathrm{um}}^2) \frac{(u_m^{\mathrm{TE}})^2}{2} \partial_t \ln F_{\mathrm{e}}(\tilde{E}_{\mathrm{um}}^2) \, \mathrm{d}z \\ &\quad \leq \sup_z |\partial_t \ln F_{\mathrm{e}}(\tilde{E}_{\mathrm{um}}^2)| \int \left(F_{\mathrm{e}}(\tilde{E}_{\mathrm{um}}^2) \frac{(u_m^{\mathrm{TE}})^2}{2} + \frac{(v_m^{\mathrm{TE}})^2}{2} + \frac{(w_m^{\mathrm{TE}})^2}{2} \right) \mathrm{d}z, \end{aligned} \tag{6.24}$$

where the last line follows only if we do not have any shocks, *i.e.*, the time derivative is bounded. If we assume the supremum is given by the dominating mode only, we

can apply Grönwall's inequality (see *e.g.*, [9, p. 624]), to find

$$\int \left(F_{\mathrm{e}}(\tilde{E}^2_{\mathrm{um}}) \frac{(u_m^{\mathrm{TE}})^2}{2} + \frac{(v_m^{\mathrm{TE}})^2}{2} + \frac{(w_m^{\mathrm{TE}})^2}{2} \right) \mathrm{d}z \Bigg|_{t=T} \leq \exp\left(\int_0^T \sup_z |\partial_t \ln F_{\mathrm{e}}(\tilde{E}^2_{\mathrm{um}})| \, \mathrm{d}t \right) \int \left(F_{\mathrm{e}}(\tilde{E}^2_{\mathrm{um}}) \frac{(u_m^{\mathrm{TE}})^2}{2} + \frac{(v_m^{\mathrm{TE}})^2}{2} + \frac{(w_m^{\mathrm{TE}})^2}{2} \right) \mathrm{d}z \Bigg|_{t=0}. \tag{6.25}$$

This seems to imply that if we put no energy in this mode from the start, it will stay silent! Though, as we clearly see in the first line of (6.13), there is a source term which depends solely on u_1^{TE} and initiates the minor modes. The estimate (6.25) is simply not valid in the limit $u_m^{\mathrm{TE}} \to 0$, since

$$\begin{aligned} \left|\partial_t \ln F_{\mathrm{e}}(\tilde{E}^2_{\mathrm{um}})\right| &= \left| \frac{F_{\mathrm{e}}'(\alpha_{\mathrm{um}}(u_1^{\mathrm{TE}})^2)}{F_{\mathrm{e}}(\alpha_{\mathrm{um}}(u_1^{\mathrm{TE}})^2)} \right| \\ &\quad \cdot \left| 2\alpha_{\mathrm{um}} u_1^{\mathrm{TE}} \partial_t u_1^{\mathrm{TE}} + 3\beta_{\mathrm{um}} \frac{(u_1^{\mathrm{TE}})^2}{u_m^{\mathrm{TE}}} \partial_t u_1^{\mathrm{TE}} - \beta_{\mathrm{um}} \frac{(u_1^{\mathrm{TE}})^3}{(u_m^{\mathrm{TE}})^2} \partial_t u_m^{\mathrm{TE}} \right| \\ &\quad \to \infty \quad \text{as} \quad u_m^{\mathrm{TE}} \to 0. \end{aligned} \tag{6.26}$$

Thus, we can expect a relatively rapid growth when u_m^{TE} is very small and $\beta_{\mathrm{um}} \neq 0$. In the case of the parallel plate waveguide, it is easily seen that the coupling factor is $\beta_{\mathrm{um}} = C\delta_{m,3}$.

7 Conclusions and discussion

The coupling between the modes produces equations for a general mode analysis which are hard to analyze. By adding the assumption of a dominant mode, we obtain a tractable problem. The dominant mode is described by a nonlinear system of homogeneous partial differential equations, and the minor modes are described by a linear system of inhomogeneous partial differential equations. The equations describing the propagation of the dominant mode are inert with respect to the minor modes, and should be object for further studies.

There is *always* a mode spreading present. The mechanisms behind this must be examined further. Some open questions are: 1) is there an equilibrium in the mode distribution, 2) when is the mode spreading strong enough to influence the dominant mode, and 3) how fast do the minor modes grow? It should be stressed that the relative ease of implementing a finite difference algorithm for the three-dimensional analysis of a rectangular waveguide makes the numerical study of the "true" mode spreading possible.

Since we have used the common waveguide modes for the analysis, the equations derived in this paper may be of interest in a mode matching algorithm, especially for the inverse scattering problem. A remaining problem is the propagation through the boundary between a nonlinear material and, *e.g.*, vacuum.

8 Acknowledgments

The author would like to acknowledge fruitful discussions with Prof. Gerhard Kristensson and several colleagues at the Electromagnetic Theory Group in Lund.

The work reported in this paper is partially supported by a grant from the Swedish Research Council for Engineering Sciences and its support is gratefully acknowledged.

A large portion of this paper was written during a stay at the Department of Mathematics and Statistics of the University of Canterbury, Christchurch, New Zealand, and their warm hospitality is most appreciated. The author would also like to thank the Royal Physiographical Society of Lund (Kungliga fysiografiska sällskapet i Lund), for a grant enabling this visit.

Appendix A Explicit representations of $\tilde{E}_m^2$

In Section 4.3 we derived the expression

$$\tilde{E}_m^2 = \sum_{kln} \frac{f_k f_l f_n}{f_m} (\boldsymbol{E}_m, \boldsymbol{E}_k \cdot \boldsymbol{E}_l \boldsymbol{E}_n) \tag{A.1}$$

if the electric field is expanded in orthonormal basis functions $\boldsymbol{E}_n$. Though, in order to derive the propagation equations for the modes, we use the expansion

$$\begin{aligned} \begin{pmatrix} \boldsymbol{E} \\ \boldsymbol{H} \end{pmatrix} = \sum_n & u_n^{\mathrm{TE}} \boldsymbol{U}_n^{\mathrm{TE}} + v_n^{\mathrm{TE}} \boldsymbol{V}_n^{\mathrm{TE}} + w_n^{\mathrm{TE}} \boldsymbol{W}_n^{\mathrm{TE}} \\ & + u_n^{\mathrm{TM}} \boldsymbol{U}_n^{\mathrm{TM}} + v_n^{\mathrm{TM}} \boldsymbol{V}_n^{\mathrm{TM}} + w_n^{\mathrm{TM}} \boldsymbol{W}_n^{\mathrm{TM}}, \end{aligned} \tag{A.2}$$

where $\boldsymbol{U}_n^{\mathrm{TE}}$, $\boldsymbol{V}_n^{\mathrm{TM}}$ and $\boldsymbol{W}_n^{\mathrm{TM}}$ are associated with the electric field and $\boldsymbol{U}_n^{\mathrm{TM}}$, $\boldsymbol{V}_n^{\mathrm{TE}}$ and $\boldsymbol{W}_n^{\mathrm{TE}}$ are associated with the magnetic field. For the sake of completeness in our presentation, we give the formulas for $\tilde{E}_m^2$ related to each of these expansion functions in this appendix. We also replace the index m with the indices um, vm and wm, depending on if the basis function $\boldsymbol{E}_m$ is $\boldsymbol{U}_m^{\mathrm{TE}}$, $\boldsymbol{V}_m^{\mathrm{TE}}$ or $\boldsymbol{W}_m^{\mathrm{TE}}$.

A.1 Electric field

Expansion function $\boldsymbol{U}_m^{\mathrm{TE}}$:

$$
\begin{aligned}
\tilde{E}_{\mathrm{um}}^2 = &\sum_{kln} \frac{u_k^{\mathrm{TE}} u_l^{\mathrm{TE}} u_n^{\mathrm{TE}}}{u_m^{\mathrm{TE}}} (\boldsymbol{U}_m^{\mathrm{TE}}, \boldsymbol{U}_k^{\mathrm{TE}} \cdot \boldsymbol{U}_l^{\mathrm{TE}} \boldsymbol{U}_n^{\mathrm{TE}}) \\
&+ \sum_{kln} \frac{v_k^{\mathrm{TM}} u_l^{\mathrm{TE}} u_n^{\mathrm{TE}}}{u_m^{\mathrm{TE}}} (\boldsymbol{U}_m^{\mathrm{TE}}, \boldsymbol{V}_k^{\mathrm{TM}} \cdot \boldsymbol{U}_l^{\mathrm{TE}} \boldsymbol{U}_n^{\mathrm{TE}}) \\
&+ \sum_{kln} \frac{u_k^{\mathrm{TE}} v_l^{\mathrm{TM}} u_n^{\mathrm{TE}}}{u_m^{\mathrm{TE}}} (\boldsymbol{U}_m^{\mathrm{TE}}, \boldsymbol{U}_k^{\mathrm{TE}} \cdot \boldsymbol{V}_l^{\mathrm{TM}} \boldsymbol{U}_n^{\mathrm{TE}}) \\
&+ \sum_{kln} \frac{v_k^{\mathrm{TM}} v_l^{\mathrm{TM}} u_n^{\mathrm{TE}}}{u_m^{\mathrm{TE}}} (\boldsymbol{U}_m^{\mathrm{TE}}, \boldsymbol{V}_k^{\mathrm{TM}} \cdot \boldsymbol{V}_l^{\mathrm{TM}} \boldsymbol{U}_n^{\mathrm{TE}}) \\
&+ \sum_{kln} \frac{w_k^{\mathrm{TM}} w_l^{\mathrm{TM}} u_n^{\mathrm{TE}}}{u_m^{\mathrm{TE}}} (\boldsymbol{U}_m^{\mathrm{TE}}, \boldsymbol{W}_k^{\mathrm{TM}} \cdot \boldsymbol{W}_l^{\mathrm{TM}} \boldsymbol{U}_n^{\mathrm{TE}}) \\
&+ \sum_{kln} \frac{u_k^{\mathrm{TE}} u_l^{\mathrm{TE}} v_n^{\mathrm{TM}}}{u_m^{\mathrm{TE}}} (\boldsymbol{U}_m^{\mathrm{TE}}, \boldsymbol{U}_k^{\mathrm{TE}} \cdot \boldsymbol{U}_l^{\mathrm{TE}} \boldsymbol{V}_n^{\mathrm{TM}}) \\
&+ \sum_{kln} \frac{v_k^{\mathrm{TM}} u_l^{\mathrm{TE}} v_n^{\mathrm{TM}}}{u_m^{\mathrm{TE}}} (\boldsymbol{U}_m^{\mathrm{TE}}, \boldsymbol{V}_k^{\mathrm{TM}} \cdot \boldsymbol{U}_l^{\mathrm{TE}} \boldsymbol{V}_n^{\mathrm{TM}}) \\
&+ \sum_{kln} \frac{u_k^{\mathrm{TE}} v_l^{\mathrm{TM}} v_n^{\mathrm{TM}}}{u_m^{\mathrm{TE}}} (\boldsymbol{U}_m^{\mathrm{TE}}, \boldsymbol{U}_k^{\mathrm{TE}} \cdot \boldsymbol{V}_l^{\mathrm{TM}} \boldsymbol{V}_n^{\mathrm{TM}}) \\
&+ \sum_{kln} \frac{v_k^{\mathrm{TM}} v_l^{\mathrm{TM}} v_n^{\mathrm{TM}}}{u_m^{\mathrm{TE}}} (\boldsymbol{U}_m^{\mathrm{TE}}, \boldsymbol{V}_k^{\mathrm{TM}} \cdot \boldsymbol{V}_l^{\mathrm{TM}} \boldsymbol{V}_n^{\mathrm{TM}}) \\
&+ \sum_{kln} \frac{w_k^{\mathrm{TM}} w_l^{\mathrm{TM}} v_n^{\mathrm{TM}}}{u_m^{\mathrm{TE}}} (\boldsymbol{U}_m^{\mathrm{TE}}, \boldsymbol{W}_k^{\mathrm{TM}} \cdot \boldsymbol{W}_l^{\mathrm{TM}} \boldsymbol{V}_n^{\mathrm{TM}}).
\end{aligned}
\tag{A.3}
$$

Expansion function $\boldsymbol{V}_m^{\mathrm{TM}}$:

$$\begin{aligned}
\tilde{E}_{\mathrm{vm}}^2 = &\sum_{kln} \frac{u_k^{\mathrm{TE}} u_l^{\mathrm{TE}} u_n^{\mathrm{TE}}}{v_m^{\mathrm{TM}}} (\boldsymbol{V}_m^{\mathrm{TM}}, \boldsymbol{U}_k^{\mathrm{TE}} \cdot \boldsymbol{U}_l^{\mathrm{TE}} \boldsymbol{U}_n^{\mathrm{TE}}) \\
&+ \sum_{kln} \frac{v_k^{\mathrm{TM}} u_l^{\mathrm{TE}} u_n^{\mathrm{TE}}}{v_m^{\mathrm{TM}}} (\boldsymbol{V}_m^{\mathrm{TM}}, \boldsymbol{V}_k^{\mathrm{TM}} \cdot \boldsymbol{U}_l^{\mathrm{TE}} \boldsymbol{U}_n^{\mathrm{TE}}) \\
&+ \sum_{kln} \frac{u_k^{\mathrm{TE}} v_l^{\mathrm{TM}} u_n^{\mathrm{TE}}}{v_m^{\mathrm{TM}}} (\boldsymbol{V}_m^{\mathrm{TM}}, \boldsymbol{U}_k^{\mathrm{TE}} \cdot \boldsymbol{V}_l^{\mathrm{TM}} \boldsymbol{U}_n^{\mathrm{TE}}) \\
&+ \sum_{kln} \frac{v_k^{\mathrm{TM}} v_l^{\mathrm{TM}} u_n^{\mathrm{TE}}}{v_m^{\mathrm{TM}}} (\boldsymbol{V}_m^{\mathrm{TM}}, \boldsymbol{V}_k^{\mathrm{TM}} \cdot \boldsymbol{V}_l^{\mathrm{TM}} \boldsymbol{U}_n^{\mathrm{TE}}) \\
&+ \sum_{kln} \frac{w_k^{\mathrm{TM}} w_l^{\mathrm{TM}} u_n^{\mathrm{TE}}}{v_m^{\mathrm{TM}}} (\boldsymbol{V}_m^{\mathrm{TM}}, \boldsymbol{W}_k^{\mathrm{TM}} \cdot \boldsymbol{W}_l^{\mathrm{TM}} \boldsymbol{U}_n^{\mathrm{TE}}) \\
&+ \sum_{kln} \frac{u_k^{\mathrm{TE}} u_l^{\mathrm{TE}} v_n^{\mathrm{TM}}}{v_m^{\mathrm{TM}}} (\boldsymbol{V}_m^{\mathrm{TM}}, \boldsymbol{U}_k^{\mathrm{TE}} \cdot \boldsymbol{U}_l^{\mathrm{TE}} \boldsymbol{V}_n^{\mathrm{TM}}) \\
&+ \sum_{kln} \frac{v_k^{\mathrm{TM}} u_l^{\mathrm{TE}} v_n^{\mathrm{TM}}}{v_m^{\mathrm{TM}}} (\boldsymbol{V}_m^{\mathrm{TM}}, \boldsymbol{V}_k^{\mathrm{TM}} \cdot \boldsymbol{U}_l^{\mathrm{TE}} \boldsymbol{V}_n^{\mathrm{TM}}) \\
&+ \sum_{kln} \frac{u_k^{\mathrm{TE}} v_l^{\mathrm{TM}} v_n^{\mathrm{TM}}}{v_m^{\mathrm{TM}}} (\boldsymbol{V}_m^{\mathrm{TM}}, \boldsymbol{U}_k^{\mathrm{TE}} \cdot \boldsymbol{V}_l^{\mathrm{TM}} \boldsymbol{V}_n^{\mathrm{TM}}) \\
&+ \sum_{kln} \frac{v_k^{\mathrm{TM}} v_l^{\mathrm{TM}} v_n^{\mathrm{TM}}}{v_m^{\mathrm{TM}}} (\boldsymbol{V}_m^{\mathrm{TM}}, \boldsymbol{V}_k^{\mathrm{TM}} \cdot \boldsymbol{V}_l^{\mathrm{TM}} \boldsymbol{V}_n^{\mathrm{TM}}) \\
&+ \sum_{kln} \frac{w_k^{\mathrm{TM}} w_l^{\mathrm{TM}} v_n^{\mathrm{TM}}}{v_m^{\mathrm{TM}}} (\boldsymbol{V}_m^{\mathrm{TM}}, \boldsymbol{W}_k^{\mathrm{TM}} \cdot \boldsymbol{W}_l^{\mathrm{TM}} \boldsymbol{V}_n^{\mathrm{TM}}).
\end{aligned} \tag{A.4}$$

Expansion function $\boldsymbol{W}_m^{\mathrm{TM}}$:

$$\begin{aligned}
\tilde{E}_{\mathrm{wm}}^2 = &\sum_{kln} \frac{u_k^{\mathrm{TE}} u_l^{\mathrm{TE}} w_n^{\mathrm{TM}}}{w_m^{\mathrm{TM}}} (\boldsymbol{W}_m^{\mathrm{TM}}, \boldsymbol{U}_k^{\mathrm{TE}} \cdot \boldsymbol{U}_l^{\mathrm{TE}} \boldsymbol{W}_n^{\mathrm{TM}}) \\
&+ \sum_{kln} \frac{v_k^{\mathrm{TM}} u_l^{\mathrm{TE}} w_n^{\mathrm{TM}}}{w_m^{\mathrm{TM}}} (\boldsymbol{W}_m^{\mathrm{TM}}, \boldsymbol{V}_k^{\mathrm{TM}} \cdot \boldsymbol{U}_l^{\mathrm{TE}} \boldsymbol{W}_n^{\mathrm{TM}}) \\
&+ \sum_{kln} \frac{u_k^{\mathrm{TE}} v_l^{\mathrm{TM}} w_n^{\mathrm{TM}}}{w_m^{\mathrm{TM}}} (\boldsymbol{W}_m^{\mathrm{TM}}, \boldsymbol{U}_k^{\mathrm{TE}} \cdot \boldsymbol{V}_l^{\mathrm{TM}} \boldsymbol{W}_n^{\mathrm{TM}}) \\
&+ \sum_{kln} \frac{v_k^{\mathrm{TM}} v_l^{\mathrm{TM}} w_n^{\mathrm{TM}}}{w_m^{\mathrm{TM}}} (\boldsymbol{W}_m^{\mathrm{TM}}, \boldsymbol{V}_k^{\mathrm{TM}} \cdot \boldsymbol{V}_l^{\mathrm{TM}} \boldsymbol{W}_n^{\mathrm{TM}}) \\
&+ \sum_{kln} \frac{w_k^{\mathrm{TM}} w_l^{\mathrm{TM}} w_n^{\mathrm{TM}}}{w_m^{\mathrm{TM}}} (\boldsymbol{W}_m^{\mathrm{TM}}, \boldsymbol{W}_k^{\mathrm{TM}} \cdot \boldsymbol{W}_l^{\mathrm{TM}} \boldsymbol{W}_n^{\mathrm{TM}}).
\end{aligned} \tag{A.5}$$

A.2 Magnetic field

Simply exchange TE for TM and vice versa in the formulas in the previous section to obtain $\tilde{H}^2$.

A.3 Derivation of leading terms for a dominant TE-mode

In Section 6 it was required to deduce the leading terms in the previous expressions when u_1^{TE} is much greater than the other expansion coefficients.

A.3.1 Expansion function $\boldsymbol{U}_m^{\mathrm{TE}}$

The terms in (A.3) proportional to at least $(u_1^{\mathrm{TE}})^2$ are

$$\begin{aligned}
\tilde{E}^2_{\mathrm{u}m} =& \frac{u_1^{\mathrm{TE}} u_1^{\mathrm{TE}} u_1^{\mathrm{TE}}}{u_m^{\mathrm{TE}}} (\boldsymbol{U}_m^{\mathrm{TE}}, \boldsymbol{U}_1^{\mathrm{TE}} \cdot \boldsymbol{U}_1^{\mathrm{TE}} \boldsymbol{U}_1^{\mathrm{TE}}) \\
&+ \sum_{k\neq 1} \frac{u_k^{\mathrm{TE}} u_1^{\mathrm{TE}} u_1^{\mathrm{TE}}}{u_m^{\mathrm{TE}}} (\boldsymbol{U}_m^{\mathrm{TE}}, \boldsymbol{U}_k^{\mathrm{TE}} \cdot \boldsymbol{U}_1^{\mathrm{TE}} \boldsymbol{U}_1^{\mathrm{TE}}) \\
&+ \sum_{l\neq 1} \frac{u_1^{\mathrm{TE}} u_l^{\mathrm{TE}} u_1^{\mathrm{TE}}}{u_m^{\mathrm{TE}}} (\boldsymbol{U}_m^{\mathrm{TE}}, \boldsymbol{U}_1^{\mathrm{TE}} \cdot \boldsymbol{U}_l^{\mathrm{TE}} \boldsymbol{U}_1^{\mathrm{TE}}) \\
&+ \sum_{n\neq 1} \frac{u_1^{\mathrm{TE}} u_1^{\mathrm{TE}} u_n^{\mathrm{TE}}}{u_m^{\mathrm{TE}}} (\boldsymbol{U}_m^{\mathrm{TE}}, \boldsymbol{U}_1^{\mathrm{TE}} \cdot \boldsymbol{U}_1^{\mathrm{TE}} \boldsymbol{U}_n^{\mathrm{TE}}) \\
&+ \sum_{k\neq 1} \frac{v_k^{\mathrm{TM}} u_1^{\mathrm{TE}} u_1^{\mathrm{TE}}}{u_m^{\mathrm{TE}}} (\boldsymbol{U}_m^{\mathrm{TE}}, \boldsymbol{V}_k^{\mathrm{TM}} \cdot \boldsymbol{U}_1^{\mathrm{TE}} \boldsymbol{U}_1^{\mathrm{TE}}) \\
&+ \sum_{l\neq 1} \frac{u_1^{\mathrm{TE}} v_l^{\mathrm{TM}} u_1^{\mathrm{TE}}}{u_m^{\mathrm{TE}}} (\boldsymbol{U}_m^{\mathrm{TE}}, \boldsymbol{U}_1^{\mathrm{TE}} \cdot \boldsymbol{V}_l^{\mathrm{TM}} \boldsymbol{U}_1^{\mathrm{TE}}) \\
&+ \sum_{n\neq 1} \frac{u_1^{\mathrm{TE}} u_1^{\mathrm{TE}} v_n^{\mathrm{TM}}}{u_m^{\mathrm{TE}}} (\boldsymbol{U}_m^{\mathrm{TE}}, \boldsymbol{U}_1^{\mathrm{TE}} \cdot \boldsymbol{U}_1^{\mathrm{TE}} \boldsymbol{V}_n^{\mathrm{TM}}).
\end{aligned} \tag{A.6}$$

In Appendix B we show that in general these scalar products are small if the free index in the sums is much separated from m. Therefore, we expect the sums in the above expression for $\tilde{E}^2_m$ can be estimated by the terms given by $k = l = n = m$. For $m = 1$ this means

$$\begin{aligned}
\tilde{E}^2_{\mathrm{u}1} &= (u_1^{\mathrm{TE}})^2 (\boldsymbol{U}_1^{\mathrm{TE}}, \boldsymbol{U}_1^{\mathrm{TE}} \cdot \boldsymbol{U}_1^{\mathrm{TE}} \boldsymbol{U}_1^{\mathrm{TE}}) \\
&= (u_1^{\mathrm{TE}})^2 \alpha_{\mathrm{u}1},
\end{aligned} \tag{A.7}$$

where

$$\alpha_{\mathrm{u}1} = \iint_\Omega |\nabla_{\mathrm{T}} \phi_1^{\mathrm{TE}}|^4 \,\mathrm{d}x \,\mathrm{d}y. \tag{A.8}$$

For $m \neq 1$ we have

$$\begin{aligned}\tilde{E}_{\mathrm{u}m}^2 =& \frac{(u_1^{\mathrm{TE}})^3}{u_m^{\mathrm{TE}}}(\boldsymbol{U}_m^{\mathrm{TE}}, \boldsymbol{U}_1^{\mathrm{TE}} \cdot \boldsymbol{U}_1^{\mathrm{TE}} \boldsymbol{U}_1^{\mathrm{TE}}) \\ &+ (u_1^{\mathrm{TE}})^2 \left[(\boldsymbol{U}_m^{\mathrm{TE}}, \boldsymbol{U}_1^{\mathrm{TE}} \cdot \boldsymbol{U}_1^{\mathrm{TE}} \boldsymbol{U}_m^{\mathrm{TE}}) + 2(\boldsymbol{U}_m^{\mathrm{TE}}, \boldsymbol{U}_m^{\mathrm{TE}} \cdot \boldsymbol{U}_1^{\mathrm{TE}} \boldsymbol{U}_1^{\mathrm{TE}})\right] \\ =& \frac{(u_1^{\mathrm{TE}})^3}{u_m^{\mathrm{TE}}} \beta_{\mathrm{u}m} + (u_1^{\mathrm{TE}})^2 \alpha_{\mathrm{u}m},\end{aligned} \tag{A.9}$$

where

$$\alpha_{\mathrm{u}m} = \iint_\Omega |\nabla_{\mathrm{T}} \phi_m^{\mathrm{TE}}|^2 |\nabla_{\mathrm{T}} \phi_1^{\mathrm{TE}}|^2 \,\mathrm{d}x\,\mathrm{d}y + 2 \iint_\Omega |\nabla_{\mathrm{T}} \phi_m^{\mathrm{TE}} \cdot \nabla_{\mathrm{T}} \phi_1^{\mathrm{TE}}|^2 \,\mathrm{d}x\,\mathrm{d}y \tag{A.10}$$

and

$$\beta_{\mathrm{u}m} = \iint_\Omega \nabla_{\mathrm{T}} \phi_m^{\mathrm{TE}} \cdot \nabla_{\mathrm{T}} \phi_1^{\mathrm{TE}} |\nabla_{\mathrm{T}} \phi_1^{\mathrm{TE}}|^2 \,\mathrm{d}x\,\mathrm{d}y. \tag{A.11}$$

We see that $\alpha_{\mathrm{u}1}$ and $\alpha_{\mathrm{u}m}$ are positive, whereas $\beta_{\mathrm{u}m}$ is not that easily analyzed.

A.3.2 Expansion functions $\boldsymbol{V}_m^{\mathrm{TM}}$ and $\boldsymbol{W}_m^{\mathrm{TM}}$

A similar analysis as in the previous section implies that the leading terms for $\boldsymbol{V}_m^{\mathrm{TM}}$ are

$$\begin{aligned}\tilde{E}_{\mathrm{v}m}^2 =& \frac{(u_1^{\mathrm{TE}})^3}{v_m^{\mathrm{TM}}}(\boldsymbol{V}_m^{\mathrm{TM}}, \boldsymbol{U}_1^{\mathrm{TE}} \cdot \boldsymbol{U}_1^{\mathrm{TE}} \boldsymbol{U}_1^{\mathrm{TE}}) \\ &+ (u_1^{\mathrm{TE}})^2 \left[(\boldsymbol{V}_m^{\mathrm{TM}}, \boldsymbol{U}_1^{\mathrm{TE}} \cdot \boldsymbol{U}_1^{\mathrm{TE}} \boldsymbol{V}_m^{\mathrm{TM}}) + 2(\boldsymbol{V}_m^{\mathrm{TM}}, \boldsymbol{U}_1^{\mathrm{TE}} \cdot \boldsymbol{V}_m^{\mathrm{TM}} \boldsymbol{U}_1^{\mathrm{TE}}\right] \\ =& \frac{(u_1^{\mathrm{TE}})^3}{v_m^{\mathrm{TM}}} \beta_{\mathrm{v}m} + (u_1^{\mathrm{TE}})^2 \alpha_{\mathrm{v}m}\end{aligned} \tag{A.12}$$

where

$$\alpha_{\mathrm{v}m} = \iint_\Omega |\nabla_{\mathrm{T}} \phi_m^{\mathrm{TM}}|^2 |\nabla_{\mathrm{T}} \phi_1^{\mathrm{TE}}|^2 \,\mathrm{d}x\,\mathrm{d}y + 2 \iint_\Omega |\nabla_{\mathrm{T}} \phi_m^{\mathrm{TM}} \times \nabla_{\mathrm{T}} \phi_1^{\mathrm{TE}}|^2 \,\mathrm{d}x\,\mathrm{d}y \tag{A.13}$$

and

$$\beta_{\mathrm{v}m} = \iint_\Omega \hat{\boldsymbol{z}} \cdot (\nabla_{\mathrm{T}} \phi_m^{\mathrm{TM}} \times \nabla_{\mathrm{T}} \phi_1^{\mathrm{TE}}) |\nabla_{\mathrm{T}} \phi_1^{\mathrm{TE}}|^2 \,\mathrm{d}x\,\mathrm{d}y. \tag{A.14}$$

The leading term for $\boldsymbol{W}_m^{\mathrm{TM}}$ is

$$\begin{aligned}\tilde{E}_{\mathrm{w}m}^2 =& (u_1^{\mathrm{TE}})^2 (\boldsymbol{W}_m^{\mathrm{TM}}, \boldsymbol{U}_1^{\mathrm{TE}} \cdot \boldsymbol{U}_1^{\mathrm{TE}} \boldsymbol{W}_m^{\mathrm{TM}}) \\ =& (u_1^{\mathrm{TE}})^2 \alpha_{\mathrm{w}m},\end{aligned} \tag{A.15}$$

where

$$\alpha_{\mathrm{w}m} = \iint_\Omega |\lambda_m^{\mathrm{TM}} \phi_m^{\mathrm{TM}}|^2 |\nabla_{\mathrm{T}} \phi_1^{\mathrm{TE}}|^2 \,\mathrm{d}x\,\mathrm{d}y. \tag{A.16}$$

Appendix B Decay of a scalar product

In this paper, we have often come across scalar products of the form $(\boldsymbol{U}_m^{\mathrm{TE}}, \boldsymbol{U}_k^{\mathrm{TE}} \cdot \boldsymbol{U}_l^{\mathrm{TE}} \boldsymbol{U}_n^{\mathrm{TE}})$, where $\boldsymbol{U}_m^{\mathrm{TE}}$ is a real-valued expansion function satisfying Helmholtz' equation in the plane. To analyze the case with a dominant TE_1-mode, we must make some estimate of this scalar product when two of the indices k, l, and n are equal to one. The canonical problem for this consists in calculating the scalar products

$$\iint_\Omega \phi_1^2 \phi_m \phi_n \,\mathrm{d}x\,\mathrm{d}y \tag{B.1}$$

where the scalar functions ϕ_k satisfy the Helmholtz' equation

$$\nabla_{\mathrm{T}}^2 \phi_k + \lambda_k^2 \phi_k = 0, \tag{B.2}$$

with Dirichlet or Neumann boundary conditions. The λ_k:s are assumed to be non-degenerate, positive and arranged in ascending order, *i.e.*, $0 < \lambda_1 < \lambda_2 < \ldots$ We choose the functions to be normalized as

$$\iint_\Omega |\phi_k|^2 \,\mathrm{d}x\,\mathrm{d}y = \iint_\Omega \left| \frac{\nabla_{\mathrm{T}} \phi_k}{\lambda_k} \right|^2 \mathrm{d}x\,\mathrm{d}y = 1, \tag{B.3}$$

which is not the normalization used previously in the paper for the eigenfunctions ϕ_k^{TE}, but simplifies the notation in this appendix. If $m \neq n$ we use the Helmholtz' equation to conclude

$$\begin{aligned}
\left| \iint_\Omega \phi_1^2 \phi_m \phi_n \,\mathrm{d}x\,\mathrm{d}y \right| &= \frac{1}{|\lambda_m^2 - \lambda_n^2|} \left| \iint_\Omega \phi_1^2 [-\phi_n \nabla_{\mathrm{T}}^2 \phi_m + \phi_m \nabla_{\mathrm{T}}^2 \phi_n] \,\mathrm{d}x\,\mathrm{d}y \right| \\
&= \frac{1}{|\lambda_m^2 - \lambda_n^2|} \left| \iint_\Omega \nabla_{\mathrm{T}} \phi_1^2 \cdot [\phi_n \nabla_{\mathrm{T}} \phi_m - \phi_m \nabla_{\mathrm{T}} \phi_n] \,\mathrm{d}x\,\mathrm{d}y \right| \\
&\leq \frac{\sup_\Omega |\nabla_{\mathrm{T}} \phi_1^2|}{|\lambda_m^2 - \lambda_n^2|} \iint_\Omega |\phi_n \nabla_{\mathrm{T}} \phi_m - \phi_m \nabla_{\mathrm{T}} \phi_n| \,\mathrm{d}x\,\mathrm{d}y.
\end{aligned} \tag{B.4}$$

Using Cauchy's inequality the last line can be estimated by

$$\begin{aligned}
&\frac{\sup_\Omega |\nabla_{\mathrm{T}} \phi_1^2|}{|\lambda_m^2 - \lambda_n^2|} \left[\lambda_m \iint_\Omega \left| \phi_n \frac{\nabla_{\mathrm{T}} \phi_m}{\lambda_m} \right| \mathrm{d}x\,\mathrm{d}y + \lambda_n \iint_\Omega \left| \phi_m \frac{\nabla_{\mathrm{T}} \phi_n}{\lambda_n} \right| \mathrm{d}x\,\mathrm{d}y \right] \\
&\quad \leq \frac{\sup_\Omega |\nabla_{\mathrm{T}} \phi_1^2|}{|\lambda_m^2 - \lambda_n^2|} \left[\frac{\lambda_m}{2} \iint_\Omega \left(|\phi_n|^2 + \left| \frac{\nabla_{\mathrm{T}} \phi_m}{\lambda_m} \right|^2 \right) \mathrm{d}x\,\mathrm{d}y \right. \\
&\qquad \left. + \frac{\lambda_n}{2} \iint_\Omega \left(|\phi_m|^2 + \left| \frac{\nabla_{\mathrm{T}} \phi_n}{\lambda_n} \right|^2 \right) \mathrm{d}x\,\mathrm{d}y \right] \\
&\quad = \frac{\sup_\Omega |\nabla_{\mathrm{T}} \phi_1^2|}{|\lambda_m^2 - \lambda_n^2|} (\lambda_m + \lambda_n) \\
&\quad = \frac{\sup_\Omega |\nabla_{\mathrm{T}} \phi_1^2|}{|\lambda_m - \lambda_n|}.
\end{aligned} \tag{B.5}$$

In two dimensions the eigenvalue λ_n grow approximately as the square root of the index n [7, p. 442], which implies the scalar product decays approximately as $1/|\sqrt{m} - \sqrt{n}|$ for large indices.

References

[1] G. B. Arfken and H. J. Weber. *Mathematical Methods for Physicists*. Academic Press, New York, 1995.

[2] P. Bernekorn, A. Karlsson, and G. Kristensson. Propagation of transient electromagnetic waves in inhomogeneous and dispersive waveguides. *J. Electro. Waves Applic.*, **10**(9), 1263–1286, 1996.

[3] A. Boström and P. Olsson. Transmission and reflection of electromagnetic waves by an obstacle inside a waveguide. *J. Appl Phys.*, **52**(3), 1187–1196, 1981.

[4] R. Y. Chiao, E. Garmire, and C. H. Townes. Self-trapping of optical beams. *Phys. Rev. Lett.*, **13**(15), 479–482, 1964.

[5] R. E. Collin. *Field Theory of Guided Waves*. IEEE Press, New York, second edition, 1991.

[6] M. Cotte. Propagation of a pulse in a waveguide. *Onde Elec.*, **34**, 143–146, 1954.

[7] R. Courant and D. Hilbert. *Methods of Mathematical Physics*, volume 1. Interscience Publishers, New York, 1953.

[8] A. C. Eringen and G. A. Maugin. *Electrodynamics of Continua I*. Springer-Verlag, New York, 1990.

[9] L. C. Evans. *Partial Differential Equations*. American Mathematical Society, Providence, Rhode Island, 1998.

[10] J. D. Jackson. *Classical Electrodynamics*. John Wiley & Sons, New York, third edition, 1999.

[11] P. L. Kelley. Self-focusing of optical beams. *Phys. Rev. Lett.*, **15**(26), 1005–1008, 1965.

[12] G. Kristensson. Transient electromagnetic wave propagation in waveguides. *J. Electro. Waves Applic.*, **9**(5/6), 645–671, 1995.

[13] G. Kristensson and D. J. N. Wall. Direct and inverse scattering for transient electromagnetic waves in nonlinear media. *Inverse Problems*, **14**, 113–137, 1998.

[14] L. D. Landau, E. M. Lifshitz, and L. P. Pitaevskiĭ. *Electrodynamics of Continuous Media*. Pergamon, Oxford, second edition, 1984.

[15] F. Olyslager. *Electromagnetic Waveguides and Transmission Lines*. Clarendon Press, Oxford, 1999.

[16] R. Petit, editor. *Electromagnetic Theory of Gratings*, volume 22 of *Topics in Current Physics*. Springer-Verlag, Heidelberg, 1980.

[17] S. V. Polstyanko, R. Dyczijedlinger, and J. F. Lee. Full wave vector Maxwell equation simulations of nonlinear self-focusing effects in three spatial dimensions. *IEEE Trans. Magnetics*, **33**(2 Part 2), 1780–1783, March 1997.

[18] A. Roberts. *Modal methods for gratings, grids and apertures*. PhD thesis, School of Physics, University of Sydney, 1988.

[19] T. Rozzi and L. Zappelli. Modal analysis of nonlinear propagation in a dielectric slab waveguide. *J. Lightwave Technol.*, **14**(2), 229–235, February 1996.

[20] D. Sjöberg. Simple wave solutions for the Maxwell equations in bianisotropic, nonlinear media, with application to oblique incidence. *Wave Motion*, **32**(3), 217–232, 2000.

[21] D. Sjöberg. Reconstruction of nonlinear material properties for homogeneous, isotropic slabs using electromagnetic waves. *Inverse Problems*, **15**(2), 431–444, April 1999.

[22] V. Tikhonenko, J. Christou, and B. Luther-Davies. Three-dimensional bright spatial soliton collision and fusion in a saturable nonlinear medium. *Phys. Rev. Lett.*, **76**, 2698–2701, 1996.

Shock structure for electromagnetic waves in bianisotropic, nonlinear materials

Daniel Sjöberg

Paper IV

Based on: D. Sjöberg. Shock structure for electromagnetic waves in bianisotropic, nonlinear materials. Technical Report LUTEDX/(TEAT-7094)/1–17/(2001), Lund Institute of Technology.

Abstract

Shock waves are discontinous solutions to quasi-linear partial differential equations, and can be studied through a singular perturbation known as the vanishing viscosity technique. The vanishing viscosity method is a means of smoothing the shock, and we study the case of electromagnetic waves in bianisotropic materials. We derive the conditions arising from this smoothing procedure for a traveling wave, and the waves are classified as fast, slow or intermediate shock waves.

1 Introduction

Electromagnetic waves propagating in an instantaneously reacting material can be modeled with a system of quasi-linear, partial differential equations. It is well known that such a model can exhibit shock solutions, *i.e.*, solutions which become discontinuous in finite time even if the initial/boundary data are smooth. This poses severe problems for numerical methods, such as finite difference schemes, which are often based on the assumption of continuous and differentiable solutions.

In order to overcome this problem, we can model the material on a finer scale, which requires a denser grid and thus increases the memory demands and the computation time. Another approach, is to develop more powerful numerical methods, which can handle discontinuous solutions. The development of these numerical schemes benefits from an understanding of the propagation of shock waves; for instance, Godunov's scheme is based on the solution of Riemann's problem [14, 15], where the shock wave is generated by discontinuous initial data. A variation of Godunov's scheme is Glimm's scheme, which is used to show global existence of solutions to certain systems of equations [13, 20].

The aim of this paper is to increase the understanding of electromagnetic shock waves, modeled with the Maxwell equations. Mainly using techniques from [31], we analyze the wave propagation in bianisotropic materials, *i.e.*, materials with different properties for different polarizations of the waves, and a possible coupling between the electric and the magnetic field [23, p. 7]. This adds insight not only to the numerical treatment of electromagnetic waves in complicated materials, but also provides some physical intuition.

The Maxwell equations can be considered as a hyperbolic system of conservation laws. A good introduction to the numerical approximation of such systems is given in [14], which introduces the analytical theory as well as some common schemes in one and two spatial dimensions. There is presently not a good mathematical understanding of systems of conservation laws in several dimensions, but some general references are [7, 14, 20, 30, 34].

Perhaps the most familiar kind of "electromagnetic" shock wave is in the field of magnetohydrodynamics, from which we give only a few references [1, 6, 10, 12, 17], [25, pp. 245–253]. Electromagnetic shock waves in isotropic media have previously been treated theoretically, see [25, pp. 388–391], [2] and references therein. Recently, a few papers on experiments concerning electromagnetic shock waves have been published [3, 4, 8]. In continuum mechanics, G. A. Maugin has recognized the

similarity between shock waves and phase transition fronts as singular sets in irreversible motion, with a dissipation related to the power expanded by a driving force on the singularity set, see [27, 28].

In this paper, we study when the shock waves can be defined as the limit of continuous traveling wave solutions to an approximate problem, where the discontinuity is smoothed over a small region. This is the *shock structure* problem, which was introduced by Gel'fand [11], and is given an extensive treatment in [33]. A thorough treatment of this problem in magnetohydrodynamics is found in [10], and a recent paper deals with the structure of electromagnetic shock waves in anisotropic ferromagnetic media [19].

This paper is organized as follows. In Section 2 we introduce the Maxwell equations and the constitutive relations used to model the electromagnetic waves, as well as the general form of the entropy condition. In Section 3 we present the vanishing viscosity method of smoothing the solutions of quasi-linear, hyperbolic equations. The consequences of the vanishing viscosity method for traveling waves are studied in Sections 4 and 5, where we show that there exists three kinds of electromagnetic shock waves: the fast, the slow, and the intermediate shock wave. In Section 6 we also mention another form of dicontinuous solutions, contact discontinuities, which cannot be analyzed with the vanishing viscosity method for traveling waves. However, they exist only under the condition of linear degeneracy, and we present this condition and its opposite, genuine nonlinearity, in Section 6. The different kinds of shock waves are illustrated with phase portraits of a certain system of ordinary differential equations in Section 7, and some concluding remarks are made in Section 8.

2 The Maxwell equations, constitutive relations and the entropy condition

In this paper we use a slight modification of the Heaviside-Lorentz units for our fields [21, p. 781], *i.e.*, all electromagnetic fields are scaled to units of $\sqrt{\text{energy/volume}}$,

$$\begin{cases} \boldsymbol{E} = \sqrt{\epsilon_0}\boldsymbol{E}_{\text{SI}} \\ \boldsymbol{H} = \sqrt{\mu_0}\boldsymbol{H}_{\text{SI}} \end{cases} \qquad \begin{cases} \boldsymbol{D} = 1/\sqrt{\epsilon_0}\boldsymbol{D}_{\text{SI}} \\ \boldsymbol{B} = 1/\sqrt{\mu_0}\boldsymbol{B}_{\text{SI}}, \end{cases} \tag{2.1}$$

where $\boldsymbol{E}$ and $\boldsymbol{H}$ is the electric and magnetic field strength, respectively, and $\boldsymbol{D}$ and $\boldsymbol{B}$ is the electric and magnetic flux density, respectively. The index SI is used to indicate the field in SI units. We use the scaled time $t = c_0 t_{\text{SI}}$, where $c_0 = 1/\sqrt{\epsilon_0\mu_0}$ is the speed of light in vacuum, and the constants ϵ_0 and μ_0 are the permittivity and permeability of free space, respectively. The six-vector notation from [18, 31], *i.e.*,

$$\boldsymbol{e} = \begin{pmatrix} \boldsymbol{E} \\ \boldsymbol{H} \end{pmatrix}, \quad \boldsymbol{d} = \begin{pmatrix} \boldsymbol{D} \\ \boldsymbol{B} \end{pmatrix}, \quad \nabla \times \mathbf{J} = \begin{pmatrix} \mathbf{0} & -\nabla \times \mathbf{I} \\ \nabla \times \mathbf{I} & \mathbf{0} \end{pmatrix}, \tag{2.2}$$

enables us to write the source free Maxwell equations in the compact form

$$\nabla \times \mathbf{J}\boldsymbol{e} + \partial_t \boldsymbol{d} = \mathbf{0}. \tag{2.3}$$

In this paper we treat the six-vectors as column vectors, *i.e.*, we write the scalar product as $\boldsymbol{e}^{\mathrm{T}}\boldsymbol{d} = \sum_{i=1}^{6} e_i d_i$. This is merely for notational convenience and does not capture the full mathematical structure, which is not needed here. On occasions, we also consider the scalar product between two three-vectors, in which case we use the standard notation $\boldsymbol{E} \cdot \boldsymbol{D} = \sum_{i=1}^{3} E_i D_i$. For more ambitious attempts to construct a six-vector notation, we refer to [18, 26].

The Maxwell equations must be supplemented by a constitutive relation, whose purpose is to model the interaction of the electromagnetic field with the material. When the material reacts very fast to stimulance, we can model it with an instantaneous constitutive model, where the values of the electric flux density $\boldsymbol{D}$ and the magnetic flux density $\boldsymbol{B}$ are completely determined by the values of the electric field strength $\boldsymbol{E}$ and magnetic field strength $\boldsymbol{H}$ at the same point in spacetime. We write this as

$$\boldsymbol{d}(\boldsymbol{r}, t) = \boldsymbol{d}(\boldsymbol{e}(\boldsymbol{r}, t)), \tag{2.4}$$

where $\boldsymbol{d}(\boldsymbol{e})$ is the gradient of a scalar function $\phi(\boldsymbol{e})$ with respect to $\boldsymbol{e}$, *i.e.*, in terms of thermodynamics, the field gradient of the thermodynamic potential (or the free energy density or the free enthalpy density) [5, 25]. We use the notation $\boldsymbol{d}(\boldsymbol{e}) = \phi'(\boldsymbol{e})$ to denote this derivative, *i.e.*, $d_i(\boldsymbol{e}) = \partial\phi/\partial e_i$, $i = 1, \ldots, 6$. The model is passive if we require that the symmetric 6×6 matrix $\boldsymbol{d}'(\boldsymbol{e}) = \phi''(\boldsymbol{e})$, where $[\boldsymbol{d}'(\boldsymbol{e})]_{ij} = \partial^2\phi/\partial e_i \partial e_j$, is a positive definite matrix, which is the case if the scalar function $\phi(\boldsymbol{e})$ is a convex function.

The initial value problem for the Maxwell equations with an instantaneously reacting constitutive model is

$$\nabla \times \mathbf{J}\boldsymbol{e} + \boldsymbol{d}'(\boldsymbol{e})\partial_t \boldsymbol{e} = \mathbf{0}, \qquad \boldsymbol{e}(\boldsymbol{x}, 0) = \boldsymbol{e}_0(\boldsymbol{x}), \tag{2.5}$$

and since $\boldsymbol{d}'(\boldsymbol{e})$ is positive definite and symmetric, this is by definition a quasi-linear, symmetric, hyperbolic system of partial differential equations [34, p. 360]. This system has been extensively studied in [31], where it is shown that the equations in general support two waves, the ordinary and the extraordinary wave, each with its own refractive index.

Due to the quasi-linearity, the system (2.5) may exhibit shock solutions, *i.e.*, even if we give smooth initial data, the solution becomes discontinuous in finite time. This means that the derivatives cannot be classically defined everywhere, but we can make a weak formulation of the problem by requiring the equality

$$\int_0^\infty \int_{\mathbb{R}^3} [\boldsymbol{e}^{\mathrm{T}} \nabla \times \mathbf{J}\boldsymbol{\varphi} + \boldsymbol{d}(\boldsymbol{e})^{\mathrm{T}} \partial_t \boldsymbol{\varphi}] \, \mathrm{d}V \, \mathrm{d}t + \int_{\mathbb{R}^3} \boldsymbol{d}(\boldsymbol{e}_0)^{\mathrm{T}} \boldsymbol{\varphi}(\boldsymbol{x}, 0) \, \mathrm{d}V = 0 \tag{2.6}$$

to hold for all six-vector test functions $\boldsymbol{\varphi}$ defined on $\mathbb{R}^3 \times [0, \infty)$, *i.e.*, vector-valued functions which are infinitely differentiable with compact support. One problem with this weak formulation is that we lose uniqueness, *i.e.*, there are several weak solutions $\boldsymbol{e}$ which satisfy the above criteria.

If the solution $\boldsymbol{e}$ to (2.5) is smooth, we can multiply the equations from the left by $\boldsymbol{e}^{\mathrm{T}}$ to obtain the Poynting theorem, or energy conservation law,

$$\nabla \cdot \boldsymbol{S}(\boldsymbol{e}) + \partial_t \eta(\boldsymbol{e}) = 0, \tag{2.7}$$

where $\boldsymbol{S}(\boldsymbol{e}) = \boldsymbol{E} \times \boldsymbol{H}$ is the Poynting vector, and $\eta(\boldsymbol{e}) = \boldsymbol{e}^{\mathrm{T}}\boldsymbol{d}(\boldsymbol{e}) - \phi(\boldsymbol{e})$ is the electromagnetic energy. When the solution $\boldsymbol{e}$ is not smooth, this inequality is no longer valid since the derivatives are not defined in the classical sense. However, as is shown in [32], it is reasonable to replace it with the inequality

$$\nabla \cdot \boldsymbol{S}(\boldsymbol{e}) + \partial_t \eta(\boldsymbol{e}) \leq 0, \tag{2.8}$$

which is interpreted in a weak sense, *i.e.*, for all scalar test functions $\varphi \geq 0$ defined on $\mathbb{R}^3 \times [0, \infty)$, the inequality

$$\int_0^\infty \int_{\mathbb{R}^3} [\boldsymbol{S}(\boldsymbol{e}) \cdot \nabla\varphi + \eta(\boldsymbol{e})\partial_t\varphi] \,\mathrm{d}V \,\mathrm{d}t + \int_{\mathbb{R}^3} \eta(\boldsymbol{e}_0)\varphi(\boldsymbol{x}, 0) \,\mathrm{d}V \geq 0 \tag{2.9}$$

holds. The inequality (2.8) is called an *entropy inequality*, and if $\boldsymbol{e}$ satisfies both (2.8) and (2.5), it is called an *entropy solution*. It is frequently conjectured that entropy solutions are unique [14, p. 32], and we refer to [32] for a discussion of the physical interpretation of this inequality. In the following section, we show how the entropy inequality is a natural consequence of the vanishing viscosity method.

3 Vanishing viscosity regularization

The loss of uniqueness for the weak solution is important to resolve if we want to make numerical approximations of the differential equations. This problem has been extensively studied for scalar conservation laws and systems of conservation laws in one space variable [9, 14, 20, 33, 34], where the conservation law is typically written $\partial_t u + \sum_i \partial_{x_i} f_i(u) = 0$. The knowledge of systems of conservation laws in several space variables is limited, but a common assumption is that reasonable (physical) solutions should arise as limits to the regularized equation $\partial_t u_\delta + \sum_i \partial_{x_i} f_i(u_\delta) = \delta\nabla^2 u_\delta$, when $\delta \to 0$. Since the second order derivative is often used as a model for a small viscous effect, this method is called the *vanishing viscosity method*. The benefit of the vanishing viscosity method is that for each $\delta > 0$ we can usually prove that the initial value problem is well posed, with unique, differentiable solutions. We can define a unique limit u as $\delta \to 0$ if we can find a convergent sequence of solutions $\{u_\delta\}$. However, this limit u must also be shown to satisfy the original conservation law, which is often nontrivial. For systems of conservation laws in several dimensions, this is still an unsolved problem [30].

We propose to use a similar method to define solutions to our quasi-linear system of equations, where we study the equations

$$\nabla \times \mathbf{J}\boldsymbol{e}_\delta + \partial_t \boldsymbol{d}(\boldsymbol{e}_\delta) = \delta\nabla^2 \boldsymbol{e}_\delta, \quad \boldsymbol{e}_\delta(\boldsymbol{x}, 0) = \boldsymbol{e}_0(\boldsymbol{x}), \quad \delta > 0. \tag{3.1}$$

Standard PDE theory guarantees a C^∞ solution $\boldsymbol{e}_\delta$ to this equation for every $\delta > 0$ for suitable $\boldsymbol{e}_0$, see [34, pp. 327–332]. An important result is that if the viscosity solution $\boldsymbol{e}_\delta$ converges boundedly almost everywhere in the limit $\delta \to 0$, the limit satisfies the entropy condition from the previous section. To see this, multiply (3.1)

with $\boldsymbol{e}_\delta$ and observe

$$\begin{cases} \boldsymbol{e}_\delta^{\mathrm{T}} \partial_t \boldsymbol{d}(\boldsymbol{e}_\delta) = \partial_t (\boldsymbol{e}_\delta^{\mathrm{T}} \boldsymbol{d}(\boldsymbol{e}_\delta) - \phi(\boldsymbol{e}_\delta)) = \partial_t \eta(\boldsymbol{e}_\delta) \\ \boldsymbol{e}_\delta^{\mathrm{T}} \nabla \times \mathbf{J} \boldsymbol{e}_\delta = \nabla \cdot (\boldsymbol{E}_\delta \times \boldsymbol{H}_\delta) = \nabla \cdot \boldsymbol{S}(\boldsymbol{e}_\delta) \\ \boldsymbol{e}_\delta^{\mathrm{T}} \nabla^2 \boldsymbol{e}_\delta = -|\nabla \boldsymbol{e}_\delta|^2 + \nabla^2 |\boldsymbol{e}_\delta|^2/2, \end{cases} \tag{3.2}$$

where $\eta(\boldsymbol{e}_\delta)$ is the electromagnetic energy in the medium and $\boldsymbol{S}(\boldsymbol{e}_\delta)$ is the Poynting vector. Note that all the derivatives are classically defined, and we have the following scalar inequality,

$$\nabla \cdot \boldsymbol{S}(\boldsymbol{e}_\delta) + \partial_t \eta(\boldsymbol{e}_\delta) \leq \delta \nabla^2 |\boldsymbol{e}_\delta|^2/2. \tag{3.3}$$

It can be shown that if $\boldsymbol{e}_\delta$ is uniformly bounded in the supremum norm and converges almost everywhere to $\boldsymbol{e}$ as $\delta \to 0$, then this limit solution $\boldsymbol{e}$ is a weak solution to (2.5) and satisfies the inequality

$$\nabla \cdot \boldsymbol{S}(\boldsymbol{e}) + \partial_t \eta(\boldsymbol{e}) \leq 0 \tag{3.4}$$

almost everywhere, see [14, p. 27] and [34, p. 438]. In the following sections, we study the consequences of the vanishing viscosity method in the case of traveling waves, which provides us with a more precise means of writing the entropy condition.

4 Inner solutions and shock structure

In this section we largely follow the ideas presented in many textbooks, *e.g.*, [9, pp. 600–603], [14, pp. 79–83], [33, pp. 508–510] and [34, p. 431]. Dropping the index δ for brevity, we investigate the singularly perturbed Maxwell equations (3.1) for the existence of solutions in the form of traveling waves,

$$\boldsymbol{e} = \boldsymbol{e}(\frac{z - vt}{\delta}) = \boldsymbol{e}(\zeta), \tag{4.1}$$

where we have chosen z to be the coordinate in the propagation direction, and v is the speed of the shock wave. We also require the derivative $\boldsymbol{e}'(\zeta)$ to disappear as $\zeta \to \pm\infty$, and a typical situation is depicted in Figure 1. In the language of singular perturbation theory [22], the traveling wave corresponds to an *inner solution* of the problem (3.1), and is a means of analyzing the microscopic behavior of the solution at a scale of order δ. The microscopic properties of a number of discontinuities which are distant at a macroscopic scale can be treated by considering them as isolated traveling waves of the type (4.1). Observe that $\zeta \to \infty$ does not necessarily mean $z \to \infty$, it is sufficient that $z > vt$ and $\delta \to 0$.

The traveling wave solution (4.1) must satisfy the ordinary differential equation

$$\hat{\boldsymbol{z}} \times \mathbf{J} \boldsymbol{e}' - v\{\boldsymbol{d}(\boldsymbol{e})\}' = \boldsymbol{e}'', \tag{4.2}$$

where $\hat{\boldsymbol{z}}$ denotes the unit vector in the z-direction. Observe that this equation does not involve the parameter δ, reflecting the fact that we are studying properties at a certain scale. Integrating the above equation once implies

$$\hat{\boldsymbol{z}} \times \mathbf{J} \boldsymbol{e} - v\boldsymbol{d}(\boldsymbol{e}) - \boldsymbol{e}' = \hat{\boldsymbol{z}} \times \mathbf{J} \boldsymbol{e}^{\mathrm{l,r}} - v\boldsymbol{d}(\boldsymbol{e}^{\mathrm{l,r}}) - (\boldsymbol{e}')^{\mathrm{l,r}}, \tag{4.3}$$

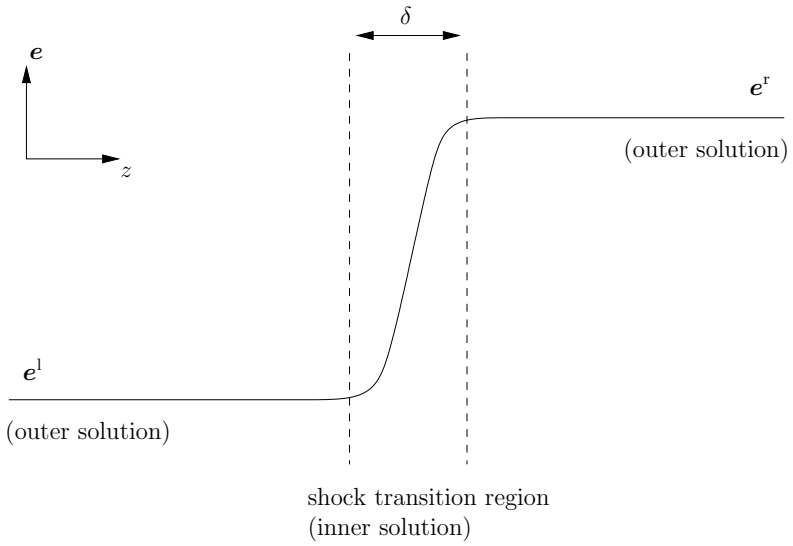

Figure 1: A typical traveling wave profile. The idea is that the inner solution shall provide a smooth transition between the outer solutions, the left and right constant states $\boldsymbol{e}_{\mathrm{l}}$ and $\boldsymbol{e}_{\mathrm{r}}$. The solution typically arises in Riemann's problem, where the initial values are $\boldsymbol{e}(\boldsymbol{x},0)=\boldsymbol{e}_0(\boldsymbol{x})=\boldsymbol{e}^{\mathrm{l}}$ for $z<0$ and $\boldsymbol{e}^{\mathrm{r}}$ for $z>0$.

where $\boldsymbol{e}^{\mathrm{l,r}}=\lim_{\zeta\to\mp\infty}\boldsymbol{e}(\zeta)$. Taking the opposite limit $\boldsymbol{e}\to\boldsymbol{e}^{\mathrm{r,l}}$ in (4.3) implies the Rankine-Hugoniot jump condition

$$\hat{\boldsymbol{z}}\times\mathbf{J}[\![\boldsymbol{e}]\!]-v[\![\boldsymbol{d}(\boldsymbol{e})]\!]=\mathbf{0}, \tag{4.4}$$

where we use the notation $[\![\boldsymbol{e}]\!]=\boldsymbol{e}^{\mathrm{r}}-\boldsymbol{e}^{\mathrm{l}}$ and $[\![\boldsymbol{d}(\boldsymbol{e})]\!]=\boldsymbol{d}(\boldsymbol{e}^{\mathrm{r}})-\boldsymbol{d}(\boldsymbol{e}^{\mathrm{l}})$ to indicate the jumps in the quantities $\boldsymbol{e}$ and $\boldsymbol{d}(\boldsymbol{e})$ over the shock. Note that the Rankine-Hugoniot condition is a vector identity, and that the jump in $\boldsymbol{d}(\boldsymbol{e})$ cannot have a component parallel to $\hat{\boldsymbol{z}}$, unless $v=0$.

We use the assumption $(\boldsymbol{e}')^{\mathrm{l,r}}=\mathbf{0}$ to write (4.3) as a system of autonomous, ordinary differential equations,

$$\boldsymbol{e}'=\hat{\boldsymbol{z}}\times\mathbf{J}(\boldsymbol{e}-\boldsymbol{e}^{\mathrm{l,r}})-v(\boldsymbol{d}(\boldsymbol{e})-\boldsymbol{d}(\boldsymbol{e}^{\mathrm{l,r}})), \tag{4.5}$$

with the asymptotic boundary conditions $\lim_{\zeta\to\mp\infty}\boldsymbol{e}(\zeta)=\boldsymbol{e}^{\mathrm{l,r}}$. It is clear that these states are critical points for the system (4.5), *i.e.*, the right hand side is zero for these states. In the following section we investigate when the system (4.5) has a solution, and what conditions this infers on the speed v. The corresponding ODE for ferromagnets described by the Landau-Lifshitz constitutive equation is studied in detail in [19] .

5 The entropy condition for a traveling wave

A solution to (4.5) that connects its critical points $\boldsymbol{e}^{\mathrm{l}}$ and $\boldsymbol{e}^{\mathrm{r}}$, where $\boldsymbol{e}^{\mathrm{l}}\neq\boldsymbol{e}^{\mathrm{r}}$, is called a heteroclinic orbit [29]. Before investigating these orbits, we show that homoclinic

orbits, *i.e.*, solutions where $\boldsymbol{e}^{\mathrm{l}} = \boldsymbol{e}^{\mathrm{r}}$ and $\boldsymbol{e} \neq \boldsymbol{e}^{\mathrm{l,r}}$ somewhere on the orbit, cannot exist. Multiplying (4.5) with $(\boldsymbol{e}')^{\mathrm{T}}$ we obtain

$$0 \leq |\boldsymbol{e}'|^2 = \left(\boldsymbol{e}^{\mathrm{T}}\hat{\boldsymbol{z}} \times \mathbf{J}(\frac{\boldsymbol{e}}{2} - \boldsymbol{e}^{\mathrm{l,r}}) - v\phi(\boldsymbol{e}) + v\boldsymbol{e}^{\mathrm{T}}\boldsymbol{d}(\boldsymbol{e}^{\mathrm{l,r}})\right)' = \psi(\boldsymbol{e})', \tag{5.1}$$

which shows there exists a scalar function $\psi(\boldsymbol{e})$ which is nondecreasing along the orbit. Such a function must be constant on a homoclinic orbit, implying $|\boldsymbol{e}'|^2 = 0$, and thus $\boldsymbol{e}$ must be constant throughout the orbit, which degenerates to a point.

The existence of a heteroclinic orbit for the system (4.5) requires that the unstable manifold of one critical point intersects the stable manifold of the other, where the unstable and the stable manifold is associated with the positive and the negative eigenvalues of the linearized problem, respectively. If the heteroclinic orbit is to be stable under small perturbations, then the sum of the dimensions of the stable and unstable manifold must exceed the dimension of the phase space [33, p. 509]. In our case, the relevant manifolds are the unstable manifold for $\boldsymbol{e}^{\mathrm{l}}$ and the stable manifold for $\boldsymbol{e}^{\mathrm{r}}$. The dimensions of these manifolds can be calculated from counting how many eigenvalues of the linearized equations that are greater/lesser than zero at each critical point. The linearized equations are

$$(\boldsymbol{e} - \boldsymbol{e}^{\mathrm{l,r}})' = \left[\hat{\boldsymbol{z}} \times \mathbf{J} - v\boldsymbol{d}'(\boldsymbol{e}^{\mathrm{l,r}})\right](\boldsymbol{e} - \boldsymbol{e}^{\mathrm{l,r}}). \tag{5.2}$$

Temporarily denoting the 6×6 matrix $\boldsymbol{d}'(\boldsymbol{e}^{\mathrm{l,r}})$ by $\mathbf{A}$, the problem of deducing the dimension of the stable and unstable manifolds consists in counting positive and negative eigenvalues for the matrix $\hat{\boldsymbol{z}} \times \mathbf{J} - v\mathbf{A}$. Since $\mathbf{A}$ is positive definite, the signs of the eigenvalues are the same as for the problem

$$[\hat{\boldsymbol{z}} \times \mathbf{J} - v\mathbf{A}]\boldsymbol{u}_i = \lambda_i \mathbf{A}\boldsymbol{u}_i \quad \Rightarrow \quad [\hat{\boldsymbol{z}} \times \mathbf{J} - (v + \lambda_i)\mathbf{A}]\boldsymbol{u}_i = \mathbf{0}. \tag{5.3}$$

Using the same technique as in [31], we formulate this eigenvalue problem as

$$c_i \boldsymbol{w}_i = \sqrt{\mathbf{A}}^{-1}[\hat{\boldsymbol{z}} \times \mathbf{J}]\sqrt{\mathbf{A}}^{-1}\boldsymbol{w}_i, \tag{5.4}$$

where $\sqrt{\mathbf{A}}$ is the symmetric, positive definite square root of $\mathbf{A}$, $c_i = v + \lambda_i$, and $\boldsymbol{w}_i = \sqrt{\mathbf{A}}\boldsymbol{u}_i$. The matrix in the right hand side is a congruence transformation of $\hat{\boldsymbol{z}} \times \mathbf{J}$, and it is well known that such a transformation does not change the signs of the eigenvalues [16, p. 251]. Since $\hat{\boldsymbol{z}} \times \mathbf{J}$ has the (double) eigenvalues ± 1 and 0, there are always two negative eigenvalues $c_{3,4} < 0$ and two zero eigenvalues $c_{5,6} = 0$. This implies $\lambda_{3,4,5,6} \leq -v < 0$. The argument concerning the dimensions of the stable and unstable manifolds can then involve only the positive eigenvalues c_1 and c_2, and the corresponding λ_1 and λ_2. In order for the sum of the dimension of the unstable manifold ($\lambda > 0$) at $\boldsymbol{e}^{\mathrm{l}}$ and the dimension of the stable manifold ($\lambda < 0$) at $\boldsymbol{e}^{\mathrm{r}}$ to be larger than six (the dimension of the phase space), one of the following conditions must hold:

$$\begin{cases} 0 < \lambda_1(\boldsymbol{e}^{\mathrm{l}}) < \lambda_2(\boldsymbol{e}^{\mathrm{l}}) & \text{and} \quad \lambda_1(\boldsymbol{e}^{\mathrm{r}}) < 0 < \lambda_2(\boldsymbol{e}^{\mathrm{r}}), & \text{or} \\ \lambda_1(\boldsymbol{e}^{\mathrm{l}}) < 0 < \lambda_2(\boldsymbol{e}^{\mathrm{l}}) & \text{and} \quad \lambda_1(\boldsymbol{e}^{\mathrm{r}}) < \lambda_2(\boldsymbol{e}^{\mathrm{r}}) < 0, & \text{or} \\ 0 < \lambda_1(\boldsymbol{e}^{\mathrm{l}}) < \lambda_2(\boldsymbol{e}^{\mathrm{l}}) & \text{and} \quad \lambda_1(\boldsymbol{e}^{\mathrm{r}}) < \lambda_2(\boldsymbol{e}^{\mathrm{r}}) < 0. & \end{cases} \tag{5.5}$$

Observe that the dimension of the unstable manifold at $\boldsymbol{e}^{\mathrm{l}}$ is calculated from the number of positive eigenvalues, *i.e.*, the number of positive eigenvalues in the left column of (5.5). The dimension of the stable manifold at $\boldsymbol{e}^{\mathrm{r}}$ is calculated from the number of negative eigenvalues, *i.e.*, the number of negative eigenvalues in the right column of (5.5) plus four, since we deduced earlier that $\lambda_{3,4,5,6}$ are always negative.

The two positive eigenvalues $c_{1,2} = v + \lambda_{1,2}$ are identified as the characteristic wave speeds in the material, which are determined from the eigenvalue problem (5.4) for each state $\boldsymbol{e}^{\mathrm{l,r}}$, as in [31]. The speeds are in general functions of both the state, $\boldsymbol{e}^{\mathrm{l}}$ or $\boldsymbol{e}^{\mathrm{r}}$, and the propagation direction, $\hat{\boldsymbol{z}}$, but we choose to suppress the dependence on the propagation direction since this is constant in this paper.

The conditions on $\lambda_{1,2}$ above can be written in terms of the shock speed v and the characteristic wave speeds $c_{1,2}$ as

$$\begin{cases} v < c_1(\boldsymbol{e}^{\mathrm{l}}) < c_2(\boldsymbol{e}^{\mathrm{l}}) & \text{and} \quad c_1(\boldsymbol{e}^{\mathrm{r}}) < v < c_2(\boldsymbol{e}^{\mathrm{r}}) \quad \text{(slow shock)} \\ c_1(\boldsymbol{e}^{\mathrm{l}}) < v < c_2(\boldsymbol{e}^{\mathrm{l}}) & \text{and} \quad c_1(\boldsymbol{e}^{\mathrm{r}}) < c_2(\boldsymbol{e}^{\mathrm{r}}) < v \quad \text{(fast shock)} \\ v < c_1(\boldsymbol{e}^{\mathrm{l}}) < c_2(\boldsymbol{e}^{\mathrm{l}}) & \text{and} \quad c_1(\boldsymbol{e}^{\mathrm{r}}) < c_2(\boldsymbol{e}^{\mathrm{r}}) < v \quad \text{(intermediate shock).} \end{cases} \tag{5.6}$$

These expressions constitute the entropy conditions for electromagnetic, plane shock waves. The nomenclature "fast shock" and "slow shock" is in accordance with [19] and [10], and "intermediate shock" is from [10]. Note that the fast and the slow shock are closely connected to the ordinary and extraordinary rays for anisotropic materials, see for instance [23, pp. 68–71] and [25, pp. 331–357].

To conclude this section, we note that our entropy condition is analogous to the Lax entropy condition for an n-dimensional, strictly hyperbolic system of conservation laws $u_t + f(u)_x = 0$. This condition is that there should exist an index k such that

$$\begin{cases} \lambda_1(u^{\mathrm{l}}) < \cdots < \lambda_{k-1}(u^{\mathrm{l}}) < v < \lambda_k(u^{\mathrm{l}}) < \cdots < \lambda_n(u^{\mathrm{l}}) \\ \lambda_1(u^{\mathrm{r}}) < \cdots < \lambda_k(u^{\mathrm{r}}) < v < \lambda_{k+1}(u^{\mathrm{r}}) < \cdots < \lambda_n(u^{\mathrm{r}}), \end{cases} \tag{5.7}$$

where $\lambda_1(u), \ldots, \lambda_n(u)$ are the eigenvalues of the $n \times n$ matrix $f'(u)$ and v is the shock speed (see for instance [9, p. 589], [14, p. 76], [20, p. 61], [33, p. 261]).

6 Genuine nonlinearity and contact discontinuities

When $c_i(\boldsymbol{e}^{\mathrm{l}}) = c_i(\boldsymbol{e}^{\mathrm{r}})$ for $i = 1$ and/or $i = 2$, one or several of the conditions (5.6) may not be applicable. This phenomenon occurs for a type of waves called *contact discontinuities*, which are characterized by

$$c_i(\boldsymbol{e}^{\mathrm{l}}) = c_i(\boldsymbol{e}^{\mathrm{r}}) = c_i(\boldsymbol{e}) \quad \text{and} \quad \hat{\boldsymbol{z}} \times \mathbf{J}(\boldsymbol{e} - \boldsymbol{e}^{\mathrm{l,r}}) - c_i(\boldsymbol{d}(\boldsymbol{e}) - \boldsymbol{d}(\boldsymbol{e}^{\mathrm{l,r}})) = \mathbf{0}, \tag{6.1}$$

for all $\boldsymbol{e} \in \gamma$, where γ is a smooth curve connecting $\boldsymbol{e}^{\mathrm{l}}$ to $\boldsymbol{e}^{\mathrm{r}}$ in $\mathbb{R}^6$. Differentiating the latter condition along the curve γ, implies $[\hat{\boldsymbol{z}} \times \mathbf{J} - c_i \boldsymbol{d}'(\boldsymbol{e})]\dot{\boldsymbol{e}} = \mathbf{0}$, where $\dot{\boldsymbol{e}}$ denotes the tangential derivative of $\boldsymbol{e}$ along this curve. This means $\dot{\boldsymbol{e}}$ is proportional to the

eigenvector $\boldsymbol{e}_i$ by definition. That the speed is constant on the curve γ can also be written

$$0 = \dot{c}_i = (\mathrm{D}_e\, c_i)^{\mathrm{T}} \dot{\boldsymbol{e}} = (\mathrm{D}_e\, c_i)^{\mathrm{T}} \boldsymbol{e}_i, \tag{6.2}$$

where $\mathrm{D}_e\, c_i$ denotes the gradient of the speed c_i with respect to the six-vector $\boldsymbol{e}$, *i.e.*, $(\mathrm{D}_e\, c_i)_k = \partial c_i / \partial e_k$. This means that the eigenvector $\boldsymbol{e}_i$ must be orthogonal to $\mathrm{D}_e\, c_i$. We say the field $\boldsymbol{e}_i$ is *linearly degenerate* if $\boldsymbol{e}_i^{\mathrm{T}}\, \mathrm{D}_e\, c_i = 0$, and *genuinely nonlinear* if $\boldsymbol{e}_i^{\mathrm{T}}\, \mathrm{D}_e\, c_i \neq 0$, see *e.g.*, [14, p. 41]. One reason for the term linearly degenerate is that contact discontinuities travel along non-crossing characteristics, just as in the linear case. An interesting feature of contact discontinuities is that their structure is not captured by the traveling wave ansatz, since the right hand side of (4.5) is identically zero. In this paper, we restrict ourselves to investigating a few explicit examples.

Our first example is a constitutive relation which always has one linearly degenerate field. For an instantaneously reacting, isotropic, nonmagnetic material, we have the constitutive relations

$$\boldsymbol{D}(\boldsymbol{E}) = F(|\boldsymbol{E}|^2)\boldsymbol{E}, \qquad \boldsymbol{B} = \boldsymbol{H}. \tag{6.3}$$

It is not difficult to prove that the characteristic speeds are

$$c_1(\boldsymbol{E}) = \frac{1}{\sqrt{F(|\boldsymbol{E}|^2) + 2F'(|\boldsymbol{E}|^2)|\boldsymbol{E}|^2}}, \qquad c_2(\boldsymbol{E}) = \frac{1}{\sqrt{F(|\boldsymbol{E}|^2)}}, \tag{6.4}$$

with the corresponding eigenvectors defined by $\boldsymbol{e}_i = (\boldsymbol{E}_i, \boldsymbol{H}_i)^{\mathrm{T}}$, where $\boldsymbol{H}_i = \hat{\boldsymbol{z}} \times \boldsymbol{E}_i$ for $i = 1, 2$, and

$$\boldsymbol{E}_1(\boldsymbol{E}) = \boldsymbol{E}/|\boldsymbol{E}|, \qquad \boldsymbol{E}_2(\boldsymbol{E}) = \hat{\boldsymbol{z}} \times \boldsymbol{E}/|\boldsymbol{E}|. \tag{6.5}$$

Since the speed is independent of $\boldsymbol{H}$, we have $\boldsymbol{e}_i^{\mathrm{T}}\, \mathrm{D}_e\, c_i = \boldsymbol{E}_i \cdot \mathrm{D}_E\, c_i$ for $i = 1, 2$. From the explicit expressions (6.4) it is seen that $\mathrm{D}_E\, c_1 \sim \mathrm{D}_E\, c_2 \sim \boldsymbol{E}$, where the $\sim$ sign indicates proportionality. It is clear that $\boldsymbol{E}_1 \cdot \mathrm{D}_E\, c_1 \neq 0$ and $\boldsymbol{E}_2 \cdot \mathrm{D}_E\, c_2 = 0$, *i.e.*, the field $\boldsymbol{E}_1$ is genuinely nonlinear and $\boldsymbol{E}_2$ is linearly degenerate. We interpret a wave where the change in $\boldsymbol{E}$ is orthogonal to $\boldsymbol{E}$, *i.e.*, $\partial_t \boldsymbol{E} \sim \boldsymbol{E}_2$, as a circularly polarized wave. This is motivated by the fact that the amplitude $|\boldsymbol{E}|$ does not change, but the vector $\boldsymbol{E}$ appears to rotate when observed as a function of time at a given point in space. Thus, we have found that circularly polarized waves in an isotropic medium are linearly degenerate.

Our second example is a constitutive model where there are no linearly degenerate fields. The model is

$$\boldsymbol{D}(\boldsymbol{E}) = (1 + \boldsymbol{C} \cdot \boldsymbol{E})\boldsymbol{E} + \frac{|\boldsymbol{E}|^2}{2}\boldsymbol{C}, \qquad \boldsymbol{B} = \boldsymbol{H}, \tag{6.6}$$

which is not valid for all $\boldsymbol{E}$, since $\boldsymbol{D}'(\boldsymbol{E}) = (1 + \boldsymbol{C} \cdot \boldsymbol{E})\mathbf{I} + \boldsymbol{C}\boldsymbol{E} + \boldsymbol{E}\boldsymbol{C}$ is not positive definite everywhere. However, it is positive definite if $|\boldsymbol{C}||\boldsymbol{E}| < 1/3$, and thus the model suffices as an approximation for $\boldsymbol{E}$ small enough. For this model, the three-vector $\boldsymbol{C}$ represents a "nonlinear axis" of the material, which is obviously

anisotropic. It is straightforward to show that when both $\boldsymbol{C}$ and $\boldsymbol{E}$ are orthogonal to $\hat{\boldsymbol{z}}$, we have

$$c_{1,2} = \frac{1}{\sqrt{1 + 2\boldsymbol{C}\cdot\boldsymbol{E} \pm |\boldsymbol{E}||\boldsymbol{C}|}}, \quad \text{and} \quad \boldsymbol{E}_{1,2} = \frac{\boldsymbol{E}}{|\boldsymbol{E}|} \pm \frac{\boldsymbol{C}}{|\boldsymbol{C}|}, \tag{6.7}$$

where the upper sign corresponds to c_1 and $\boldsymbol{E}_1$, and $\boldsymbol{H}_{1,2} = \hat{\boldsymbol{z}} \times \boldsymbol{E}_{1,2}$. The scalar product $\boldsymbol{E}_i \cdot \mathrm{D}_E\, c_i$ from which we analyze genuine nonlinearity can be shown to be

$$\boldsymbol{E}_{1,2} \cdot \mathrm{D}_E\, c_{1,2} = -\frac{3}{2} \frac{\boldsymbol{C}\cdot\boldsymbol{E}/|\boldsymbol{E}| \pm |\boldsymbol{C}|}{(1 + 2\boldsymbol{C}\cdot\boldsymbol{E} \pm |\boldsymbol{C}||\boldsymbol{E}|)^{3/2}}. \tag{6.8}$$

We see that one of these quantities is zero if $\boldsymbol{E}$ is parallel or antiparallel to $\boldsymbol{C}$, but any situation inbetween means $\boldsymbol{E}_1 \cdot \mathrm{D}_E\, c_1 \neq 0$ and $\boldsymbol{E}_2 \cdot \mathrm{D}_E\, c_2 \neq 0$. This shows that this model usually has no linearly degenerate fields, and contact discontinuities occurs only when the electric field is parallel or antiparallel to the axis $\boldsymbol{C}$. We conclude this example by noting the peculiarity that when the scalar product $\boldsymbol{C}\cdot\boldsymbol{E}$ is negative, the characteristic speeds $c_{1,2}$ may be larger than one, which is the speed of light in vacuum in our units. This may further restrict the validity of this model.

7 Numerical demonstration of shock structure for an anisotropic material

In this section we show numerically that there exists a structure (an inner solution dissipatively connecting two states) for a nonlinear anisotropic material. In order to present a concise example, we regularize the Maxwell equations in the electric field only, *i.e.*,

$$\begin{cases} -\nabla \times \boldsymbol{H} + \partial_t \boldsymbol{D} = \delta \nabla^2 \boldsymbol{E} \\ \nabla \times \boldsymbol{E} + \partial_t \boldsymbol{B} = \boldsymbol{0}. \end{cases} \tag{7.1}$$

The benefit of this approach is to reduce the phase space of the resulting system of ordinary differential equations to two dimensions, which enables us to plot the phase space easily. The approach is reasonable if we consider the Faraday law to be exact, and a similar technique is sometimes used for equations describing gas dynamics [9, p. 602]. The anisotropic material is described by the constitutive equation

$$\boldsymbol{D}(\boldsymbol{E}) = \begin{pmatrix} (2 + |\boldsymbol{E}|^2)E_x \\ (3 + |\boldsymbol{E}|^2)E_y \\ (4 + |\boldsymbol{E}|^2)E_z \end{pmatrix}, \quad \boldsymbol{B} = \boldsymbol{H}, \tag{7.2}$$

where in this section the fields are dimensionless, see [31] for details on the scaling. This model has an anisotropic linear part and an isotropic nonlinear part, *i.e.*, practically the same example material as in [31].

Fig.	E_x^{l}	E_y^{l}	E_x^{r}	E_y^{r}	v	c_1^{l}	c_2^{l}	c_1^{r}	c_2^{r}	Δ
2	0.000	0.000	0.500	0.000	0.667	0.577	0.707	0.555	0.603	−0.011
3	0.200	0.000	1.000	0.000	0.556	0.573	0.687	0.447	0.500	−0.087
4	0.788	0.000	1.000	0.000	0.476	0.509	0.525	0.447	0.500	−0.002
5	0.617	0.472	1.000	1.000	0.400	0.478	0.574	0.342	0.475	−0.059

Table 1: Relevant values for the phase portraits. The last column is the entropy difference $\Delta = \hat{\boldsymbol{z}} \cdot (\boldsymbol{S}(\boldsymbol{e}^{\mathrm{r}}) - \boldsymbol{S}(\boldsymbol{e}^{\mathrm{l}})) - v(\eta(\boldsymbol{e}^{\mathrm{r}}) - \eta(\boldsymbol{e}^{\mathrm{l}}))$, and since all the numbers in the column are negative, we see that all the waves satisfy the original entropy condition (2.8).

The system of ordinary differential equations corresponding to (4.5) becomes

$$\begin{pmatrix} E_x' \\ E_y' \\ E_z' \\ 0 \\ 0 \\ 0 \end{pmatrix} = \begin{pmatrix} 0 & 0 & 0 & 0 & 1 & 0 \\ 0 & 0 & 0 & -1 & 0 & 0 \\ 0 & 0 & 0 & 0 & 0 & 0 \\ 0 & -1 & 0 & 0 & 0 & 0 \\ 1 & 0 & 0 & 0 & 0 & 0 \\ 0 & 0 & 0 & 0 & 0 & 0 \end{pmatrix} \begin{pmatrix} E_x - E_x^{\mathrm{l,r}} \\ E_y - E_y^{\mathrm{l,r}} \\ E_z - E_z^{\mathrm{l,r}} \\ H_x - H_x^{\mathrm{l,r}} \\ H_y - H_y^{\mathrm{l,r}} \\ H_z - H_z^{\mathrm{l,r}} \end{pmatrix} - v \begin{pmatrix} (2 + |\boldsymbol{E}|^2)E_x - (2 + |\boldsymbol{E}^{\mathrm{l,r}}|^2)E_x^{\mathrm{l,r}} \\ (3 + |\boldsymbol{E}|^2)E_y - (3 + |\boldsymbol{E}^{\mathrm{l,r}}|^2)E_y^{\mathrm{l,r}} \\ (4 + |\boldsymbol{E}|^2)E_z - (4 + |\boldsymbol{E}^{\mathrm{l,r}}|^2)E_z^{\mathrm{l,r}} \\ H_x - H_x^{\mathrm{l,r}} \\ H_y - H_y^{\mathrm{l,r}} \\ H_z - H_z^{\mathrm{l,r}} \end{pmatrix}. \quad (7.3)$$

With $E_z^{\mathrm{l,r}} = H_z^{\mathrm{l,r}} = 0$ we have $E_z = H_z = 0$ throughout the shock, and $|\boldsymbol{E}|^2 = E_x^2 + E_y^2$. By eliminating the magnetic field and the z-components, we obtain the following 2×2 system of ordinary differential equations,

$$\begin{pmatrix} E_x \\ E_y \end{pmatrix}' = \frac{1}{v} \begin{pmatrix} E_x - E_x^{\mathrm{l,r}} \\ E_y - E_y^{\mathrm{l,r}} \end{pmatrix} - v \begin{pmatrix} (2 + E_x^2 + E_y^2)E_x - (2 + (E_x^{\mathrm{l,r}})^2 + (E_y^{\mathrm{l,r}})^2)E_x^{\mathrm{l,r}} \\ (3 + E_x^2 + E_y^2)E_y - (3 + (E_x^{\mathrm{l,r}})^2 + (E_y^{\mathrm{l,r}})^2)E_y^{\mathrm{l,r}} \end{pmatrix}, \quad (7.4)$$

which contains all the qualitative information we need. We remark that this system can be integrated exactly for certain values of $E_x^{\mathrm{l,r}}$ and $E_y^{\mathrm{l,r}}$, but we refrain from exploiting this possibility in this paper. Phase portraits, *i.e.*, plots of the vector fields on the right hand side of the equations above, are found in Figures 2, 3 and 4 for a fast shock, an intermediate shock and a slow shock, respectively. Figure 5 depicts the phase portrait for a shock with mixed polarization, and Table 1 lists the relevant numbers used in each phase portrait. It is clearly seen from the figures that there exists a path connecting the critical points.

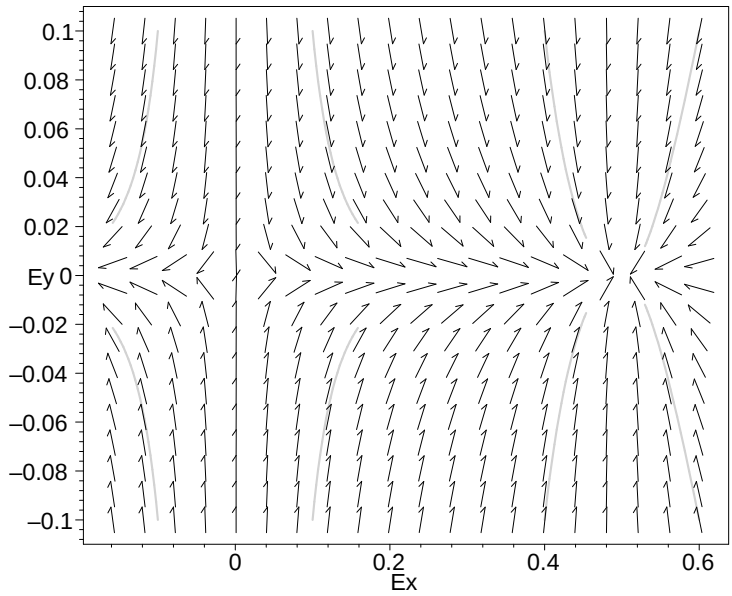

Figure 2: Phase portrait of a fast shock wave structure problem. The critical points are $(E_x^{\mathrm{l}}, E_y^{\mathrm{l}}) = (0.000, 0.000)$ and $(E_x^{\mathrm{r}}, E_y^{\mathrm{r}}) = (0.500, 0.000)$.

8 Discussion and conclusions

By studying a parabolic regularization of the quasi-linear Maxwell equations, we have proposed a classification of electromagnetic shock waves into three categories: slow, fast and intermediate. This classification depends on how the shock speed relates to the characteristic speeds in the material, which in turn depend on the field strengths on both sides of the shock. These shock conditions can probably be improved with the help of Conley's index theory, as in [10, 33].

There also exists an additional kind of discontinuity, the contact discontinuity, which only occurs for linearly degenerate fields. In particular, we have showed that circularly polarized waves in isotropic, nonlinear media, exhibits contact discontinuities. The further study of contact discontinuities is beyond the scope of this paper, but it is seen from the analysis in Section 6 that it is important to understand which constitutive relations that permit a linearly degenerate field.

We consider the parabolic regularization term $\nabla^2 \boldsymbol{e}$ merely as a mathematical technique used in order to obtain a well posed problem, and do not require it to have a physical interpretation. Though, it is noteworthy that it may arise as a consequence of a multiple scale analysis of a more detailed constitutive relation, for instance when temporal and/or spatial dispersion is taken into account. The dispersion can be modeled with a convolution, for instance $\boldsymbol{d} = \chi_1 * \boldsymbol{e} + \chi_2 * \boldsymbol{e} * \boldsymbol{e}$, where $*$ denotes temporal and/or spatial convolution. Introducing a microscopic and a macroscopic time or space variable and performing a formal multiple scale expansion, it is found that the leading order term of the solution should satisfy $\nabla \times \mathbf{J}\boldsymbol{e} + \partial_t \boldsymbol{d}(\boldsymbol{e}) = \delta\, \mathrm{D}^2\, \boldsymbol{e}$, where D^2 is a second order differential operator in time and/or space. In the case of $\mathrm{D}^2 = \partial_t^2$, *i.e.*, "temporal viscosity", we note that even

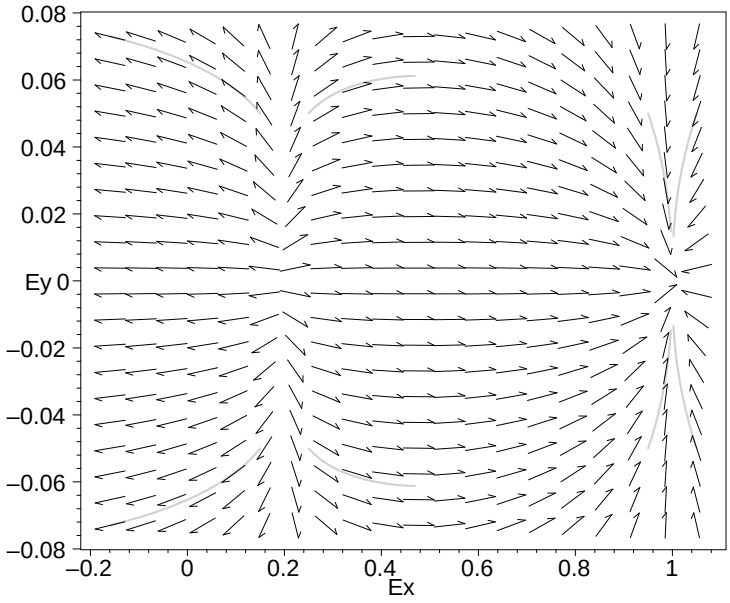

Figure 3: Phase portrait of an intermediate shock wave structure problem. The critical points are $(E_x^{\mathrm{l}}, E_y^{\mathrm{l}}) = (0.200, 0.000)$ and $(E_x^{\mathrm{r}}, E_y^{\mathrm{r}}) = (1.000, 0.000)$.

though we obtain exactly the same analysis for a traveling wave profile as for the term $\nabla^2 \boldsymbol{e}$ used in this paper, this version of the Maxwell equations is noncausal, and very difficult to treat in more than one spatial dimension. A similar system of equations in one dimension is studied as a boundary value problem in [24], and the influence of the noncausality is found to be small when δ is small.

9 Acknowledgments

The work reported in this paper is partially supported by a grant from the Swedish Research Council for Engineering Sciences and its support is gratefully acknowledged.

This work was largely conducted during visits to the Department of Mathematics and Statistics of the University of Canterbury, Christchurch, New Zealand, and the Department of Mathematics and Computer Science of the University of Akron, Ohio. Their warm hospitality is most appreciated. The author would also thanks the Royal Physiographical Society of Lund (Kungliga fysiografiska sällskapet i Lund) for a grant enabling these visits.

The author thanks Prof. Gerhard Kristensson and Dr. Mats Gustafsson for many valuable discussions on this paper.

References

[1] G. Bekefi and S. C. Brown. Plasma physics: Waves and radiation processes in plasma. *Am. J. Phys*, **34**, 1001, 1966.

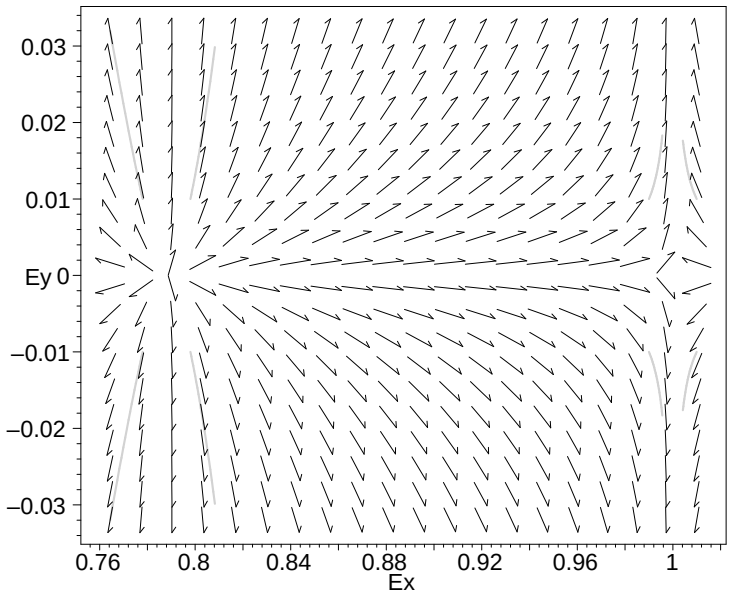

Figure 4: Phase portrait of a slow shock wave structure problem. The critical points are $(E_x^{\mathrm{l}}, E_y^{\mathrm{l}}) = (0.788, 0.000)$ and $(E_x^{\mathrm{r}}, E_y^{\mathrm{r}}) = (1.000, 0.000)$.

[2] F. Bloom. *Mathematical problems of classical nonlinear electromagnetic theory.* Longman Scientific & Technical, Burnt Mill, Harlow, England, 1993.

[3] G. Branch and P. W. Smith. Fast-rise-time electromagnetic shock waves in nonlinear, ceramic dielectrics. *J. Phys. D: Applied Phys.*, **29**(8), 2170–2178, August 1996.

[4] C. Brooker, N. Altieri, G. Eastwood, R. Hoad, and J. E. Dolan. 90kV 1800A 85ps rise time electromagnetic shock line for UWB applications. *Electronics Letters*, **35**(25), 2210–2212, December 1999.

[5] B. D. Coleman and E. H. Dill. Thermodynamic restrictions on the constitutive equations of electromagnetic theory. *Z. angew. Math. Phys.*, **22**, 691–702, 1971.

[6] C. C. Conley and J. A. Smoller. On the structure of magnetohydrodynamic shock waves. *Comm. Pure Appl. Math.*, **28**, 367–375, 1974.

[7] C. M. Dafermos. *Hyperbolic conservation laws in continuum physics.* Grundlehren der mathematischen Wissenschaften 325. Springer-Verlag, Berlin, 2000.

[8] J. E. Dolan. Simulation of shock waves in ferrite-loaded coaxial transmission lines with axial bias. *J. Phys. D: Applied Phys.*, **32**(15), 1826–1831, August 1999.

[9] L. C. Evans. *Partial Differential Equations.* American Mathematical Society, Providence, Rhode Island, 1998.

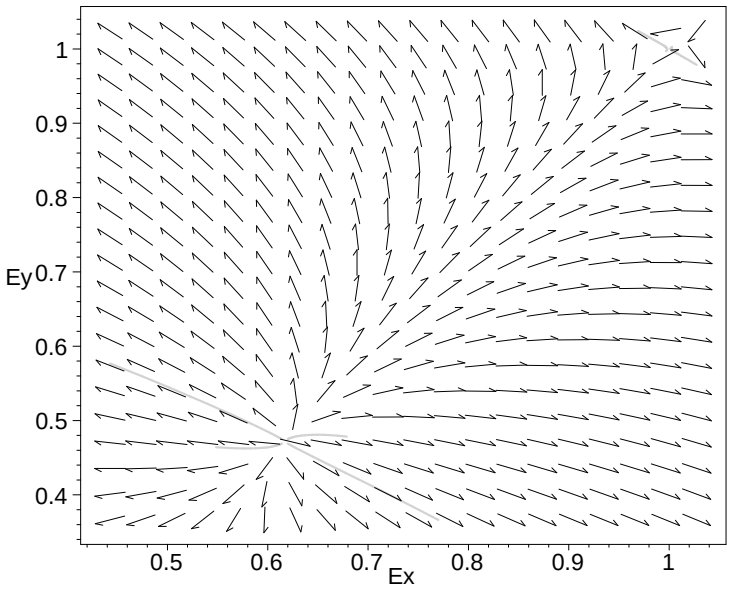

Figure 5: Phase portrait of a slow shock wave structure problem with mixed polarizations. The critical points are $(E_x^{\mathrm{l}}, E_y^{\mathrm{l}}) = (0.617, 0.472)$ and $(E_x^{\mathrm{r}}, E_y^{\mathrm{r}}) = (1.000, 1.000)$.

[10] Y. Farjami and M. Hesaaraki. Structure of shock waves in planar motion of plasma. *Nonlinearity*, **11**, 797–821, 1998.

[11] I. Gel'fand. Some problems in the theory of quasilinear equations. *Amer. Math. Soc. Transl.*, **29**, 295–381, 1963. Translated from Russian, Usp. Mat. Nauk 14 (1959), 87–115.

[12] P. Germain. Shock waves and shock waves structure in magneto-fluid dynamics. *Rev. Mod. Phys.*, **32**, 951–958, 1960.

[13] J. Glimm. Solutions in the large for nonlinear hyperbolic systems of equations. *Comm. Pure Appl. Math.*, **18**, 697–715, 1965.

[14] E. Godlewski and P.-A. Raviart. *Numerical Approximation of Hyperbolic Systems of Conservation Laws*. Springer-Verlag, Berlin, 1996.

[15] S. K. Godunov. A difference scheme for numerical computation of discontinuous solutions of equations of fluid dynamics. *Mat. Sb.*, **47**(89), 217–306, 1959.

[16] H. Goldstein. *Classical Mechanics*. Addison-Wesley, Reading, MA, USA, second edition, 1980.

[17] C. L. Grabbe. Plasma waves and instabilities. *Am. J. Phys*, **52**, 970, 1984.

[18] M. Gustafsson. *Wave Splitting in Direct and Inverse Scattering Problems*. PhD thesis, Lund Institute of Technology, Department of Electromagnetic Theory, P.O. Box 118, S-211 00 Lund, Sweden, 2000. `http://www.es.lth.se/home/mats`.

[19] N. I. Gvozdovskaya and A. G. Kulikovskii. Investigation of electromagnetic shock-wave structure in anisotropic ferromagnets with easy axis. *Wave Motion*, **29**, 23–34, 1999.

[20] L. Hörmander. *Lectures on Nonlinear Hyperbolic Differential Equations*. Number 26 in Mathémathiques & Applications. Springer-Verlag, Berlin, 1997.

[21] J. D. Jackson. *Classical Electrodynamics*. John Wiley & Sons, New York, third edition, 1999.

[22] J. Kevorkian and J. D. Cole. *Multiple Scale and Singular Perturbation Methods*. Springer-Verlag, Berlin, 1996.

[23] J. A. Kong. *Electromagnetic Wave Theory*. John Wiley & Sons, New York, 1986.

[24] G. Kristensson. Condon's model on optical rotatory power and causality — a scientific trifle. Technical Report LUTEDX/(TEAT-7080)/1–23/(1999), Lund Institute of Technology, Department of Electromagnetic Theory, P.O. Box 118, S-211 00 Lund, Sweden, 1999.

[25] L. D. Landau, E. M. Lifshitz, and L. P. Pitaevskiĭ. *Electrodynamics of Continuous Media*. Pergamon, Oxford, second edition, 1984.

[26] I. V. Lindell, A. H. Sihvola, and K. Suchy. Six-vector formalism in electromagnetics of bi-anisotropic media. *J. Electro. Waves Applic.*, **9**(7/8), 887–903, 1995.

[27] G. A. Maugin. On shock waves and phase-transition fronts in continua. *ARI*, **50**, 141–150, 1998.

[28] G. A. Maugin. On the universality of the thermomechanics of forces driving singular sets. *Archive of Applied Mechanics*, **70**, 31–45, 2000.

[29] H. Poincaré. *Méthodes nouvelles de la mécanique céleste (New methods of celestial mechanics, english translation)*. American Institute of Physics, Woodbury, NY, 1993. Originally published: Gauthier-Villars et fils, Paris, 1892–99.

[30] D. Serre. Systems of conservation laws: A challenge for the XXIst century. In B. Engquist and W. Schmid, editors, *Mathematics Unlimited — 2001 and Beyond*, pages 1061–1080. Springer-Verlag, Berlin, 2001.

[31] D. Sjöberg. Simple wave solutions for the Maxwell equations in bianisotropic, nonlinear media, with application to oblique incidence. *Wave Motion*, **32**(3), 217–232, 2000.

[32] D. Sjöberg. On uniqueness and continuity for the quasi-linear, bianisotropic Maxwell equations, using an entropy condition. Technical Report

LUTEDX/(TEAT-7095)/1–20/(2001), Lund Institute of Technology, Department of Electroscience, Electromagnetic Theory, P.O. Box 118, S-211 00 Lund, Sweden, 2001.

[33] J. Smoller. *Shock Waves and Reaction–Diffusion Equations*. Grundlehren der mathematischen Wissenschaften 258. Springer-Verlag, Berlin, second edition, 1994.

[34] M. Taylor. *Partial Differential Equations III: Nonlinear Equations*. Springer-Verlag, New York, 1996.

On uniqueness and continuity for the quasi-linear, bianisotropic Maxwell equations, using an entropy condition

Daniel Sjöberg

Paper V

Based on: D. Sjöberg. On uniqueness and continuity for the quasi-linear, bianisotropic Maxwell equations, using an entropy condition. Technical Report LUTEDX/(TEAT-7095)/1–20/(2001), Lund Institute of Technology.

Abstract

The quasi-linear Maxwell equations describing electromagnetic wave propagation in nonlinear media permit several weak solutions, which may be discontinuous (shock waves). It is often conjectured that the solutions are unique if they satisfy an additional entropy condition. The entropy condition states that the energy contained in the electromagnetic fields is irreversibly dissipated to other energy forms, which are not described by the Maxwell equations. We use the method employed by Kružkov to scalar conservation laws to analyze the implications of this additional condition in the electromagnetic case, *i.e.*, systems of equations in three dimensions. It is shown that if a certain term can be ignored, the solutions are unique.

1 Introduction

There are three classical questions regarding a given mathematical problem: does it have a solution, is the solution unique, and does the solution change only little when we perturb the data? When all these questions are answered in the positive, we say the problem is well posed, in the sense of Hadamard [9]. One reason for this statement is that these properties guarantee reproducible results from simulations. For instance, if the model permits multiple solutions, how can we be sure which one we are calculating and that it is physically relevant?

In this paper, we treat the questions of uniqueness and continuity for solutions of the Maxwell equations, when modeling nonlinear media. Using a technique developed by Kružkov [17] for scalar conservation laws, we study the consequences of postulating an additional condition to the Maxwell equations, known as the entropy condition. We show that if a certain term can be ignored, the solution is indeed unique and depends continuously on given data.

The Maxwell equations alone are not sufficient to describe wave propagation through a material. They must be supplemented by constitutive relations, modeling the interaction between the electromagnetic fields and the material. These relations are often linear, but for large field strengths it is necessary to include some nonlinear interactions as well. When the material reacts much faster than the typical time scale of the wave, we may assume an instantaneous model. In this case, the Maxwell equations takes the mathematical structure of a symmetric system of hyperbolic conservation laws. In our case, the key word in this classification is "hyperbolic" [6, p. 401], in the sense that we can diagonalize the system of equations into a system of weakly coupled, scalar transport equations, allowing wave solutions.

Nonlinear hyperbolic conservation laws have been extensively studied, mostly from the perspective of continuum mechanics and thermodynamics. Much of the early engineering work up to 1948 is reported in [3], and a recent survey of mainly the mathematical aspects of this field is given in [5]. A nice introduction to the numerical treatment as well as a summary of theoretical results is found in [7], and the subject is treated in text books on partial differential equations [6, 12, 30]. One of the key results is that these equations permit solutions which become discontinuous in finite time, even if the initial data is infinitely differentiable. This means we

cannot guarantee the existence of classical derivatives, and the solution must be interpreted in a weak sense, *e.g.*, as a distribution or a measure.

It is well known that weak solutions to nonlinear hyperbolic conservation laws are not necessarily unique, see *e.g.*, [6, p. 142]. One remedy to this problem is to define the hyperbolic conservation law as the limit of a parabolic equation, which has well-defined solutions. This is the technique of vanishing viscosity, and was first introduced in [10]. This programme has been quite successful, but some difficulties remain, especially for systems of equations in several space variables. However, it has been shown that if the limit can be suitably defined, the solution satisfies an *entropy condition*, which can be defined independently of the limit process. This entropy condition is well motivated from a modeling point of view, and can often be shown to be a means of selecting the unique, physically relevant solution. When uniqueness proofs fail, it is often conjectured that the entropy condition provides unique solutions [7, p. 32].

There are many kinds of entropy conditions. Probably the first was considered by Jouguet [14], followed by Oleĭnik's condition E for a scalar equation [25], which was later extended by Liu [22], and a similar condition for strictly hyperbolic systems was formulated by Lax [20]. These conditions essentially require that when the equations allow a discontinuous solution, the characteristics should cross each other, which can be interpreted as "loss of information" or increase of entropy. There are also conditions for systems of conservation laws which are directly linked to the physical entropy, especially in gas dynamics. From an energy conservation point of view, this can also be considered as the dissipation of the energy defined by the conservation law. Dafermos has proposed an entropy condition requiring this dissipation to be maximal [4].

This paper is organized as follows. In Section 2 we present the notation used in the paper and the constitutive relations leading to the formulation of the Maxwell equations as a symmetric system of hyperbolic, quasi-linear conservation laws. We postulate the entropy condition in Section 3, and discuss the relevant interpretation of this condition. In Section 4 we treat the questions of uniqueness and continuous dependence on data for our solution using the technique of "doubling the variables" introduced by Kružkov for a scalar conservation law in [17]. We conclude by giving an explicit example in Section 5 of a situation where the Maxwell equations alone permit two solutions, and use the entropy condition to choose the relevant one. Some final remarks are made in Section 6.

2 The quasi-linear Maxwell equations

In this paper we use a slight modification of the Heaviside-Lorentz units for our fields [13, p. 781], *i.e.*, all electromagnetic fields are scaled to units of $\sqrt{\text{energy/volume}}$,

$$\begin{cases} \boldsymbol{E} = \sqrt{\epsilon_0}\boldsymbol{E}_{\text{SI}} \\ \boldsymbol{H} = \sqrt{\mu_0}\boldsymbol{H}_{\text{SI}}, \end{cases} \qquad \begin{cases} \boldsymbol{D} = 1/\sqrt{\epsilon_0}\boldsymbol{D}_{\text{SI}} \\ \boldsymbol{B} = 1/\sqrt{\mu_0}\boldsymbol{B}_{\text{SI}}, \end{cases} \qquad \boldsymbol{J} = \sqrt{\mu_0}\boldsymbol{J}_{\text{SI}}, \tag{2.1}$$

where $\boldsymbol{E}$ and $\boldsymbol{H}$ is the electric and magnetic field strength, respectively, and $\boldsymbol{D}$ and $\boldsymbol{B}$ is the electric and magnetic flux density, respectively, and $\boldsymbol{J}$ is the electric current density. The index SI is used to indicate the field in SI units. We use the scaled time $t = c_0 t_{\mathrm{SI}}$, where $c_0 = 1/\sqrt{\epsilon_0 \mu_0}$ is the speed of light in vacuum, and the constants ϵ_0 and μ_0 are the permittivity and permeability of free space, respectively. The six-vector notation from [8, 27], *i.e.*,

$$\boldsymbol{e} = \begin{pmatrix} \boldsymbol{E} \\ \boldsymbol{H} \end{pmatrix}, \quad \boldsymbol{d} = \begin{pmatrix} \boldsymbol{D} \\ \boldsymbol{B} \end{pmatrix}, \quad \boldsymbol{j} = \begin{pmatrix} \boldsymbol{J} \\ \boldsymbol{0} \end{pmatrix} \quad \nabla \times \mathbf{J} = \begin{pmatrix} \mathbf{0} & -\nabla \times \mathbf{I} \\ \nabla \times \mathbf{I} & \mathbf{0} \end{pmatrix}, \tag{2.2}$$

enables us to write the Maxwell equations in the compact form

$$\nabla \times \mathbf{J}\boldsymbol{e} + \partial_t \boldsymbol{d} = -\boldsymbol{j}. \tag{2.3}$$

In this paper we treat the six-vectors as column vectors, *i.e.*, we write the scalar product as $\boldsymbol{e}^{\mathrm{T}}\boldsymbol{d} = \sum_{i=1}^{6} e_i d_i$. This is merely for notational convenience and does not capture the full mathematical structure, which is not needed here. For more ambitious attempts to construct a six-vector notation, we refer to [8, 21].

The Maxwell equations must be supplemented by a constitutive relation, whose purpose is to model the interaction of the electromagnetic field with the material. When the material reacts very fast to stimulance, we can model it with an instantaneous constitutive model, where the values of the electric flux density $\boldsymbol{D}$ and the magnetic flux density $\boldsymbol{B}$ are completely determined by the values of the electric field strength $\boldsymbol{E}$ and magnetic field strength $\boldsymbol{H}$ at the same point in spacetime. We write this as

$$\boldsymbol{d}(\boldsymbol{r}, t) = \boldsymbol{d}(\boldsymbol{e}(\boldsymbol{r}, t)), \tag{2.4}$$

where $\boldsymbol{d}(\boldsymbol{e})$ is the gradient of a scalar function $\phi(\boldsymbol{e})$ with respect to $\boldsymbol{e}$, *i.e.*, in terms of thermodynamics, the field gradient of the thermodynamic potential (or the free energy density or the free enthalpy density) [2, 18]. We use the notation $\boldsymbol{d}(\boldsymbol{e}) = \phi'(\boldsymbol{e})$ to denote this derivative, *i.e.*, $d_i(\boldsymbol{e}) = \partial\phi/\partial e_i$, $i = 1, \ldots, 6$. The model is passive if we require that the symmetric 6×6 matrix $\boldsymbol{d}'(\boldsymbol{e}) = \phi''(\boldsymbol{e})$, where $[\boldsymbol{d}'(\boldsymbol{e})]_{ij} = \partial^2\phi/\partial e_i \partial e_j$, is a positive definite matrix, which is the case if the scalar function $\phi(\boldsymbol{e})$ is a convex function.

The Maxwell equations with an instantaneously reacting constitutive model is

$$\nabla \times \mathbf{J}\boldsymbol{e} + \boldsymbol{d}'(\boldsymbol{e})\partial_t \boldsymbol{e} = -\boldsymbol{j}, \tag{2.5}$$

and since $\boldsymbol{d}'(\boldsymbol{e})$ is positive definite and symmetric, this is by definition a quasi-linear, symmetric, hyperbolic system of partial differential equations [30, p. 360]. The source free version of this system has been extensively studied in [27], where it is shown that the equations in general support two waves, the ordinary and the extraordinary wave, each with its own refractive index.

Due to the quasi-linearity, the system (2.5) may exhibit shock solutions, *i.e.*, even if we give smooth data, the solution becomes discontinuous in finite time. This means the derivatives cannot be classically defined everywhere, but we can make a weak formulation of the problem by requiring the equality

$$\int_{\mathbb{R}} \int_{\mathbb{R}^3} [-\boldsymbol{e}^{\mathrm{T}} \nabla \times \mathbf{J}\boldsymbol{\varphi} - \boldsymbol{d}(\boldsymbol{e})^{\mathrm{T}} \partial_t \boldsymbol{\varphi} + \boldsymbol{j}^{\mathrm{T}} \boldsymbol{\varphi}] \, \mathrm{d}V \, \mathrm{d}t = 0 \tag{2.6}$$

to hold for all six-vector test functions $\boldsymbol{\varphi}$ defined on $\mathbb{R}^3 \times \mathbb{R}$, *i.e.*, vector-valued functions which are infinitely differentiable with compact support. We do not consider static fields in this paper, *i.e.*, if $\boldsymbol{j} = \mathbf{0}$ for $t < 0$, then $\boldsymbol{e} = \mathbf{0}$ for $t < 0$.

One problem with the weak formulation is that we lose uniqueness, *i.e.*, there are several weak solutions $\boldsymbol{e}$ which satisfy the above criteria. In the following section we present an entropy condition which guarantees uniqueness of the weak solutions.

3 The entropy condition

When the solutions to (2.5) are smooth, we can derive an equation representing the conservation of energy. First, we note the identities

$$\begin{cases} \boldsymbol{e}^{\mathrm{T}} \nabla \times \mathbf{J}\boldsymbol{e} = \nabla \cdot (\boldsymbol{E} \times \boldsymbol{H}) = \nabla \cdot \boldsymbol{S}(\boldsymbol{e}) \\ \boldsymbol{e}^{\mathrm{T}} \partial_t \boldsymbol{d}(\boldsymbol{e}) = \partial_t (\boldsymbol{e}^{\mathrm{T}} \boldsymbol{d}(\boldsymbol{e}) - \phi(\boldsymbol{e})) = \partial_t \eta(\boldsymbol{e}), \end{cases} \tag{3.1}$$

where the last identity follows from $\boldsymbol{d}(\boldsymbol{e}) = \phi'(\boldsymbol{e})$. The vector $\boldsymbol{S}(\boldsymbol{e})$ is the Poynting vector, and the scalar, convex function $\eta(\boldsymbol{e})$ is the electromagnetic energy density. Multiplying (2.5) with $\boldsymbol{e}^{\mathrm{T}}$ now implies the Poynting theorem (conservation of energy)

$$\nabla \cdot \boldsymbol{S}(\boldsymbol{e}) + \partial_t \eta(\boldsymbol{e}) = -\boldsymbol{e}^{\mathrm{T}} \boldsymbol{j}. \tag{3.2}$$

When the solutions to (2.5) are not smooth, this equation is no longer valid since the derivatives are not defined. We propose to replace it with the inequality

$$\boxed{\nabla \cdot \boldsymbol{S}(\boldsymbol{e}) + \partial_t \eta(\boldsymbol{e}) \leq -\boldsymbol{e}^{\mathrm{T}} \boldsymbol{j},} \tag{3.3}$$

which is interpreted in a weak sense, *i.e.*, for all nonnegative test functions φ, the inequality

$$\int_{\mathbb{R}} \int_{\mathbb{R}^3} [-\boldsymbol{S}(\boldsymbol{e}) \cdot \nabla \varphi - \eta(\boldsymbol{e}) \partial_t \varphi + \boldsymbol{e}^{\mathrm{T}} \boldsymbol{j} \varphi] \, \mathrm{d}V \, \mathrm{d}t \leq 0 \tag{3.4}$$

holds. The inequality (3.3) is called the *entropy condition*, and is here postulated in addition to the Maxwell equations. Observe that since (3.3) is postulated and interpreted in the weak sense, it is valid for non-smooth solutions. The pair of functions $\eta(\boldsymbol{e})$ and $\boldsymbol{S}(\boldsymbol{e})$ are known in the mathematical literature as an entropy/entropy-flux pair, see *e.g.*, [6, pp. 604–611], [12, pp. 70–71], and [30, pp. 436–445]. The existence of such a pair is nontrivial in the general case, and is a special property of the system. Similar conditions are often present for systems of nonlinear conservation laws, such as the equations governing gas dynamics, see *e.g.*, [7, pp. 21–35] and [4, 19, 22].

3.1 Why the term "entropy"?

It is quite obvious that no constitutive relation can capture all of the physical processes which occur when electromagnetic waves interact with matter. There is always some interaction that is left out, and if we choose not to model it, we must assume that the electromagnetic energy used in the interaction is lost in an irreversible

process. If the process were not irreversible, we would have to include it in our equations if the equations are supposed to be realistic. Since the electromagnetic energy is lost, it must be a nonincreasing function of time (except for the energy fed to the system), which is the essence of the entropy inequality (3.3). Namely, we can choose a suitable sequence of test functions $\{\varphi\}$ converging to a function constant on $\mathbb{R}^3 \times [t_1, t_2]$ to find[1]

$$\int_{\mathbb{R}^3} \eta(\boldsymbol{e})\,\mathrm{d}V\bigg|_{t=t_2} \leq \int_{\mathbb{R}^3} \eta(\boldsymbol{e})\,\mathrm{d}V\bigg|_{t=t_1} - \int_{t_1}^{t_2}\int_{\mathbb{R}^3} \boldsymbol{e}^{\mathrm{T}}\boldsymbol{j}\,\mathrm{d}V\,\mathrm{d}t, \tag{3.5}$$

when all the integrals are defined. For active sources $\boldsymbol{j}$, *i.e.*, sources which radiate electromagnetic energy, the term $-\int_{t_1}^{t_2}\int_{\mathbb{R}^3} \boldsymbol{e}^{\mathrm{T}}\boldsymbol{j}\,\mathrm{d}V\,\mathrm{d}t$ is positive when $t_1 < t_2$ and represents the energy fed to the system.

The inequality sign in (3.5) represents the fact that there is a loss of electromagnetic energy with increasing time. The irreversible processes that are not modeled by the Maxwell equations can be represented with an energy density term TS, where T is the temperature and S is the entropy density. The first law of thermodynamics states that the total internal energy

$$\mathcal{U} = \int_{\mathbb{R}^3} (\eta(\boldsymbol{e}) + TS)\,\mathrm{d}V \tag{3.6}$$

is constant for an isolated system (no exchange of heat or work, *i.e.*, for time intervals when $\boldsymbol{j} = \boldsymbol{0}$). If the integral of the electromagnetic energy is nonincreasing, it then follows that the integral of TS must be nondecreasing. This means the entropy must be nondecreasing under isothermal conditions, which is consistent with the second law of thermodynamics. This shows that the term "entropy condition" is justified for electromagnetic waves, if we interpret entropy as a representation of the dissipative processes not modeled by the Maxwell equations. Thus, we think of entropy as "missing information" about the system. For a further discussion on the interpretation of entropy, we refer to [29].

3.2 The entropy condition for vanishing viscosity solutions

We have previously postulated the entropy condition in addition to the Maxwell equations. The question may be raised if there exists solutions that satisfy both these criteria. There is at present no definite answer to this question, but we can show that if we make a parabolic regularization of the Maxwell equations,

$$\nabla \times \mathbf{J}\boldsymbol{e}_\delta + \partial_t \boldsymbol{d}(\boldsymbol{e}_\delta) = -\boldsymbol{j} + \delta\nabla^2\boldsymbol{e}_\delta, \tag{3.7}$$

and the solution $\boldsymbol{e}_\delta$ is uniformly bounded in the supremum norm and converges almost everywhere to $\boldsymbol{e}$ as $\delta \to 0$, this limit solution satisfies the entropy condition (3.3), see [7, p. 27] and [30, p. 438]. This method of constructing solutions to quasi-linear hyperbolic equations is called the vanishing viscosity method, and is a

[1] This procedure is performed in detail in Section 4.2.

standard method in partial differential equation theory. It can be shown that for each $\delta > 0$, the initial value problem for (3.7) is well posed with solutions infinitely differentiable in the interior domain and continuous on the boundary [30, p. 338]. For similar systems of equations in one spatial dimension and scalar equations in several dimensions, there exists a limiting function as $\delta \to 0$. However, there are still some questions regarding the convergence for systems of equations in several space dimensions, that have not been resolved, and we can only conjecture the existence of a limit $\boldsymbol{e} = \lim_{\delta \to 0} \boldsymbol{e}_\delta$, see [26] and [7, p. 32].

The parabolic equation (3.7) is actually the equivalent[2] (or modified) equation corresponding to certain numerical schemes used to solve hyperbolic equations, *e.g.*, the Lax-Friedrichs scheme in one spatial dimension [7, p. 181]. The viscosity parameter δ is then typically of order $(\Delta x)^2/\Delta t$, where Δx and Δt is the discretization in space and time, respectively, implying $\delta \to 0$ as the discretization is refined. In this context, the entropy is a measure of what goes on on a finer scale than we are observing, *i.e.*, on a scale of order δ.

4 Kružkov's method for entropy solutions

In this section we use a method due to Kružkov (see [17] and [6, pp. 608–611]) to study uniqueness and continuous dependence on data for solutions which satisfy the Maxwell equations as well as an entropy condition,

$$\begin{cases} \nabla \times \mathbf{J}\boldsymbol{e} + \partial_t \boldsymbol{d}(\boldsymbol{e}) = -\boldsymbol{j} \\ \nabla \cdot \boldsymbol{S}(\boldsymbol{e}) + \partial_t \eta(\boldsymbol{e}) \leq -\boldsymbol{e}^{\mathrm{T}} \boldsymbol{j}, \end{cases} \tag{4.1}$$

where $\boldsymbol{S}(\boldsymbol{e}) = \boldsymbol{E} \times \boldsymbol{H}$ and $\eta(\boldsymbol{e}) = \boldsymbol{e}^{\mathrm{T}} \boldsymbol{d}(\boldsymbol{e}) - \phi(\boldsymbol{e})$. The idea is to study the difference between the energies for two potentially different solutions, slightly perturbed in space and time. This enables us to obtain an inequality similar to (3.5), but with a new energy which is zero only when the two solutions are equal almost everywhere. However, the inequality also comprises a term which eludes further analysis. This is further commented at the end of Section 4.1.

Suppose we have two solutions, $\boldsymbol{e}$ and $\tilde{\boldsymbol{e}}$, satisfying

$$\begin{cases} \nabla_{\boldsymbol{x}} \times \mathbf{J}\boldsymbol{e} + \partial_t \boldsymbol{d}(\boldsymbol{e}) = -\boldsymbol{j} \\ \nabla_{\boldsymbol{x}} \cdot \boldsymbol{S}(\boldsymbol{e}) + \partial_t \eta(\boldsymbol{e}) \leq -\boldsymbol{e}^{\mathrm{T}} \boldsymbol{j}, \end{cases} \quad \text{and} \quad \begin{cases} \nabla_{\boldsymbol{y}} \times \mathbf{J}\tilde{\boldsymbol{e}} + \partial_s \boldsymbol{d}(\tilde{\boldsymbol{e}}) = -\tilde{\boldsymbol{j}} \\ \nabla_{\boldsymbol{y}} \cdot \boldsymbol{S}(\tilde{\boldsymbol{e}}) + \partial_s \eta(\tilde{\boldsymbol{e}}) \leq -\tilde{\boldsymbol{e}}^{\mathrm{T}} \tilde{\boldsymbol{j}}, \end{cases} \tag{4.2}$$

where $\boldsymbol{j}$ and $\tilde{\boldsymbol{j}}$ may be different. Note that we have labeled the independent variables differently for the two solutions, *i.e.*, $\boldsymbol{e} = \boldsymbol{e}(\boldsymbol{x}, t)$, $\boldsymbol{j} = \boldsymbol{j}(\boldsymbol{x}, t)$, $\tilde{\boldsymbol{e}} = \tilde{\boldsymbol{e}}(\boldsymbol{y}, s)$ and $\tilde{\boldsymbol{j}} = \tilde{\boldsymbol{j}}(\boldsymbol{y}, s)$. This is helpful when handling the differential operators in the following. We add[3] $-\tilde{\boldsymbol{e}}^{\mathrm{T}}(\nabla_{\boldsymbol{x}} \times \mathbf{J}\boldsymbol{e} + \partial_t \boldsymbol{d}(\boldsymbol{e}) + \boldsymbol{j}) + \tilde{\boldsymbol{e}}^{\mathrm{T}} \nabla_{\boldsymbol{x}} \times \mathbf{J}\tilde{\boldsymbol{e}} + \partial_t \phi(\tilde{\boldsymbol{e}}) = 0$ to the entropy

[2] For a numerical scheme of order n approximating a given equation, the equivalent (or modified) equation is defined as the equation which is approximated to order $n + 1$ by the scheme.

[3] This distribution is well-defined, since $\tilde{\boldsymbol{e}}(\boldsymbol{y}, s)$ does not depend on $\boldsymbol{x}$ or t. This implies that the derivatives operate only on the test function.

condition for $\boldsymbol{e}$, which implies

$$\begin{aligned} 0 &\geq \nabla_{\boldsymbol{x}} \cdot \boldsymbol{S}(\boldsymbol{e}) + \partial_t \eta(\boldsymbol{e}) + \boldsymbol{e}^{\mathrm{T}} \boldsymbol{j} - \tilde{\boldsymbol{e}}^{\mathrm{T}} (\nabla_{\boldsymbol{x}} \times \mathbf{J}\boldsymbol{e} + \partial_t \boldsymbol{d}(\boldsymbol{e}) + \boldsymbol{j}) + \tilde{\boldsymbol{e}}^{\mathrm{T}} \nabla_{\boldsymbol{x}} \times \mathbf{J}\tilde{\boldsymbol{e}} + \partial_t \phi(\tilde{\boldsymbol{e}}) \\ &= \nabla_{\boldsymbol{x}} \cdot \boldsymbol{S}(\boldsymbol{e} - \tilde{\boldsymbol{e}}) + \partial_t \eta(\boldsymbol{e}, \tilde{\boldsymbol{e}}) + (\boldsymbol{e} - \tilde{\boldsymbol{e}})^{\mathrm{T}} \boldsymbol{j}, \end{aligned} \tag{4.3}$$

where

$$\eta(\boldsymbol{e}, \tilde{\boldsymbol{e}}) = (\boldsymbol{e} - \tilde{\boldsymbol{e}})^{\mathrm{T}} \boldsymbol{d}(\boldsymbol{e}) - \phi(\boldsymbol{e}) + \phi(\tilde{\boldsymbol{e}}). \tag{4.4}$$

Note that the terms $\tilde{\boldsymbol{e}}^{\mathrm{T}} \nabla_{\boldsymbol{x}} \times \mathbf{J}\tilde{\boldsymbol{e}}$ and $\partial_t \phi(\tilde{\boldsymbol{e}})$ are identically zero since $\tilde{\boldsymbol{e}}$ does not depend on $\boldsymbol{x}$ or t, and are included in order to obtain better symmetry in the inequality (4.3). Repeating the procedure for the set of equations with independent variables $(\boldsymbol{y}, s)$, results in the entropy inequalities

$$\begin{cases} \nabla_{\boldsymbol{x}} \cdot \boldsymbol{S}(\boldsymbol{e} - \tilde{\boldsymbol{e}}) + \partial_t \eta(\boldsymbol{e}, \tilde{\boldsymbol{e}}) + (\boldsymbol{e} - \tilde{\boldsymbol{e}})^{\mathrm{T}} \boldsymbol{j} \leq 0 \\ \nabla_{\boldsymbol{y}} \cdot \boldsymbol{S}(\tilde{\boldsymbol{e}} - \boldsymbol{e}) + \partial_s \eta(\tilde{\boldsymbol{e}}, \boldsymbol{e}) + (\tilde{\boldsymbol{e}} - \boldsymbol{e})^{\mathrm{T}} \tilde{\boldsymbol{j}} \leq 0. \end{cases} \tag{4.5}$$

These inequalities are interpreted in a weak sense, *i.e.*, they are defined through their effect on nonnegative test functions. Thus, the inequalities

$$\begin{cases} \displaystyle\iiiint \Big\{ - \boldsymbol{S}(\boldsymbol{e} - \tilde{\boldsymbol{e}}) \cdot \nabla_{\boldsymbol{x}} \varphi - \eta(\boldsymbol{e}, \tilde{\boldsymbol{e}}) \partial_t \varphi + (\boldsymbol{e} - \tilde{\boldsymbol{e}})^{\mathrm{T}} \boldsymbol{j} \varphi \Big\} \, \mathrm{d}V(\boldsymbol{x}) \, \mathrm{d}V(\boldsymbol{y}) \, \mathrm{d}t \, \mathrm{d}s \leq 0 \\ \displaystyle\iiiint \Big\{ - \boldsymbol{S}(\tilde{\boldsymbol{e}} - \boldsymbol{e}) \cdot \nabla_{\boldsymbol{y}} \varphi - \eta(\tilde{\boldsymbol{e}}, \boldsymbol{e}) \partial_s \varphi + (\tilde{\boldsymbol{e}} - \boldsymbol{e})^{\mathrm{T}} \tilde{\boldsymbol{j}} \varphi \Big\} \, \mathrm{d}V(\boldsymbol{x}) \, \mathrm{d}V(\boldsymbol{y}) \, \mathrm{d}t \, \mathrm{d}s \leq 0, \end{cases} \tag{4.6}$$

must hold for all test functions $\varphi(\boldsymbol{x}, \boldsymbol{y}, t, s) \geq 0$. The integrations are performed over $\mathbb{R}^3 \times \mathbb{R}^3 \times \mathbb{R} \times \mathbb{R}$, but we suppress the integration limits in order to simplify the notation. We now observe the symmetry $\boldsymbol{S}(\boldsymbol{e} - \tilde{\boldsymbol{e}}) = \boldsymbol{S}(\tilde{\boldsymbol{e}} - \boldsymbol{e})$, and expand $\partial_t \varphi$ and $\partial_s \varphi$ as $\partial_t \varphi = \frac{1}{2}\partial_t \varphi + \frac{1}{2}\partial_s \varphi + \frac{1}{2}\partial_t \varphi - \frac{1}{2}\partial_s \varphi$ and $\partial_s \varphi = \frac{1}{2}\partial_s \varphi + \frac{1}{2}\partial_t \varphi + \frac{1}{2}\partial_s \varphi - \frac{1}{2}\partial_t \varphi$. After adding the inequalities we obtain

$$\begin{aligned} 0 \geq \iiiint \Big\{ &- \boldsymbol{S}(\boldsymbol{e} - \tilde{\boldsymbol{e}}) \cdot (\nabla_{\boldsymbol{x}} \varphi + \nabla_{\boldsymbol{y}} \varphi) - \frac{1}{2}[\eta(\boldsymbol{e}, \tilde{\boldsymbol{e}}) + \eta(\tilde{\boldsymbol{e}}, \boldsymbol{e})](\partial_t \varphi + \partial_s \varphi) \\ &- \frac{1}{2}[\eta(\boldsymbol{e}, \tilde{\boldsymbol{e}}) - \eta(\tilde{\boldsymbol{e}}, \boldsymbol{e})](\partial_t \varphi - \partial_s \varphi) + (\boldsymbol{e} - \tilde{\boldsymbol{e}})^{\mathrm{T}} (\boldsymbol{j} - \tilde{\boldsymbol{j}}) \varphi \Big\} \, \mathrm{d}V(\boldsymbol{x}) \, \mathrm{d}V(\boldsymbol{y}) \, \mathrm{d}t \, \mathrm{d}s, \end{aligned} \tag{4.7}$$

which is the general expression with an arbitrary test function φ. To proceed with the analysis, we now choose a special test function which somewhat simplifies this inequality.

4.1 Choosing the proper test function

Following Kružkov's classical uniqueness proof, we employ the special test function

$$\varphi(\boldsymbol{x}, \boldsymbol{y}, t, s) = J_\delta^{(3)} \left(\frac{\boldsymbol{x} - \boldsymbol{y}}{2} \right) J_\delta \left(\frac{t - s}{2} \right) \psi \left(\frac{\boldsymbol{x} + \boldsymbol{y}}{2}, \frac{t + s}{2} \right), \tag{4.8}$$

where J_δ is a nonnegative mollifier, having unit integral and converging to the Dirac measure as $\delta \to 0$. The mollifier in space $J_\delta^{(3)}$ can be written as the product $J_\delta^{(3)}(\boldsymbol{x}) =$

$J_\delta(x_1)J_\delta(x_2)J_\delta(x_3)$. Since the support of the mollifiers shrinks to zero when $\delta \to 0$, this choice of test function brings the variables $\boldsymbol{x}$ and $\boldsymbol{y}$, and t and s, respectively, close to each other as the parameter $\delta \to 0$. This is similar to restricting the tensor product between two distributions to the diagonal, see [11].

Introducing the new variables

$$\bar{\boldsymbol{x}} = \frac{\boldsymbol{x}+\boldsymbol{y}}{2}, \quad \bar{\boldsymbol{y}} = \frac{\boldsymbol{x}-\boldsymbol{y}}{2}, \quad \bar{t} = \frac{t+s}{2}, \quad \bar{s} = \frac{t-s}{2}, \tag{4.9}$$

the inequality (4.7) is written

$$\iiiint \left\{ -\boldsymbol{S}(\boldsymbol{e}-\tilde{\boldsymbol{e}}) \cdot \nabla_{\bar{\boldsymbol{x}}}\psi - \frac{1}{2}[\eta(\boldsymbol{e},\tilde{\boldsymbol{e}}) + \eta(\tilde{\boldsymbol{e}},\boldsymbol{e})]\partial_{\bar{t}}\psi + (\boldsymbol{e}-\tilde{\boldsymbol{e}})^{\mathrm{T}}(\boldsymbol{j}-\tilde{\boldsymbol{j}})\psi \right\}$$
$$J_\delta^{(3)} J_\delta \,\mathrm{d}V(\bar{\boldsymbol{x}})\,\mathrm{d}V(\bar{\boldsymbol{y}})\,\mathrm{d}\bar{t}\,\mathrm{d}\bar{s}$$
$$\leq \iiiint \frac{1}{2}[\eta(\boldsymbol{e},\tilde{\boldsymbol{e}}) - \eta(\tilde{\boldsymbol{e}},\boldsymbol{e})] J_\delta^{(3)} J_\delta' \psi \,\mathrm{d}V(\bar{\boldsymbol{x}})\,\mathrm{d}V(\bar{\boldsymbol{y}})\,\mathrm{d}\bar{t}\,\mathrm{d}\bar{s}. \tag{4.10}$$

The explicit expression for the energy term $\frac{1}{2}[\eta(\boldsymbol{e},\tilde{\boldsymbol{e}}) + \eta(\tilde{\boldsymbol{e}},\boldsymbol{e})]$ is found from the definition of $\eta(\boldsymbol{e},\tilde{\boldsymbol{e}})$,

$$\frac{1}{2}[\eta(\boldsymbol{e},\tilde{\boldsymbol{e}}) + \eta(\tilde{\boldsymbol{e}},\boldsymbol{e})] = \frac{1}{2}(\boldsymbol{e}-\tilde{\boldsymbol{e}})^{\mathrm{T}}(\boldsymbol{d}(\boldsymbol{e}) - \boldsymbol{d}(\tilde{\boldsymbol{e}})), \tag{4.11}$$

and in Appendix A it is shown that we can introduce a third rank tensor $K_{ijk}(\boldsymbol{e},\tilde{\boldsymbol{e}})$, defined in (A.8), to write

$$\frac{1}{2}[\eta(\boldsymbol{e},\tilde{\boldsymbol{e}}) - \eta(\tilde{\boldsymbol{e}},\boldsymbol{e})] = K_{ijk}(\boldsymbol{e},\tilde{\boldsymbol{e}})(e_i-\tilde{e}_i)(e_j-\tilde{e}_j)(e_k-\tilde{e}_k), \tag{4.12}$$

where summation over repeated indices is assumed. As seen in Appendix A, the tensor K_{ijk} is related to the third derivative of the thermodynamic potential, ϕ'''. Since ϕ is a quadratic function for linear materials, we see that this term must be due to the nonlinearity of our constitutive relation.

The explicit form of the entropy inequality (4.7) is thus

$$\iiiint \left\{ -\boldsymbol{S}(\boldsymbol{e}-\tilde{\boldsymbol{e}}) \cdot \nabla_{\bar{\boldsymbol{x}}}\psi - \frac{1}{2}(\boldsymbol{e}-\tilde{\boldsymbol{e}})^{\mathrm{T}}(\boldsymbol{d}(\boldsymbol{e}) - \boldsymbol{d}(\tilde{\boldsymbol{e}}))\partial_{\bar{t}}\psi + (\boldsymbol{e}-\tilde{\boldsymbol{e}})^{\mathrm{T}}(\boldsymbol{j}-\tilde{\boldsymbol{j}})\psi \right\}$$
$$J_\delta^{(3)} J_\delta \,\mathrm{d}V(\bar{\boldsymbol{x}})\,\mathrm{d}V(\bar{\boldsymbol{y}})\,\mathrm{d}\bar{t}\,\mathrm{d}\bar{s}$$
$$\leq \iiiint K_{ijk}(\boldsymbol{e},\tilde{\boldsymbol{e}})(e_i-\tilde{e}_i)(e_j-\tilde{e}_j)(e_k-\tilde{e}_k) J_\delta^{(3)} J_\delta' \psi \,\mathrm{d}V(\bar{\boldsymbol{x}})\,\mathrm{d}V(\bar{\boldsymbol{y}})\,\mathrm{d}\bar{t}\,\mathrm{d}\bar{s}, \tag{4.13}$$

where no approximations are made so far. It is conjectured that the term on the right hand side of the inequality is negligible, since it is cubic in the difference $\boldsymbol{e}-\tilde{\boldsymbol{e}}$ and should therefore be small compared to the other terms when $|\boldsymbol{e}-\tilde{\boldsymbol{e}}|$ is small. However, the differentiated mollifier J_δ' could change this assumption. It should be noted that in the case of a scalar conservation law, which Kružkov studied, it is possible to choose the functions corresponding to $\boldsymbol{S}$ and η such that this term does not appear. To see why it is desirable to obtain control over this term, we spend the following subsections showing that this implies that our solutions are unique and depend continuously on data.

4.2 Uniqueness and continuous dependence on data

If we assume the term on the right hand side of (4.13) can be replaced with zero, we are free to take the limit $\delta \to 0$ in the mollifiers since the terms inside the curly brackets are summable over $\bar{\boldsymbol{x}}$ and $\bar{t}$. This implies that the integrals over $\bar{\boldsymbol{y}}$ and $\bar{s}$ only contribute when $(\bar{\boldsymbol{y}}, \bar{s})$ is close to $(\boldsymbol{0}, 0)$, which implies $\bar{\boldsymbol{x}} \approx \boldsymbol{x} \approx \boldsymbol{y}$ and $\bar{t} \approx t \approx s$. Hence the limit $\delta \to 0$ provides the inequality

$$\iint \Big\{ -\boldsymbol{S}(\boldsymbol{e}-\tilde{\boldsymbol{e}}) \cdot \nabla_{\bar{\boldsymbol{x}}}\psi - \frac{1}{2}(\boldsymbol{e}-\tilde{\boldsymbol{e}})^{\mathrm{T}}(\boldsymbol{d}(\boldsymbol{e})-\boldsymbol{d}(\tilde{\boldsymbol{e}}))\partial_{\bar{t}}\psi + (\boldsymbol{e}-\tilde{\boldsymbol{e}})^{\mathrm{T}}(\boldsymbol{j}-\tilde{\boldsymbol{j}})\psi \Big\} \,\mathrm{d}V(\bar{\boldsymbol{x}})\,\mathrm{d}\bar{t} \le 0, \quad (4.14)$$

and from this point on we use the variables $\bar{\boldsymbol{x}}$ and $\bar{t}$ to emphasize that they are the mean values of the variables $\boldsymbol{x}$ and $\boldsymbol{y}$, and t and s, respectively. Following [6, pp. 608–611] we choose the test function $\psi(\bar{\boldsymbol{x}}, \bar{t}) = \alpha(\bar{\boldsymbol{x}})\beta(\bar{t})$ according to

$$\begin{cases} \alpha : \mathbb{R}^3 \to \mathbb{R} \quad \text{is smooth,} \\ \alpha(\bar{\boldsymbol{x}}) = 1 \quad \text{if} \quad |\bar{\boldsymbol{x}}| \le r, \\ \alpha(\bar{\boldsymbol{x}}) = 0 \quad \text{if} \quad |\bar{\boldsymbol{x}}| \ge r + r_0, \\ |\nabla_{\bar{\boldsymbol{x}}}\alpha(\bar{\boldsymbol{x}})| \le 2/r_0, \end{cases} \quad (4.15)$$

and

$$\begin{cases} \beta : \mathbb{R} \to \mathbb{R} \text{ is Lipschitz continuous,} \\ \beta(\bar{t}) = 0 \quad \text{if} \quad \bar{t} \le t_1 \text{ or } \bar{t} \ge t_2 + \Delta t, \\ \beta(\bar{t}) = 1 \quad \text{if} \quad t_1 + \Delta t \le \bar{t} \le t_2, \\ \beta \text{ is linear on } [t_1, t_1+\Delta t] \text{ and } [t_2, t_2+\Delta t], \end{cases} \quad (4.16)$$

where Δt satisfies $0 < \Delta t < t_2 - t_1$. Strictly speaking, β is not a test function, but we can use a suitable sequence of proper test functions to construct this limit. Our inequality is now written

$$\begin{aligned} \frac{1}{\Delta t}\int_{t_2}^{t_2+\Delta t} \frac{1}{2}\int_{\mathbb{R}^3} (\boldsymbol{e}-\tilde{\boldsymbol{e}})^{\mathrm{T}}(\boldsymbol{d}(\boldsymbol{e})-\boldsymbol{d}(\tilde{\boldsymbol{e}}))\alpha(\bar{\boldsymbol{x}})\,\mathrm{d}V(\bar{\boldsymbol{x}})\,\mathrm{d}\bar{t} \\ + \int_{t_1}^{t_2+\Delta t}\int_{r<|\bar{\boldsymbol{x}}|<r+r_0} \boldsymbol{S}(\boldsymbol{e}-\tilde{\boldsymbol{e}}) \cdot \nabla_{\bar{\boldsymbol{x}}}\alpha(\bar{\boldsymbol{x}})\beta(\bar{t})\,\mathrm{d}V(\bar{\boldsymbol{x}})\,\mathrm{d}\bar{t} \\ \le \frac{1}{\Delta t}\int_{t_1}^{t_1+\Delta t} \frac{1}{2}\int_{\mathbb{R}^3} (\boldsymbol{e}-\tilde{\boldsymbol{e}})^{\mathrm{T}}(\boldsymbol{d}(\boldsymbol{e})-\boldsymbol{d}(\tilde{\boldsymbol{e}}))\alpha(\bar{\boldsymbol{x}})\,\mathrm{d}V(\bar{\boldsymbol{x}})\,\mathrm{d}\bar{t} \\ - \int_{t_1}^{t_2+\Delta t}\int_{\mathbb{R}^3} (\boldsymbol{e}-\tilde{\boldsymbol{e}})^{\mathrm{T}}(\boldsymbol{j}-\tilde{\boldsymbol{j}})\alpha(\bar{\boldsymbol{x}})\beta(\bar{t})\,\mathrm{d}V(\bar{\boldsymbol{x}})\,\mathrm{d}\bar{t} \end{aligned} \quad (4.17)$$

and the integral containing $\boldsymbol{S}(\boldsymbol{e}-\tilde{\boldsymbol{e}})$ vanishes as $r \to \infty$ since $\boldsymbol{S}(\boldsymbol{e}-\tilde{\boldsymbol{e}})$ is a quadratic function of $\boldsymbol{e}-\tilde{\boldsymbol{e}}$ and $|\boldsymbol{e}|^2$ and $|\tilde{\boldsymbol{e}}|^2$ are integrable, which means the integral must disappear in this limit. We next let $\Delta t \to 0$ to deduce the fundamental energy

estimate

$$\frac{1}{2}\int_{\mathbb{R}^3}(\boldsymbol{e}-\tilde{\boldsymbol{e}})^{\mathrm{T}}(\boldsymbol{d}(\boldsymbol{e})-\boldsymbol{d}(\tilde{\boldsymbol{e}}))\,\mathrm{d}V(\bar{\boldsymbol{x}})\bigg|_{\bar{t}=t_2} \leq \frac{1}{2}\int_{\mathbb{R}^3}(\boldsymbol{e}-\tilde{\boldsymbol{e}})^{\mathrm{T}}(\boldsymbol{d}(\boldsymbol{e})-\boldsymbol{d}(\tilde{\boldsymbol{e}}))\,\mathrm{d}V(\bar{\boldsymbol{x}})\bigg|_{\bar{t}=t_1} - \int_{t_1}^{t_2}\int_{\mathbb{R}^3}(\boldsymbol{e}-\tilde{\boldsymbol{e}})^{\mathrm{T}}(\boldsymbol{j}-\tilde{\boldsymbol{j}})\,\mathrm{d}V(\bar{\boldsymbol{x}})\,\mathrm{d}\bar{t} \quad (4.18)$$

for every pair $t_1 < t_2$. We emphasize that this estimate was obtained by assuming that a term cubic in the difference $\boldsymbol{e}-\tilde{\boldsymbol{e}}$ could be ignored.

Our first question concerns the uniqueness of entropy solutions, *i.e.*, can different solutions be generated by the same data? From (4.18) we see the answer is negative. The currents may be assumed to start at a specific time, *i.e.*, $\boldsymbol{j}=\tilde{\boldsymbol{j}}=\boldsymbol{0}$ for $t\leq 0$, and causality implies $\boldsymbol{e}=\tilde{\boldsymbol{e}}=\boldsymbol{0}$ for $\bar{t}=0$. By choosing $t_2=T$ and $t_1=0$ and using the same currents for the two solutions, $\boldsymbol{j}=\tilde{\boldsymbol{j}}$ everywhere, we obtain

$$\frac{1}{2}\int_{\mathbb{R}^3}(\boldsymbol{e}-\tilde{\boldsymbol{e}})^{\mathrm{T}}(\boldsymbol{d}(\boldsymbol{e})-\boldsymbol{d}(\tilde{\boldsymbol{e}}))\,\mathrm{d}V(\bar{\boldsymbol{x}})\bigg|_{\bar{t}=T} \leq 0 \quad (4.19)$$

for every finite time $T>0$. Assuming the model saturates for high field strengths, *i.e.*, $\boldsymbol{d}(\boldsymbol{e})$ can be bounded by a linear function of $\boldsymbol{e}$, there exists positive constants $C_<$ and $C_>$ such that

$$C_<|\boldsymbol{e}-\tilde{\boldsymbol{e}}|^2 \leq (\boldsymbol{e}-\tilde{\boldsymbol{e}})^{\mathrm{T}}(\boldsymbol{d}(\boldsymbol{e})-\boldsymbol{d}(\tilde{\boldsymbol{e}})) \leq C_>|\boldsymbol{e}-\tilde{\boldsymbol{e}}|^2, \quad (4.20)$$

we see that (4.19) implies $\boldsymbol{e}=\tilde{\boldsymbol{e}}$ almost everywhere. Thus we have uniqueness.

Our second question concerns the continuous dependence of the solution on given data. We use Hölder's inequality to estimate the source term

$$-\int_0^T\int_{\mathbb{R}^3}(\boldsymbol{e}-\tilde{\boldsymbol{e}})^{\mathrm{T}}(\boldsymbol{j}-\tilde{\boldsymbol{j}})\,\mathrm{d}V(\bar{\boldsymbol{x}})\,\mathrm{d}\bar{t} \leq \int_0^T\int_{\mathbb{R}^3}|(\boldsymbol{e}-\tilde{\boldsymbol{e}})^{\mathrm{T}}(\boldsymbol{j}-\tilde{\boldsymbol{j}})|\,\mathrm{d}V(\bar{\boldsymbol{x}})\,\mathrm{d}\bar{t} \leq \int_0^T\left(\int_{\mathbb{R}^3}|\boldsymbol{e}-\tilde{\boldsymbol{e}}|^2\,\mathrm{d}V(\bar{\boldsymbol{x}})\right)^{1/2}\left(\int_{\mathbb{R}^2}|\boldsymbol{j}-\tilde{\boldsymbol{j}})|^2\,\mathrm{d}V(\bar{\boldsymbol{x}})\right)^{1/2}\mathrm{d}\bar{t}. \quad (4.21)$$

Using the notation $\|\boldsymbol{e}-\tilde{\boldsymbol{e}}\| = \left(\int_{\mathbb{R}^3}|\boldsymbol{e}-\tilde{\boldsymbol{e}}|^2\,\mathrm{d}V\right)^{1/2}$ and (4.20), the estimate (4.18) implies

$$\frac{C_<}{2}\|\boldsymbol{e}-\tilde{\boldsymbol{e}}\|^2_{\bar{t}=T} \leq \int_0^T\|\boldsymbol{e}-\tilde{\boldsymbol{e}}\|\cdot\|\boldsymbol{j}-\tilde{\boldsymbol{j}}\|\,\mathrm{d}\bar{t}, \quad (4.22)$$

where we used $\|\boldsymbol{e}-\tilde{\boldsymbol{e}}\|^2_{\bar{t}=0}=0$. Since this inequality is valid for all $T>0$, the term on the left hand side can be replaced by its supremum. After dividing by $\sup_{\bar{t}\in[0,T]}\|\boldsymbol{e}-\tilde{\boldsymbol{e}}\|$, we find

$$\sup_{\bar{t}\in[0,T]}\|\boldsymbol{e}-\tilde{\boldsymbol{e}}\| \leq \frac{2}{C_<}\int_0^T\|\boldsymbol{j}-\tilde{\boldsymbol{j}}\|\,\mathrm{d}\bar{t}, \quad (4.23)$$

for every $T>0$. This shows that the norm of the difference between two solutions is bounded by the norms of the difference between the difference between the sources. Thus we have continuous dependence of the solution on input data for each finite time T.

4.3 Initial/boundary-value problem

To simplify and streamline the presentation, the analysis so far has been for all of space and time, which means there are no initial or boundary values involved. In this subsection, we give a brief review on how to treat a finite region $\Omega \subset \mathbb{R}^3$ instead of all space. We also allow for initial values by making the following weak formulation of the Maxwell equations instead of (2.6),

$$\int_0^\infty \int_\Omega [-\boldsymbol{e}^{\mathrm{T}} \nabla \times \mathbf{J}\boldsymbol{\varphi} - \boldsymbol{d}(\boldsymbol{e})^{\mathrm{T}} \partial_t \boldsymbol{\varphi} + \boldsymbol{j}^{\mathrm{T}} \boldsymbol{\varphi}] \,\mathrm{d}V \,\mathrm{d}t + \int_0^\infty \int_{\partial\Omega} \boldsymbol{S}(\boldsymbol{\varphi}, \boldsymbol{e}) \cdot \hat{\boldsymbol{n}} \,\mathrm{d}S \,\mathrm{d}t - \int_\Omega \boldsymbol{d}(\boldsymbol{e}_0)^{\mathrm{T}} \boldsymbol{\varphi} \,\mathrm{d}V \Big|_{t=0} = 0, \quad (4.24)$$

where $\hat{\boldsymbol{n}}$ denotes the unit normal pointing out of the region Ω, and $\boldsymbol{S}(\boldsymbol{\varphi}, \boldsymbol{e}) = \boldsymbol{\varphi}_E \times \boldsymbol{H} - \boldsymbol{\varphi}_H \times \boldsymbol{E}$, with $\boldsymbol{\varphi}_E$ and $\boldsymbol{\varphi}_H$ denoting the parts of the six-vector test function $\boldsymbol{\varphi}$ corresponding to the electric and magnetic field, respectively. We denote the initial values by $\boldsymbol{e}(\boldsymbol{x}, 0) = \boldsymbol{e}_0(\boldsymbol{x})$. Instead of the estimate (4.18) we now obtain

$$\int_0^T \int_{\partial\Omega} \boldsymbol{S}(\boldsymbol{e} - \tilde{\boldsymbol{e}}) \cdot \hat{\boldsymbol{n}} \,\mathrm{d}S(\bar{\boldsymbol{x}}) \,\mathrm{d}\bar{t} + \frac{1}{2} \int_\Omega (\boldsymbol{e} - \tilde{\boldsymbol{e}})^{\mathrm{T}} (\boldsymbol{d}(\boldsymbol{e}) - \boldsymbol{d}(\tilde{\boldsymbol{e}})) \,\mathrm{d}V(\bar{\boldsymbol{x}}) \Big|_{\bar{t}=T} \leq \frac{1}{2} \int_\Omega (\boldsymbol{e}_0 - \tilde{\boldsymbol{e}}_0)^{\mathrm{T}} (\boldsymbol{d}(\boldsymbol{e}_0) - \boldsymbol{d}(\tilde{\boldsymbol{e}}_0)) \,\mathrm{d}V(\bar{\boldsymbol{x}}) - \int_0^T \int_\Omega (\boldsymbol{e} - \tilde{\boldsymbol{e}})^{\mathrm{T}} (\boldsymbol{j} - \tilde{\boldsymbol{j}}) \,\mathrm{d}V(\bar{\boldsymbol{x}}) \,\mathrm{d}\bar{t}, \quad (4.25)$$

once again under the assumption that we can ignore the cubic term in (4.13). The initial values are given from the problem formulation, but it remains to divide the integral of Poynting's vector over the boundary, representing the net flow of energy across the boundary, into parts representing energy flow in and out of the region. We use the energy splitting (change of variables) [8, 15]

$$\boldsymbol{E}_\pm = \frac{-\hat{\boldsymbol{n}} \times (\hat{\boldsymbol{n}} \times \boldsymbol{E}) \pm \hat{\boldsymbol{n}} \times \boldsymbol{H}}{2}, \quad (4.26)$$

to decompose the energy flux into

$$\boldsymbol{S}(\boldsymbol{e} - \tilde{\boldsymbol{e}}) \cdot \hat{\boldsymbol{n}} = |\boldsymbol{E}_+ - \tilde{\boldsymbol{E}}_+|^2 - |\boldsymbol{E}_- - \tilde{\boldsymbol{E}}_-|^2. \quad (4.27)$$

Assuming we can choose boundary data such that the incoming energy flux $|\boldsymbol{E}_- - \tilde{\boldsymbol{E}}_-|^2$ is given, we obtain

$$\int_0^T \int_{\partial\Omega} |\boldsymbol{E}_+ - \tilde{\boldsymbol{E}}_+|^2 \,\mathrm{d}S(\bar{\boldsymbol{x}}) \,\mathrm{d}\bar{t} + \frac{1}{2} \int_\Omega (\boldsymbol{e} - \tilde{\boldsymbol{e}})^{\mathrm{T}} (\boldsymbol{d}(\boldsymbol{e}) - \boldsymbol{d}(\tilde{\boldsymbol{e}})) \,\mathrm{d}V(\bar{\boldsymbol{x}}) \Big|_{\bar{t}=T} \leq \int_0^T \int_{\partial\Omega} |\boldsymbol{E}_- - \tilde{\boldsymbol{E}}_-|^2 \,\mathrm{d}S(\bar{\boldsymbol{x}}) \,\mathrm{d}\bar{t} + \frac{1}{2} \int_\Omega (\boldsymbol{e}_0 - \tilde{\boldsymbol{e}}_0)^{\mathrm{T}} (\boldsymbol{d}(\boldsymbol{e}_0) - \boldsymbol{d}(\tilde{\boldsymbol{e}}_0)) \,\mathrm{d}V(\bar{\boldsymbol{x}}) - \int_0^T \int_\Omega (\boldsymbol{e} - \tilde{\boldsymbol{e}})^{\mathrm{T}} (\boldsymbol{j} - \tilde{\boldsymbol{j}}) \,\mathrm{d}V(\bar{\boldsymbol{x}}) \,\mathrm{d}\bar{t}, \quad (4.28)$$

with everything on the right hand side given by initial/boundary data or the sources $\boldsymbol{j} - \tilde{\boldsymbol{j}}$. It is easy to see that this estimate provides us with the same conclusions regarding uniqueness and continuous dependence on data as in the previous subsection.

5 One-dimensional example

We give an example of a situation where we have several solutions to the Maxwell equations (2.5), but the entropy condition (3.3) helps us finding the relevant solution. Assuming no sources and the initial values

$$\boldsymbol{e}(\boldsymbol{x},0) = \begin{cases} \boldsymbol{e}^{\mathrm{l}} & z<0 \\ \boldsymbol{e}^{\mathrm{r}} & z>0, \end{cases} \tag{5.1}$$

where the constant six-vectors $\boldsymbol{e}^{\mathrm{l}}$ and $\boldsymbol{e}^{\mathrm{r}}$ denote the left and right state, respectively, the Maxwell equations reduce to the one-dimensional equations,

$$\hat{\boldsymbol{z}} \times \mathbf{J}\partial_z \boldsymbol{e} + \partial_t \boldsymbol{d}(\boldsymbol{e}) = \mathbf{0}, \tag{5.2}$$

where $\hat{\boldsymbol{z}}$ is the unit vector in the z direction. This is a Riemann problem, *i.e.*, the propagation of a step function, which is the archetype problem when studying discontinuous solutions, or shock waves. For an isotropic, nonmagnetic material, we can further reduce the Maxwell equations to the well investigated system [1, 16, 28]

$$\begin{cases} \partial_z H + \partial_t D(E) = 0 \\ \partial_z E + \partial_t H = 0. \end{cases} \tag{5.3}$$

Note that this can be converted to the p-system in gas dynamics by making D the dependent variable instead of E.

The entropy condition reduces to

$$\partial_z(EH) + \partial_t \eta(E,H) \leq 0, \tag{5.4}$$

where

$$\eta(E,H) = ED(E) - \int_0^E D(E')\,\mathrm{d}E' + \frac{H^2}{2}. \tag{5.5}$$

We study the constitutive relation for an instantaneously reacting Kerr medium,

$$D(E) = E + E^3 \quad \Rightarrow \quad \eta(E,H) = \frac{E^2}{2} + \frac{3E^4}{4} + \frac{H^2}{2}, \tag{5.6}$$

and choose the initial values, corresponding to (5.1), as

$$\begin{pmatrix} E^{\mathrm{l}} \\ H^{\mathrm{l}} \end{pmatrix} = \begin{pmatrix} 1 \\ \sqrt{2} \end{pmatrix} \quad \text{and} \quad \begin{pmatrix} E^{\mathrm{r}} \\ H^{\mathrm{r}} \end{pmatrix} = \begin{pmatrix} 0 \\ 0 \end{pmatrix}. \tag{5.7}$$

It can be verified that the one-dimensional Maxwell equations (5.3) allow two solutions for these initial values (see Figure 1): the shock wave solution

$$\begin{pmatrix} E \\ H \end{pmatrix} = \begin{cases} (1,\sqrt{2})^{\mathrm{T}} & z < \frac{1}{\sqrt{2}}t \\ (0,0)^{\mathrm{T}} & z > \frac{1}{\sqrt{2}}t \end{cases} \tag{5.8}$$

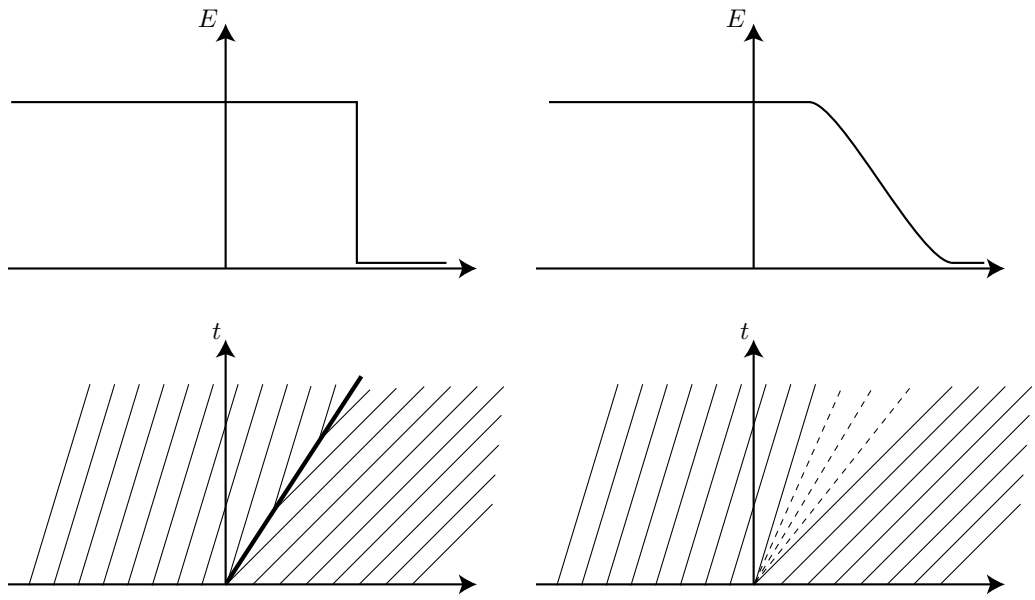

Figure 1: Top row: the two solutions with initial values (5.7) for a given time t. The solution to the left is the (nonphysical) shock wave (5.8), and the one to the right is the rarefaction (5.9). Bottom row: the '+'-characteristics for the two solutions. The '+'-characteristics are the curves in spacetime along which the waves propagating in the positive z-direction are constant, *i.e.*, in order to find the field at a certain point in space and time, we follow the characteristic curve back in time to the initial values. There are also '−'-characteristics, corresponding to waves propagating in the negative z-direction, but we have chosen initial values such that these waves can be ignored. Note that for the discontinuous solution, the characteristics originate from the shock front, indicated by the bold line.

and the rarefaction wave solution[4]

$$\begin{pmatrix} E \\ H \end{pmatrix} = \begin{cases} (1, \sqrt{2})^{\mathrm{T}} & z < \frac{1}{2}t \\ (f(z/t), g(z/t))^{\mathrm{T}} & \frac{1}{2}t < z < t \\ (0,0)^{\mathrm{T}} & z > t, \end{cases} \tag{5.9}$$

where f and g are differentiable functions satisfying

$$f(1/2) = 1, \quad g(1/2) = \sqrt{2}, \quad f(1) = g(1) = 0, \tag{5.10}$$

thus providing a smooth transition from the left state $(1, \sqrt{2})$ to the right state $(0,0)$. For a discontinuous solution which is equal to $(E^{\mathrm{l}}, H^{\mathrm{l}})$ when $z < vt$ and equal to $(E^{\mathrm{r}}, H^{\mathrm{r}})$ when $z > vt$, the entropy condition becomes

$$(E^{\mathrm{r}}H^{\mathrm{r}} - E^{\mathrm{l}}H^{\mathrm{l}}) - v(\eta(E^{\mathrm{r}}, H^{\mathrm{r}}) - \eta(E^{\mathrm{l}}, H^{\mathrm{l}})) \leq 0. \tag{5.11}$$

[4]Actually, this is not the true solution; it should also contain an additional, small shock wave of amplitude $[\![E]\!] \sim 0.01$ propagating to the left with speed ~ -0.5, where $[\![E]\!]$ denotes the discontinuity in E over the shock. We have chosen to exclude it to keep the example simple. The qualitative behavior of the solution is dominated by the continuous rarefaction wave (5.9), which is drastically different from the nonphysical shock solution (5.8).

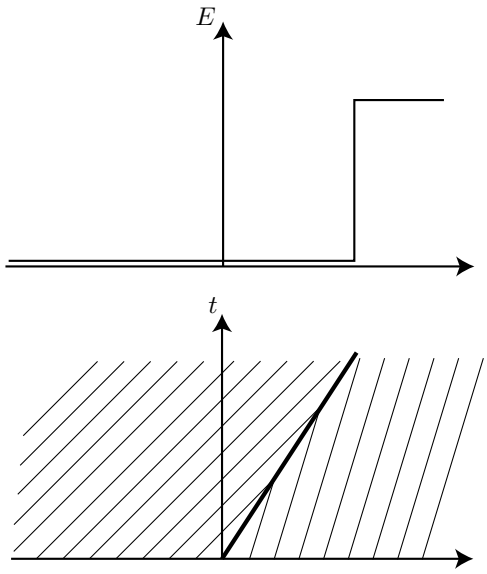

Figure 2: Top: the (physical) shock wave (5.13) for a given time t. Bottom: the '+'-characteristics corresponding to this solution. Note that the characteristics cross each other on the shock front, indicated by the bold line.

Calculating the expression on the left hand side for the discontinuous solution (5.8), we find it is equal to $1/4\sqrt{2} \not\leq 0$. The entropy condition is violated, and the true solution must be (5.9), which can be shown to satisfy the entropy condition. Thus, the entropy condition has helped us in choosing the correct solution, where the Maxwell equations alone are not sufficient.

It should be noted that if we exchange the left and the right states in the initial value problem, *i.e.*,

$$\begin{pmatrix} E^{\mathrm{l}} \\ H^{\mathrm{l}} \end{pmatrix} = \begin{pmatrix} 0 \\ 0 \end{pmatrix} \quad \text{and} \quad \begin{pmatrix} E^{\mathrm{r}} \\ H^{\mathrm{r}} \end{pmatrix} = \begin{pmatrix} 1 \\ \sqrt{2} \end{pmatrix}, \tag{5.12}$$

the entropy condition is satisifed for the shock solution

$$\begin{pmatrix} E \\ H \end{pmatrix} = \begin{cases} (0,0)^{\mathrm{T}} & z < \frac{1}{\sqrt{2}}t \\ (1,\sqrt{2})^{\mathrm{T}} & z > \frac{1}{\sqrt{2}}t, \end{cases} \tag{5.13}$$

since in this case $(E^{\mathrm{r}}H^{\mathrm{r}} - E^{\mathrm{l}}H^{\mathrm{l}}) - v(\eta(E^{\mathrm{r}}, H^{\mathrm{r}}) - \eta(E^{\mathrm{l}}, H^{\mathrm{l}})) = -1/4\sqrt{2} \leq 0$. Thus, the initial values (5.12) generates a unique, physical, shock solution, where electromagnetic energy is dissipated. This solution is depicted in Figure 2.

6 Conclusions

In the previous sections, the constitutive relation $\boldsymbol{d}(\boldsymbol{e})$ may depend on additional parameters without any change in the analysis. In particular, we allow for a dependence on the spatial variable, *i.e.*, $\boldsymbol{d}(\boldsymbol{x}, \boldsymbol{e})$. It is also easily seen that this form of

constitutive relation allows for a coupling between the electric and magnetic field and any anisotropic effects, as long as the 6×6 matrix $\boldsymbol{d}'(\boldsymbol{e})$ is positive definite for all $\boldsymbol{e}$. Thus, our presentation comprises inhomogeneous, bianisotropic, instantaneously reacting nonlinear models.

It must be stressed that the results obtained in this paper are subject to the assumption that the cubic term in (4.13) is negligible. We have not been able to prove this conjecture, but one way might be to study the conservation of pseudo-momentum $\boldsymbol{D}\times\boldsymbol{B}$, as is done for one-dimensional shock profiles in continuum mechanics [23, 24]. This results in three additional conservation laws (one for each component of the pseudo-momentum), which might bring additional information to the problem. For instance, the problematic term can be related to the balance of forces across shock fronts, but the usefulness of this approach in three-dimensional electromagnetics is unclear.

Since it seems reasonable that entropy solutions to the Maxwell equations are unique and depend continuously on data, numerical methods for treating these equations should incorporate the entropy condition. One way to do this is by choosing a numerical scheme based on vanishing viscosity, where the viscosity parameter is of the same order as the discretization as explained at the end of Section 3.2.

In the Introduction, we listed the three questions of existence, uniqueness and continuity. The latter two have been treated in this paper using Kružkov's method, but the questions remain open. There is also only empirical evidence regarding the existence of solutions satisfying the entropy condition. If it is possible to answer these questions by the vanishing viscosity technique, that answer will most probably also shed additional light on the problems with uniqueness and continuity treated in this paper.

7 Acknowledgments

The work reported in this paper is partially supported by a grant from the Swedish Research Council for Engineering Sciences and its support is gratefully acknowledged.

The author thanks the staff at the Department of Electroscience, Electromagnetic Theory, for many valuable discussions and suggestions on this paper. Special thanks go to Dr. Mats Gustafsson and Prof. Gerhard Kristensson for reading this manuscript and providing constructive discussions.

Appendix A Analysis of an energy term

In this appendix, we analyze the term $\frac{1}{2}[\eta(\boldsymbol{e},\tilde{\boldsymbol{e}})-\eta(\tilde{\boldsymbol{e}},\boldsymbol{e})]$. The definition of the energy $\eta(\boldsymbol{e},\tilde{\boldsymbol{e}})$ is

$$\eta(\boldsymbol{e},\tilde{\boldsymbol{e}})=(\boldsymbol{e}-\tilde{\boldsymbol{e}})^{\mathrm{T}}\boldsymbol{d}(\boldsymbol{e})-\phi(\boldsymbol{e})+\phi(\tilde{\boldsymbol{e}}), \tag{A.1}$$

which enables us to write

$$\frac{1}{2}[\eta(\boldsymbol{e},\tilde{\boldsymbol{e}})-\eta(\tilde{\boldsymbol{e}},\boldsymbol{e})]=(\boldsymbol{e}-\tilde{\boldsymbol{e}})^{\mathrm{T}}\frac{\boldsymbol{d}(\boldsymbol{e})+\boldsymbol{d}(\tilde{\boldsymbol{e}})}{2}-\phi(\boldsymbol{e})+\phi(\tilde{\boldsymbol{e}}). \tag{A.2}$$

This is in fact a cubic function of $\boldsymbol{e} - \tilde{\boldsymbol{e}}$. To see this, first note that we can write

$$\begin{aligned}\phi(\boldsymbol{e}) - \phi(\tilde{\boldsymbol{e}}) &= \int_0^1 \frac{\mathrm{d}}{\mathrm{d}r}\phi(r\boldsymbol{e} + (1-r)\tilde{\boldsymbol{e}})\,\mathrm{d}r \\ &= (\boldsymbol{e} - \tilde{\boldsymbol{e}})^{\mathrm{T}} \int_0^1 \phi'(r\boldsymbol{e} + (1-r)\tilde{\boldsymbol{e}})\,\mathrm{d}r \\ &= (\boldsymbol{e} - \tilde{\boldsymbol{e}})^{\mathrm{T}} \int_0^1 \boldsymbol{d}(r\boldsymbol{e} + (1-r)\tilde{\boldsymbol{e}})\,\mathrm{d}r. \end{aligned} \tag{A.3}$$

We then have

$$\begin{aligned}(\boldsymbol{e} - \tilde{\boldsymbol{e}})^{\mathrm{T}} \frac{\boldsymbol{d}(\boldsymbol{e}) + \boldsymbol{d}(\tilde{\boldsymbol{e}})}{2} - \phi(\boldsymbol{e}) + \phi(\tilde{\boldsymbol{e}}) = \frac{1}{2}(\boldsymbol{e} - \tilde{\boldsymbol{e}})^{\mathrm{T}} \\ \left\{\boldsymbol{d}(\boldsymbol{e}) - \int_0^1 \boldsymbol{d}(r\boldsymbol{e} + (1-r)\tilde{\boldsymbol{e}})\,\mathrm{d}r + \boldsymbol{d}(\tilde{\boldsymbol{e}}) - \int_0^1 \boldsymbol{d}(r\boldsymbol{e} + (1-r)\tilde{\boldsymbol{e}})\,\mathrm{d}r\right\}, \end{aligned} \tag{A.4}$$

and we repeat the trick in (A.3) to find

$$\begin{aligned}\boldsymbol{d}(\boldsymbol{e}) - \int_0^1 \boldsymbol{d}(r\boldsymbol{e} + (1-r)\tilde{\boldsymbol{e}})^{\mathrm{T}}\,\mathrm{d}r &= \int_0^1 \{\boldsymbol{d}(\boldsymbol{e}) - \boldsymbol{d}(r\boldsymbol{e} + (1-r)\tilde{\boldsymbol{e}})\}\,\mathrm{d}r \\ = \int_0^1 (\boldsymbol{e} - (r\boldsymbol{e} + (1-r)\tilde{\boldsymbol{e}}))^{\mathrm{T}} &\int_0^1 \boldsymbol{d}'(q\boldsymbol{e} + (1-q)(r\boldsymbol{e} + (1-r)\tilde{\boldsymbol{e}}))\,\mathrm{d}q\,\mathrm{d}r \\ = (\boldsymbol{e} - \tilde{\boldsymbol{e}})^{\mathrm{T}} \int_0^1 (1-r) &\int_0^1 \boldsymbol{d}'(q\boldsymbol{e} + (1-q)(r\boldsymbol{e} + (1-r)\tilde{\boldsymbol{e}}))\,\mathrm{d}q\,\mathrm{d}r, \end{aligned} \tag{A.5}$$

and

$$\begin{aligned}\boldsymbol{d}(\tilde{\boldsymbol{e}}) - \int_0^1 \boldsymbol{d}(r\boldsymbol{e} + (1-r)\tilde{\boldsymbol{e}})^{\mathrm{T}}\,\mathrm{d}r &= \int_0^1 \{\boldsymbol{d}(\tilde{\boldsymbol{e}}) - \boldsymbol{d}(r\boldsymbol{e} + (1-r)\tilde{\boldsymbol{e}})\}\,\mathrm{d}r \\ = \int_0^1 (\tilde{\boldsymbol{e}} - (r\boldsymbol{e} + (1-r)\tilde{\boldsymbol{e}}))^{\mathrm{T}} &\int_0^1 \boldsymbol{d}'(q\tilde{\boldsymbol{e}} + (1-q)(r\boldsymbol{e} + (1-r)\tilde{\boldsymbol{e}}))\,\mathrm{d}q\,\mathrm{d}r \\ = (\tilde{\boldsymbol{e}} - \boldsymbol{e})^{\mathrm{T}} \int_0^1 r &\int_0^1 \boldsymbol{d}'(q\tilde{\boldsymbol{e}} + (1-q)(r\boldsymbol{e} + (1-r)\tilde{\boldsymbol{e}}))\,\mathrm{d}q\,\mathrm{d}r \\ = (\tilde{\boldsymbol{e}} - \boldsymbol{e})^{\mathrm{T}} \int_0^1 (1-r) &\int_0^1 \boldsymbol{d}'(q\tilde{\boldsymbol{e}} + (1-q)(r\tilde{\boldsymbol{e}} + (1-r)\boldsymbol{e}))\,\mathrm{d}q\,\mathrm{d}r, \end{aligned} \tag{A.6}$$

where the last line follows from a change of variables $r \to 1-r$. The sum of these terms involve the expression

$$\int_0^1 (1-r) \int_0^1 \{\boldsymbol{d}'(q\boldsymbol{e} + (1-q)(r\boldsymbol{e} + (1-r)\tilde{\boldsymbol{e}})) - \boldsymbol{d}'(q\tilde{\boldsymbol{e}} + (1-q)(r\tilde{\boldsymbol{e}} + (1-r)\boldsymbol{e}))\} \,\mathrm{d}q \,\mathrm{d}r$$
$$= \int_0^1 (1-r) \int_0^1 (\boldsymbol{e} - \tilde{\boldsymbol{e}})^{\mathrm{T}} (q + (1-q)(r - (1-r)))$$
$$\int_0^1 \boldsymbol{d}''(p(q\boldsymbol{e} + (1-q)(r\boldsymbol{e} + (1-r)\tilde{\boldsymbol{e}})) + (1-p)(q\boldsymbol{e} + (1-q)(r\boldsymbol{e} + (1-r)\tilde{\boldsymbol{e}}))) \,\mathrm{d}p \,\mathrm{d}q \,\mathrm{d}r$$
$$= (\boldsymbol{e} - \tilde{\boldsymbol{e}})^{\mathrm{T}} \int_0^1 \int_0^1 \int_0^1 (1-r)(2q + 2r - 2qr - 1)$$
$$\boldsymbol{d}''(p(q\boldsymbol{e} + (1-q)(r\boldsymbol{e} + (1-r)\tilde{\boldsymbol{e}})) + (1-p)(q\boldsymbol{e} + (1-q)(r\boldsymbol{e} + (1-r)\tilde{\boldsymbol{e}}))) \,\mathrm{d}p \,\mathrm{d}q \,\mathrm{d}r. \tag{A.7}$$

Since $\boldsymbol{d}'' = \phi'''$ we can introduce the third rank tensor

$$K_{ijk}(\boldsymbol{e}, \tilde{\boldsymbol{e}}) = \int_0^1 \int_0^1 \int_0^1 (1-r)(2q + 2r - 2qr - 1)$$
$$\frac{\partial^3 \phi}{\partial e_i \partial e_j \partial e_k}(p(q\boldsymbol{e}+(1-q)(r\boldsymbol{e}+(1-r)\tilde{\boldsymbol{e}}))+(1-p)(q\boldsymbol{e}+(1-q)(r\boldsymbol{e}+(1-r)\tilde{\boldsymbol{e}}))) \,\mathrm{d}p \,\mathrm{d}q \,\mathrm{d}r, \tag{A.8}$$

to write

$$(\boldsymbol{e} - \tilde{\boldsymbol{e}})^{\mathrm{T}} \frac{\boldsymbol{d}(\boldsymbol{e}) + \boldsymbol{d}(\tilde{\boldsymbol{e}})}{2} - \phi(\boldsymbol{e}) + \phi(\tilde{\boldsymbol{e}}) = K_{ijk}(\boldsymbol{e}, \tilde{\boldsymbol{e}})(e_i - \tilde{e}_i)(e_j - \tilde{e}_j)(e_k - \tilde{e}_k), \tag{A.9}$$

where summation over repeated indices is assumed. With ϕ a quadratic function for linear materials, we see that this term must be due to the nonlinearity of the constitutive relation.

References

[1] F. Bloom. *Mathematical problems of classical nonlinear electromagnetic theory.* Longman Scientific & Technical, Burnt Mill, Harlow, England, 1993.

[2] B. D. Coleman and E. H. Dill. Thermodynamic restrictions on the constitutive equations of electromagnetic theory. *Z. angew. Math. Phys.*, **22**, 691–702, 1971.

[3] R. Courant and K. O. Friedrichs. *Supersonic Flow and Shock Waves.* Springer-Verlag, New York, 1948.

[4] C. M. Dafermos. The entropy rate admissibility criteria for solutions of hyperbolic conservation laws. *Journal of Differential Equations*, **14**, 202–212, 1973.

[5] C. M. Dafermos. *Hyperbolic conservation laws in continuum physics.* Grundlehren der mathematischen Wissenschaften 325. Springer-Verlag, Berlin, 2000.

[6] L. C. Evans. *Partial Differential Equations.* American Mathematical Society, Providence, Rhode Island, 1998.

[7] E. Godlewski and P.-A. Raviart. *Numerical Approximation of Hyperbolic Systems of Conservation Laws.* Springer-Verlag, Berlin, 1996.

[8] M. Gustafsson. *Wave Splitting in Direct and Inverse Scattering Problems.* PhD thesis, Lund Institute of Technology, Department of Electromagnetic Theory, P.O. Box 118, S-211 00 Lund, Sweden, 2000. `http://www.es.lth.se/home/mats`.

[9] J. Hadamard. *Lectures on the Cauchy Problem in Linear Partial Differential Equations.* Yale University Press, New Haven, 1923.

[10] E. Hopf. The partial differential equation $u_t + uu_x = \mu u_{xx}$. *Comm. Pure Appl. Math.*, **3**, 201–230, 1950.

[11] L. Hörmander. *The Analysis of Linear Partial Differential Operators I.* Grundlehren der mathematischen Wissenschaften 256. Springer-Verlag, Berlin Heidelberg, 1983.

[12] L. Hörmander. *Lectures on Nonlinear Hyperbolic Differential Equations.* Number 26 in Mathémathiques & Applications. Springer-Verlag, Berlin, 1997.

[13] J. D. Jackson. *Classical Electrodynamics.* John Wiley & Sons, New York, third edition, 1999.

[14] E. Jouguet. Sur la propagation des discontinuités dans les fluides. *C. R. Acad. Sci., Paris, Sér I*, **132**, 673–676, 1901.

[15] H.-O. Kreiss and J. Lorenz. *Initial-Boundary Value Problems and the Navier-Stokes Equations.* Academic Press, San Diego, 1989.

[16] G. Kristensson and D. J. N. Wall. Direct and inverse scattering for transient electromagnetic waves in nonlinear media. *Inverse Problems*, **14**, 113–137, 1998.

[17] S. Kružkov. First order quasilinear equations with several space variables. *Math. USSR Sbornik*, **10**, 217–273, 1970.

[18] L. D. Landau, E. M. Lifshitz, and L. P. Pitaevskiĭ. *Electrodynamics of Continuous Media.* Pergamon, Oxford, second edition, 1984.

[19] P. D. Lax. Shock waves and entropy. In E. A. Zarantonello, editor, *Contributions to nonlinear functional analysis*, pages 603–634. Academic Press, New York, 1971.

[20] P. D. Lax. *Hyperbolic systems of conservation laws and the mathematical theory of shock waves*. Conf. Board. Math. Sci. Regional Conference Series in Applied Mathematics 11. SIAM, Philadelphia, 1973.

[21] I. V. Lindell, A. H. Sihvola, and K. Suchy. Six-vector formalism in electromagnetics of bi-anisotropic media. *J. Electro. Waves Applic.*, **9**(7/8), 887–903, 1995.

[22] T.-P. Liu. The entropy condition and the admissibility of shocks. *J. Math. Anal. Appl.*, **53**, 78–88, 1976.

[23] G. A. Maugin. On shock waves and phase-transition fronts in continua. *ARI*, **50**, 141–150, 1998.

[24] G. A. Maugin. On the universality of the thermomechanics of forces driving singular sets. *Archive of Applied Mechanics*, **70**, 31–45, 2000.

[25] O. A. Oleĭnik. Uniqueness and stability of the generalized solution of the Cauchy problem for a quasi-linear equation. *Amer. Math. Soc. Transl.*, **33**(2), 285–290, 1963. Translated from Russian, Uspehi Mat. Nauk 14 (1959), no. 2 (86), 87–158.

[26] D. Serre. Systems of conservation laws: A challenge for the XXIst century. In B. Engquist and W. Schmid, editors, *Mathematics Unlimited — 2001 and Beyond*, pages 1061–1080. Springer-Verlag, Berlin, 2001.

[27] D. Sjöberg. Simple wave solutions for the Maxwell equations in bianisotropic, nonlinear media, with application to oblique incidence. *Wave Motion*, **32**(3), 217–232, 2000.

[28] D. Sjöberg. Reconstruction of nonlinear material properties for homogeneous, isotropic slabs using electromagnetic waves. *Inverse Problems*, **15**(2), 431–444, April 1999.

[29] D. F. Styer. Insight into entropy. *Am. J. Phys*, **68**(12), 1090–1096, December 2000.

[30] M. Taylor. *Partial Differential Equations III: Nonlinear Equations*. Springer-Verlag, New York, 1996.